UNIVERSITÀ DEGLI STUDI DI MILANO

FACOLTÀ DI SCIENZE E TECNOLOGIE

Doctorate in

Industrial Chemistry XXXIII Cycle

Heterohelicenes as appealing chiral systems: innovative methodologies for their preparation also in enantiomerically pure form

Valentina Pelliccioli

Tutor: Dr. Silvia Cauteruccio

Coordinator: Prof. Dominique Roberto

A.A. 2017/2021

Table of Contents

Abstract

Helicenes are *ortho*-annulated polycyclic aromatic or heteroaromatic compounds, endowed with inherent chirality owing to the helical shape of their π-conjugated system. Carbohelicenes only include benzene rings in their structure, while in heterohelicenes one or more heterocycles are present. Interestingly, the introduction of heteroatoms into the fused polycyclic frameworks adds remarkable changes to the electronic structures of helicenes, and additional chemical and physical properties. Their unique structural features and physicochemical properties have stimulated manifold studies in several fields, including optoelectronics, material science, asymmetric catalysis, and chiral recognition.[1] Many of these applications require the use of enantiomerically pure helicenes, although the resolution of racemates by means of analytical methods as well as the separation of diastereomers still remain the most common ways to obtain non-racemic helicenes, whose peculiar geometry makes them extremely difficult targets for stereoselective synthesis. This Ph.D. thesis was intended to provide a meaningful contribution in the development of innovative and versatile syntheses of heterohelicenes, also in enantiopure form, and has focused on the following main goals:

1. Study of methodologies for the synthesis of functionalised tetrathia[7]helicenes (7-THs).

2. Synthesis of different classes of thiahelicenes through methodologies set up for the preparation of 7-THs.

3. Enantioselective synthesis of thia[5]helicenes via Au-catalysed alkyne hydroarylation.

In the course of this thesis, a sub-topic has also been developed:

4. Functionalisation of benzo[1,2-*b*:4,3-*b*']dithiophenes by Suzuki reactions in Deep Eutectic Solvents (DESs).

1. Study of methodologies for the synthesis of functionalised tetrathia[7]helicenes (7-THs)

a) Synthesis of differently functionalised 7-TH derivatives

Tetrathia[7]helicenes (7-THs), in which thiophene rings are fused to alternating benzene rings, are configurationally stable heterohelicenes.[2] Thank to the possibility of combining the electronic features of oligothiophenes with the peculiar chiroptical properties of helical shaped molecules, these systems are potentially interesting for applications in optoelectronics,[3] catalysis,[4] and biology.[5] In spite of their great potential, general and versatile methods to prepare differently functionalised 7-TH frameworks, also by asymmetric procedures, are still scarce. In this context, three novel and versatile routes were developed to prepare 7-TH derivatives **1**, **2** and **3** through cyclisation reactions of bis(benzodithiophene) species **4**, **5** and **6**, respectively (*Scheme 1*).[6]

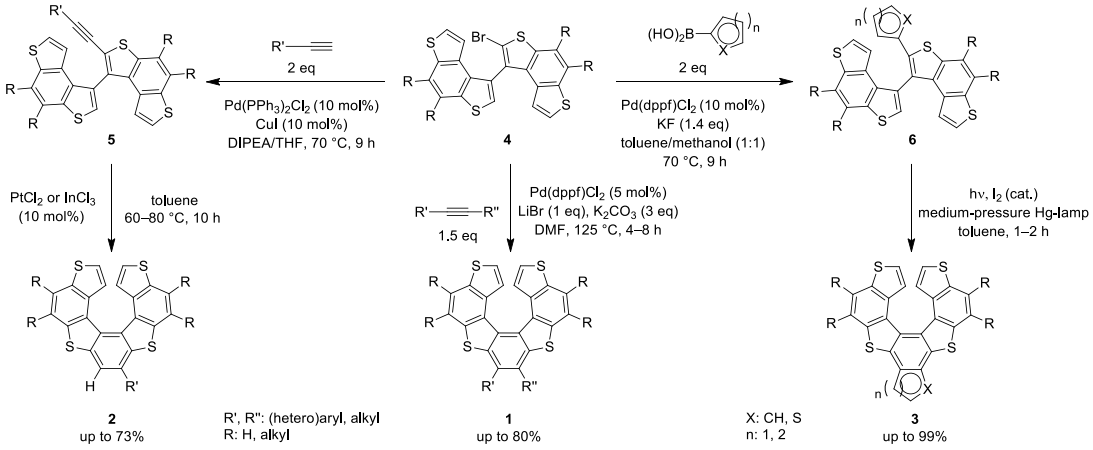

***Scheme 1*:** Synthesis of functionalised 7-TH derivatives **1**, **2** and **3**.

More in detail, a set of 7,8-disubstituted compounds **1** was prepared through Pd-catalysed annulation of bromides **4** with internal alkynes (yields up to 80%), while the synthesis of 7-monosubstituted derivatives **2** was accomplished via a two-step procedure involving a Sonogashira cross-coupling of **4** with terminal alkynes, followed by the metal-promoted cycloisomerisation of intermediates **5** (yields up to 73%). Finally, the synthesis of benzo fused 7-TH systems **3** was performed by means of a two-step procedure involving a Suzuki coupling of **4** with (hetero)aryl boronic acids, followed by the photochemical cyclisation of intermediates **6** (yields up to 99%). This study affords an important contribution to thiahelicene chemistry since the substrate scope of these protocols can be easily extended thanks to the wide range of easily available alkynes and (hetero)arylboronic acids.

*b) Study of the stereochemical properties of atropisomeric intermediates **4**, **5** and **6***

To consider an asymmetric version of the latter protocols and obtain enantioenriched 7-THs, the stereochemical properties of atropisomeric intermediates **4**, **5** and **6** were evaluated by variable-temperature chiral HPLC[7] in combination with kinetic studies. All compounds were found to be configurationally stable even at high temperatures (estimated free energy rotation $\Delta G^{\ddagger} > 34$ kcal/mol at 150 °C). The chiroptical properties of single enantiomers of **4**, **5** and **6** were also analysed by experimental and theoretical electronic and vibrational circular dichroism spectra, and the good agreement between experimental and computational data allowed us to assign their absolute configuration.[8] Furthermore, to evaluate the potentialities of these compounds in chiroptics materials, Circularly Polarized Luminescence (CPL) properties of the enantiopure **4**, **5** and **6** in solution were preliminary investigated, and especially compounds **5**, containing an alkyne pendant, displayed interesting luminescent features.

*c) Preliminary studies of asymmetric cycloisomerisation of intermediates **5***

Taking into account the configurational stability of intermediates **5**, a first study of the cycloisomerisation of (±)-**5** promoted by chiral Au(I)-catalysts to obtain enantioenriched 7-monosubstituted derivatives **2** through a kinetic resolution was performed. This work has been carried out in collaboration with Prof. Manuel Alcarazo from Georg-August University of Göttingen. Initially, the intramolecular hydroarylation promoted by a non-chiral Au(I)-catalyst **L1**[9] was studied to evaluate the efficacy of this kind of catalysts for the cyclisation of **5**, and helicenes (±)-**2** were isolated in good to excellent yields (*Scheme 2*, left).

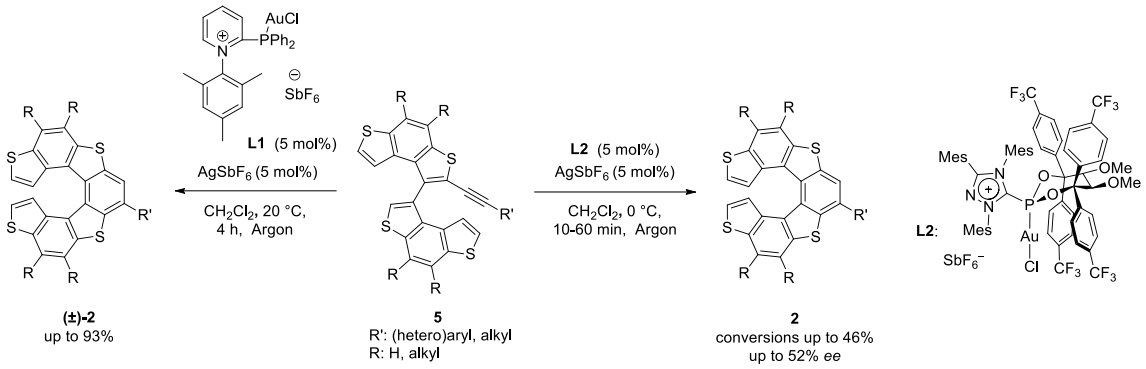

***Scheme 2*:** Au(I)-promoted cycloisomerisation of intermediates **5**.

Next, the kinetic resolution of (±)-**5** was performed using chiral Au(I)-catalysts, and the best results were achieved using **L2**[10] in the presence of $AgSbF_6$ in CH_2Cl_2 at 0 °C (*Scheme 2*, right). In this case, conversions up to 46% and moderate to good enantiomeric excesses (up to 52%) were obtained.[11]

2. Synthesis of different classes of thiahelicenes through methodologies set up for the preparation of 7-THs

The versatility of the methodologies developed for the synthesis of 7-THs was further demonstrated for the preparation of a novel class thiahelicenes. In particular, a very similar synthetic approach used to prepare 7,8-disubstituted 7-TH derivatives **1** was also applied for the synthesis of functionalised thia[6]helicenes **7** through a three-step procedure starting from commercially available boronic acid **8** and bromides **9** (*Scheme 3*).

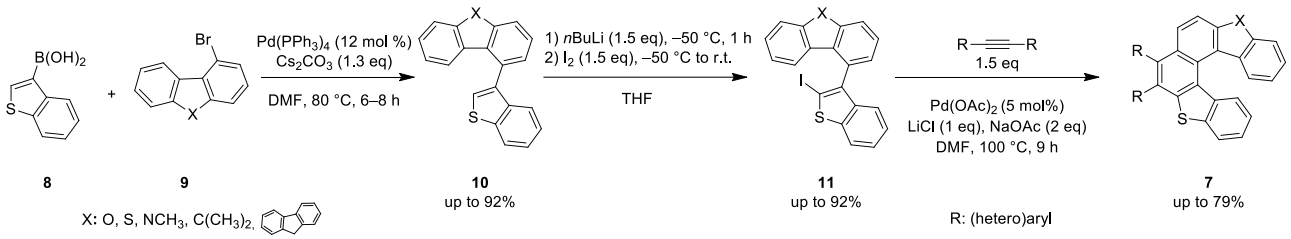

Scheme 3: Synthesis of thia[6]helicenes **7**.

Indeed, intermediates **10** were prepared in very good yields (up to 92%) through the Suzuki reaction between boronic acid **8** and bromides **9** in the presence of $Pd(PPh_3)_4$ as catalyst, Cs_2CO_3 as base in DMF at 80 °C. Next, the iodination of dimers **10** was performed by the deprotonation of α-position of the terminal thiophene ring with *n*BuLi at −50 °C followed by the addition of a solution of iodine in THF, and iodides **11** were isolated in high yields (up to 92%). Finally, the $Pd(OAc)_2$-catalysed annulation of some iodides **11** with internal alkynes was performed in the presence of NaOAc and LiCl in DMF at 100 °C, and the corresponding thia[6]helicenes **7** were isolated in moderate to good yields (up to 79%), so demonstrating that dimers **11** were also reactive towards the Pd-catalysed annulation of internal alkynes. These results are very promising because they demonstrate the efficacy and the versatility of our synthetic protocol also for the

synthesis of different classes of thiahelicenes. Further studies on the configurational stability of thia[6]helicenes **7** will be carried out.

3. Enantioselective synthesis of thia[5]helicenes via Au-catalysed alkyne hydroarylation

In our continuing search aimed at finding versatile syntheses of heterohelicenes, also in enantiopure form, in Alcarazo's laboratories a highly enantioselective synthesis of thia[5]helicenes was developed. In particular, a novel class of thia[5]helicenes **12** was synthesised starting from configurationally unstable dialkynes **13** (*Scheme 4*).

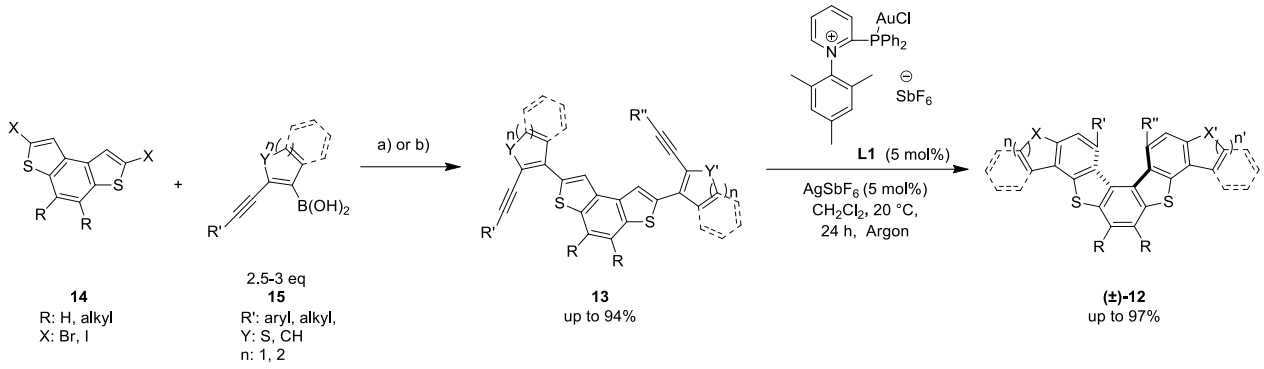

Scheme 4: Synthesis of dialkynes **13** and their Au(I)-catalysed cycloisomerisation to thiahelicenes (±)-**12**.

More in detail, dialkynes **13** were prepared in good to excellent yields (up to 94%) by Suzuki coupling between dihalides of benzo[1,2-*b*:4,3-*b*']dithiophenes **14** and boronic acids **15** following two different procedures previously set up for the Suzuki coupling of benzodithiophene derivatives[12] and boronic acids **15**.[9,10] Next, dialkynes **13** were reacted in CH_2Cl_2 at room temperature in the presence of Au(I) pre-catalyst **L1** and $AgSbF_6$ (*Scheme 4*). After 24 hours, no starting material was found in the reaction mixture, and the expected products (±)-**12** were isolated in excellent yields (up to 97%). These new helicenes **12** were analysed by chiral HPLC and two peaks were observed for each compound. No on-column interconversion was observed at 37 °C, and this suggested that these new helicenes were configurationally stable at this temperature. Based on these results, the enantioselective intramolecular hydroarylation of dialkynes **13** promoted by chiral catalyst **L2** was performed using experimental conditions very similar than those reported in literature for the enantioselective synthesis of carbohelicenes[10] (*Scheme 5*).

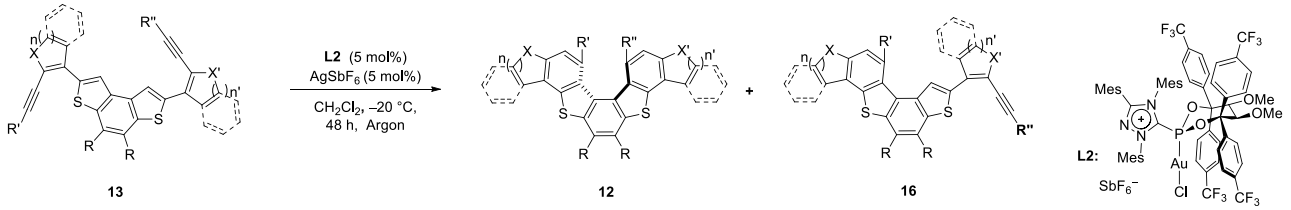

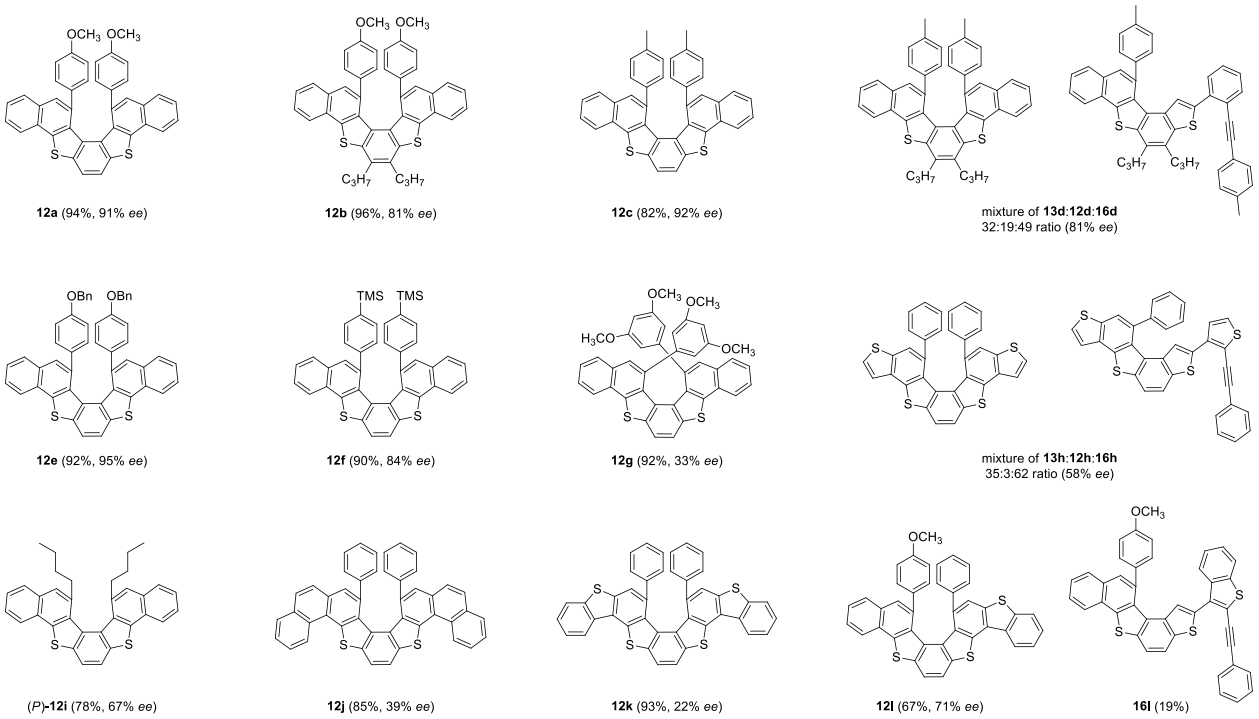

Scheme 5: Enantioselective double Au(I)-catalysed cycloisomerisation of dialkynes **13**.

Dialkynes **13** were reacted in CH_2Cl_2 at – 20 °C in the presence of 5 mol% of pre-catalyst **L2** and 5 mol% of $AgSbF_6$ under argon for 48 hours, and excellent yields (82–96%) and very good *ee* (81–95%) were achieved with electron-rich and electron-withdrawing substituents in the *para* position of the phenyl ring (**12a**–**c, 12e**,**f**). For compounds **12d** and **12h**, no complete conversion of the starting material was observed and the side-products **16d** and **16h** were also found in the reaction mixture, while moderate yield and *ee* were obtained in case of **12i** (78% yield and 67% *ee*). Otherwise, low *ee* were obtained in the hydroarylation of more conjugated (hetero)aryl systems, such as **12j** and **12k** (39% and 22% *ee*, respectively) and in case of substituents in *meta*-positions of the phenyl ring **12g** (33% *ee*), although they were isolated in very good yield (up to 93%). The first example of enantioenriched helicene **12l**, bearing two different aryl pendants, was also obtained in moderate yield and good *ee*, along with a small amount of the side-product **16l** (19%). Finally, X-ray studies on the enantioenriched mixture of **12i** suggested that the enantiomer of **L2** used as catalyst in these reactions favoured the formation of the thiahelicenes with right-handed helicity (the *P*-configuration). Several X-ray structures of dimers **13** and helicenes **12** were also obtained, so confirming their 3D-structure.[13]

4. Functionalisation of benzo[1,2-*b*:4,3-*b*']dithiophenes by Suzuki reactions in Deep Eutectic Solvents (DESs)

Benzo[1,2-*b*:4,3-*b*']dithiophene (BDT) is not only the key intermediate for the synthesis of thiahelicenes,[6,13] but its derivatives are widely studied as units in mono and polydisperse oligomers for the synthesis of conductive materials used in electronic devices.[12] Thus, BDT represents a key starting molecule, which can allow access to more complex and interesting systems, for example through the functionalisation of the α-

positions of the terminal thiophene rings with aryl,[12] alkenyl and alkynyl pendants,[14] that can be introduced by Pd-catalysed cross-coupling reactions starting from α-halogenated BDT derivatives. In collaboration with Prof. Capriati (Università degli Studi di Bari), a general procedure was set up for the synthesis of 2,7-disubstituted BDTs **17** (up to 79% yield) through the $Pd(OAc)_2$-catalysed ligandless Suzuki reaction between dihalides **14** and aryl-, alkenyl- and alkynyl-trifluoroborate salts using the eutectic mixture formed by choline chloride/glycerol as sustainable and environmentally responsible green reaction media[15] (*Scheme 6*).

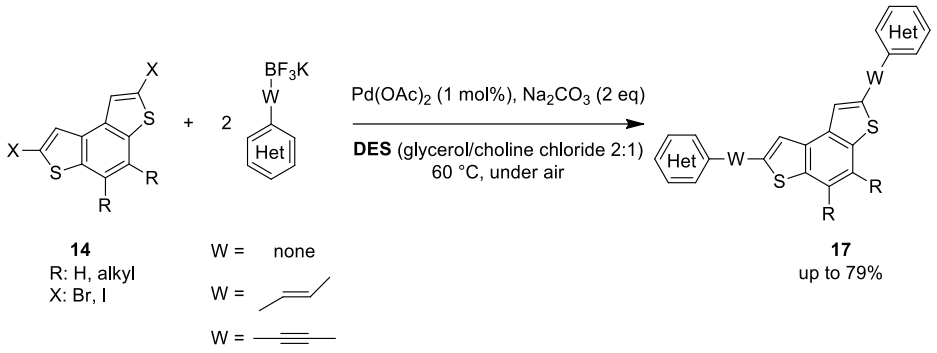

***Scheme 6*:** Synthesis of 2,7-disubstituted BDTs **17** through Suzuki reaction in DES.

The optical and electrochemical characterisation of these systems were also carried out, and some derivatives displayed a photoluminescent quantum yield in solution significantly high (up to 80%).

References

1. C. F. Chen and Y. Shen *Helicene Chemistry: From Synthesis to Applications* 1st ed.; Springer-Verlag Berlin 352. Heidelberg, 2017.
2. S. Cauteruccio, D. Dova and E. Licandro, *Adv. Heterocycl. Chem.,* 2016, **118**, 1.
3. A. Bossi, E. Licandro, S. Maiorana, C. Rigamonti, S. Righetto, G. R. Stephenson, M. Spassova, E. Botek and B. Champagne, *J. Phys. Chem. C*, 2008, **112**, 7900.
4. S. Cauteruccio, A. Loos, A. Bossi, D. Dova, F. Rominger, S. Prager, M. C. Blanco Jaimes, A. Dreuw, E. Licandro, A. S. K. Hashmi and A. K. Stephen, *Inorg. Chem.,* 2013, **52**, 7995; S. Cauteruccio, D. Dova, A. Genoni, M. Orlandi, M. Benaglia and E. Licandro, *Eur. J. Org. Chem.,* 2014, 2694.
5. S. Cauteruccio, C. Bartoli, C. Carrara, D. Dova, C. Errico, G. Ciampi, D. Dinucci, F. Chiellini and E. Licandro, *ChemPlusChem*, 2015, **80**, 490.
6. V. Pelliccioli, D. Dova, C. Baldoli, C. Graiff, E. Licandro and S. Cauteruccio, *Eur. J. Org. Chem.*, 2021, **3**, 383.
7. I. D'Acquarica, F. Gasparrini, M. Pierini, C. Villani and G. Zappia, *J. Sep. Sci*., 2006, **29**, 1508.
8. V. Pelliccioli, R. Franzini, G. Mazzeo, G. Longhi, C. Villani, S. Abbate, E. Licandro and S. Cauteruccio, *Manuscript in preparation.*
9. H. Tinnermann, L. D. M. Nicholls, T. Johannsen, C. Wille, C. Golz, R. Goddard and M. Alcarazo, *ACS Catalysis*, 2018, **8**, 10457.

10. L. D. M. Nicholls, M. Marx, T. Hartung, E. González-Fernández, C. Golz and M. Alcarazo, *ACS Catalysis*, 2018, **8**, 6079; T. Hartung, R. Machleid, M. Simon, C. Golz and M. Alcarazo, *Angew. Chem. Int. Ed.*, 2020, **59**, 5660.
11. V. Pelliccioli, T. Hartung, M. Simon, C. Golz, L. Emanuela, M. Alcarazo and S. Cauteruccio, *Manuscript in preparation.*
12. A. Bedi and S. Zade, *Macromolecules*, 2013, **46**, 8864.
13. V. Pelliccioli, T. Hartung, M. Simon, C. Golz, L. Emanuela, S. Cauteruccio and M. Alcarazo *Manuscript in preparation.*
14. Y. Nishide, H. Osuga, M. Saito, T. Aiba, Y. Inagaki, Y. Doge and K. Tanaka *J. Org. Chem*., 2007, **72**, 9141.
15. V. Pelliccioli, G. Dilauro, S. Grecchi, S. Arnaboldi, C. Graiff, F. M. Perna, P. Vitale, E. Licandro, A. Aliprandi, S. Cauteruccio and V. Capriati, *Eur. J. Org. Chem*., **2020**, 6981.

List of Schemes

Introduction

Chapter 1

Chapter 2

Chapter 4

Chapter 5

Chapter 6

List of Figures

Introduction

Chapter 1

Chapter 2

Chapter 3

Chapter 4

Chapter 5

Chapter 6

List of Tables

Chapter 1

Chapter 2

Chapter 3

Chapter 4

Chapter 6

Abbreviations

°C	degrees celcius
7-TH	tetrathia[7]helicene
Å	Ångström
Ar	general arene
BDT	benzo[1,2-b:4,3-b']dithiophene
BINAP	2,2‘-bis(diphenylphosphino)-1,1‘-binaphthalene
BINOL	1,1'-bi-2-naphthol
Bn	benzyl
Bu	butyl
c	concentration
cal	calorie
cald.	calculated
cat	catalytic
CD	circular dichroism
ChCl	cholina chloride
CPL	circular polarized luminescence
CSP	chiral stationary phase
Dba	dibenzylideneacetone
DDQ	2,3-dichloro-5,6-dicyano-1,4-benzoquinone
DES	Deep Eutectic Solvent
DFT	Density Functional Theory
DIPEA	N,N,-diisopropylethylamine
DMF	N,N-dimethylformamide
dppf	1,1’-(diphenylphosphino)ferrocene
DSSC	dey sensitised solar cell
ECD	Electronic Circular Dichroism
ee	enantiomeric excess
EI	Electron Ionisation
$E_{p(Ox.)}$	Electrochemical oxidation potential
$E_{p(Red.)}$	Electrochemical reduction potential
ESI-MS	Electrospray Ionisation Mass Spectrometry
eV	electron volt
Fc	ferrocene
g	dissym. factor
Gly	glycerol
HOMO	Highest Occupied Molecular Obital
HPLC	High Performance Liquid Chromatography
HRMS	High Resolution Mass Spectrometry
hυ	light irradiation
Hz	Hertz
k	kinetic rate constant
***i*Pr**	iso-propyl
IR	InfraRed spectroscopy
LEP	Light Emitting Polymer
LUMO	Lowest Unoccupied Molecular Orbital
m/z	mass to charge ratio
MBSC	Miyaura Borylation/Suzuki Coupling
Me	methyl
NBS	N-bromosuccinamide
NMR	Nuclear Magnetic Resonance
OFET	Organic Field-Effect Transistor
OLED	Organic Light Emitting Diode

ORD	Optical Rotatory Dispersion
ORTEP	Oak Ridge Thermal Ellipsoid Plot Program
PCE	power conversion efficiency
Ph	phenyl
PLQY	photoluminescent quantum yields
PVSC	perovskite solar cells
rac	racemic
RP	reverse phase
rt	room temperature
SEGPHOS	5,5‘-Bis(diphenylphosphino)-4,4‘-bi-1,3-benzodioxole
Sphos	2-Dicyclohexylphosphino-2′,6′-dimethoxybiphenyl
$t_{1/2}$	half life
TADDOL	α,α,α',α'-tetraaryl-2,2-disubstituted 1,3-dioxolane-4,5-dimethanol
$TBAPF_6$	tetrabutylammonium hexafluorophosphate
Th	thiophene
THF	tetrahydrofuran
TLC	Thin Layer Chromatography
TMS	trimethylsilyl
$TS^{\neq}$	transition state

Introduction

Introduction: Helicenes

1. General properties

Polycyclic (hetero)aromatic compounds are a group of molecules characterised by two or more condensed (hetero)aromatic rings that are considered of great interest in several fields.[1,2] In this fascinating class, helicenes have received notable attention owing to their non-planar screw-shaped skeletons formed by a minimum of four *ortho*-fused aromatic or heteroaromatic rings, which form a helically chiral axis, due to geometrical constraints and overlapping of the terminal rings (*Figure 1*).[3,4]

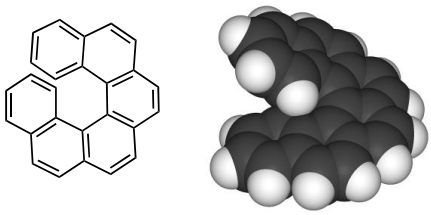

Figure 1: Example of helicene structure.

The definition "helicene" was introduced in 1956,[5] but the first helicenes were synthetised in 1903.[6] The number of aromatic rings in the helical backbone is indicated by the number *n* in backets [*n*] before the helicene name. Helicenes can be divided into two main classes: carbohelicenes, which are composed solely of benzene rings in the backbone, and heterohelicenes that contain at least one heterocycle in the screw skeleton. Heteroatoms generally found in the helical scaffolds are: nitrogen (pyrroles, imidazoles or pyridines), sulphur (thiophenes), oxygen (furans), phosphorus (phospholanes), and silicon (siloles). They are named aza[n]helicenes, thia[n]helicenes, oxa[n]helicenes, phospha[n]helicenes, and sila[n]helicenes, respectively (*Figure 2*).[7,8] Sometimes, these could also be named as [n]heterohelicenes or [n]helicenes for simplicity. Moreover, a prefix of type "di" for 2, "tri" for 3, "tetra" for 4, etcetera, is used to define the number of heterocyclic rings.

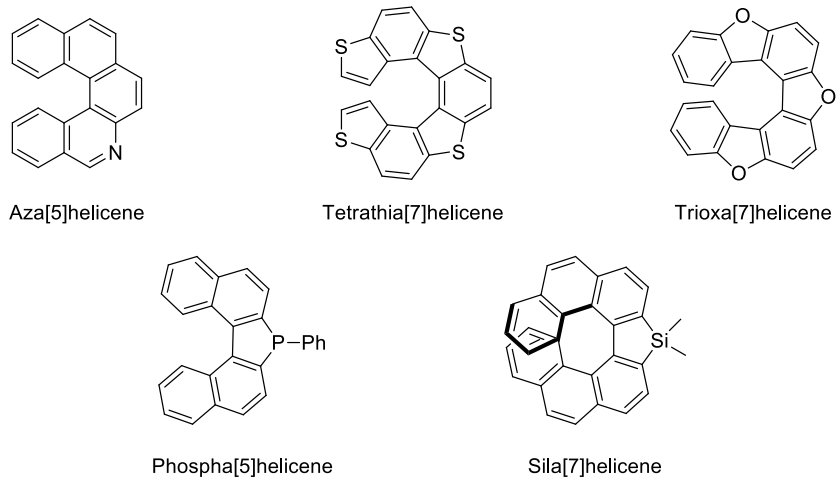

Figure 2: Examples of heterohelicenes.

Besides, helicene must be fully aromatic. In the case of at least one cycle is not aromatic, the correct nomenclature of this helical molecule is "pseudo-helicene" or helicene-like compound and represents the third family of helicenes.

The defining property of a helicene is its helical structure. Because of the steric hindrance of the terminal rings, helicenes have a C_2-symmetric axis, which is perpendicular to the helical axis (*Figure 3, left*). This axis can either wind clockwise or anti-clockwise and for this reason helicenes are chiral even though they have no stereogenic centres.

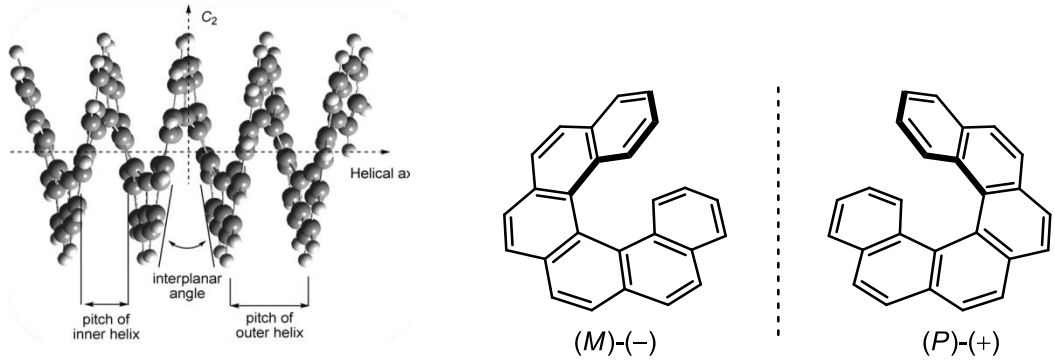

Figure 3: (*M*)- and (*P*)-helicene.

According to the Cahn-Ingold-Prelog rules, a left-handed helix (anti-clockwise) is designated "*minus*" and denoted as the *M* enantiomer, whereas a right-handed helix (clockwise) is designated "*plus*" and denoted as the *P* enantiomer (*Figure 3, right*).[9] Moreover, according to the results of CD and ORD spectroscopy, as a general trend in a homochiral series, the *M* and *P* series of helicenes have a (–) levorotatory and a (+) dextrorotatory specific rotation, respectively.[10]

When there is an increase in the number of fused rings, the helicene spirals up along the helical axis to form a cylindrical structure with a steady pitch in the inner and the outer helixes.[11] In case of helicenes composed of six-member aromatic rings, it takes almost six rings to cover a complete 360 °C rotation of a screw,[12] while in case of helicenes with at least one five-member heterocycles incorporated into the skeleton, more rings are required, because of the smaller in-plane turn (θ) of them that contribute to the helical structure (*Figure 4*).

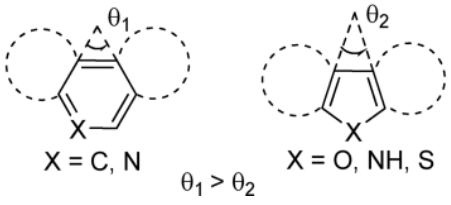

Figure 4: In-plane turn (θ).

1.1 Structural properties

As previously reported, the non-planar structure arises due to the steric repulsion of the terminal rings and therefore the connections between the rings are twisted. The dihedral angles of terminal ring rely on the helicenes' lengths and the substituents present. As shown in *Figure 5*, the dihedral angles of carbohelicenes increase as the elongation of the helicenes increase from [4]helicene (26.7°) to [6]helicene (58.5°), but decreased with further elongation (e.g. for [7]helicene the dihedral angle is 30.7° and for [11]helicene it is only 4.0°).

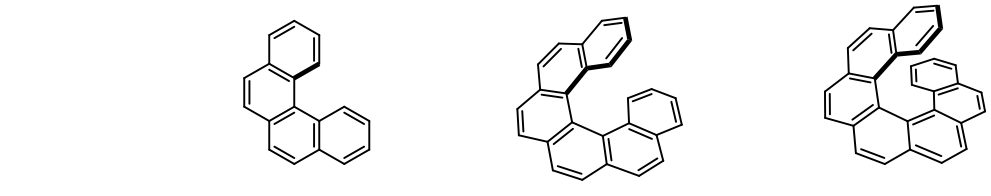

Figure 5: Dihedral angles of model helicenes.

Moreover, the dihedral angles can be also modulated by the number and the nature of substituents on the helical backbone as shown in *Figure 6*, in which the examples suggest that the extent of steric hindrance is Me > MeO > H.

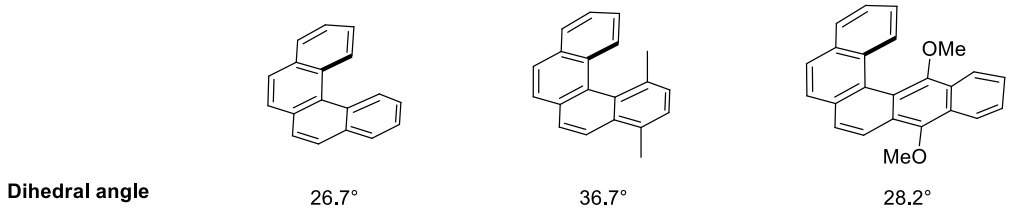

Figure 6: Dihedral angles of model substituted-helicenes.

Furthermore, shielding and deshielding effects in the ^{1}H-NMR spectra of helicenes have demonstrated the overlap of the rings as well as the van der Waals interactions between nearby groups.[13] Because of the torsional strain, there are diverse C−C bond lengths in the skeleton having features of a single bond or a double bond. More in details, the average C−C bond length in inner helix is about 1.430 Å, while on the periphery is only about 1.360 Å[13] (the bond length of benzene is 1.393 Å).[14]

1.2 Racemization barrier of helicenes

Another fascinating property of helicenes is their racemization. Commonly, [6+n]carbohelicenes are considered to have a stable helical axis of chirality. Therefore, [5]helicene racemizes at 22 °C with a $t_{1/2}$ of 1100 min,[15] while [6]helicene has a $t_{1/2}$ of 187 min at 187.6 °C.[16,17] In order to explain the racemization process, two transition states ($TS^{\neq}$) of [5]helicene have been proposed (*Figure 7*).[18]

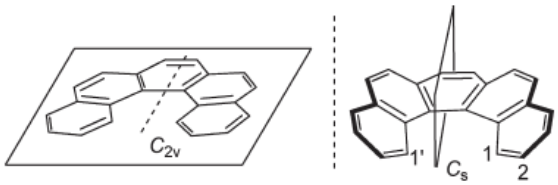

Figure 7: Transition states ($TS^{\neq}$) of [5]helicene.

The $TS^{\neq}$ with C_{2v} symmetry has the rings stretch outward but all the atoms are coplanar (*Figure 7*, left), while in the $TS^{\neq}$, with Cs symmetry, the terminal rings bending to the same side (*Figure 7*, right). In most theoretical calculations, Cs symmetry $TS^{\neq}$ has been adopted. These hint that unsubstituted [5]carbohelicene in the ground state first twists into the non-chiral $TS^{\neq}$ with Cs symmetry, the torsional strain is released by subsequent transformation to (*P*)- or (*M*)-configuration with equal probability and results in racemization. This suggests that the racemization barrier dramatically increases fixing one or both of the terminal rings or incorporating substituents into the internal *bay area* of the helix (*Figure 8*). In a general way, a substituent effect in the *bay area* causes an increase in the energy barrier of racemization, while two substituents are present, such steric effects are even higher. Sometimes, even the electronic effects of different substituents on the backbones may affect the racemization barrier.[19]

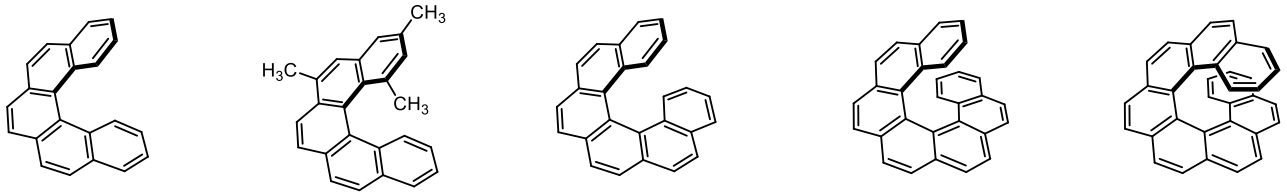

[5]helicene	3,8,10-trimetyl[5]helicene	[6]helicene	[7]helicene	[8]helicene
24.6	38.7	**36.9**	41.7	42.4

Figure 8: Racemization barriers (in kcal/mol) for [5]helicene,[20] 3,8,10-trimethyl[5]helicene,[21] [6]helicene,[22] [7]helicene and [8]helicene.[16]

Again, [6]carbohelicene racemizes *via* a $TS^{\neq}$ with C_{2v} symmetry, whereby the helix simultaneously extends to minimize the peripheral overlap and the last aromatic rings of the helix invert their respective positions. Obviously, longer helicenes undergo racemization via more complicated processes in which more than one $TS^{\neq}$ might be involved. When one or more five-membered aromatic rings are present on the helicene backbone, a higher number of rings is required to have a stable chiral axis, because of the smaller in-plane-turn of five-membered aromatic cycles compared to six-membered rings. For example, the heterohelicenes 5,8-dithia[6]helicene and 3,6,9-trithia[6]helicene have significantly lower barriers to racemization than [6]carbohelicene (*Figure 9*) and are not configurationally stable at room temperature.[23]

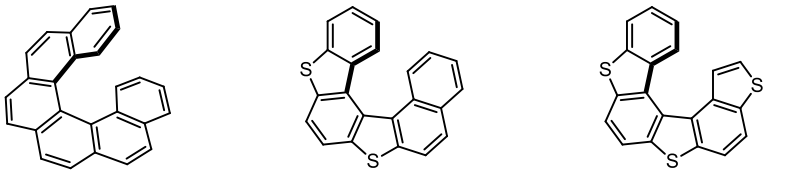

Figure 9: Racemization barriers (in kcal/mol) for [6]helicene, 5,8-dithia[6]helicene and 3,6,9-trithia[6]helicene.

1.3 Photophysical properties

The π-interactions of their polyaromatic system and the resulting absorbance and emission spectra are a further interesting property of helicenes. The electronic delocalization is enables throughout the helical structure, although the extent of π-conjugation is not as good as other planar polyaromatic systems, because of slight loss of aromatic character owing to the helical axis.[24] However, the HOMO-LUMO gap of isomeric [6+*n*]helicenes are smaller than phanacenes, due to π-π overlap across the helical pitches and this value decreases inversely proportional to *n*.[25] Other methods to decrease the HOMO-LUMO gap include: the incorporation of furan and thiophene sub-units,[26] the incorporation of push-pull elements,[27] the annulation of additional rings onto the structure[28] or of an anti-aromatic subunit[29] (*Figure 10*).

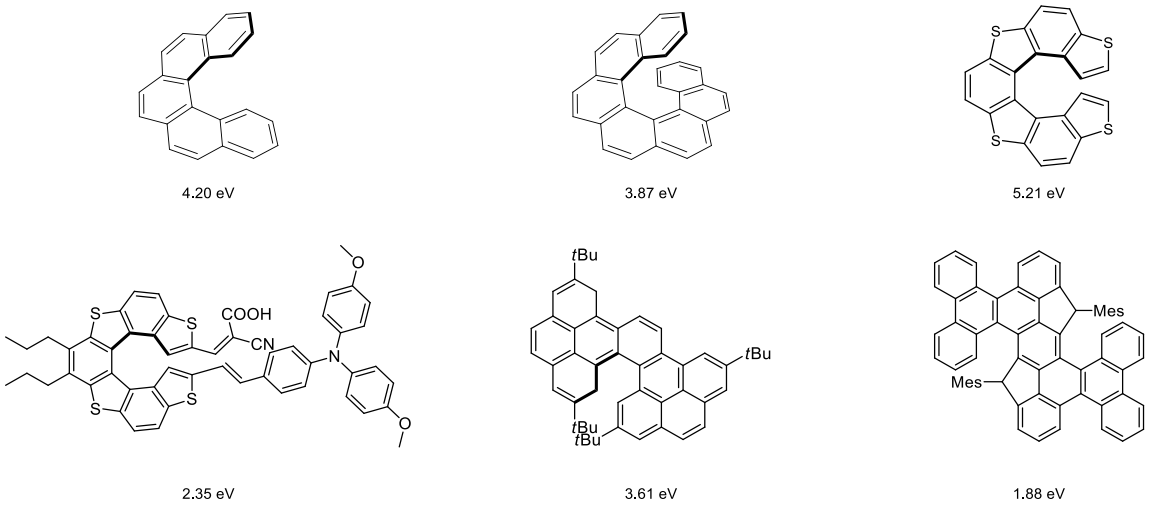

Figure 10: HOMO-LUMO gaps for some model helicenes.

Helicenes are also fluorescent molecules, although the quantum yield (Φ_F) can be quite low because of non-emissive quenching events decreasing the efficiency of fluorescence. Nevertheless, this can be increased by properly functionalisation of the helicene skeleton (*Figure 11*)[30] or introduction of heteroaromatic rings into the backbone.[31,32]

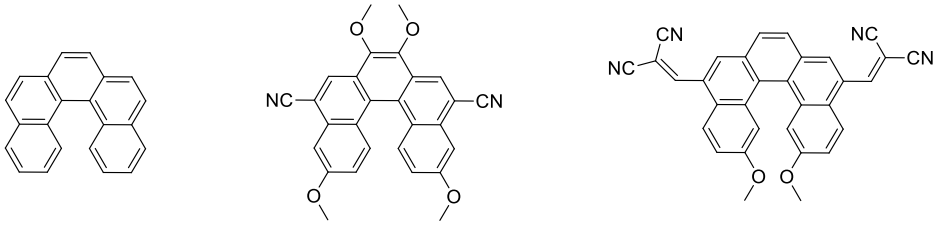

Φ_f= 4% Φ_f= 15% Φ_f= 23%

Figure 11: Quantum yield (Φ_F) of model helicenes.

Furthermore, helicenes with twisted extended π-conjugated molecular structure could exhibit excellent CPL properties[33] and this is highly interesting. Indeed, CPL materials have attracted wide attention in last decade for their great applications in several fields.

In the following sections, the most common strategies to synthetise carbo- and heterohelicenes also in enantiopure way are described.[3,34-36,]

2. Synthesis of helicenes

2.1 Transition metal-free synthesis

2.1.a Photocyclisation

In 1967, Martin[37] reported the first photochemical strategy for the synthesis of [7]helicene (*Scheme 1*).

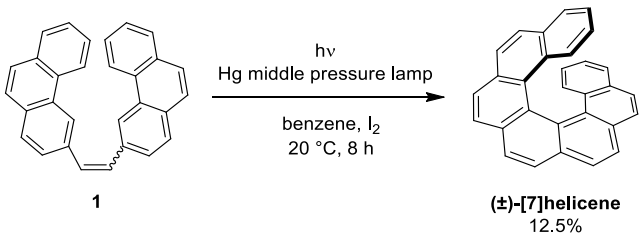

Scheme 1: First photochemical strategy for the synthesis of [7]helicene.

After this work, the photocyclisation has become one of the most popular method for the preparation of many carbo- and heterohelicenes due to the easy preparation of stilbene-type precursors.[3,38] Afterwards, later optimisations of Martin and Katz led to improved yields and regioselectivities.[4] In particular, Katz[39] optimised the photochemical cyclisation using excess propylene oxide and a stoichiometric amount of iodine under inert atmosphere. These conditions not only increase the yields compared to previous procedures but also prevents photo-oxidative or photo-reduction side reactions of the double bonds. Drawbacks of photocyclisation are the high purity of solvents and the extremely high dilutions necessary to avoid the dimerization reactions, which limits large-scale preparation. Next, this reaction requires specific photochemical equipment. Additionally, it lacks tolerance to some functional groups as NH_2 and NO_2 that prevent cyclisation. Moreover, no general enantioselective procedure for these reactions currently exists.[35]

Nevertheless, it is still a convenient procedure for the preparation of a plethora of helicenes because of the easy synthesis of a stilbene-type precursors and mild reaction conditions.[40]

2.1.b Diels-Alder Reactions

In 1990, Katz[41] described the first synthesis of helicenes *via* a Diels-Alder reaction (selected example, *Scheme 2*).

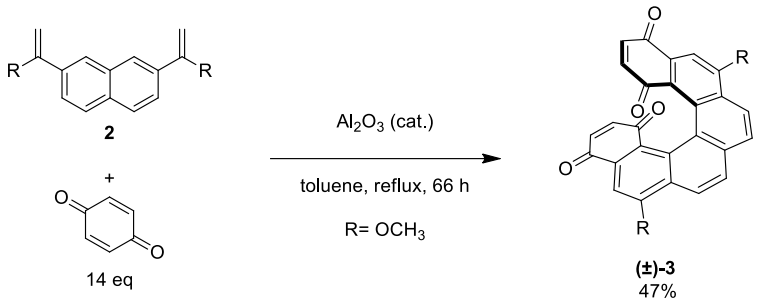

Scheme 2: First synthesis of helicenes *via* a Diels-Alder reaction.

This reaction is an effective method to prepare helical frameworks owing to its moderate to good yields and its ability to be used in large-scale synthesis. Furthermore, the yields and rates of the reaction could be improved by adding electron-donating substituents to the diene molecules. Besides, the functional groups can modify the electronic properties of the helicenes and improve the solubility and optical resolution. Although, the yields are in many cases not as good as other procedures, this strategy enabled rapid access to gram quantities of helicenes and accelerated further study of these molecules.

2.1.c Friedel-Crafts reactions

Newman[5,42] described the first synthesis of [6]helicenes using a Friedel-Crafts/dehydration sequence (*Scheme 3a*). Moreover, the resolution could be obtained by repeated crystallization with TAPA (2-(2,4,5,7-tetranitro-9-fluorenylideneaminooxy)propionic acid). Although low yield was achieved, this was highly innovative for its time and confirmed the helical chirality of [6]helicene (*Scheme 3b*).

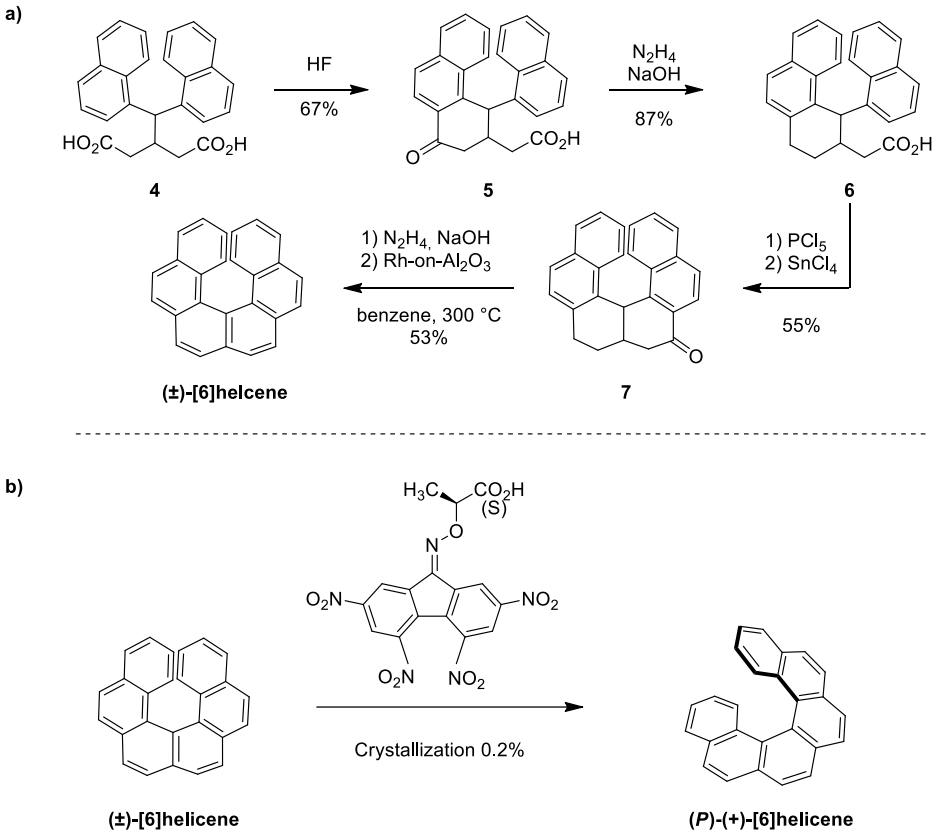

Scheme 3: a) First synthesis of [6]helicenes using a Friedel-Crafts/dehydration sequence. b) Resolution of [6]helicene.

2.2 Transition metal-mediated synthesis

Several transition metal-mediated syntheses have been described for the preparation of helicenes. Among them, Pd-catalysed coupling reaction has a great importance.[43-46] For example, a double Stille reaction was used for the synthesis of one of the first laterally extended [5]helicenes (*Scheme 4*).[44]

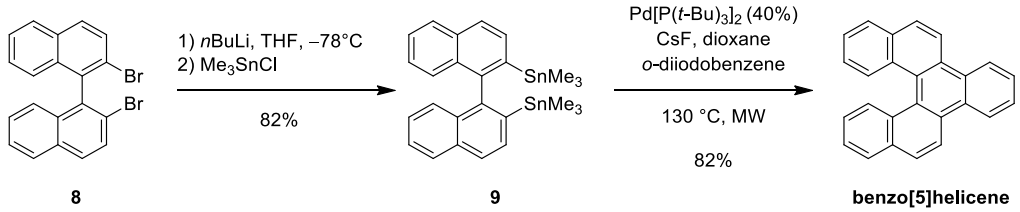

Scheme 4: Synthesis of one of the first laterally extended [5]helicenes.

2.2.a Ring-Closing Metathesis (RCM)

In 2006, Collins[47] reported the first synthesis of helicenes by ring-closing metathesis (*Scheme 5*).

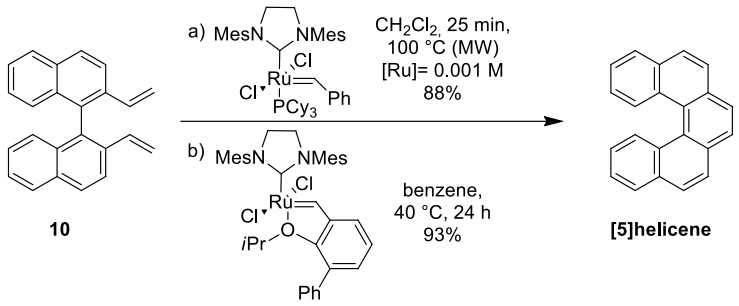

Scheme 5: First synthesis of helicenes by ring-closing metathesis.

As shown in *Scheme 5*, two different routes were developed. The first one is very fast, but requires high temperatures, that can result in pyrolysis. The second one demands mild conditions, but it requires a longer time. Thus, this method is a facile way to efficiently synthetise substituted [5]-, [6]- and [7]helicenes with good tolerance towards different functional groups.

2.2.b Metal-catalysed [2 + 2 + 2] cyclisations

Stará and Starý developed a largely successful and wide-ranging strategy for the synthesis of helicenes, based on the Co(I) or Ni(0) catalysed intramolecular [2+2+2] cycloisomerisation.[48,49] At the beginning, this procedure allowed the preparation of several partially saturated [5]-, [6]- and [7]- aza-, oxa- and carbohelicenes in good yields and later a variety of *O*-, *N*-, *S*-, and *P*-functionalised helicenes. This work was then extended to use preferentially Ni(0), which was generally more reactive (*Scheme 6*).[50]

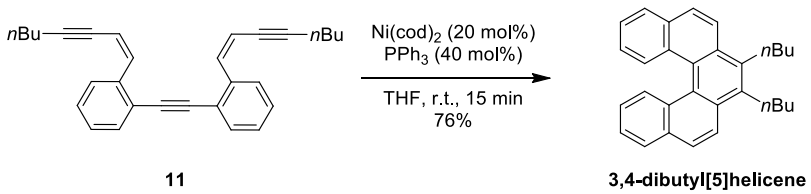

Scheme 6: Ni(0) catalysed intramolecular [2+2+2] cycloisomerisation.

This strategy is very interesting because it allows to prepared several carbo- and heterohelicenes in good yield and high efficiency because of the 100% atom economy and the short reaction time.[51,52]

Variants of this methodology could be also promoted by other transition metal. In 2004, Scott and Donovan[53] developed a procedure using Ru(II)-catalysts, while Tilley[54] exploited Ir(I)-catalysts in 2017. Furthermore, Fürstner[55] performed a π-acid-catalysed cycloisomerisation using Pt(II)-catalyst (*Scheme 7*).

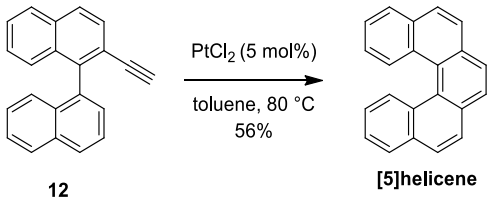

Scheme 7: A π-acid-catalysed cycloisomerisation using Pt(II)-catalyst.

Nowadays, π-acid-catalysed cycloisomerisation became a suitable and valuable method to prepare diverse carbo- and heterohelicenes.[31,56-59]

2.3 Construction of 5-member rings

Helicenes prepared by constructing *ortho*-fused hetero five-membered rings have been less utilised, because of the limited transformations exploitable for cyclisation.

2.3.a Furan rings

Most of the strategies to construct furan rings start from diverse functionalised BINOLs. In 1973, Högberg[60] proposed the first synthesis of oxahelicene forming the furan rings. Afterwards, further modifications of this methodology have been reported in order to simplify and optimise the synthesis of this class of heterohelicenes (a selected example[61] in *Scheme 8*).

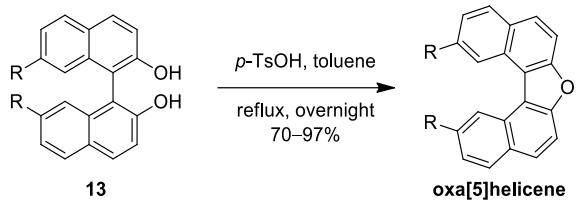

Scheme 8: Synthesis of oxa[5]helicene through the formation of the furan ring.

2.3.b Thiophene rings

As furan rings, also the construction of thiophenes can be performed starting from BINOL derivatives (*Scheme 9*).[62]

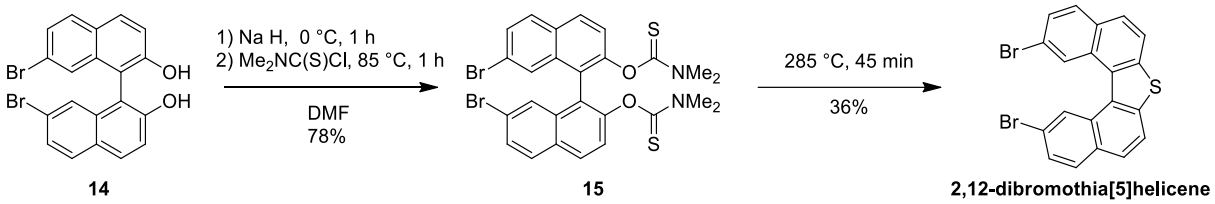

Scheme 9: Construction of thiophene ring starting from BINOL derivative **14**.

Moreover, a lot of different strategies were developed in last decades to form this hetero-ring.[63-67] Recently, Xu and co-workers proposed a cyclisation under $PdCl_2$/DMSO catalytic system, in which $PdCl_2$ is the sole metal catalyst and DMSO acts as oxidant and solvent (*Scheme 10*).[68]

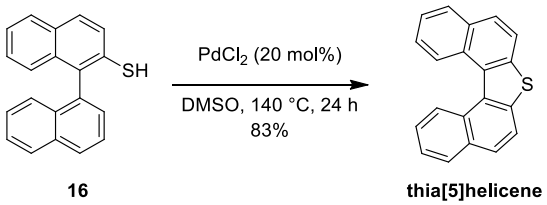

Scheme 10: Synthesis of thia[5]helicene.

2.3.c Silole rings

In 2001, Kurita[69] reported a smoothly way to prepare sila[5]helicenes starting from a properly functionalised BINOL **8** (*Scheme 11*).

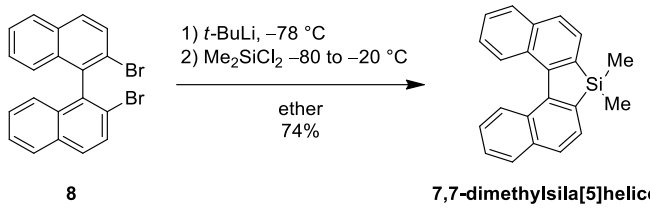

Scheme 11: Synthesis of sila[5]helicenes starting from BINOL dibromide **8**.

Recently, Takay[70] proposed an efficient synthesis of sila[n]helicenes through *via* dehydrogenative silylation of C−H bonds using rhodium catalyst with (*R*)-(*S*)-BPPFA ([R,R]-1-[1-dimethylaminoethyl]-1′,2-bis[diphenylphosphino]ferrocene) ligand (*Scheme 12*).

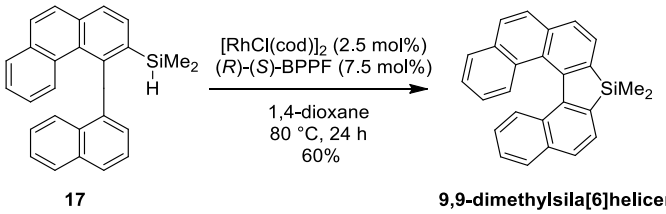

Scheme 12: Sila[n]helicenes through via dehydrogenative silylation.

2.3.d Phosphole rings

The first example of synthesis of phosphahelicenes through the final construction of phosphole rings was developed in 1993 by De Lucchi (*Scheme 13*),[71] but variants of this strategy have been used also recently.[72]

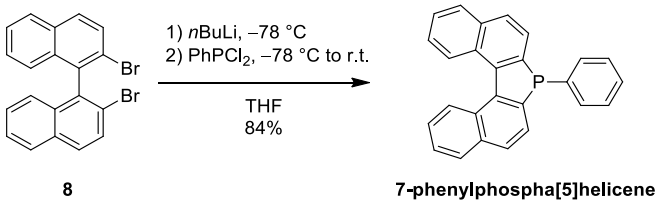

Scheme 13: Synthesis of phospha[5]helicene.

Lately, Tanaka[73] disclosed a rhodium-mediated enantioselective synthesis of phosphahelicenes with the building of final hetero-cycles as crucial step.

2.3.e Imidazole, pyrrole and pyridine rings

Few approaches have been reported in literature for the incorporation of an imidazole ring in the helical backbone. In 1990, Leonard[74] performed the synthesis of helicene **18** by an oxidative ring closure in presence of iodobenzene diacetilene starting from the diarylamine **19** (*Scheme 14*).

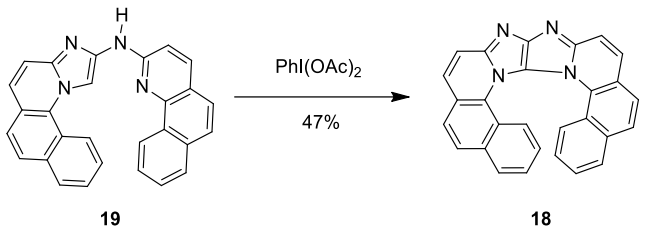

Scheme 14: Synthesis of azahelicene **18** containing imidazole rings.

Regarding pyrrole rings, Meghsoodlou[75] developed a convenient method for the preparation of [5]helicenes with two pyrrole units **20** treating phenanthroline derivatives **21** with acetylenic esters in MeOH (*Scheme 15*).

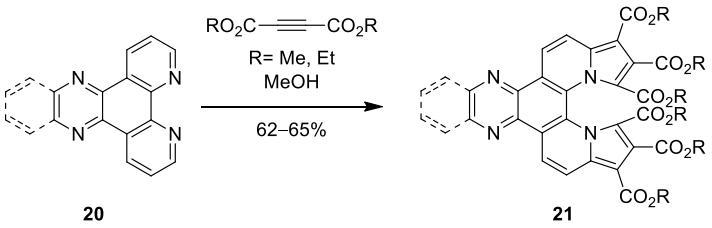

Scheme 15: Synthesis of azahelicene with pyrrole rings.

Concerning the construction of pyridine rings, Stará[76] reported the synthesis of benzo fused aza[6]helicenes **23** exploiting the versatility of [2+2+2] alkyne cycloisomerisation mediated by Co(I) and Ni (0)-catalysts (*Scheme 16*).

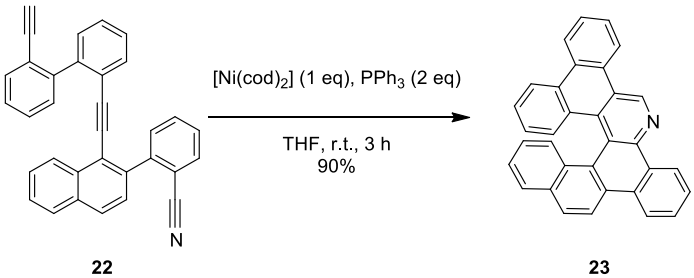

Scheme 16: Synthesis of azahelicene with pyridine rings.

3. Enantioselective synthesis of helicenes

3.1 Asymmetric Diels-Alder

In 1999, Urbano[77] reported a diastereoselective Diels-Alder reaction for the synthesis of helicene (*M*)-**25** using a chiral auxiliary of quinone (*S*)-**24** (*Scheme 17*).

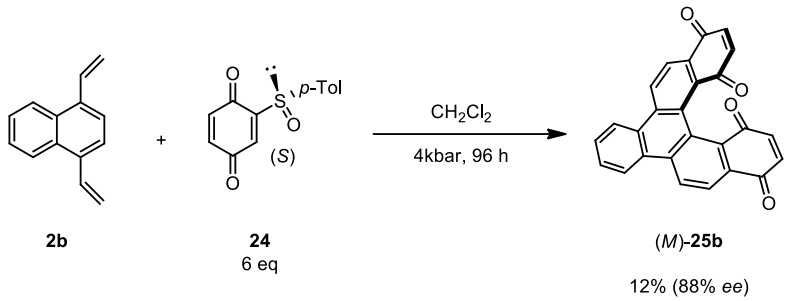

Scheme 17: Diastereoselective Diels-Alder reaction for the synthesis of (*M*)-**25b**.

The helicenes were obtained in up to 88% *ee* but the yields were low, because of the high pressures required. Moreover, another disadvantage is the excess of chiral auxiliary that are needed. Afterwards, another route with milder conditions was performed using activated dienes. As shown in *Scheme 18*,[78] the use of activated dienes **26** significantly improves the yields of helicenes **27** in good to excellent *ee*.

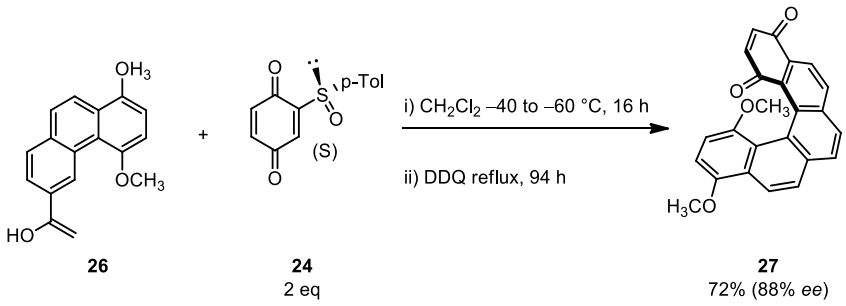

Scheme 18: Diastereoselective Diels-Alder reaction for the synthesis of helicene **27**.

3.2 Metal-catalysed asymmetric synthesis

3.2.a Asymmetric catalytic ring closing olefin metathesis

As previously reported in the *Section 2.2.a*, Collins[47] investigated the use of ring closing alkene metathesis for the synthesis of a variety of functionalised racemic carbohelicenes. An enantioselective variant with chiral carbine-derived catalyst allowed to form [7]helicene from the racemic precursor **28** via a kinetic resolution.[79] After a deep screening of the experimental conditions, the [7]helicene was obtained in 80% *ee* and 38% conversion using hexafluorobenzene as solvent and vinylcyclohexane as additive (*Scheme 19*).

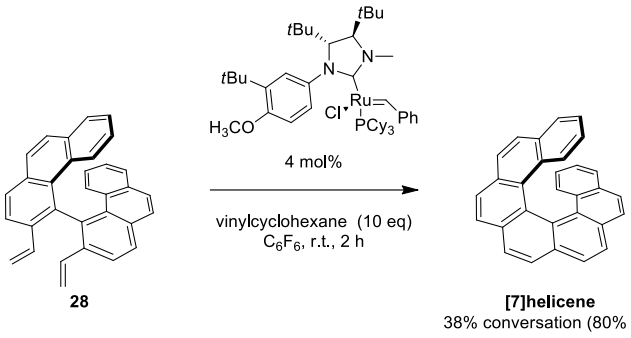

Scheme 19: Asymmetric catalytic ring closing olefin metathesis.

3.2.b Asymmetric metal-catalysed [2 + 2 + 2] cyclisations

Enantioselective [2+2+2] cycloisomerisation is an effective strategy to prepare a wide range of enantioenriched helicenes. Nickel-base catalysts are largely used, as they are commonly more reactive and do not require high temperatures.[80] Recently, Stará[81] reported the enantioselective synthesis of a laterally extended [6]carbohelicene **29** using oxahelicene NHC ligands **31** (*Scheme 20*), which were, in turn, themselves obtained through a diastereoselective [2+2+2] cyclisation.

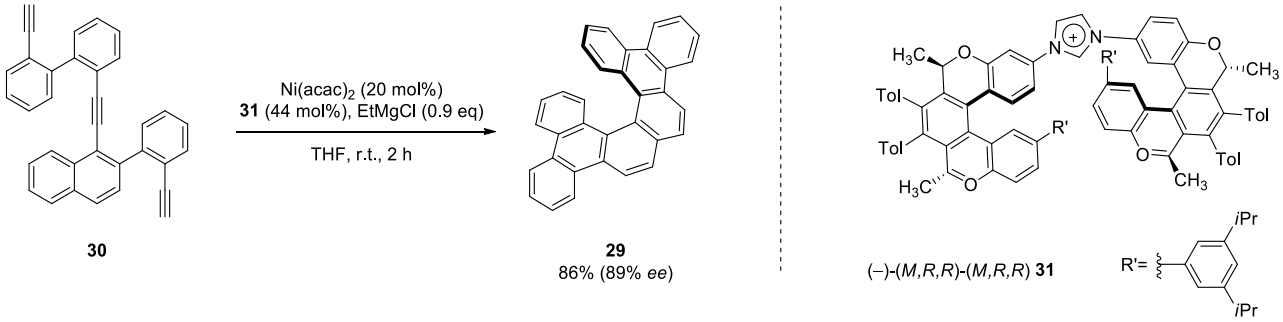

Scheme 20: Ni-catalysed asymmetric metal-catalysed [2 + 2 + 2] cyclisation.

Besides, Tanaka described Rh(I)-based complexes as suitable catalysts in order to synthetise not only carbohelicenes,[82,83] but also heterohelicenes such as silahelicenes[84] (*Scheme 21*) and phosphahelicenes. [73,85]

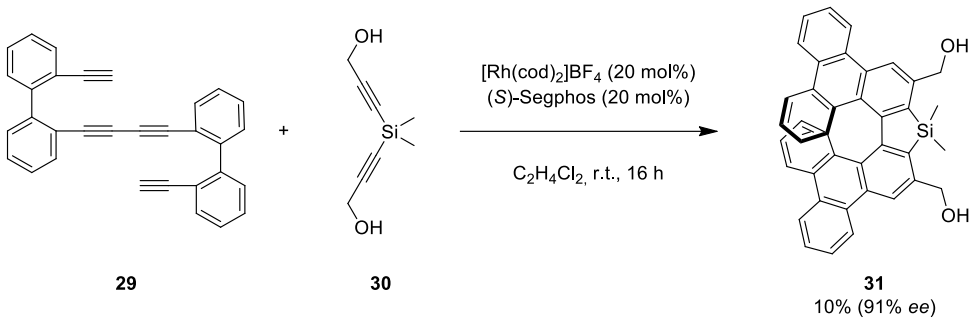

Scheme 21: Rh-catalysed asymmetric metal-catalysed [2 + 2 + 2] cyclisations.

However, transition-metal-catalysed [2 + 2 + 2] cycloisomerisation of π-electron systems is a robust, general and practical method for the synthesis of a plethora of helicene molecules not only in racemic mixture, but also in enantio-/diastereo-selective way.[51]

3.2.c π-acid-catalysed cycloisomerisation

As previously reported, π-acid-catalysed cycloisomerisation is another effective strategy to prepare helicenes.[55] Diverse asymmetric variants of this procedure have been attempted by Tanaka and co-workers (*Scheme 22*).[86]

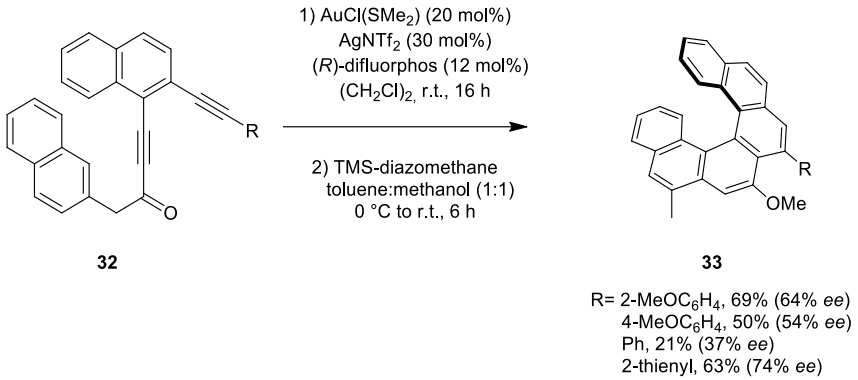

Scheme 22: π-acid-catalysed cycloisomerisation.

The reaction proceeds by a tandem gold-catalysed hydroarylation/carbocyclisation of **32** and a subsequent methylation. The [6]carbohelicenes **33** were prepared in moderate to good yield, with *ee* values between 37 and 74%. This strategy was also used to prepare [6]-[87] and [10]-[88] azahelicenes, which were obtained with interesting *ee* values, although yields remained low and catalyst loadings were still high.

Recently, enantioselective π-acid-catalysed cycloisomerisation of helicenes promoted by gold-catalysts has been widely studied[89] especially by the group of Alcarazo.[90-93] Further explanations of their work are reported in *Chapter 4.*

3.3 Optical resolution

Most of the asymmetric syntheses so far reported for the synthesis of enantioenriched helicenes have not satisfactory optical purity, which is the necessary property to investigate and utilize these fascinating molecules. To date, the most practical way to obtain optically pure helicenes is the optical resolution.[35] Since the first reported example,[94] diverse approaches have been discovered whereby crystal picking and recrystallization,[95,96] resolution by HPLC,[97,98] the use of chiral auxiliaries[99,100] and enzymes.[101]

4. Applications of helicenes

Helicenes show a unique combination of large aromatic π-system and exceptionally strong chiral transfer, which confers those interesting electronic and optical properties as well as the capability to form complexes

with transition metals[102,103] and influence the formation of higher order structure. Thus, helicenes find manifold applications in several fields and some of them are described in this section to highlight the research areas where these fascinating compounds have attracted interest.

4.1 Chiral recognition

In 1985, Martin[104] demonstrated the high efficiency of helical compounds in stereocontrol phenomena related to chiral induction (a selected example in *Scheme 23*).

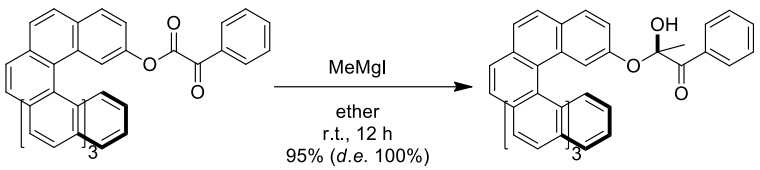

Scheme 23: Selected example of chiral recognition.

As shown in the previous scheme,[105] the (±)-[7]helicene **34** undergoes addition of Grignard reagents with excellent yield and complete diastereoselectivity. Moreover, the authors firstly reported the use of an enantioenriched carbohelicene to induce asymmetry in organic syntheses.[105] Afterwards, the capability of helicenes to transfer chirality to other molecules has also explored in the field of chiral recognition, where helicenes have been exploited in the sensing of single chiral molecules.[34,36] For instance, Reetz[106] reported the use of 2,15-dihydroxy-[6]helicene ([6]-HELIXOL) as fluorescent sensor for chiral aminoalcohols and amines. More recently, Qui[107] developed a tri-helicene organic cage (*Figure 12*), in which the cavity inside the cage can discriminate enantiomers of racemic mixtures of chiral alcohols and amines, incorporating one enantiomer as a guest molecule, that could be later extracted, and the enantiomeric excesses are excellent.

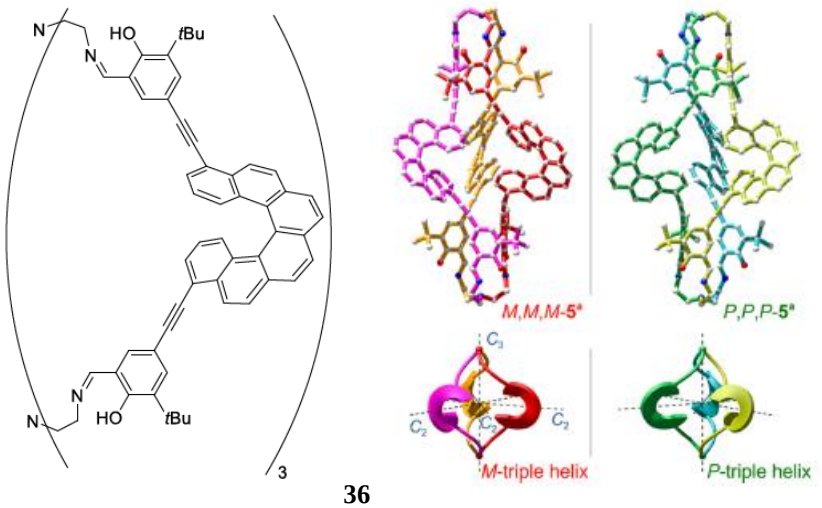

36

Figure 12: Tri-helicene **36** (left), its crystal structure (top) and representation of triple helix geometry (bottom) on the right. Figure taken from: *J. Am. Chem. Soc*. **2018**, *140*, 2769.[107]

4.2 Asymmetric catalysis

One application of helicenes is in the field of asymmetric catalysis.[34,102,108] Compounds bearing helical chirality were used as ligand in asymmetric catalysis only after 1997, while many different chiral ligands and catalyst have been developed so far. Probably, it was due to the difficulties in the preparation of large amount of them. Nowadays, thanks to the development of new methodologies for their diastereoselective or enantioselective synthesis,[3,34,35] among with the possibility to separate racemic helicenes by chiral HPLC,[97,98,109] their use in catalysis is growing significantly. One advantage is the high configurational stability of helicenes, because reactions at higher temperatures might be possible without the racemization of ligands.

Soai[8,110] reported the use of [6]helicene and 7,8-diisopropyltetrathia[7]helicene (7-TH2C$_3$) as chiral additives for the autocatalytic reaction between dialkylzinc and pyrimidyl aldehyde with very good results (*Scheme 24*).

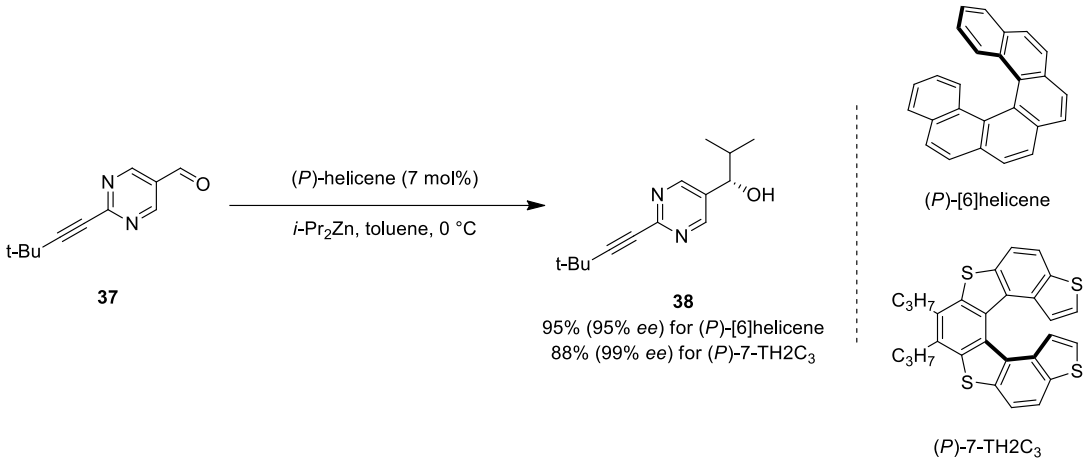

Scheme 24: Selective example of chiral additives.

Recently, Marinetti and co-workers published a series of examples of phosphahelicene-based catalysts that were used as organocatalyst in [3+2]cyclisation of allenes and electron-poor olefines.[111] Moreover, phosphahelicene-based catalysts found application also as efficient ligands in enantioselective Au(I) catalysis[112,113,114] (*Scheme 25*).

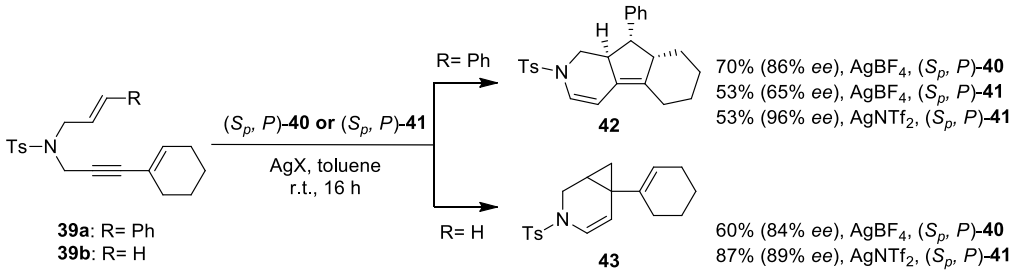

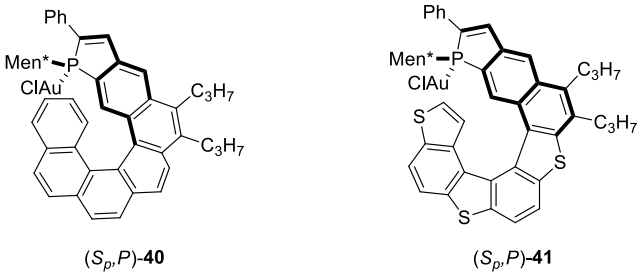

(S_p,*P*)-**40** (S_p,*P*)-**41**

Scheme 25: Cycloisomerisation of enynes **39**.[113,114]

In general, diverse phospha-helicenes or helicenes with a P-functionalisation have been recently studied and attracted attention, because their significant contribution in this field.[115] Newly, Storch[116] designed a palladium complex with a P-functionalised helicene as ligand (*Figure 13*) for homogeneous catalysis, while for asymmetric catalysis the optimisation of structure and conditions are currently under progress.

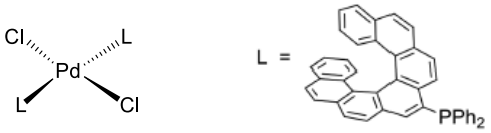

Figure 13: Palladium complex with a P-functionalised helicene as ligand.

4.3 Nonlinear optics and optoelectronic materials

The fascinating polyaromatic system of helicenes caught attention towards their possible applications in nonlinear optics and optoelectronic materials. Optical devices with a direct emission of circularly polarized light have been considered more useful in terms of compactness, energy efficiency and cost. In 2013, Fuchter[117] explored this concept through doping a light emitting polymer (LEP) with either the enantiopure [7]carbohelicene or 1-aza[6]helicene and investigating the influence on the structure and the emissive properties (*Figure 14*).

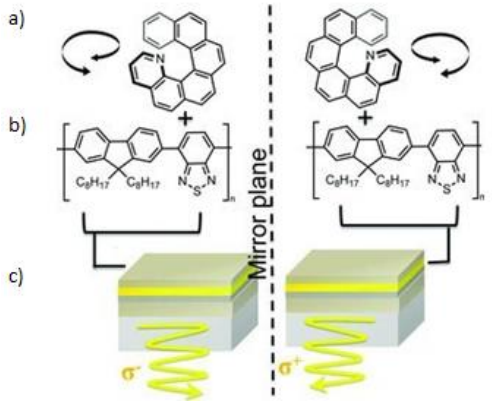

Figure 14. a) 1-aza[6]helicenes doped into the circularly polarized light emitting device; b) light emitting polymer used in the study; c) schematic of circularly polarized light emitting device.
Figure taken from *Adv. Mater*. **2013**, *25*, 2624.[117]

These studies exhibited that devices doped with the enantiopure helicenes emitted strongly circularly polarized light and showed a strong brightness, indicating that helicenes had a significant influence on the higher order structure of the material. The advantage of this method is that helicenes could be potentially doped into a variety of established PLED and OLED materials across the full visual spectrum. Moreover, bespoke chiral polymer synthesis is not required. Besides, the same authors demonstrated a circularly polarised light-detecting organic field-effect transistor (OFET) based on enantiopure (*M*)- or (*P*)-1-aza[6]helicene as the active element of a semiconducting thin film[118] and, more recently, they also described remarkable differences in hole mobility measured in OFETs constructed from either racemic or enantiopure 1-aza[6]-helicene in a thin film.[119] Furthermore, they studied the promising chiral emission within CP-OLEDs developed using a single-handed aza[6]helicene additive, without the need for an alignment layer,[120] thus demonstrating that high-dissymmetry CP emission in CP-PLED is not originated only from the propagation of light through a thick chiral medium, but also by the interplay of other effects.

Starting from the first reported example in 1998,[121] also Langmuir-Blodgett films bearing enantiopure helicene units have attracted a lot of attention[122-124] because of the amplification of chiroptical properties of helicenes through aggregation and the strong second order non-linear optical response of the aggregates, which is a direct consequence of the supramolecular chirality of the system. For this reasons, simple access to Langmuir-Blodgett films is required. In this context, Stará and Starý[124] recently reported a preliminary study on self-assembly of amphiphilic helicenes at the air-water interface (selected example, *Figure 15*).

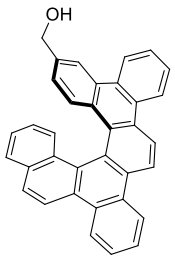

44

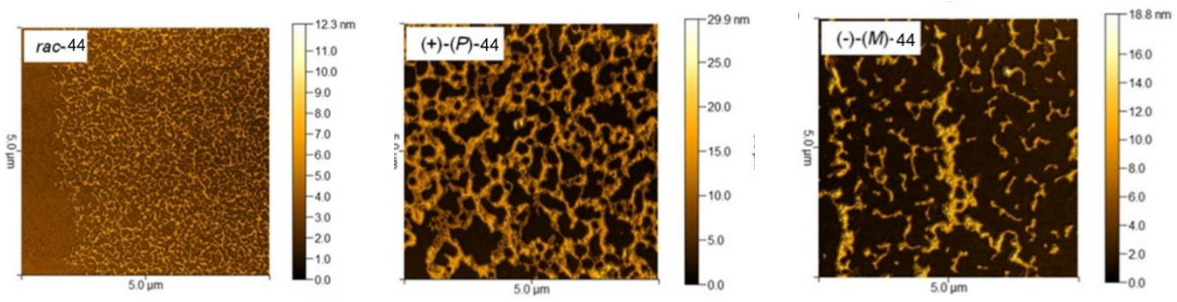

Figure 15: AFM tapping-mode images of the Langmuir layers of racemic and enantiopure helicene **44** transferred on the vertically oriented silicon chips at a constant surface pressure.
Figure taken from *Chem. Eur. J.* **2019**, *25*, 11494.[124]

Another stimulating application of helicenes is in perovskite solar cells (PVSCs). Organic-inorganic hybrid perovskites have great potential in multifunctional optoelectronic devices because of their properties,[125,126] for instance broad and tunable light-harvesting range, low excitation binding energy and good ambipolar

charge-transporting capability. Moreover, these compounds show promising advantage of low-cost fabrication and massive production thanks to the facile solution processability similar to the organic semiconductors. In 2019, Wu and Chueh[127] investigated the use of a series of [7]helicene as hole-extraction/transporting layer in PVSCs (*Figure 16*).

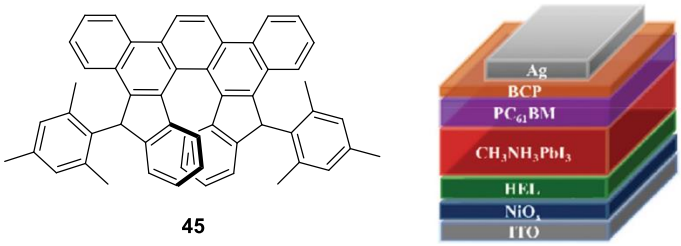

Figure 16: Selected example (on the left) and the schematic structure of the studied PVSC.

The obtained helicenes-modified PVSCs could deliver PCEs (power conversion efficiency) of over 18% and the maximum could reach 19%. These results demonstrated that helicenes could be a suitable class for realizing high-performance PVSCs.

More recently, Wang[128] presented the construction of D-π-D molecular semiconductors for PVSCs containing helicene **46a** or planar π-linker **46b**, in order to compare the materials and evaluate the possible advantage to use helical structures in place of planar compounds (*Figure 17*).

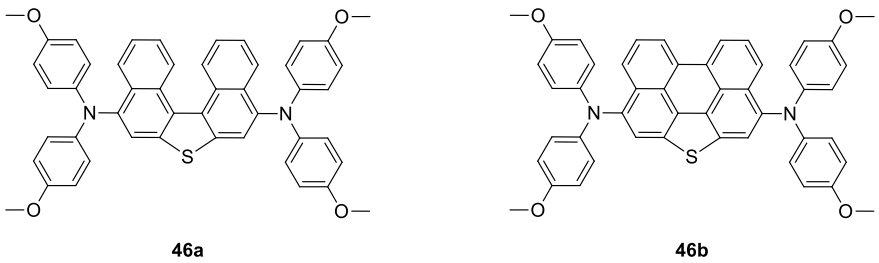

Figure 17: D-π-D molecular semiconductors for PVSCs containing helicene **46a** or planar π-linker **46b**.

They demonstrated that the simple D–π–D type molecular semiconductor with **45** can be used to fabricated more efficient PVSCs compared to the one containing **46**. Indeed, the first one had higher hole-mobility than the other. Moreover, photoluminescence measurements suggested that it can efficiently extract holes from photoexcited perovskite film.

There are several other optoelectronic applications of helicenes such as organic light-emitting diodes (OLEDs),[129,130] organic semi-conductors,[131,132] dye sensitised solar cells (DSSCs),[133,134,27] organic spin filters[135] chiroptical switches,[136,137] as well as biological imaging agents[138] to name a few.[139]

5. Aims of this PhD thesis

This Ph.D. thesis aims to develop innovative and versatile syntheses of heterohelicenes, especially thiahelicene derivatives, also in enantiopure form. Besides this main object, the synthesis of functionalised benzo[1,2-*b*:4,3-*b*']dithiophenes (BDTs) in more eco-friendly reaction media, such as Deep Eutectic Solvents (DESs) has also been carried out. On the other hand, BDTs represent key intermediates for the synthesis of the thiahelicene derivatives set up in this thesis, as well as they found several applications as functional organic materials to use in electronic devices.

More in detail, the main goals of the present thesis can be divided into:

i. The study of methodologies for the synthesis of functionalised tetrathia[7]helicenes (7-THs)

ii. The synthesis of diverse classes of thiahelicenes through the methodologies set up for the preparation of 7-THs.

iii. The study of the stereochemical and chiroptical properties of atropisomeric bis(benzodithiophene) intermediates.

iv. The synthesis of enantioenriched 7-TH derivatives through cycloisomerisations promoted by chiral Au(I)-catalysts.

v. The enantioselective synthesis of thia[5]helicenes via double chiral Au-catalysed alkyne hydroarylation.

vi. The functionalisation of benzo[1,2-*b*:4,3-*b*']dithiophenes (BDTs) by Suzuki reaction in *Deep Eutectic Solvents* (*DESs*).

For the sake of clarity, the results concerning the topics covered in this PhD thesis have been organized in six chapters.

Chapter 1 deals with the development of novel and versatile routes to prepare differently functionalised 7-TH derivatives through transition metal-catalysed annulation reactions of bis(benzodithiophene) intermediates as key steps.

In *Chapter 2*, the synthetic approach discussed in *Chapter 1* has been successfully applied for the synthesis of a novel class of thia[6]helicenes.

Chapter 3 deals with the systematic study of the stereochemical and chiroptical properties of the atropisomeric bis(benzodithiophene) intermediates by means of experimental techniques, including variable-temperature chiral HPLC, ECD and VCD spectroscopy, in combination with theoretical calculations. A preliminary investigation on the CPL properties of these atropisomers has also been reported.

A first study on the synthesis of enantioenriched 7-monosubstituted 7-THs through cycloisomerisation reactions promoted by chiral Au(I)-catalysts has been described in *Chapter 4*, while the enantioselective synthesis of a novel class of thia[5]helicenes by a double chiral Au(I)-catalysed intramolecular hydroarylation has been thoroughly discussed in *Chapter 5*.

Finally, the synthesis of 2,7-disubstituted BDT derivatives by Suzuki-Miyaura reaction in *DES* along with their photophysical and electrochemical characterization have been discussed in *Chapter 6*.

Chapter 1

Diversified syntheses of tetrathia[7]helicenes by metal-catalysed cross coupling reactions

This chapter describes the design and the development of novel versatile syntheses of tetrathia[7]helicenes (7-THs) that make use of metal-catalysed cross coupling reactions as key steps. X-ray analysis of an intermediate obtained from these protocols was performed in collaboration with Prof. Claudia Graiff (Università di Parma).

1.1 Tetrathia[7]helicenes: general concepts and synthetic strategies

Tetrathia[7]helicenes (7-THs, *Figure 18*) are a fascinating class of thiahelicenes, in which four thiophene rings are fused to three alternating arene rings.[140]

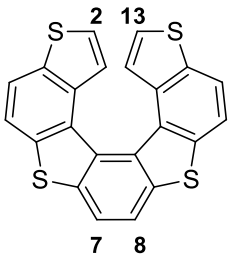

Figure 18: Structure of 7-TH scaffold.

7-THs have an extended conjugated π-system and their helix is configurationally stable with an intrinsic asymmetry, which can be separated into *M* and *P* enantiomers. Moreover, these systems can be easily functionalised in α-positions of the two terminal thiophene rings, allowing the modulation of physical and chemical properties by changing the substituents.[141] Furthermore, the introduction of diverse substituents with different steric hindrance in C2 and C13 positions can tune the distance between the two terminal thiophene rings, resulting in considerable variations in the dihedral angle of the molecule. Thanks to the possibility of combining the electronic properties of oligothiophenes with the unique chiroptical features of helical shaped molecules, these systems have stimulated manifold studies in optoeletronics, [27,142] catalysis,[143-145] sensors[146] and biology,[147-149] to name a few.

Regarding the synthesis of 7-TH backbone, two main approaches have been reported in literature: *i*) the formation of the C-C bond between the β-positions of the thiophene rings (*Figure 19,* **a**); *ii*) the annulation of 3,3'-bis(benzo[1,2-*b*:4,3-*b*']dithiophene) derivatives (*Figure 19,* **b**).

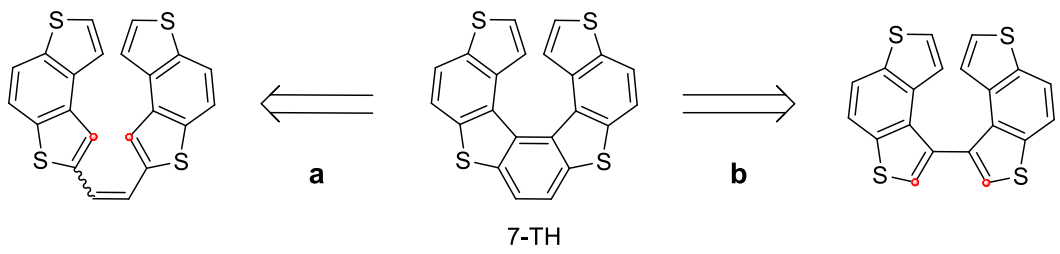

Figure 19: Approaches for the synthesis of the 7-TH scaffold.

Concerning the pathway **a**, this is the most common method to prepare carbo- and heterohelicenes, which involves a photocyclisation of the corresponding stilbene-like precursors as key step, and it is the most popular route to prepare 7-TH systems. For example, alkenes **47** can be converted into the corresponding 7-THs in a range of 60–70% yields by an oxidative photocyclisation using a medium pressure Hg lamp in diluted solutions (*Scheme 26*).[150]

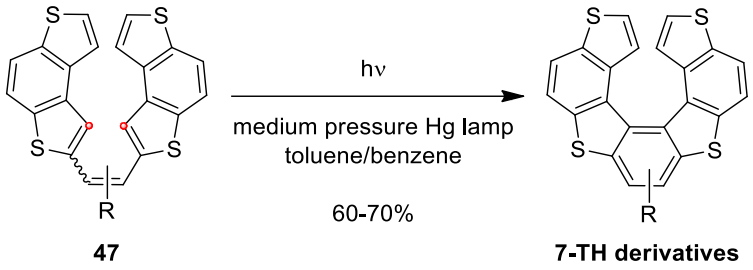

Scheme 26: Photocyclisation of alkenes **47**.

The efficiency of this reaction is strongly influenced by the concentration of the reaction solution as well as the stereochemistry of the precursors **47**. Indeed, the configuration (*Z*)- or (*E*)- of the alkenes **47** plays a crucial role in the performance of the photocyclisation, since (*Z*)-isomers are often more soluble in organic solvents than the corresponding (*E*)-isomers. Moreover, (*E*)-isomers require the isomerization into (*Z*)-isomers to close, and it often takes place longer reaction times. In particular, two alternative procedures were developed by Licandro's group[151,152] to synthetise these precursors starting from properly functionalised BDTs (*Scheme 27*).

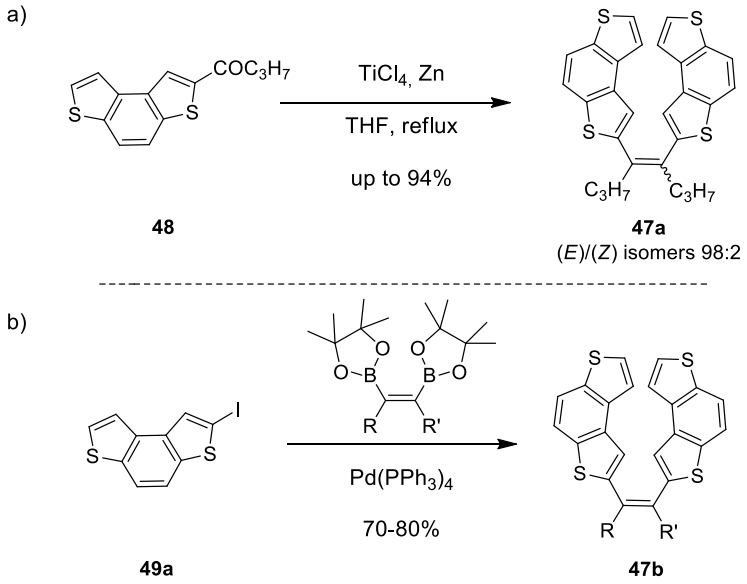

Scheme 27: Synthesis of alkenes **47**.

The first procedure involved the synthesis of the alkyl ketone **48** starting from the parent BDT, followed by a McMurry coupling in the presence of $TiCl_4$ and Zn in THF that gave the desired intermediate **47a** in

excellent yield and very good stereoselectivity (mixture of (*E*)/(*Z*)-isomers in ratio ca. 98:2) (*Scheme 27*, a).[151] In the second strategy, BDT was converted into the corresponding iodide **49a** which underwent a subsequent palladium-catalysed Suzuki coupling with symmetrical or unsymmetrical bis-boronates (*Scheme 27*, b).[152] In this case, also 7-TH scaffolds **47b** with different substituents could be obtained.

Alternatively, concerning the formation of C-C bond between the β-positions of thiophene rings (pathway **a**, Figure 19), benzo fused 7-TH systems were also prepared by non-photochemical procedures that exploited the oxidative cyclodehydrogenation of 1,2-bis(2-thienyl)benzene precursors induced by the use of DDQ in combination with $BF_3{\cdot}OEt_2$ [153] or $FeCl_3$[154] as oxidants.

Although the oxidative cyclisation of olefins represents a direct and low-cost method to prepare 7-TH systems, this approach presents some limitations especially in terms of versatility. Indeed, a limited number of substituents in the 7- and 8- position can be present because of the low compatibility of many functional groups under photochemical and/or oxidative conditions.[151]

Regarding the route **b** (*Figure 19*), Tanaka[155,156] reported the non-photochemical diastereoselective synthesis of the 2,13-dimethyl-tetrathia[7]helicene (*Scheme 28*).

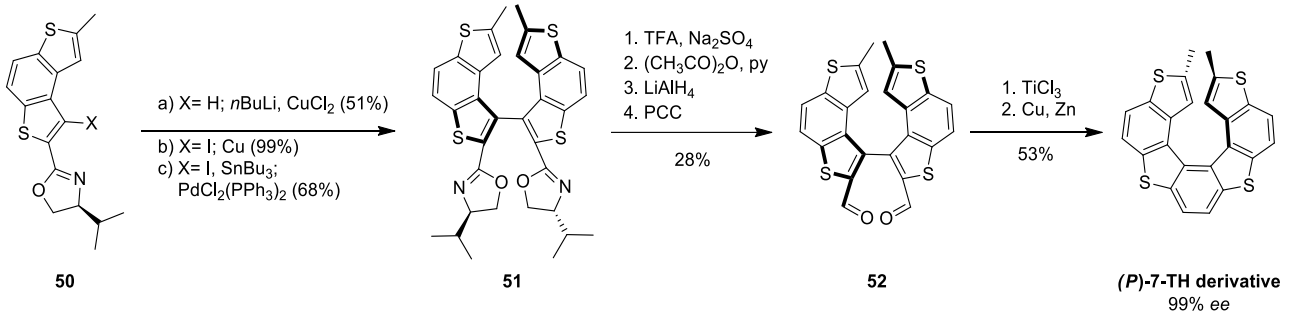

Scheme 28: Diastereoselective synthesis of 2,13-dimethyl-tetrathia[7]helicene.

In particular, the Ullmann or Stille coupling of the starting BDT precursor **50** bearing a chiral oxazoline substituent in the α-position provided an atropisomeric biaryl system **51**, with stable C_2 symmetry, which was subsequently converted into a dialdehyde **52.** The intramolecular McMurry coupling of enantiopure **52**, gave the 7-TH scaffold in 99% *ee*. This strategy was quite innovative because it was possible to prepare enantiopure 7-TH derivative thanks to the transformation of a stereogenic centre into a stereogenic axis, and then in a helical stereogenic element. Despite that, this second approach is still much underdeveloped compared to the first one, and only two examples of cyclisation of 3,3'-bis(benzo[1,2-*b*:4,3-*b*']dithiophene) have been reported for the synthesis of the enantiopure 2,13-dimethyltetrathia[7]helicene[155,156] (reported in *Scheme 28*), and of a pentathia[7]helicene.[157] On the other hand, this method represents the most promising way to obtain highly functionalised 7-THs, especially in enantioenriched form exploiting the potential axial chirality of bis(benzodithiophene) intermediates.

1.2 Development of novel procedures for the synthesis of tetrathia[7]helicenes

Inspired by strategies reported for the preparation of BDT derivatives,[158,159] we investigated novel methodologies for the cyclisation of bis(benzo[1,2-*b*:4,3-*b*']dithiophene) species involving transition metal-catalysed cross-coupling reactions (*Scheme 29*).

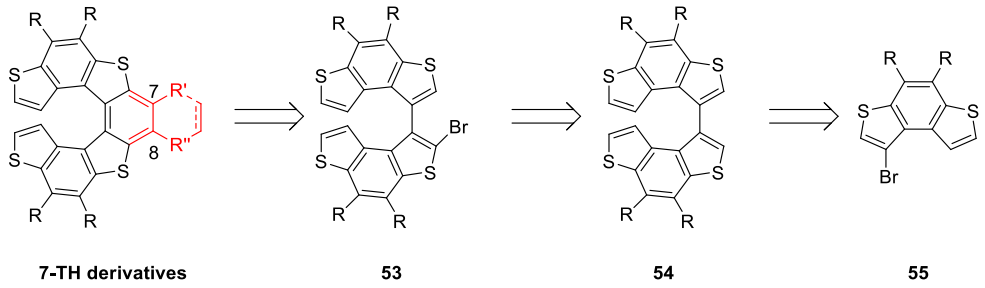

Scheme 29: Novel approach for the synthesis of 7-THs through annulation reaction of bis(benzodithiophene) intermediates.

In particular, this alternative route to prepare diverse classes of 7-THs involves the use of 3,3'-bis(benzo[1,2-*b*:4,3-*b*']dithiophene)-based bromides **53**, that can be obtained by a regioselective bromination of the corresponding biaryls **54**, which in turn can be synthetised by a palladium-catalysed homocoupling reaction of bromides **55**.

1.2.1 Synthesis of bromides 55

The first intermediates of our synthetic approach are bromides **55**, which were synthetised through a two-step procedure involving the electrophilic bromination of benzo[1,2-*b*:4,3-*b*']dithiophenes **56**, followed by a regioselective debromination of tribromo derivatives **57** by lithium-halogen exchange reaction with *n*BuLi and quenching with methanol[87] (*Scheme 30*).

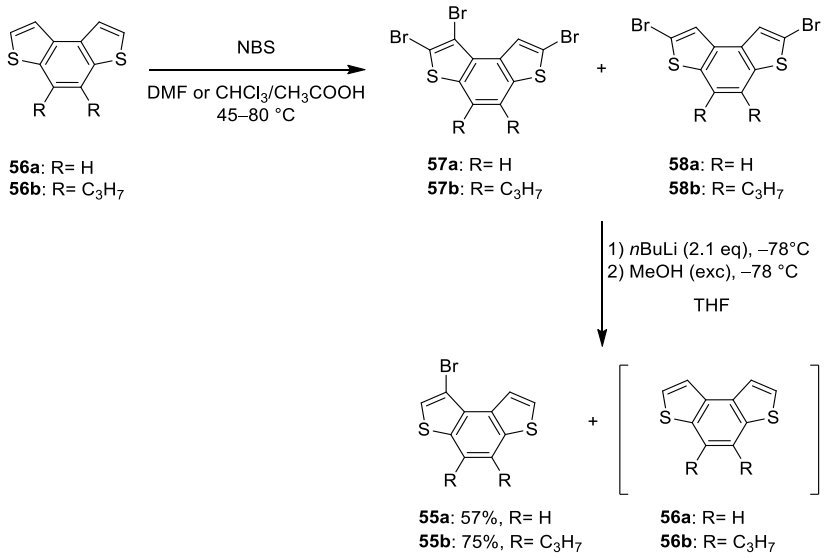

Scheme 30: Two-step synthesis of 1-bromobenzodithiophenes **55**.

More in detail, BDTs **56a**[160] was converted into the corresponding tribromo derivative **57a** by the treatment with a large amount of *N*-bromosuccinimide (NBS) in chloroform/acetic acid (1:1) at 45 °C. These conditions allowed to get the mixture of tribromide **57a** and dibromide **58a** in 24:1 molar ratio (71% yield of **57a** in the mixture by ^{1}H-NMR). Otherwise, the bromination of **56b**[161] required 3.3 equiv. of NBS in DMF at 80 °C. Tribromide **57b** was obtained in mixture with dibromide **58b** in 1:0.14 molar ratio (76% yield of **57b** in the mixture by NMR). Next, the regioselective debromination of the α-positions of **57a**,**b** was carried out using *n*BuLi and MeOH[161]. In particular, a solution of **57a** in THF was treated with *n*BuLi at –78 °C and then with an excess of MeOH. The desired compound **55a** was isolated in 57% yield. Otherwise, a better regioselectivity was observed in case of **55b**, where the debromination of **57b** at –78 °C provided **55b** in 75% yield. Small amounts of benzodithiophene **56a** and **56b** were also recovered (10–20%). This strategy represents a useful method to prepare β-bromo BDTs **55**, although the atom economy is quite low because of the waste of two bromo atoms. In order to improve the atom economy of the overall procedure as well as the yield of **55a**, we designed an alternative procedure, that involved the construction of the benzene ring through a photochemical reaction starting from a properly brominated alkene **59**, which in turn could be synthetised by a Wittig reaction between phosphonium salt **60**[162] and commercially available 4-bromo-2-tiofen-carbaldeide **61** (*Scheme 31*).

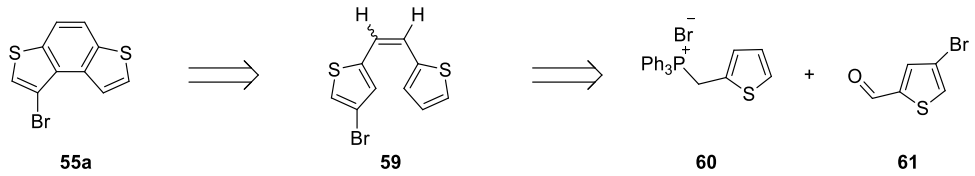

Scheme 31: Alternative retrosynthetic pathway for bromide **55a**.

Thus, phosphonium salt **60** and aldehyde **61** in equimolar ratio were dissolved in DMF and treated with K_2CO_3 to form phosphorus ylide in the presence of 18-crown-6 as phase transfer at room temperature (*Scheme 32*).

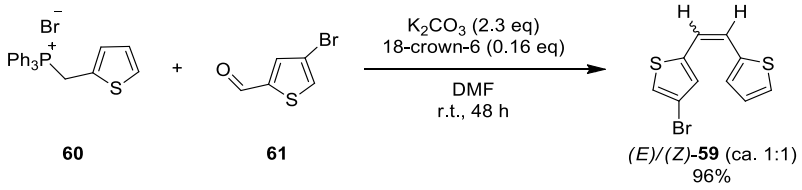

Scheme 32: Synthesis of alkene **59**.

After 48 hours, no starting materials were found in the reaction mixture and alkene **59** was isolated in 96% yield as a mixture of (*E*)/(*Z*) isomers in ca. 1:1 molar ratio, calculated by ^{1}H-NMR and confirmed by RP-HPLC. Next, the alkene **59**, obtained as pale-yellow solid, was converted into the corresponding β-brominated BDT **55a** through an oxidative photochemical reaction (*Scheme 33*).

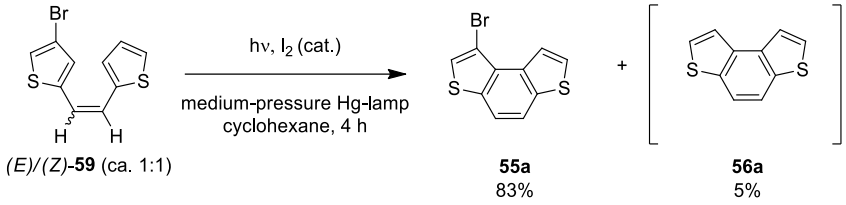

Scheme 33: Photocyclisation of alkene (*E*)/(*Z*)-**59**.

More in detail, the reaction was performed in the presence of a catalytic amount of I_2 using a medium-pressure Hg lamp with a 125-watt generator in cyclohexane solution (1.5×10^{-3} M) under air, whose oxygen acts as re-oxidising agent. After 4 hours, no starting material was observed in the reaction mixture and the bromide **55a** was isolated in 83% yield, along with a small amount of debrominated by-product **56a** (ca. 5%). We then demonstrated that this approach represents a valid alternative to the two-step procedure reported in *Scheme 30* for the synthesis of β-bromo BDT **55a**.

1.2.2 Synthesis of dimeric intermediates 53 and 54

According to the retrosynthetic pathway reported in *Scheme 29*, we then turned our attention on the synthesis of 3,3'-bis(benzo[1,2-*b*:4,3-*b*']dithiophenes **54** and **53**. Initially, the homocoupling reaction of bromides **55** to prepare the corresponding biaryls **54** was investigated following the dimerization procedures reported in literature for similar benzo[1,2-*b*:4,3-*b*']dithiophene-based species. In particular, Raja and co-workers reported the successful reductive homocoupling reaction of a β-bromobenzodithiophene derivative using $Pd[P(t\text{-}Bu)_3]_2$ as catalyst in the presence of K_3PO_4 as base in toluene at 50 °C.[157] In our hands, only traces of the desired bis(benzodithiophene) **54b** were obtained using bromide **55b**. No apparent difference in the reactivity was observed when other catalytic systems (e.g. $Pd(OAc)_2$/SPhos, $Pd(OAc)_2$/Xantphos, $Pd(dppf)Cl_2$/CsF or $Pd(PPh_3)_4$) were used instead of $Pd[P(t\text{-}Bu)_3]_2$, and the starting bromide was generally recovered in almost quantitative yield. Unsatisfactory yields of **54b** (20–30%) were also obtained by Li/Br exchange reaction of **55b** with *n*BuLi followed by *in situ* oxidation with $CuCl_2$. We then considered an alternative approach for the synthesis of **54** that exploits the one-pot Miyaura Borylation/Suzuki Coupling (MBSC) reaction, that is a well-established method to prepare symmetrical and unsymmetrical (hetero)biaryl systems, avoiding the isolation of arylboron intermediates since it involves the *in situ* formation of boron species.[163-166] Among different experimental conditions so far reported in literature for the MBSC reactions, we selected the procedure reported by Miura and co-workers in 1997, that was found to be suitable also for thienyl bromides. In particular, Miura *et al.*[167] demonstrated that the $PdCl_2(PPh_3)_2$-catalysed one-pot Suzuki reaction to prepare several biaryls could be efficiently promoted by the use of a phase-transfer catalyst, such as $n\text{-}Bu_4NHSO_4$, in a biphasic solvent system formed by toluene and water. Thus, we initially examined very similar conditions by reacting bromide **54b** with 0.65 equiv. of bis(pinacolato)diboron in the presence of 7 mol% of $PdCl_2(PPh_3)_2$, 10 mol% of $n\text{-}Bu_4NHSO_4$ and 3 equiv. of CsF as base in a mixture of toluene/water (2:1) at reflux (*Table 1*, entry 1).

Table 1. Optimisation of MBSC reaction to synthesise homodimers **54a,b**.

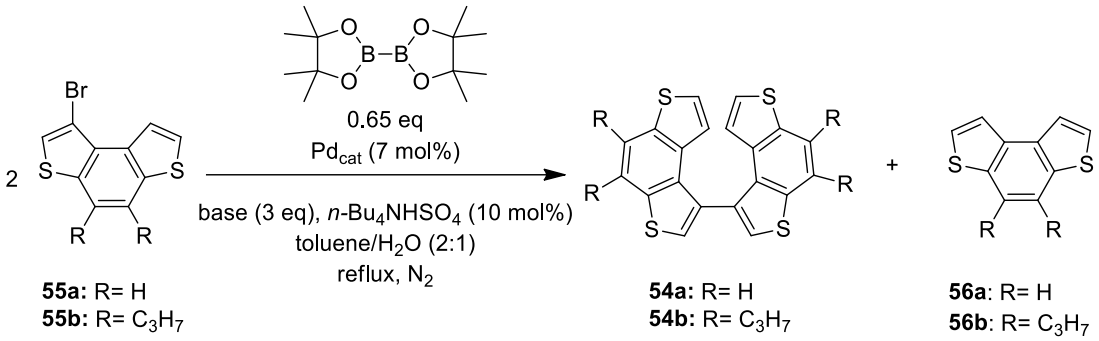

Entry[a]	**55**	Pd_{cat}	t (h)[b]	Yield of **54** (%)[c]	Yield of **56** (%)[c]
1	**55b**	$Pd(PPh_3)_2Cl_2/PPh_3$[d]	8	60	20
2	**55b**	$Pd(PPh_3)_4$	8	52	31
3	**55b**	$Pd_2(OAc)_2/PCy_3$[e]	8	58	27
4	**55b**	$Pd_2(OAc)_2/P(o\text{-tolyl})_3$[e]	8	49	30
5	**55b**	$Pd(dppf)Cl_2$	8	75	10
6[f]	**55b**	$Pd(dppf)Cl_2$	8	49	15
7[g]	**55b**	$Pd(dppf)Cl_2$	6	81	-
8[g,h]	**55b**	$Pd(dppf)Cl_2$	6	85	-
9	**55a**	$Pd(dppf)Cl_2$	12	78	9
10[g]	**55a**	$Pd(dppf)Cl_2$	4	81	-
11[g,i]	**55a**	$Pd(dppf)Cl_2$	4	86	-
12[g,j]	**55a**	$Pd(dppf)Cl_2$	4	85	-

[a] Unless otherwise stated, the reactions were performed using 0.4 mmol of **55a**,**b**, bis(pinacolato)diboron (0.65 eq), 7 mol% of palladium-catalyst, 3 equiv. of base, 10 mol% of *n*-Bu_4NHSO_4 in a mixture of toluene/water (2:1, 0.05 M) at reflux. [b] The conversion of the starting bromide **55** was complete. [c] Isolated yield. [d] The reaction was run using 4:1 molar ratio of PPh_3 and $Pd(PPh_3)_2Cl_2$. [e] The reaction was run using 7 mol% of $Pd(OAc)_2$ and 14 mol% of phosphine ligand. [f] Na_2CO_3 (2 M) was used in place of CsF. [g] The concentration of the reaction mixture was 0.5 M. [h] The reaction was run using 1.42 mmol of **55b**. [i] The reaction was run using 1.48 mmol of **55a**. [j] The reaction was run using 3.70 mmol of **55a**.

After 8 hours no starting bromide was observed in the reaction mixture and **54b** was isolated in 60% yield along with the dehalogenated product **56b** (20%) (*Table 1*, entry 1). To enhance the efficiency of this coupling and minimize the formation of by-products, different palladium catalysts were tested. The use of $Pd(OAc)_2/P(o\text{-tolyl})_3$, $Pd(OAc)_2/P(Cy)_3$ or $Pd(PPh_3)_4$ did not afford relevant improvements (*Table 1*, entries 2–4), since **54b** was obtained in 49–58% yield and significant amounts of **56b** were recovered (27–31%). On the contrary, when $Pd(dppf)Cl_2$ was used as the catalyst the yield of **54b** improved up to 75% recovering **56b** in only in 10% (*Table 1*, entry 5). As far as the base is concerned, upon replacing CsF with Na_2CO_3 the yield

of **54b** dropped off to 49% (*Table 1*, entry 6). We also found that the concentration of the reaction mixture played an important role. Indeed, when the reaction was run at a higher molar concentration (0.5 M instead of 0.05 M) starting from 0.4 (*Table 1*, entry 7) as well as 1.5 mmol (*Table 1*, entry 8) of **55b**, after 6 hours the reaction mixture did not contain bromide **55b**, and **54b** was isolated in very good yields (81% and 85%, respectively, entries 7 and 8, *Table 1*). Furthermore, these reactions displayed a higher selectivity as only traces of the by-product **56b** were detected in the mixture. The optimised experimental conditions reported in entry 8 of *Table 1* were also used for the homocoupling of bromide **55a** (*Table 1*, entries 9–12), and the product **54a** was isolated in 86% after 4 hours (entry 11, *Table 1*). It is noteworthy that these reactions were found to be scalable, allowing us to prepare up to 1 g of **54a** in a single run (*Table 1*, entry 12).

Having successfully prepared dimers **54** in very good yields, their regioselective bromination was studied to obtain monobromides **53**. Although compounds **54** displayed four terminal thiophene rings with free α and β positions, which could undergo electrophilic substitution, the thiophene rings involved in the C_β-C_β biaryl bond could be, in principle, more reactive because of the presence of the electron-rich benzodithienyl moiety in the β-position. Indeed, a similar behaviour was also observed for the synthesis of 2-bromo-3,3'-dithiophene through the selective α-bromination of 3,3'-dithiophene with NBS.[168] In order to verify this hypothesis, a brief screening of the experimental conditions for the bromination of **54b** with NBS was carried out, evaluating the effect on the outcome of this reaction of the solvent (DMF, CCl_4, CH_3Cl and CH_3COOH), the reaction temperature (25–60 °C) and the number of equivalents of NBS (1–2.5 eq). We were pleased to find that reacting **54b** with a small molar excess of NBS (1.2 eq) in chloroform/acetic acid 1:1 mixture at 35 °C, the required bromide **53b** was the major product in the final reaction mixture after 8 hours, and the chromatographic purification on silica gel of this mixture provided **53b** in 60% yield (*Scheme 34*).

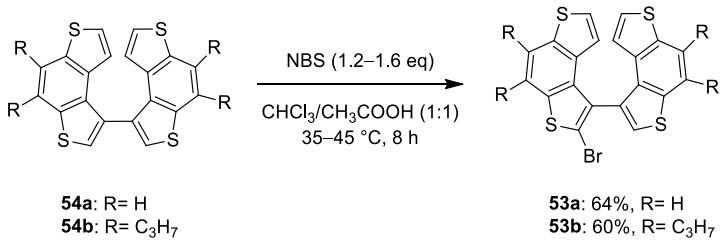

54a: R= H
54b: R= C_3H_7

53a: 64%, R= H
53b: 60%, R= C_3H_7

Scheme 34: Bromination of dimers **54**.

Similar reaction conditions were also used to prepare bromide **53a**, which was isolated in 64% yield using in this case 1.6 equiv. of NBS at 45 °C (*Scheme 34*). The mixture of these reactions generally contained small amounts of the unreacted starting material **54** (10–15%) and other brominated side-products (mono- and dibromurated derivatives, 10–15%), whose presence was confirmed by LC-MS and GC-MS analysis of the crude mixtures.

With these bromides in hand, we then focused our attention on the synthesis of diverse classes of 7-THs through metal-catalysed coupling reactions as key steps (*Scheme 35*). More in detail, three different strategies were investigated: *i)* the Pd-catalysed carboannulation of internal acetylenes to prepare 7,8-

disustituted 7-THs **62**; *ii)* the Sonogashira coupling with terminal alkynes, followed by metal-promoted intramolecular hydroarylation of intermediates **63** to obtain 7-monosubstituted helicenes **64**; *iii)* the Suzuki coupling with (hetero)aryl boronic acids, followed by the oxidative photochemical cyclisation of intermediates **65** to synthesize benzo fused 7-TH systems **66**.

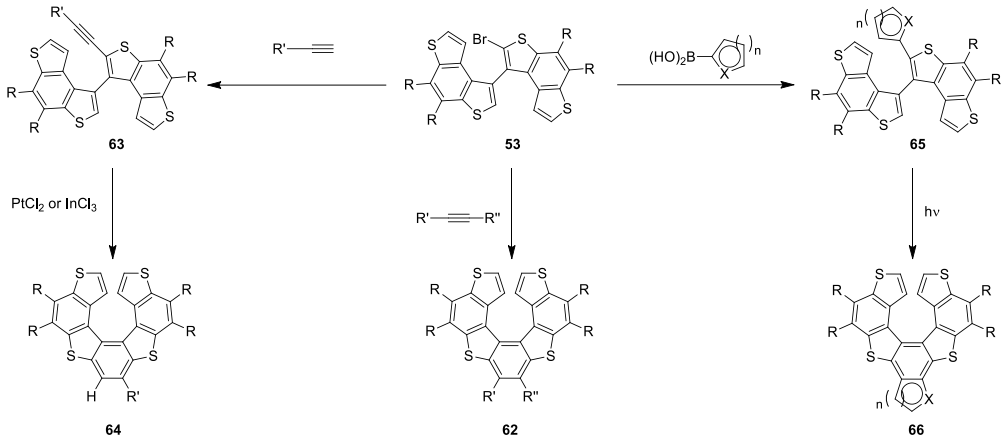

Scheme 35: General synthetic scheme for the synthesis of 7-TH derivatives **62**, **64** and **66**.

1.2.3 Synthesis of 7,8-disubstituted tetrathia[7]helicenes 62

To prepare 7,8-disubstituted 7-TH derivatives **62**, we though to exploit a Pd-catalysed carboannulation of bromides **53** with internal acetylenes **67**. Initially, the annulation of **53b** with diphenylacetylene **67a** was studied as a model reaction under experimental conditions very similar to those reported for the annulation of 2-bromo-3,3'-dithiophene to give the corresponding 4,5-disubstituted benzo[1,2-*b*:4,3-*b*']dithiophenes.[169]

Table 2. Optimisation of Pd-catalysed carboannulation of bromide **53b** with diphenylacetylene (**67a**).

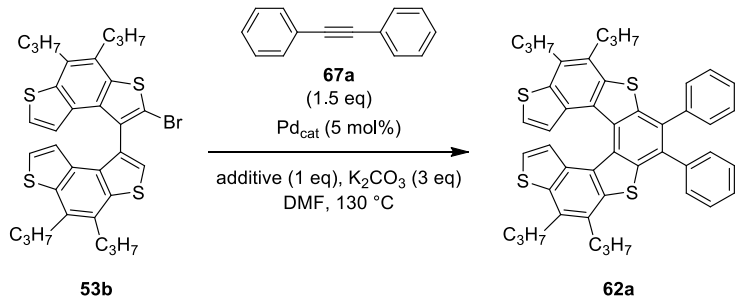

Entry[a]	Pd_{cat}	Additive	t (h)[b]	Yield of **67a** (%)[c]
1	$Pd(PPh_3)_2Cl_2$	LiBr	8	60[d]
2	$Pd[P(t\text{-}Bu)_3]_2$	LiBr	8	62[d,e]
3	$Pd(dppf)Cl_2$	LiBr	6	78[e]
4	$Pd(dppf)Cl_2$	-	12	58[d]

[a] Rection conditions: 0.07 mmol of **53b**, 1.5 equiv. of **67a**, 5 mol% of palladium catalyst, 1 equiv. of LiBr, 3 equiv. of K_2CO_3 in DMF (0.03 M). [b] The reactions were stopped when they did not further progress. [c] Isolated yield. [d] Small amounts of **53b** was also recovered (5–10%). [e] Debrominated by-product **54b** was also recovered (ca. 10%).

In particular, the use of $Pd(PPh_3)_2Cl_2$ (5 mol%) as catalyst, K_2CO_3 (3 eq) as base, LiBr (1 eq) as additive, in DMF at 130 °C under nitrogen gave thiahelicene **62a** in 60% yield (*Table 2*, entry 1). Next, a couple of diverse palladium catalysts were examined (*Table 2*, entries 2–3). A lower reactivity was observed using $Pd([P(tBu)_3])_2$ (*Table 2*, entry 2), while the use of $Pd(dppf)Cl_2$ increased the yield of **62a** up to 78% (*Table 2*, entry 3), so this latter was selected as the best catalyst for this reaction. Finally, this reaction was performed using $Pd(dppf)Cl_2$ without LiBr and **62a** was isolated in lower yield than that obtained using the same catalyst with additive (78% *vs.* 58%, compare entry 3 with entry 4, *Table 2*), thus demonstrating the important role of the additive[170] in this reaction.

The experimental conditions of entry 3 of *Table 2* were then used to prepare a set of 7,8-disubstituted 7-THs **62** through the palladium-catalysed annulation of bromides **53a**,**b** and various (hetero)aryl- and alkyl-containing internal alkynes (*Scheme 36*).

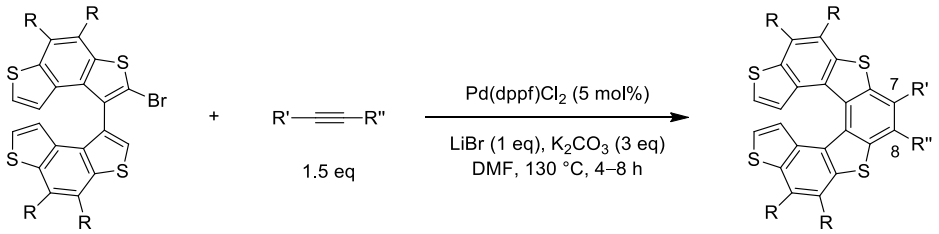

53a: R= H
53b: R= C_3H_7

67a: R'= R"= Ph
67b: R'= R"= 2-Th
67c: R'= R"= C_3H_7
67d: R'= R"= CH_2OCH_3
67e: R'= Ph, R"= 2-Th
67f: R'= Ph, R"= CH_2CH_3

62a–h

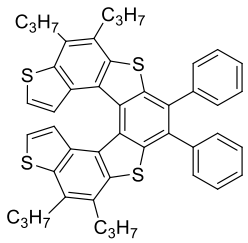

62a (78%)

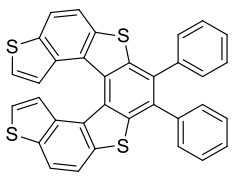

62b (80%)

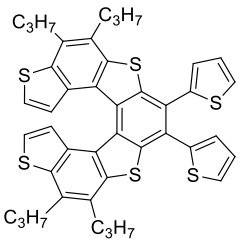

62c (68%)

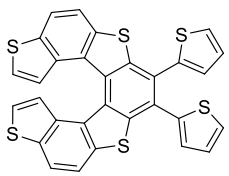

62d (63%)

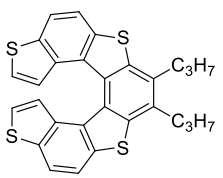

62e (50%)

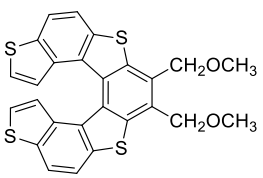

62f (46%)

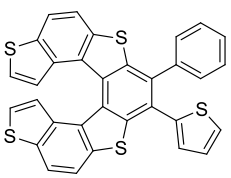

62g (60%)

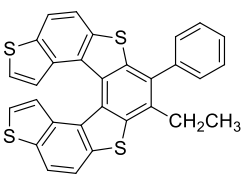

62h (75%)

Scheme 36: Synthesis of 7-TH derivatives **62a**–**h.**

As shown in *Scheme 36*, both bromides **53a**,**b** were effective in the coupling process hereby delivering the expected products **62a–h** in moderate to good yields. The use of (hetero)aryl alkynes **67a**, **67b**, **67e** and **67f** afforded best results, and the final helicenes were isolated 63–80% yield, while the use of internal alkynes with both alkyl substituents such as **67c**,**d** were found to be less reactive towards the annulation of **53a** since the expected products **62e**,**f** were isolated in lower yields (46–50%). It should be noted that this strategy allowed us to prepare not only 7-THs with the same substituents in the 7 and 8 position such as **62a–f** but also derivatives with two different pendants (R'≠ R" in compounds **62g**,**h**). These results demonstrated the versatility of this procedure since different 7-TH derivatives can be easily obtained bearing different alkyl or (hetero)aryl groups in the 7 and 8 position. Unfortunately, attempts to perform this reaction with terminal alkynes (e.g. phenylacetylene) did not provide the required 7-substituted 7-TH since complex reaction mixtures were obtained.

1.2.4 Synthesis of 7-monosubstituted tetrathia[7]helicenes 64

Since the preparation of 7-monosubstituted 7-THs **64** was not possible through Pd-catalysed carboannulation of bromides **53** with terminal acetylenes, we though an alternative two-step procedure that involved the construction of the central benzene ring by a metal-catalysed intramolecular hydroarylation of the alkynes **63**, which in turn could be obtained through a Sonogashira coupling between bromides **53** and terminal alkynes **68** (*Scheme 37*).

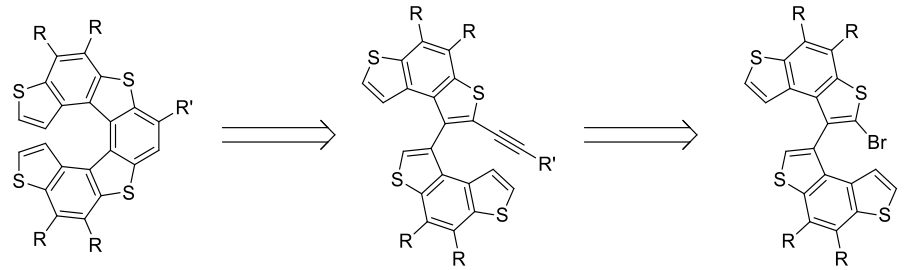

Scheme 37: Retrosynthetic approach for the preparation of monosubstituted 7-THs **64**.

Concerning the first step of this procedure, the Sonogashira reaction between bromides **53** and terminal alkynes **68**, we initially studied the $Pd(PPh_3)_2Cl_2$/CuI-catalysed reaction between bromide **53a** and phenylacetylene **68a** in the presence of DIPEA and THF at 70 °C, that are classical conditions for the Sonogashira coupling involving benzodithiophene halides.[171,172] In particular, we evaluated the influence of the number of equivalents of alkyne **68a** and the amount of the catalytic system on the outcome of this reaction (*Table 3*).

Table 3. Optimisation of Sonogashira reaction between bromide **53a** and phenylacetylene (**68a**).

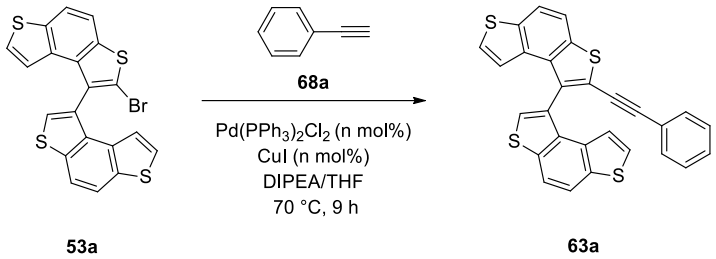

53a **63a**

Entry[a]	**68a** (eq)	n mol%	Yield of **63a** (%)[b]
1	1.1	10	68
2	1.5	10	87
3	2.0	10	87
4	1.5	7	87
5	1.5	5	73
6[c]	1.5	7	74
7[c]	2.0	10	84
7[d]	2.0	10	85

[a]Rection conditions: 0.20 mmol **53a**, DIPEA (5 mL) and THF (5 mL) at 70 °C (oil bath). [b] Isolated yield. [c] 0.50 mmol of **53a**. [d] 1 mmol of **53a**.

While the conversion of the starting material **53a** was not complete after 9 hours adding 1.1 equiv. of **68a** and the desired compound was obtained in 68% yield along with 20% of recovered bromide **53a** (*Table 3*, entry 1), when 1.5 equiv. (*Table 3*, entry 2) or 2 equiv. (*Table 3*, entry 3) of **68a** were used, the product **63a** was isolated in 87% yield. Next, the reaction was performed using 1.5 equiv. of alkyne **68a** and changing the amount of the catalytic system. While a complete conversion of the starting material **53a** was observed using 10 mol% or 7 mol% of $Pd(PPh_3)_2Cl_2$/CuI and **63a** was isolated in 87% yield (*Table 3*, compare entry 2 and entry 4), when the reaction was carried out with 5 mol% of $Pd(PPh_3)_2Cl_2$/CuI **63a** was isolated in a slighter yield (73% vs. 87%), and some bromide **53a** was also recovered (16%) (*Table 3*, entry 5). Again, when a scale up of the reaction from 0.20 mmol to 0.50 mmol of **53a** was performed under the optimised conditions reported in entry 4 of *Table 3*, **63a** was isolated in 74% yield, and bromide **53a** was recovered in 14% (*Table 3*, entry 6). Better results were obtained for the same reaction scale using a higher amount of the catalyst and alkyne **68a** (*Table 3*, entry 7). Finally, when the reaction was performed starting from 1 mmol of **53a**, **63a** was isolated in 85% yield, that is very similar than that obtained starting from 0.5 mmol of **53b**.

The experimental conditions reported in entry 2 of *Table 3* were used to prepare a set of alkynes **63a–g** starting from bromides **53a**,**b** and commercially available alkynes **68a–f** (*Scheme 38*).

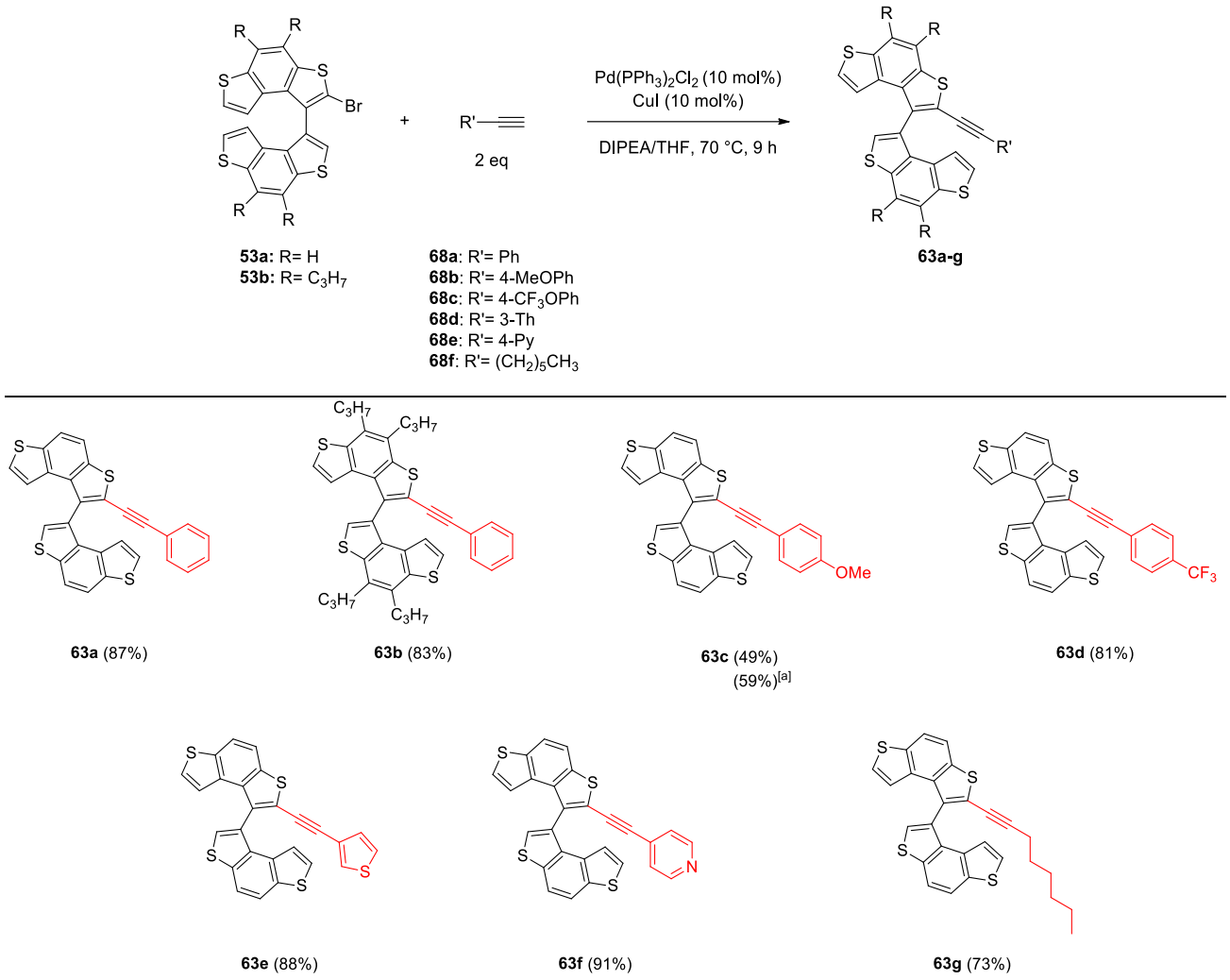

Scheme 38: Synthesis of alkynes **63**. [a] 1.05 equiv. of alkyne **68b**.

As shown in *Scheme 38*, both bromides **53a**,**b** were effective in the Sonogashira coupling delivering the expected products **63a–g** in good yields (59–91%). It should be noted that in the presence of electron-donor group such as the methoxy group in alkyne **68b**, we obtained a complex reaction mixture from which the desired product **63c** was isolated in 59% yield using in this case 1.05 equiv. of alkyne **68b**, along with some unreacted bromide **53a** (13%). On the contrary, the presence of electron-withdrawing groups such as the trifluoromethyl group in alkyne **68c** afforded the product **63d** in 81% yield. Good results were also achieved using both electron-rich and electron-poor heteroaryl alkynes **68d** and **68e**, containing a thienyl and a pyridyl ring, respectively. Indeed, the products **63e** and **63f** were isolated in 88% and 91% yield, respectively. Finally, alkyne **68f**, containing an alkyl chain, was effective in the coupling delivering the expected compound **63g** in 73% yield. These results demonstrated the versatility of this procedure which allowed us to prepare a small library of intermediates **63**.

For compound **63c** we were able to obtain colourless needles by layering hexane over a dichloromethane solution, and their single crystal X-ray diffraction analysis confirmed the structure of the molecule. The ORTEP view of the molecule and the atomic numbering scheme are reported in *Figure 20*.

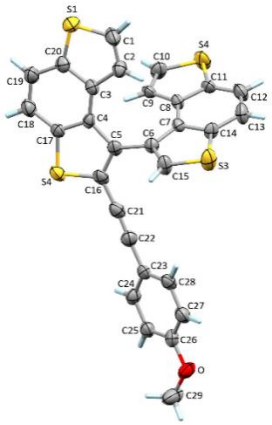

Figure 20: ORTEP view of compound **63c**. Ellipsoids are drawn at their 50% level.

The two benzodithienyl moieties are practically planar and they are connected via C5-C6 bond. The dihedral angle between the mean planes is 65.76°. Noteworthy, the C12-C13 and C18-C19 bond lengths in the benzene rings are significantly shorter than the C3-C4 and C7-C8 ones, in accordance with parent systems and their precursors reported in literature.[142] The mean plane of the methoxyphenyl substituent is twisted and showed a dihedral angle of 27.49° with respect to the benzodithienyl group. The carbon atoms involved in the triple bond are at a distance of 0.066 and 0.153 Å, respectively, for C21 and C22 from the mean plane of the substituted benzodithienyl moiety. A racemic mixture of the two atropisomers is present in the crystals.

Afterwards, the metal-catalysed intramolecular hydroarylation of some alkynes **63** was studied to obtain the corresponding 7-monosubstituted 7-THs **64**. At the onset of this study, we carried out a preliminary screening of the reaction conditions for the $PtCl_2$-catalysed hydroarylation of the model alkyne **63a** taking into account that the hydroarylation reactions performed for the preparation of heterohelicenes are generally promoted by $PtCl_2$[31, 58, 59,173,174] (*Table 4*).

Table 4. Brief screening for the $PtCl_2$-catalysed intramolecular hydroarylation of alkyne **63a**.

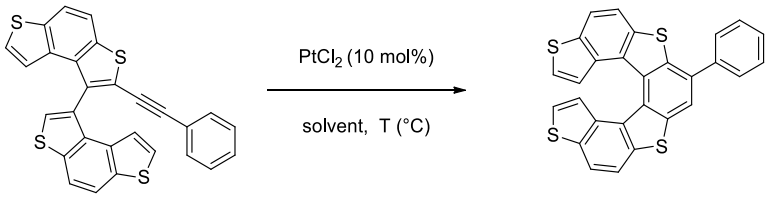

63a **64a**

Entry[a]	Solvent	T (°C)/t (h)	Conversion[b] (%)	Yield of **64a** (%)[c]
1	Toluene	80 / 10	100	32
2	Dichloroethane	90 / 10	100	32
3	Toluene/CH_3CN	120 / 10	100	17
4	Toluene	60 / 10	100	36
5	Toluene	r.t. / 10	< 3	-[d]
6	Toluene	r.t. / 24	<10	-[d]
7	Toluene	r.t. / 504	100	25

[a] Reaction conditions: 0.20 mmol of **63a**, 10 mol% of the catalyst. Concentration: 0.2 M. [b] The conversion of **63a** was evaluated by RP-HPLC (eluent: CH_3CN) on the crude reaction mixture. [c] Isolated yield. [d] The reaction mixture was not purified.

We initially evaluated the effect of the solvent on the outcome of this reaction (*Table 4*, entries 1–3). While **64a** was isolated in 32% yield using toluene at 80 °C (*Table 4*, entry 1) or dichloroethane[31] at 90 °C (*Table 4*, entry 2), when a mixture of toluene/acetonitrile[59] (1:1 ratio) was used as reaction media at 120 °C the final 7-TH **64a** was recovered in 17% yield (*Table 4*, entry 3). Next, the final yield of **64a** increased up to 36% decreasing the temperature at 60 °C using toluene as solvent (*Table 4*, entry 4). On the other hand, when the reaction was performed at room temperature the reaction time dramatically increased. Indeed, the conversation of starting alkyne **63a** was trifling after 10 or 24 hours (*Table 4*, entry 5 and entry 6), and 21 days was necessary to have a complete conversion of **63a** (*Table 4*, entry 7), but the crude was very complicated because of the formation of several unknown side-products.

With these results in hand, this process was extended by exploring the substrate scope of the reaction with alkynes **64a–d** also using different metal-based catalysts generally employed to promote cycloisomerisation of 2-alkynyl derivatives[55] (*Scheme 39*).

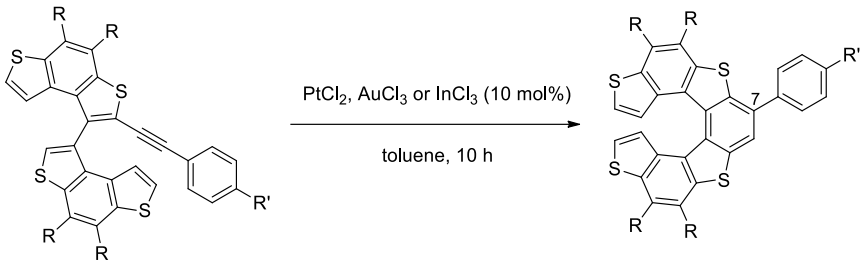

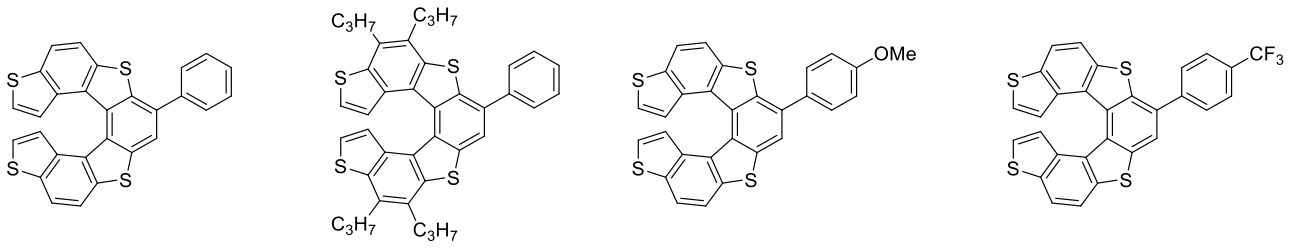

64a (36%, $PtCl_2$, 60 °C)
(NR, $AuCl_3$, 80 °C)
(NR, $InCl_3$, 80 °C)

64b (42%, $PtCl_2$, 60 °C)

64c (28%, $PtCl_2$, 60 °C)
(NR, $AuCl_3$, 80 °C)
(73%, $InCl_3$, 80 °C)

64d (27%, $PtCl_2$, 60 °C)
(NR, $AuCl_3$, 80 °C)
(NR, $InCl_3$, 80 °C)

Scheme 39: Synthesis of 7-THs **64a**–**d**.

As can be seen in *Scheme 39*, both alkynes **63a**,**b** were moderately effective in the ring closing process promoted by $PtCl_2$ hereby delivering the expected products **64a,b** in 36% and 42%, respectively. The same trend was observed in the presence of electron-donor group such as OMe (**63c**) and electron-withdrawing group such as CF_3 (**63d**). More in detail, the 7-TH **64c** was isolated in 28% yield and the final helicene **64d** was obtained in 27% yield along with 28% of recovered alkyne **63d**. At this point, the role of metal-based catalyst was briefly investigated. Unfortunately, no cyclised product was observed using $AuCl_3$ in place of $PtCl_2$. On the other hand, an interesting result was achieved in case of $InCl_3$. While starting material was quantitatively recovered in case of **63a** and **63d**, the alkyne with electron-donor substituent **63c** gave the final 7-TH **64c** in 73% yield. These results clearly demonstrate that this latter reaction is widely influenced by the nature of the catalyst and the electronic features of the alkynes. This two-step strategy allowed us to prepare some 7-monosubstituted 7-THs **64**, though the last step was not optimised yet. Further studies on the intramolecular hydroarylation of alkynes **63** also with chiral ligands will be discussed in *Chapter 4*.

1.2.5 Synthesis of benzo fused tetrathia[7]helicenes 66

To further expand the usefulness of bromides **53**, we also developed a novel two-step strategy for the preparation of benzo fused 7-THs **66**, in which the formation of the central benzene ring could be accomplished by an oxidative photochemical cyclisation of dimers **65**, which could be synthetised through a Suzuki coupling between bromides **53** and (hetero)aryl boron species **69** (*Scheme 40*).

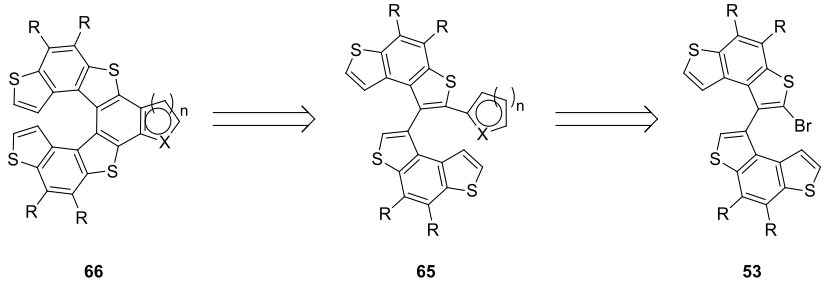

66 **65** **53**

Scheme 40: Retrosynthetic approach for the preparation of benzo-fused helicenes **66**.

We initially studied the Suzuki coupling between bromides **53a**,**b** and boron species **69a–d** using two different methods (*Method A* and *Method B, Table 5*).

Table 5. Suzuki coupling between bromides **53a**,**b** and (hetero)arylboronic derivatives **69a–d**.

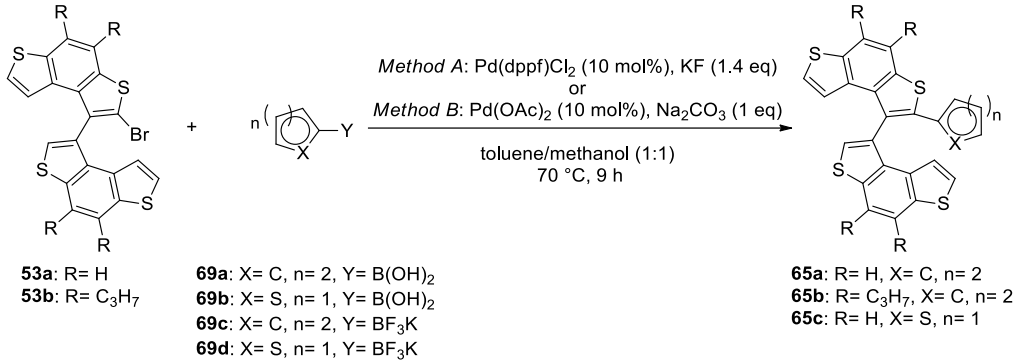

Entry	**53**	**69**	Method[a,b]	Yield of **65** (%)[c]
1	**53a**	**69a**	*A*	91
2	**53b**	**69a**	*A*	86
3	**53a**	**69b**	*A*	80
4	**53a**	**69c**	*B*	89
5	**53b**	**69c**	*B*	61
6	**53a**	**69d**	*B*	-[d]

[a] *Method A*: 0.1 mmol of **53**, 2 equiv. of (hetero)arylboronic acids **69a**,**b**, 10 mol% of Pd(dppf)Cl_2, 1.4 equiv. of KF at 70 °C, under nitrogen. [b] *Method B*: 0.1 mmol of **53**, 1 equiv. of trifluoroborate salt **69c**,**d**, 10 mol% of $Pd(OAc)_2$, 1 equiv. of Na_2CO_3 at 70 °C, under air. [c] Isolated yield. [d] The strarting material **53a** was quantitatively recovered.

More in detail, *Method A* involves the use of Pd(dppf)Cl_2 as catalyst and KF as base in a mixture of toluene and methanol, that are experimental conditions previously reported in literature for the Suzuki coupling of benzodithiophene halides with (hetero)aryl boronic acids.[175] Otherwise, we also tried a more environmentally convenient method that makes use of trifluoroarylborate salts and a less expensive catalyst, such as $Pd(OAc)_2$ without phosphine-based ligands under air [176,177] (*Method B*). As reported in *Table 5*, *Method A* provided very good results for the Suzuki coupling between both bromides **53a**,**b** and (hetero)arylboronic acids **69a**,**b** delivering the expected products **65a–c** in 80–91% yield (*Table 5*, entries 1–3). Concerning *Method B*, **65a** was obtained in a similar yield (89%, entry 4 of *Table 5*) than that obtained with *Method A* (91%, entry 1 of *Table 5*), while **65b** was obtained in a significant lower yield (61%, entry 5 of *Table 5*) than that obtained with *Method A* (86%, entry 2 of *Table 5*). Unfortunately, the formation of **65c** was not observed using *Method B* (*Table 5*, entry 6), and the starting material **53a** was quantitatively recovered. Overall, these results are quite interesting, because they demonstrate that a less expensive and more environmentally convenient

protocol (*Method B*) could be used for the synthesis of some intermediates **65**. Taking into account the good yields achieved for compounds **65a–c** under the experimental conditions reported in entries 1–3 of *Table 5*, we did not perform further studies for this Suzuki coupling, and we focused on the final step involving the oxidative photochemical cyclisation of dimers **65a–c**.

In particular, this reaction was performed in the presence of a catalytic amount of I_2 using a medium-pressure Hg lamp with a 125-watt generator in toluene solution (10^{-4} M) under air at room temperature (*Scheme 41*).

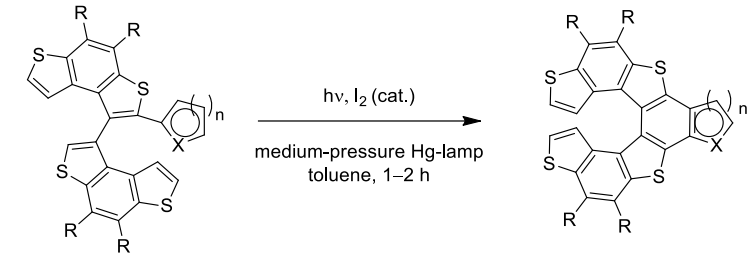

65a: R= H, X= C, n= 2
65b: R= C_3H_7, X= C, n= 2
65c: R= H, X= S, n= 1

66a–c

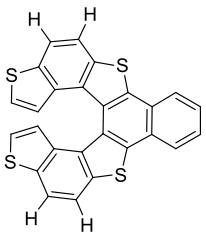

66a (99%, 1.5 h)

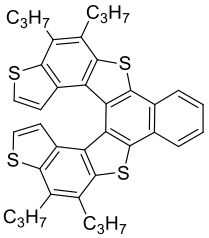

66b (91%, 1 h)

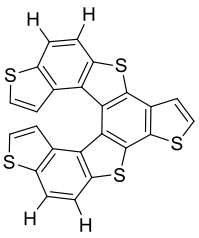

66c (94%, 2 h)

Scheme 41: Synthesis of benzo fused 7-THs **66a**–**c**.

As shown in *Scheme 41*, the desired benzo fused systems **66a**–**c** were obtained in excellent yields in very short reaction time (1–2 hours), also thanks to the high dilution conditions (C = 10^{-4} M) used in these reactions. Further studies should be carried out to expand the library of laterally extended 7-THs **66**.

1.3 Conclusions and perspectives

In summary, general and versatile synthetic methodologies have been developed to prepare different classes of 7-TH derivatives **62**, **64** and **66**, exploiting transition metal-catalysed cross coupling reactions as key steps.

In particular, starting from the same building block, namely bromides **53**, three different functionalised 7-TH frameworks have been obtained: *i*) 7,8-disubstituted 7-TH derivatives **62** through palladium-catalysed annulation of **53** with internal alkynes; *ii*) 7-substituted 7-TH derivatives **64** through Sonogashira coupling with terminal alkynes, followed by $InCl_3$- or $PtCl_2$-catalysed intramolecular hydroarylation of alkynes **63**; *iii*) benzo fused 7-THs derivatives **66** through Suzuki coupling with (hetero)aryl boronic acids, followed by the oxidative photochemical cyclisation of intermediates **65**.
Noteworthy, the versatility of this synthetic approach could allow the synthesis not only of 7-TH scaffolds but also of heterohelicenes with different number of condensed rings and heteroatoms in the backbone. A preliminary study on the synthesis of different thiahelicene derivatives through the synthetic approach described for 7-TH is reported in the *Chapter 2*.
Moreover, these procedures involve the synthesis of atropisomeric intermediates **53**, **54**, **66** and **69** whose stereochemical properties could be exploited to set up an asymmetric version of these protocols. To this purpose, their stereochemical and chiroptical properties have been fully elucidated by experimental and theoretical studies (see *Chapter 3*), while a first study on the synthesis of enantioenriched 7-THs **64** by cycloisomerisation of intermediates **63** with chiral Au(I) complexes has been faced in *Chapter 4*.

In perspective, the photophysical and electronic properties of some 7-THs reported in this *Chapter*, such as 7,8-diaryl substituted derivatives or benzo fused systems, will be investigated by means of absorption/emission measurements and cyclic voltammetry experiments, respectively. Again, the chiroptical properties, including Circularly Polarized Luminescence (CPL) features, of these 7-THs will be evaluated.

1.4 Experimental part

1.4.1 General methods

Unless otherwise stated, the reactions were run under inert atmosphere (nitrogen or argon atmosphere) by means of standard Schlenk technique for manipulating air-sensitive compounds. All commercially available reagents and solvents were purchased from Sigma-Aldrich and used without further purification. 4-Bromo-2-tiofen-carbaldehyde **61** and the alkynes **68** and **69** were purchased from Fluorochem. NBS was recrystallised from water.[178] Solutions of *n*BuLi (1.6 M in hexane) were purchased from Sigma-Aldrich and titrated prior to use. Anhydrous THF was purchased from Sigma-Aldrich 250 mL bottles on molecular sieves with crown cap. Benzo[1,2-*b*:4,3-*b*']dithiophene **56a**,[160] 4,5-dipropylbenzo[1,2-*b*:4,3-*b*']dithiophene **56b**,[179] phosphonium salt **60**[162] were synthesised as reported in literature. Thin-layer chromatography (TLC) was performed with Aldrich silica gel 60 F254 precoated plates, and plates were visualized with short-wave UV light (254 and 366 nm). Column chromatography was carried out with Aldrich silica gel (70-230 mesh). Melting points were determined with a Büchi Melting Point B-540 apparatus and are uncorrected. The IR spectra were recorded on powders using ATR Fourier Transform Infrared (FTIR) spectrometer (PerkinElmer spectrum 100). The ^{1}H and ^{13}C NMR spectra were recorded in $CDCl_3$ or CD_2Cl_2 at 25 °C using a Bruker AC-300, Bruker AC-400 and Bruker AC-600 MHz spectrometer. Chemical shifts were reported relative to the residual protonated solvent resonances (^{1}H: δ = 7.26 ppm, ^{13}C: δ = 77.00 for $CDCl_3$, ^{1}H: δ = 5.32 ppm for CD_2Cl_2). The chemical shifts are given in ppm and coupling constants in Hz. High Resolution Electron Ionization (HR EI) mass spectra were recorded on a FISONS - Vg Autospec- M246 spectrometer. The purity of compounds was evaluated by Reverse-Phase RP-HPLC analyses that were performed on Agilent 1100 series system, equipped with DAD 300 analyzer, using the analytical column Zorbax Eclipse XDB-C18 (150 mm x 4.6 mm 5 µm).

1.4.2 Synthesis and characterization of new compounds

Synthesis of 1,2,7-tribromobenzo[1,2-*b*:4,3-*b*']dithiophene (57a). To a mixture of **56a** (1.05 mmol, 200 mg) in $CHCl_3$ (6 mL) and AcOH (6 mL) NBS (6.8 mmol, 1.21 g, 6.5 equiv.) was added in portions and the resulting suspension was stirred at 45 °C. The outcome of the reaction was monitored by RP-HPLC analysis (acetonitrile as the eluent). After 8 hours, the mixture was cooled to room temperature, and a saturated solution of $NaHCO_3$ was slowly added under vigorously stirring until neutralization. The aqueous phase was extracted with CH_2Cl_2 (3 × 20 mL), and the collected organic phases were washed with H_2O (2 × 20 mL), dried over Na_2SO_4, and concentrated under reduced pressure. The residue was purified by column chromatography on silica gel with hexane as the eluent to afford a mixture of bromides **57a** and **58a** (332 mg, **57a**:**58a** = 24:1 NMR molar ratio): bromide **57a** (319 mg, 0.749 mmol, 71%), bromide **58a** (13 mg, 0.0312 mmol). ^{1}H NMR (300 MHz, mixture **57a** and **58a**, $CDCl_3$): δ = 8.65 (s, 1H, **57a**), 7.72 (d, *J* = 8.6 Hz, 1H, **58a**), 7.64 (d, *J* = 8.6 Hz, 1H, **57a**), 7.63 (s, 2H, **58a**), 7.59 (s, 2H, **58a**). The assignment has been made taking into account NMR data for **57a**[180] and **58a**.[181]

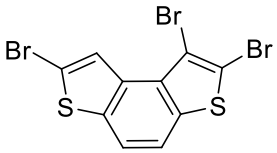

Synthesis of 1,2,7-tribromo-4,5-dipropylbenzo[1,2-*b*:4,3-*b*']dithiophene (57b). To a solution of **56b** (6.19 mmol, 1.7 g) in dry DMF (15 mL) NBS (19.2 mmol, 3.42 g, 3.1 equiv.) was added at room temperature and the resulting mixture was stirred at 80 °C. The outcome of the reaction was monitored by RP-HPLC analysis (acetonitrile as the eluent). After 6 hours, the reaction mixture was cooled to room temperature, diluted with CH_2Cl_2 and poured into water (70 mL). The aqueous phase was extracted with CH_2Cl_2 (4 × 40 mL), and the collected organic phases were washed with water (4 × 20 mL), dried over Na_2SO_4, and concentrated under reduced pressure. The residue was purified by column chromatography on silica gel with hexane as the eluent to afford a mixture of bromides **57b** and **58b** (2.69 g, **57b**:**58b** = 1:0.14 NMR molar ratio): bromide **57b** (2.40 g, 76%), bromide **58b** (336 mg). ^{1}H NMR (300 MHz, mixture **57b** and **58b**, $CDCl_3$): δ = 8.61 (s, 1H, **57b**), 7.55 (s, 2H, **58b**), 2.88–2.83 (m, 4H, **57b** + **58b**), 1.77–1.68 (m, 4H, **57b** + **58b**), 1.10–1.04 (m, 6H, **57b** + **58b**). The assignment has been made taking into account NMR data reported in literature for **57b** and **58b**.[161]

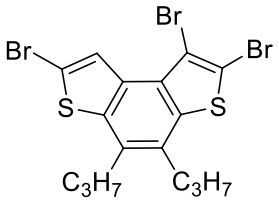

Synthesis of (*E*/*Z*)-4-bromo-2-(2-(thiophen-2-yl)vinyl)thiophene (59). A mixture of phosphonium salt **60** (9.4 g, 21.5 mmol), K_2CO_3 (6.8 g, 49.4 mmol, 2.3 equiv.), 18-crown-6 ether (0.9 g, 3.4 mmol, 0.16) and aldehyde **61** (4.4 g, 23.1 mmol, 1.07 eq) in DMF (40 mL) was stirred at room temperature. After 48 hours, the solvent was removed under reduced pressure, and the residue was poured into water (50 mL). The aqueous phase was extracted with CH_2Cl_2 (4 × 15 mL), and the collected organic phases were washed with H_2O (2 × 30 mL), dried over Na_2SO_4, and concentrated under reduced pressure. The residue was purified by column chromatography on silica gel with hexane as the eluent to afford **59** (5.62 g, 20.7 mmol, 96%) as mixture of *E/Z* isomers in 1:1 molar ratio. ^{1}H NMR (300 MHz, $CDCl_3$): δ = 7.28 (d, *J* = 5.0 Hz, 1H, *Z*), 7.22 (d, *J* = 5.0 Hz, 1H, *E*), 7.15–6.99 (m, 7H, *E*+*Z*), 6.96–6.91 (d, *J* = 15.8 Hz, 1H, *E* + bs 2H), 6.66 (d, *J* = 11.7 Hz, 1H, *Z*), 6.49 (d, *J* = 11.7 Hz, 1H, *Z*). ^{13}C NMR (75 MHz, $CDCl_3$): δ = 143.2, 141.6, 140.2, 138.3, 130.2, 128.7, 127.7 (2C), 126.9, 126.7 (2C), 125.0, 124.5, 123.2, 122.6, 121.2, 121.1, 120.0, 110.2, 109.5. IR (neat): $\tilde{\nu}$ = 3109, 3076, 1618, 1523, 1492, 1459, 1435, 1365, 1325, 1269, 1183, 1162, 1078, 1042, 942, 867, 853, 828, 769, 727, 703, 592, 557, 527, 475, 431 cm^{-1}. HRMS (EI): calcd for $C_{10}H_7BrS_2$ $[M]^+$: 269.9170, found 269.9163.

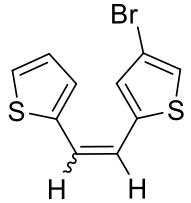

Synthesis of 1-bromobenzo[1,2-*b*:4,3-*b*']dithiophene (55a). *Method A.* To a stirring solution of **57a**:**58a** in 24:1 NMR molar ratio (290 mg, 0.65 mmol of **57a** and 0.03 mmol of **58b**) in dry THF (10 mL) at –78 °C a solution of *n*BuLi (0.89 mL, 1.43 mmol, 1.6 M in hexane) was added dropwise under an argon atmosphere, and the resulting mixture was stirred for 1 hour at –78 °C. MeOH (1 mL) was added dropwise to the mixture at –78 °C, and after 15 minutes the mixture was warmed at room temperature. A saturated aqueous solution of NH_4Cl (20 mL) was slowly added, and the aqueous phase was extracted with CH_2Cl_2 (3 × 20 mL). The collected organic phases

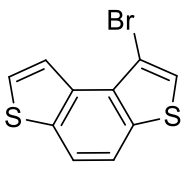

were washed with H_2O (2 × 20 mL), dried over Na_2SO_4, and concentrated under reduced pressure. The residue was purified by column chromatography on silica gel with hexane as the eluent to afford **55a** (100 mg, 57%) as colourless solid. M.p. (hexane) 122–124 °C. ^{1}H NMR (300 MHz, $CDCl_3$): δ = 8.69 (d, *J* = 5.5 Hz, 1H), 7.89 (d, *J* = 8.7 Hz, 1H), 7.79 (d, *J* = 8.6 Hz, 1H), 7.62 (d, *J* = 5.5 Hz, 1H), 7.54 (s, 1H). ^{13}C NMR (75 MHz, $CDCl_3$): δ = 138.3 (Cq), 136.2 (Cq), 134.0 (Cq), 131.4 (Cq), 126.1 (CH), 124.0 (CH), 121.5 (CH), 120.0 (CH), 118.9 (CH), 106.2 (Cq). IR (neat): ν̃ = 2959, 2923, 2868, 2853, 1461, 1378, 1329, 1259, 1185, 1160, 1158, 1146, 1089, 967, 884, 851, 830, 790, 738, 703, 619, 555, 479, 460, 440 cm^{-1}. HRMS (EI): calcd for $C_{10}H_5BrS_2$ [M]+: 267.9016, found 267.9016. Compound **56a** was also recovered (33 mg).

Method B. A stirred solution of compound **59** (300 mg, 1.12 mmol) and a catalytic amount of iodine in cyclohexane (750 mL) was irradiated at room temperature with a 125 W unfiltered medium-pressure Hg lamp. The outcome of the reaction was monitored by HPLC analysis (eluent: H_2O/CH_3CN = 95:5). After completion of the reaction, the solvent was removed under reduced pressure, and the residue was purified by column chromatography on silica gel with hexane as eluent to give **55a** (225 mg, 75%) as colourless solid. Compound **57a** was also recovered (11 mg). Spectroscopic data in accordance with what previously reported in method A.

Synthesis of 1-bromo-4,5-dipropylbenzo[1,2-*b*:4,3-*b*']dithiophene (55b). To a stirring solution of **57b**:**58b** in 1:0.14 NMR molar ratio (1.5 g, 2.58 mmol of **57b** and 0.42 mmol of **58b**) in dry THF (22 mL) at –78 °C a solution of *n*BuLi (4.5 mL, 6.3 mmol, 1.4 M in hexane,) was added dropwise under an argon atmosphere, and the resulting mixture was stirred for 1 hour at –78 °C. MeOH (1 mL) was added dropwise to the mixture at –78 °C, and after 15 minutes the mixture was warmed at room temperature. A saturated aqueous solution of NH_4Cl (20 mL) was slowly added, and the aqueous phase was extracted with CH_2Cl_2 (3 × 20 mL). The collected organic phases were washed with H_2O (2 × 20 mL), dried over Na_2SO_4, and concentrated under reduced pressure. The residue was purified by column chromatography on silica gel with hexane as the eluent to afford **55b** (658 mg, 1.86 mmol, 75%) as colourless solid. ^{1}H NMR (300 MHz, $CDCl_3$): δ = 8.66 (d, *J* = 5.6 Hz, 1H), 7.53 (d, *J* = 5.6 Hz, 1H), 7.47 (s, 1H), 3.03–2.95 (m, 4H), 1.82–1.72 (m, 4H), 1.12–1.06 (m, 6H). Spectroscopic data are in agreement with those reported in literature.[161] Compound **56b** was also recovered (123 mg).

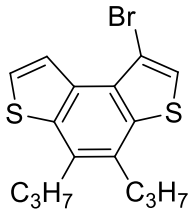

General procedure for the synthesis of dimers 54a,b. A deaerated mixture of bromide **55** (1.5 mmol), bis(pinacolato)diboron (247.6 mg, 0.98 mmol), $Pd(dppf)Cl_2$ (76.8 mg, 0.105 mmol), CsF (683.5 mg, 4.5 mmol) and nBu$_4$NHSO$_4$ (50.9 mg, 0.15 mmol) in toluene (2 mL) and water (1 mL) was refluxed under nitrogen for 4–6 h. The outcome of the reaction was monitored by TLC analysis (hexane). After completion of the reaction, the mixture was cooled to room temperature and poured into water (10 mL). The aqueous phase was extracted with CH_2Cl_2 (4 × 5 mL), and the collected organic phases were dried over Na_2SO_4, and

concentrated under reduced pressure. The residue was purified by column chromatography on silica gel to provide the required product **54**.

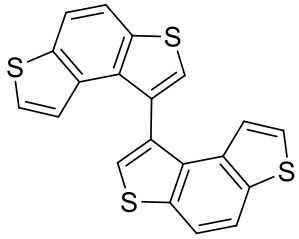

Dimer 54a. The crude product obtained from the Pd-catalysed homocoupling reaction of bromide **55a** was purified by chromatography on silica gel (hexane) to give **54a** (243 mg, 86%) as colourless solid. M.p. (hexane) 178–180 °C. ^{1}H NMR (300 MHz, $CDCl_3$): δ = 7.93 (d, J = 8.7 Hz, 2H), 7.89 (d, J = 8.7 Hz, 2H), 7.58 (s, 2H), 7.09 (d, J = 5.5 Hz, 2H), 6.49 (d, J = 5.5 Hz, 2H). ^{13}C NMR (75 MHz, $CDCl_3$): δ = 137.5 (Cq), 136.7 (Cq), 134.6 (Cq), 133.8 (Cq), 132.8 (Cq), 126.1 (CH), 125.7 (CH), 121.5 (CH), 119.5 (CH), 118.9 (CH). IR (neat): $\tilde{\nu}$ = 1382, 1269, 1260, 1153, 1090, 875, 855, 822, 813, 794, 784, 763, 741, 712, 462 cm^{-1}. HRMS (EI): calcd for $C_{20}H_{10}S_4$ $[M]^+$: 377.9665, found 377.9650.

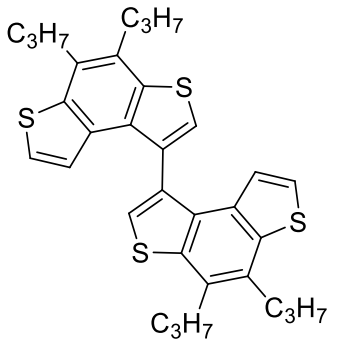

Dimer 54b. The crude product obtained from the Pd-catalysed homocoupling reaction of bromide **55b** was purified by chromatography on silica gel (hexane) to give **54b** (348 mg, 85%) as colourless solid. M.p. (pentane) 170–171 °C. ^{1}H NMR (300 MHz, $CDCl_3$): δ = 7.44 (s, 2H), 7.02 (d, J = 5.5 Hz, 2H), 6.55 (d, J = 5.5 Hz, 2H), 3.12–2.98 (m, 8H, CH_2), 1.88–1.80 (m, 8H, CH_2), 1.20–1.09 (m, 6H, CH_3). ^{13}C NMR (75 MHz, $CDCl_3$): δ = 139.8 (Cq), 139.0 (Cq), 133.7 (Cq), 132.8 (Cq), 132.1 (Cq), 130.7 (Cq), 130.2 (Cq), 124.5 (CH), 124.2 (CH), 122.3 (CH), 34.5 (CH_2), 34.2 (CH_2), 23.3 (CH_2), 23.1 (CH_2), 14.8 (CH_3), 14.7 (CH_3). IR (neat): $\tilde{\nu}$ = 2955, 2917, 2849, 1464, 1366, 1261, 1087, 1018, 1006, 854, 831, 817, 802, 766, 753, 709, 688, 645, 635, 423 cm^{-1}. HRMS (EI): calcd for $C_{32}H_{34}S_4$ $[M]^+$: 546.1543, found 546.1540.

General procedure for the synthesis of bromides 53a,b. To a mixture of **54** (0.20 mmol) in $CHCl_3$ (2 mL) and AcOH (2 mL) NBS (0.28–0.32 mmol, 50.0–56.6 mg) was added in portions and the resulting suspension was stirred at 35–45 °C. The outcome of the reaction was monitored by RP-HPLC analysis (acetonitrile as the eluent). After 8 hours, the mixture was cooled to room temperature, and a saturated solution of $NaHCO_3$ was slowly added under vigorously stirring until neutralization. The aqueous phase was extracted with CH_2Cl_2 (4 × 10 mL), and the collected organic phases were washed with H_2O (2 × 10 mL), dried over Na_2SO_4, and concentrated under reduced pressure. The residue was purified by column chromatography on silica gel to provide the required product **53.**

Bromide 53a. The crude product obtained from the bromination of **54a** was purified by column chromatography on silica gel with hexane as the eluent to give **53a** (58 mg, 64%) as colourless solid (RP-HPLC purity up to 90%). ^{1}H NMR (300 MHz, $CDCl_3$): δ = 7.96–7.86 (m, 3H), 7.79 (d, J = 8.7 Hz, 1H), 7.60 (s, 1H), 7.18 (d, J = 5.5 Hz, 1H), 7.12 (d, J = 5.5 Hz, 1H), 6.58 (d, J = 5.5 Hz, 1H), 6.38 (d, J = 5.5 Hz, 1H). ^{13}C NMR (75 MHz, $CDCl_3$): δ = 138.0 (Cq), 137.6 (Cq), 137.1 (Cq), 136.2 (Cq), 134.3 (Cq), 133.9 (Cq), 133.5 (Cq), 133.2 (Cq), 133.1 (Cq), 130.9 (Cq), 126.6 (CH), 126.5 (2CH), 121.2 (CH), 121.0 (CH), 119.7 (CH), 119.6 (CH), 119.0 (CH), 117.9 (CH), 116.2 (Cq). IR (neat): ν̃ = 1383, 1328, 1156, 1148, 1084, 866, 848, 822, 770, 756, 707, 679, 659, 633, 517, 462, 433, 423 cm^{-1}. HRMS (ESI): calcd for $C_{20}H_9BrS_4$ [M]$^+$: 455.8770, found 455.8794.

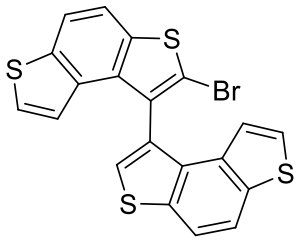

Bromide 53b. The crude product obtained from the bromination of **54b** was purified by column chromatography on silica gel with hexane as the eluent to give **53b** (76 mg, 60%) as colourless solid. M.p. (hexane) 155–157 °C. ^{1}H NMR (300 MHz, $CDCl_3$): δ = 7.46 (s, 1H, Het), 7.09 (d, J = 5.5 Hz, 1H, Het), 7.03 (d, J = 5.5 Hz, 1H, Het), 6.62 (d, J = 5.6 Hz, 1H, Het), 6.40 (d, J = 5.6 Hz, 1H, Het), 3.12–2.95 (m, 8H, CH_2), 1.95–1.75 (m, 8H, CH_2), 1.26–1.07 (m, 12H, CH_3). ^{13}C NMR (75 MHz, $CDCl_3$): δ = 140.1 (Cq), 139.8 (Cq), 139.3 (Cq), 138.5 (Cq), 134.1 (Cq), 132.5 (Cq), 132.2 (Cq), 131.8 (Cq), 131.7 (Cq), 131.3 (Cq), 131.1 (Cq), 130.8 (Cq), 130.2 (Cq), 129.3 (Cq), 125.0 (CH), 124.9 (CH), 124.8 (CH), 121.9 (CH), 121.8 (CH), 114.5 (Cq), 34.5 (CH_2), 34.4 (CH_2), 34.2 (CH_2), 34.1 (CH_2), 23.3 (CH_2), 23.2 (CH_2), 23.1 (CH_2), 23.0 (CH_2), 14.8 (CH_3), 14.7 (CH_3). IR (neat): ν̃ = 2955, 2924, 2865, 2852, 1467, 1451, 1375, 1364, 1267, 1172, 1160, 1087, 854, 828, 817, 768, 753, 709, 644, 637, 422 cm^{-1}. HRMS (EI): calcd for $C_{32}H_{33}S_4Br$ [M]$^+$: 624.0649, found 624.0686.

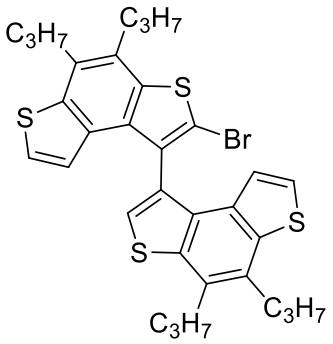

General procedure for the synthesis of 7,8-disubstituted tetrathia[7]helicenes 62a–h. To a flame-dried reaction vessel bromide **53** (0.10 mmol), $Pd(dppf)Cl_2$ (3.7 mg, 0.005 mmol), LiBr (8.6 mg, 0.10 mmol), K_2CO_3 (41.5 mg, 0.30 mmol) and alkyne **67** (0.15 mmol), if a solid, were added. The reaction vessel was fitted with a silicon septum, evacuated and back-filled with nitrogen, and this sequence was repeated twice. Deaerated DMF (5 mL) and alkyne **67** (0.15 mmol), if a liquid, were then added successively under a stream of nitrogen at room temperature. The resulting mixture was stirred at reflux under nitrogen for 4–6 h. The outcome of the reaction was monitored by TLC analysis. After completion of the reaction, the mixture was cooled to room temperature and poured into water (20 mL). The aqueous phase was extracted with CH_2Cl_2 (4 × 10 mL), and the collected organic phases were washed with brine (2 × 20 mL), dried over Na_2SO_4, and concentrated under reduced pressure. The residue was purified by column chromatography on silica gel to provide the required product **62**.

Helicene 62a. The crude product obtained from the Pd-catalysed annulation reaction between bromide **53b** and alkyne **67a** was purified by column chromatography on silica gel with hexane as the eluent to give **62a** (56 mg, 78%) as yellow solid. M.p. (heptane) 298–300 °C. ^{1}H NMR (300 MHz, $CDCl_3$): δ = 7.52–7.28 (m, 10H, phenyl), 6.82 (d, *J* = 5.6 Hz, 2H, thiophene-7TH), 6.80 (d, *J* = 5.6 Hz, 2H, thiophene-7TH), 3.14–3.01 (m, 8H, CH_2), 1.89–1.81 (m, 8H, CH_2), 1.16–1.09 (m, 12H, CH_3). ^{13}C NMR (150 MHz, $CDCl_3$): δ = 139.3 (2Cq), 139.1 (Cq), 138.7 (Cq), 134.2 (Cq), 132.8 (Cq), 132.4 (Cq), 130.4 (2CH), 129.9 (Cq), 129.8 (Cq), 129.5 (Cq), 128.2 (2CH), 127.5 (CH), 125.9 (CH), 122.4 (CH), 34.6 (CH_2), 34.3 (CH_2), 23.3 ($2CH_2$), 14.7 ($2CH_3$). IR (neat): ν̃ = 2956, 2922, 2866, 2863, 1741, 1599, 1555, 1462, 1455, 1441, 1376, 1346, 1327, 1263, 1234, 1207, 1105, 1089, 1028, 916, 886, 843, 832, 818, 768, 753, 741, 698, 666, 647, 633, 609, 542, 433 cm^{-1}. HRMS (EI): calcd for C46H42S4 [M]$^{+}$: 722.2169, found 722.2155.

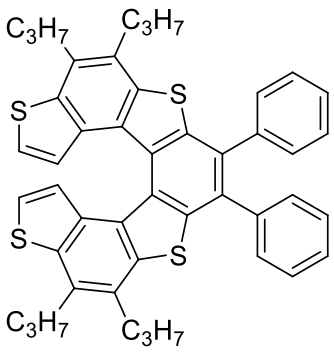

Helicene 62b. The crude product obtained from the Pd-catalysed annulation reaction between bromide **53a** and alkyne **67a** was purified by column chromatography on silica gel with hexane as the eluent to give **62b** (44 mg, 80%) as yellow solid. M.p. (hexane/CH_2Cl_2) 308–310 °C. ^{1}H NMR (300 MHz, $CDCl_3$): *δ* = 8.02 (d, *J* = 8.5 Hz, 2H, Ar-7TH), 7.89 (d, *J* = 8.3 Hz, 2H, Ar-7TH), 7.50–7.30 (m, 10H, phenyl), 6.95 (d, *J* = 5.6 Hz, 2H, thiophene-7TH), 6.84 (d, *J* = 5.5 Hz, 2H, thiophene-7TH). ^{13}C NMR (75 MHz, $CDCl_3$): *δ* = 140.5 (Cq), 138.7 (Cq), 137.4 (Cq), 136.7 (Cq), 136.1 (Cq), 133.0 (Cq), 131.2 (Cq), 130.3 (2CH), 129.2 (Cq), 128.3 (2CH), 127.7 (CH), 125.3 (CH), 124.4 (CH), 121.3 (CH), 118.5 (CH). IR (neat): ν̃ = 3091, 3061, 2955, 2921, 2851, 1867, 1734, 1599, 1493, 1441, 1399, 1379, 1354, 1327, 1260, 1223, 1191, 1157, 1092, 1069, 1025, 913, 899, 887, 853, 842, 825, 809, 791, 771, 761, 743, 730, 712, 700, 680, 641, 612, 602, 594, 566, 552, 523, 490, 482, 464, 451, 429 cm^{-1}. HRMS (ESI): calcd for $C_{34}H_{18}S_4$ [M]$^{+}$: 554.0291, found 554.0291.

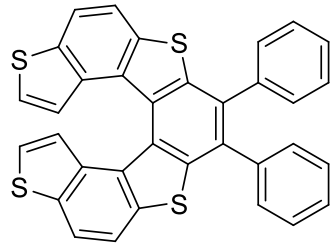

Helicene 62c. The crude product obtained from the Pd-catalysed annulation reaction between bromide **53b** and alkyne **67b** was purified by column chromatography on silica gel with the mixture of hexane/CH_2Cl_2 (9:1) as the eluent to give **62c** (50 mg, 68%) as yellow solid. M.p. (heptane) 254–256 °C. ^{1}H NMR (300 MHz, $CDCl_3$): *δ* = 7.43 (dd, *J* = 5.1, 1.0 Hz, 2H, thienyl), 7.31 (dd, *J* = 3.5, 1.0 Hz, 2H, thienyl), 7.14 (dd, *J* = 5.1, 3.5 Hz, 2H, thienyl), 6.81 (d, *J* = 5.6 Hz, 2H, thiophene-7TH), 6.72 (d, *J* = 5.6 Hz, 2H, thiophene-7TH), 3.17–2.99 (m, 8H, CH_2), 1.92–1.81 (m, 8H, CH_2), 1.14 (t, *J* = 7.3 Hz, 12H, CH_3). ^{13}C NMR (150 MHz, $CDCl_3$): *δ* = 140.1 (Cq), 139.7 (Cq), 139.5 (Cq), 138.8 (Cq), 134.2 (Cq), 133.2 (Cq), 130.3 (Cq), 129.7 (Cq), 129.2 (Cq), 129.1 (CH), 127.2 (CH), 126.8 (CH), 126.3 (Cq), 125.8

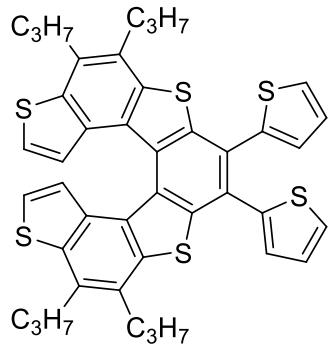

(CH), 122.6 (CH), 34.6 (CH_2), 34.3 (CH_2), 23.3 ($2CH_2$), 14.74 (CH_3), 14.67 (CH_3). IR (neat): ν˜ = 2956, 2922, 2852, 1737, 1464, 1260, 1207, 1168, 1090, 1019, 851, 800, 696, 646 cm^{-1}. HRMS (EI): calcd for $C_{42}H_{38}S_6$ $[M]^+$: 734.1298, found 734.1300.

Helicene 62d.

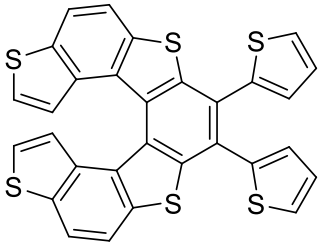

The crude product obtained from the Pd-catalysed annulation reaction between bromide **53a** and alkyne **67b** was purified by column chromatography on silica gel with the mixture of hexane/CH_2Cl_2 (95:5) as the eluent to give **62d** (35 mg, 63%) as yellow solid. M.p. (heptane) 348–349 °C. ^{1}H NMR (300 MHz, $CDCl_3$): δ = 8.04 (d, J = 8.5 Hz, 2H, Ar-7TH), 7.92 (d, J = 8.5 Hz, 2H, Ar-7TH), 7.44 (dd, J = 5.1, 1.0 Hz, 2H, thienyl), 7.33 (dd, J = 3.5, 1.0 Hz, 2H, thienyl), 7.13 (dd, J = 5.1, 3.6 Hz, 2H, thienyl), 6.94 (d, J = 5.6 Hz, 2H, thiophene-7TH), 6.76 (d, J = 5.6 Hz, 2H, thiophene-7TH). ^{13}C NMR (75 MHz, $CDCl_3$): δ = 142.4 (Cq), 141.2 (Cq), 139.2 (Cq), 137.6 (Cq), 136.7 (Cq), 136.1 (Cq), 130.9 (Cq), 129.7 (Cq), 129.1 (CH), 127.4 (CH), 126.8 (CH), 125.2 (CH), 124.6 (CH), 121.6 (CH), 118.5 (CH). IR (neat): ν˜ = 1381, 1325, 1293, 1212, 1194, 1181, 1159, 1091, 1078, 1046, 1024, 900, 890, 853, 827, 793, 770, 754, 698, 649, 596, 545, 492, 474, 454, 434, 421 cm^{-1}. HRMS (EI): calcd for $C_{30}H_{14}S_6$ $[M]^+$: 565.9420, found 565.9420.

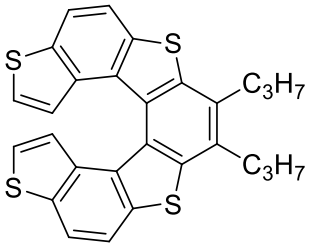

Helicene 62e. The crude product obtained from the Pd-catalysed annulation reaction between bromide **53a** and alkyne **67c** was purified by column chromatography on silica gel with hexane as the eluent to give **62e** (24 mg, 50%) as colourless solid. ^{1}H NMR (300 MHz, $CDCl_3$): δ = 7.99 (d, J = 8.6 Hz, 2H, Ar-7TH), 7.95 (d, J = 8.6 Hz, 2H, Ar-7TH), 6.88 (d, J = 5.6 Hz, 2H thiophene-7TH), 6.74 (d, J = 5.6 Hz, 2H, thiophene-7TH), 3.22–3.03 (m, 4H, CH_2), 1.91–1.85 (m, 4H, CH_2), 1.16 (t, J = 7.3 Hz, 6H, CH_3). Spectroscopic data are in agreement with those reported in literature. [182]

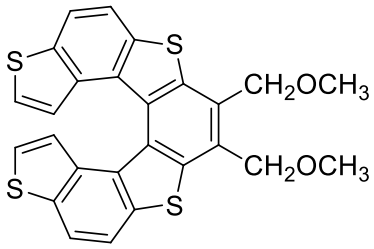

Helicene 62f. The crude product obtained from the Pd-catalysed annulation reaction between bromide **53a** and alkyne **67d** was purified by column chromatography on silica gel with the mixture of hexane/CH_2Cl_2 (1:1) as the eluent to give **62f** (22 mg, 46%) as yellow solid. M.p. (heptane) 167–168 °C. ^{1}H NMR (300 MHz, $CDCl_3$): δ = 8.04 (d, J = 8.5 Hz, 2H, Ar-7TH), 7.97 (d, J = 8.5 Hz, 2H, Ar-7TH), 6.89 (d, J = 5.5 Hz, 2H, thiophene-7TH), 6.68 (d, J = 5.5 Hz, 2H, thiophene 7-TH), 5.15 (d, J = 12.2 Hz, 2H, CH_2), 5.05 (d, J = 12.2 Hz, 2H, CH_2), 3.51 (s, 6H, OCH_3). ^{13}C NMR (75 MHz, $CDCl_3$): δ = 139.4 (Cq), 137.1 (Cq), 136.6 (Cq), 136.0 (Cq), 130.7 (Cq), 130.1 (Cq), 128.5 (Cq), 125.1 (CH), 124.4 (CH), 121.5 (CH), 118.5 (CH), 70.3 (CH_2), 58.3 (OCH_3). IR (neat): ν˜ = 3096, 2921, 2873, 2814, 1716, 1659, 1559, 1447, 1379, 1326, 1187,

1160, 1145, 1086, 997, 950, 885, 821, 788, 769, 704, 655, 540, 528, 469, 458 cm^{-1}. HRMS (EI): calcd for $C_{26}H_{18}O_2S_4$ $[M]^+$: 490.0190, found 490.0189.

Helicene 62g. The crude product obtained from the Pd-catalysed annulation reaction between bromide **53a** and alkyne **67e** was purified by column chromatography on silica gel with the mixture of hexane/CH_2Cl_2 (95:5) as the eluent to give **62g** (33 mg, 60%) as yellow solid. M.p. (hexane/CH_2Cl_2) 344–345 °C. ^{1}H NMR (400 MHz, $CDCl_3$): δ = 8.04–8.01 (m, 2H, Ar-7TH), 7.93 (d, J = 8.5 Hz, 1H, Ar-7TH), 7.88 (d, J = 8.6 Hz, 1H, Ar-7TH), 7.52–7.38 (m, 5H, phenyl), 7.36 (dd, J = 5.2, 1.1 Hz, 1H, thienyl), 7.23 (dd, J = 3.5, 1.1 Hz, 1H, thienyl), 7.06 (dd, J = 5.1, 3.6 Hz, 1H, thienyl), 6.95–6.93 (m, 2H, thiophene-7TH), 6.82–6.79 (m, 2H, thiophene-7TH). ^{13}C NMR (75 MHz, $CDCl_3$): δ = 141.2 (Cq), 140.4 (Cq), 139.3 (Cq), 138.8 (Cq), 137.8 (Cq), 137.3 (Cq), 136.7 (Cq), 136.2 (Cq), 136.1 (Cq), 134.1 (Cq), 131.6 (Cq), 131.1 (Cq), 131.0 (Cq), 130.1 (2CH), 129.6 (Cq), 129.2 (Cq), 128.9 (CH), 128.4 (2CH), 128.1 (CH), 127.1 (CH), 126.7 (CH), 125.8 (Cq), 125.2 (2CH), 124.5 (CH), 124.4 (CH), 121.5 (CH), 121.4 (CH), 118.5 (2CH). IR (neat): ν̃ = 1382, 1327, 1288, 1189, 1158, 899, 887, 854, 833, 825, 792, 769, 752, 733, 713, 702, 646, 597, 593, 546, 490, 482, 451 cm^{-1}. HRMS (EI): calcd for $C_{32}H_{16}S_5$ $[M]^+$: 559.9856, found 559.9856.

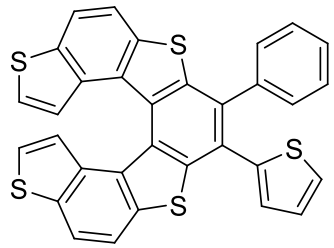

Helicene 62h. The crude product obtained from the Pd-catalysed annulation reaction between bromide **53a** and alkyne **67f** was purified by column chromatography on silica gel with the mixture of hexane/CH_2Cl_2 (9:1) as the eluent to give **62h** (38 mg, 75%) as colourless solid. M.p. (heptane) 279–282 °C. ^{1}H NMR (300 MHz, $CDCl_3$): δ = 8.06–7.96 (m, 3H, Ar-7TH), 7.84 (d, J = 8.5 Hz, 1H, Ar-7TH), 7.61–7.49 (m, 5H, phenyl), 6.93-6.90 (m, 2H, thiophene-7TH), 6.82–6.78 (m, 2H, thiophene 7TH), 3.01 (q, J = 7.7 Hz, 2H, CH_2), 1.32 (t, J = 7.5 Hz, 3H, CH_3). ^{13}C NMR (75 MHz, $CDCl_3$): δ = 140.7 (Cq), 139.0 (Cq), 138.8 (Cq), 137.1 (Cq), 136.7 (Cq), 136.5 (Cq), 136.4 (Cq), 136.2 (Cq), 136.0 (Cq), 133.7 (Cq), 133.3 (Cq), 131.4 (Cq), 131.2 (Cq), 129.8 (CH), 129.5(CH), 129.4 (Cq), 128.85 (CH), 128.78 (CH), 128.2 (CH), 127.9 (Cq), 125.3 (CH), 125.2 (CH), 124.3 (CH), 124.1 (CH), 121.2 (CH), 120.9 (CH), 118.6 (CH), 118.5 (CH), 25.9 (CH_2), 14.3 (CH_3). IR (neat): ν̃ = 2962, 2920, 2850, 1732, 1599, 1459, 1441, 1381, 1326, 1260, 1187, 1159, 1058, 1024, 901, 884, 856, 814, 790, 764, 700, 634, 594, 486, 470 cm^{-1}. HRMS (EI): calcd for $C_{30}H_{18}S_4$ $[M]^+$: 506.0291, found 506.0304.

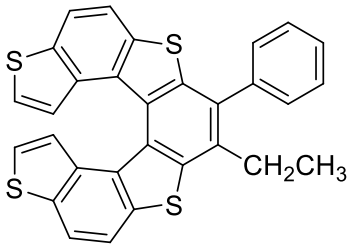

General Procedure for the synthesis of alkynes 63a–g. A deaerated mixture of bromide **53** (0.2 mmol), alkyne **68** (0.21–0.4 mmol), $Pd(PPh_3)_2Cl_2$ (14 mg, 0.02 mmol), CuI (3.8 mg, 0.02 mmol) in dry THF (5 mL) and DIPEA (5 mL) was stirred at 70 °C for 9 hours under a nitrogen atmosphere. The outcome of the reaction was monitored by TLC analysis. After completion of the reaction, the mixture was cooled to room

temperature and poured into a saturated NH_4Cl solution (10 mL). The aqueous phase was extracted with CH_2Cl_2 (4 × 15 mL), and the collected organic phases were washed with water (2 × 15 mL), dried over Na_2SO_4, and concentrated under reduced pressure. The residue was purified by column chromatography on silica gel to provide the required product **63**.

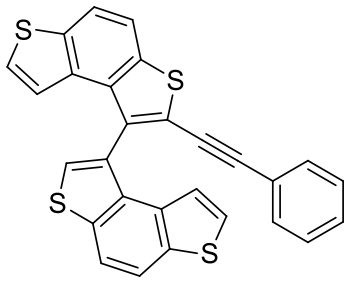

Alkyne 63a. The crude product obtained from the Sonogashira reaction between bromide **53a** and alkyne **68a** (0.4 mmol) was purified by column chromatography on silica gel with the mixture of hexane/CH_2Cl_2 (9:1) as the eluent to give **63a** (83 mg, 87%) as colourless solid, m.p. (hexane/CH_2Cl_2) 203–206 °C. ^{1}H NMR (300 MHz, CD_2Cl_2): δ = 8.01–7.87 (m, 4H, Ar), 7.75 (s, 1H, thiophene), 7.26–7.10 (m, 7H), 6.60 (d, J = 5.5 Hz, 1H, thiophene), 6.52 (d, J = 5.5 Hz, 1H, thiophene). ^{13}C NMR (125 MHz, $CDCl_3$): δ = 137.9 (Cq), 137.5 (Cq), 137.0 (Cq), 136.8 (Cq), 136.2 (Cq), 134.6 (Cq), 134.5 (Cq), 133.60 (Cq), 133.59 (Cq), 131.43 (Cq), 131.35 (2CH), 128.5 (CH), 128.2 (2CH), 126.51 (CH), 126.48 (CH), 126.1 (CH), 122.5 (Cq), 122.4 (Cq), 121.7 (CH), 121.6 (CH), 120.6 (CH), 119.4 (CH), 119.0 (CH), 118.4 (CH), 97.8 (C≡C), 82.7 (C≡C). IR (neat): $\tilde{\nu}$ = 1594, 1566, 1493, 1440, 1383, 1332, 1252, 1193, 1158, 1146, 1067, 1024, 962, 920, 887, 854, 835, 822, 807, 789, 770, 760, 743, 714, 704, 690, 666, 643, 555, 534, 516, 495, 482, 471, 456, 427 cm^{-1}. HRMS (EI): calcd for $C_{28}H_{14}S_4$ $[M]^+$: 477.9978, found 477.9987.

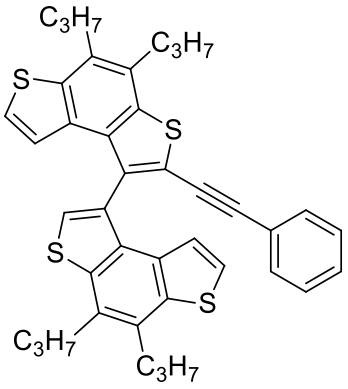

Alkyne 63b. The crude product obtained from the Sonogashira reaction between bromide **53b** and alkyne **68a** (0.4 mmol) was purified by column chromatography on silica gel with the mixture of hexane/CH_2Cl_2 (19:1) as the eluent to give **63b** (107 mg, 83%) as colourless solid. M.p. (heptane) 80–85 °C. ^{1}H NMR (300 MHz, $CDCl_3$): δ = 7.55 (s, 1H, thiophene), 7.20–7.12 (m, 3H, phenyl), 7.05 (d, J = 5.6 Hz, 2H, thiophene), 7.02–6.99 (m, 2H, phenyl), 6.71 (d, J = 5.6 Hz, 1H, thiophene), 6.63 (d, J = 5.6 Hz, 1H, thiophene), 3.14–2.95 (m, 8H, CH_2), 1.93–1.80 (m, 8H, CH_2), 1.18 (t, J = 7.3 Hz, 6H, CH_3), 1.12 (t, J = 7.3 Hz, 6H, CH_3). ^{13}C NMR (75 MHz, $CDCl_3$): δ = 140.2 (Cq), 139.7 (Cq), 139.2 (Cq), 138.4 (Cq), 137.9 (Cq), 132.8 (Cq), 132.7 (Cq), 132.2 (Cq), 132.1 (Cq), 131.8 (Cq), 131.3 (2CH), 130.6 (Cq), 130.1 (Cq), 129.8 (Cq), 128.2 (CH), 128.1 (2CH), 124.9 (2CH), 124.4 (CH), 122.7 (Cq), 122.5 (CH), 122.4 (CH), 120.8 (Cq), 97.2 (C≡C), 83.2 (C≡C), 34.5 ($2CH_2$), 34.2 ($2CH_2$), 23.3 (CH_2), 23.1 ($3CH_2$), 14.7 ($4CH_3$). IR (neat): $\tilde{\nu}$ = 2956, 2927, 2868, 1454, 1444, 1087, 884, 851, 830, 818, 769, 752, 710, 687, 644, 525, 506 cm^{-1}. HRMS (EI): calcd for $C_{40}H_{38}S_4$ $[M]^+$: 646.1856, found 646.1858.

Alkyne 63c. The crude product obtained from the Sonogashira reaction between bromide **53a** and alkyne **68b** (0.21 mmol) was purified by column chromatography on silica gel with the mixture of hexane/CH_2Cl_2 (7:3) as the eluent to give **63c** (60 mg, 59%) as colourless solid, M.p. (hexane/ CH_2Cl_2) 208–212 °C. ^{1}H NMR (300 MHz, $CDCl_3$): δ = 7.96–7.88 (m, 3H, Ar), 7.83 (d, *J* = 8.6 Hz, 1H, Ar), 7.68 (s, 1H, thiophene), 7.14–7.10 (m, 2H, thiophene), 7.03 (d, *J* = 8.7 Hz, 2H, phenyl), 6.72 (d, *J* = 8.8 Hz, 2H, phenyl), 6.66 (d, *J* = 5.5 Hz, 1H, thiophene), 6.53 (d, *J* = 5.5 Hz, 1H, thiophene), 3.75 (s, 3H, OCH_3). ^{13}C NMR (75 MHz, $CDCl_3$): δ = 159.8 (Cq), 137.9 (Cq), 137.4 (Cq), 136.9 (Cq), 136.1 (Cq), 135.9 (Cq), 134.6 (Cq), 134.4 (Cq), 133.7 (2Cq), 132.9 (2CH), 131.6 (Cq), 126.44 (CH), 126.39 (CH), 126.0 (CH), 122.9 (Cq), 121.7 (2CH), 120.4 (CH), 119.4 (CH), 119.0 (CH), 118.4 (CH), 114.5 (Cq), 113.9 (2CH), 98.0 (C≡C), 81.5 (C≡C), 55.2 (OCH_3). IR (neat): ν˜ = 2955, 2920, 2850, 1739, 1601, 1505, 1462, 1439, 1386, 1290, 1247, 1173, 1155, 1108, 1090, 1056, 1020, 973, 854, 826, 786, 761, 708, 671, 525, 473, 457 cm^{-1}. HRMS (EI): calcd for $C_{29}H_{16}OS_4$ [M]+: 508.0084, found 508.0080.

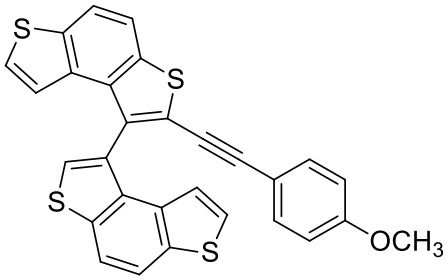

Alkyne 63d. The crude product obtained from the Sonogashira reaction between bromide **53a** and alkyne **68c** (0.4 mmol) was purified by column chromatography on silica gel with the mixture of hexane/ CH_2Cl_2 (7:3) as the eluent to give **63d** (90 mg, 82%) as colourless solid. M.p. (hexane/ CH_2Cl_2) 192–195 °C. ^{1}H NMR (300 MHz, $CDCl_3$): *δ* = 7.98–7.90 (m, 3H, Ar), 7.85 (d, *J* = 8.7 Hz, 1H, Ar), 7.69 (s, 1H, thiophene), 7.44 (d, *J* = 8.2 Hz, 2H, phenyl), 7.16–7.14 (m, 4H), 6.63 (d, *J* = 5.5 Hz, 1H, thiophene), 6.57 (d, *J* = 5.5 Hz, 1H, thiophene). ^{13}C NMR (125 MHz, $CDCl_3$): *δ* = 138.1 (Cq), 137.9 (Cq), 137.6 (Cq), 137.0 (Cq), 136.5 (Cq), 134.6 (Cq), 134.5 (Cq), 133.5 (Cq), 133.5 (Cq), 131.5 (CH), 131.2 (Cq), 130.1 (m, *J* = 130 Hz, C-CF_3), 126.8 (CH), 126.5 (CH), 126.2 (CH), 126.2 (Cq), 125.1 (m, *J* = 15 Hz, CH), 123.8 (m, *J* = 1080 Hz, CF_3), 121.6 (CH), 121.5 (Cq), 121.5 (CH), 121.0 (CH), 119.5 (CH), 119.0 (CH), 118.4 (CH), 96.2 (C≡C), 85.1 (C≡C). ^{19}F NMR (300 MHz, $CDCl_3$): *δ* = – 62.94. IR: (neat) ν̃ = 3091, 2917, 2848, 2360, 2341, 2204, 1612, 1387, 1318, 1255, 1160, 1116, 1104, 1065, 1014, 970, 918, 884, 835, 819, 781, 757, 731, 708, 670, 594, 570, 517, 458 cm^{-1}. HRMS (EI): calcd for $C_{29}H_{13}F_3S_4$ $[M]^+$: 545.9852, found 545.9852.

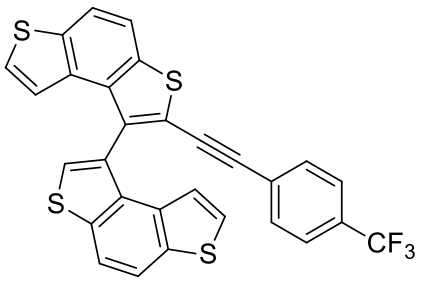

Alkyne 63e. The crude product obtained from the Sonogashira reaction between bromide **53a** and alkyne **68d** (0.4 mmol) was purified by column chromatography on silica gel with the mixture of hexane/CH_2Cl_2 (7:3) as the eluent to give **63e** (85 mg, 88%) as colourless solid. M.p. (hexane/ CH_2Cl_2) 208–210 °C. ^{1}H NMR (300 MHz, $CDCl_3$): δ = 7.99–7.87 (m, 3H, Ar), 7.83 (d, J = 8.7 Hz, 1H, Ar), 7.67 (s, 1H, Het), 7.21–7.09 (m, 4H), 6.80 (dd, J = 4.8, 1.4 Hz, 1H, thiophene), 6.65 (d, J = 5.5 Hz, 1H, thiophene), 6.52 (d, J = 5.5 Hz, 1H, thiophene). ^{13}C NMR (125 MHz, $CDCl_3$): δ = 137.9 (Cq), 137.4 (Cq), 136.9 (Cq), 136.6 (Cq), 136.1 (Cq), 134.6 (Cq), 134.5 (Cq), 134.4 (Cq), 133.6 (Cq), 131.4 (Cq), 129.6 (CH), 129.1 (CH), 126.5 (CH), 126.5 (CH), 126.1 (CH), 125.3 (CH), 122.4 (Cq), 121.7 (CH), 121.6 (CH), 121.5 (Cq), 120.5 (CH), 119.4 (CH), 119.0 (CH), 118.4 (CH), 92.9 (C≡C), 82.1 (C≡C). IR: (neat) $\tilde{\nu}$ = 3104, 3082, 2962, 2907, 2853, 1779, 1587, 1564, 1525, 1482, 1396, 1326, 1300, 1258, 1194, 1149, 1132, 1078, 1044, 1014, 947, 937, 855, 784, 767, 744, 731, 704, 665, 627, 596, 579, 564, 537, 514, 490, 452 cm^{-1}. HRMS (EI): calcd for $C_{26}H_{12}S_5$ [M]$^+$: 483.9543, found 483.9549.

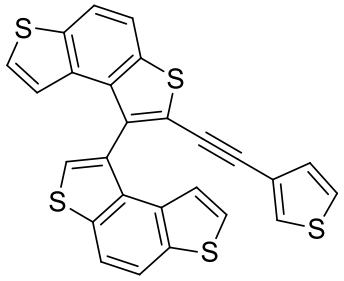

Alkyne 63f. The crude product obtained from the Sonogashira reaction between bromide **53a** and alkyne **68e** (0.4 mmol) was purified by column chromatography on silica gel with the mixture of hexane/CH_2Cl_2 (7:3) as the eluent to give **63f** (87 mg, 91%) as yellow solid. ^{1}H NMR (300 MHz, $CDCl_3$): δ = 8.43 (d, J = 5.9 Hz, 2H, pyridine), 7.99–7.88 (m, 3H, Ar), 7.84 (d, J = 8.7 Hz, 1H, Ar), 7.69 (s, 1H, thiophene), 7.15–7.12 (m, 2H, thiophene), 6.91 (dd, J = 4.5, 1.5 Hz, 2H, pyridine), 6.61 (d, J = 5.5 Hz, 1H, thiophene), 6.57 (d, J = 5.5 Hz, 1H, thiophene). ^{13}C NMR (75 MHz, $CDCl_3$): δ = 147.7 (CH), 139.4 (Cq), 138.2 (Cq), 137.6 (Cq), 137.1 (Cq), 137.0 (Cq), 134.7 (Cq), 134.4 (Cq), 133.3 (Cq), 132.4 (Cq), 130.9 (Cq), 127.1 (CH), 126.6 (CH), 126.4 (CH), 125.5 (CH), 121.6 (CH), 121.5 (CH), 121.3 (CH), 120.4 (Cq), 119.7 (CH), 119.0 (CH), 118.3 (CH), 94.4 (C≡C), 89.4 (C≡C). HRMS (EI): calcd for $C_{27}H_{13}NS_4$ [M]+: 478.9931, found 478.9932.

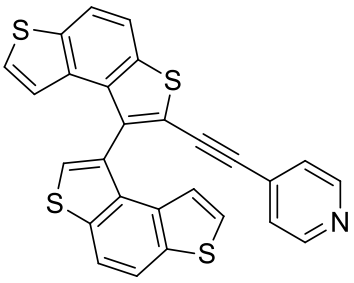

Alkyne 63g. The crude product obtained from the Sonogashira reaction between bromide **53a** and alkyne **68f** (0.4 mmol) was purified by column chromatography on silica gel with the mixture of hexane/CH_2Cl_2 (7:3) as the eluent to give **63g** (71 mg, 73%) as a colourless solid. M.p. (hexane) 74–76 °C. ^{1}H NMR (300 MHz, $CDCl_3$): δ = 7.94–7.86 (m, 3H, Ar), 7.79 (d, J = 8.6 Hz, 1H, Ar), 7.60 (s, 1H, thiophene), 7.11 (d, J = 5.5 Hz, 1H, thiophene), 7.09 (d, J = 5.5 Hz, 1H, thiophene), 6.62 (d, J = 5.5 Hz, 1H, thiophene), 6.47 (d, J = 5.5 Hz, 1H, thiophene), 2.17 (t, J = 7.0 Hz, 2H, CH_2), 1.31–0.96 (m, 8H, CH_2), 0.82 (t, J = 7.0 Hz, 3H, CH_3). ^{13}C NMR (125 MHz, $CDCl_3$): δ = 137.8 (Cq), 137.4 (Cq), 136.9

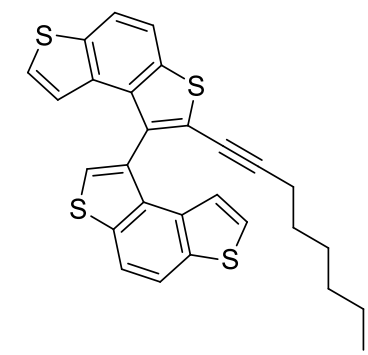

(Cq), 135.7 (Cq), 137.4 (Cq), 134.6 (Cq), 134.4 (Cq), 133.6 (Cq), 133.6 (Cq), 131.7 (Cq), 126.2 (CH), 126.2 (CH), 126.0 (CH), 123.5 (Cq), 121.6 (CH), 121.6 (CH), 120.1 (CH), 119.3 (CH), 118.9 (CH), 118.3 (CH), 94.8 (C≡C), 73.7 (C≡C), 31.2 (CH_2), 28.0 (CH_2), 28.0 (CH_2), 22.4 (CH_2), 19.6 (CH_2), 14.1 (CH_3). IR: (neat) $\tilde{\nu}$ = 3091, 2949, 2919, 2850, 1855, 1779, 1693, 1564, 1533, 1480, 1455, 1410, 1397, 1378, 1322, 1298, 1259, 1193, 1147, 1087, 1049, 1017, 896, 846, 817, 784, 767, 742, 700, 654, 635, 531, 509, 472, 454, 406 cm^{-1}. HRMS (EI): calcd for $C_{28}H_{22}S_4$ $[M]^+$: 486.0604, found 486.0604.

General procedure for the synthesis of 7-substituted tetrathia[7]helicenes 64a–d. To a flame-dried reaction vessel, alkynes **63** (0.20 mmol), $PtCl_2$ (5.3 mg, 0.02 mmol) or $InCl_3$ (4.4 mg, 0.02 mmol) were added. The reaction vessel was fitted with a silicon septum, evacuated and back-filled with argon, and this sequence was repeated twice. Deaerated toluene (1 mL) was added successively under a stream of argon at room temperature. The resulting mixture was stirred at 60 or 80 °C under argon for 10 hours. The outcome of the reaction was monitored by TLC analysis. After completion of the reaction, the mixture was cooled to room temperature and the solvent was removed under reduced pressure. The crude mixture was purified by column chromatography on silica gel to provide the required product **64**.

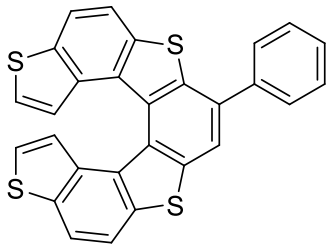

Helicene 64a. The crude product obtained from the cycloisomerisation of **63a** in the presence of $PtCl_2$ (5.3 mg, 0.02 mmol) at 60 °C was purified by column chromatography on silica gel with the mixture of hexane/CH_2Cl_2 (7:3) as the eluent to give **64a** (34 mg, 36%) as yellow solid. M.p. (hexane/CH_2Cl_2) 301–308 °C. ^{1}H NMR (500 MHz, $CDCl_3$): δ = 8.06–8.02 (m, 3H, Ar-7TH), 7.99 (d, *J* = 8.5 Hz, 1H, Ar-7TH), 7.94 (d, *J* = 8.5 Hz, 1H, Ar-7TH), 7.86–7.84 (m, 2H, phenyl), 7.60–7.57 (m, 2H, phenyl), 7.52–7.49 (m, 1H, phenyl), 6.94–6.91 (m, 2H, thiophene-7TH), 6.78–6.76 (m, 2H, thiophene-7TH). ^{13}C NMR (125 MHz, $CDCl_3$): δ = 140.0 (Cq), 138.5 (Cq), 137.6 (Cq), 137.2 (Cq), 136.9 (Cq), 136.74 (Cq), 136.66 (Cq), 136.2 (Cq), 136.1 (Cq), 134.8 (Cq), 131.1 (Cq), 130.8 (Cq), 130.4 (Cq), 129.0 (Cq), 128.9 (2CH), 128.6 (2CH), 128.4 (CH), 125.2 (2CH), 124.4 (2CH), 121.4 (CH), 121.3 (CH), 120.2 (CH), 118.7 (CH), 118.5 (CH). IR (neat): $\tilde{\nu}$ = 2953, 2921, 2852, 1564, 1444, 1382, 1327, 1260, 1196, 1152, 1086, 1027, 922, 895, 873, 821, 794, 788, 768, 745, 735, 697, 659, 622, 588, 578, 541, 519, 471, 455, 443 cm^{-1}. HRMS (EI) calcd for $C_{28}H_{14}S_4$ $[M]^+$: 477.9978, found 477.9986.

Helicene 64b. The crude product obtained from the cycloisomerisation of **63b** in the presence of $PtCl_2$ (0.02 mmol) at 60 °C was purified by column chromatography on silica gel with the mixture of hexane/CH_2Cl_2 (9:1) as the eluent to give **64b** (54 mg, 42%) as yellow solid. M.p. (heptane) 220–225 °C. ^{1}H NMR (300 MHz, $CDCl_3$): δ = 7.97 (s, 1H, Ar-7TH), 7.87–7.85 (m, 2H, phenyl), 7.62–7.58 (m, 2H, phenyl), 7.53–7.49 (m, 1H, phenyl), 6.82–6.79 (m, 2H, thiophene-7TH), 6.75 (d, *J* = 5.6 Hz, 2H, thiophene-7TH), 3.20–2.99 (m, 8H, CH_2), 1.98–1.81 (m, 8H, CH_2), 1.23–1.12 (m, 12H, CH_3). ^{13}C NMR (75 MHz, $CDCl_3$): δ = 140.4 (Cq), 139.0 (Cq), 138.9 (Cq), 138.8 (Cq), 138.7 (Cq), 137.7 (Cq), 136.6 (Cq), 134.25 (2Cq), 134.16 (Cq), 132.93 (Cq), 132.88 (Cq), 131.0 (Cq), 129.8 (Cq), 129.7 (Cq), 129.6 (Cq), 129.4 (Cq), 129.0 (Cq), 128.9 (2CH), 128.7 (2CH), 128.1 (CH), 125.9 (2CH), 122.4 (2CH), 119.7 (CH), 34.64 ($2CH_2$), 34.57 (CH_2), 34.3 (CH_2), 23.3 ($4CH_2$), 14.81 (CH_3), 14.76 (CH_3), 14.69 ($2CH_3$). IR (neat): ν̃ = 2957, 2927, 2868, 1495, 1469, 1454, 1334, 1158, 1029, 1088, 930, 881, 826, 818, 763, 751, 699, 646, 591 cm^{-1}. HRMS (EI): calcd for $C_{40}H_{38}S_4$ [M]$^+$: 646.1856, found 646.1865

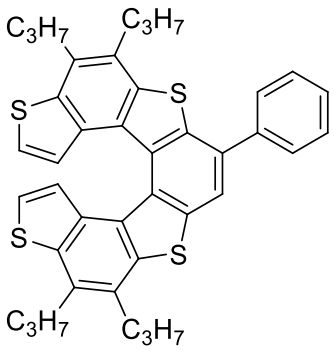

Helicene 64c. The crude product obtained from the cycloisomerisation of **63c** in the presence of $InCl_3$ (4.4 mg, 0.02 mmol) at 80 °C was purified by column chromatography on silica gel with the mixture of hexane/CH_2Cl_2 (9:1) as the eluent to give **64c** (74 mg, 73%) as yellow solid. M.p. (hexane/CH_2Cl_2) 245–248 °C. ^{1}H NMR (300 MHz, $CDCl_3$): δ = 8.05–7.92 (m, 5H), 7.78 (d, *J* = 8.6 Hz, 2H, phenyl), 7.12 (d, *J* = 8.6 Hz, 2H, phenyl), 6.93–6.91 (m, 2H, thiophene-7TH), 6.77 (d, *J* = 5.6 Hz, 2H, thiophene-7TH), 3.93 (s, 3H, OCH_3). ^{13}C NMR (75 MHz, $CDCl_3$): δ = 159.8 (Cq), 138.6 (Cq), 137.7 (Cq), 137.1 (Cq), 136.7 (2Cq), 136.6 (Cq), 136.1 (2Cq), 134.6 (Cq), 132.4 (Cq), 131.2 (Cq), 130.8 (Cq), 130.3 (Cq), 129.8 (2CH), 128.7 (Cq), 125.3 (2CH), 124.3 (2CH), 121.4 (CH), 121.2 (CH), 120.0 (CH), 118.7 (CH), 118.5 (CH), 114.4 (2CH), 55.4 (OCH_3). IR (neat): ν̃ = 3083, 3013, 2955, 2924, 2832, 1607, 1575, 1508, 1458, 1437, 1415, 1383, 1327, 1281, 1247, 1198, 1175, 1154, 1116, 1090, 1043, 1030, 923, 894, 884, 875, 831, 823, 809, 786, 768, 748, 737, 708, 695, 682, 658, 642, 602, 570, 556, 540, 512, 495, 474, 451, 420, 411, 407 cm^{-1}. HRMS (EI) calcd for $C_{29}H_{16}OS_4$ [M]+: 508.0084, found 508.0084.

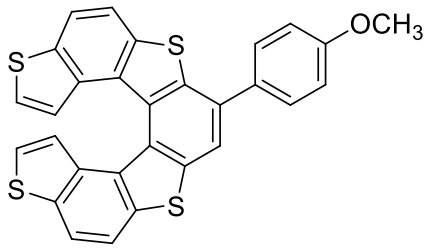

Helicene 64d. The crude product obtained from the cycloisomerisation of **63d** in the presence of $InCl_3$ (4.4 mg, 0.02 mmol) at 80 °C was purified by column chromatography on silica gel with the mixture of hexane/CH_2Cl_2 (9:1) as the eluent to give **64d** (74 mg, 73%) as yellow solid. M.p. (hexane/ CH_2Cl_2) 150–153 °C. ^{1}H NMR (500 MHz, $CDCl_3$): *δ* = 8.08–8.04 (m, 3H), 8.00–7.97 (m, 3H), 7.85 (d, *J* = 8.1 Hz, 2H, Ph), 6.94 (t, *J* = 5.4 Hz, 2H, Het), 6.76 (ddd, *J* = 5.6, 2.5, 0.6 Hz, 2H, Het). ^{13}C NMR (125 MHz, $CDCl_3$): *δ* =

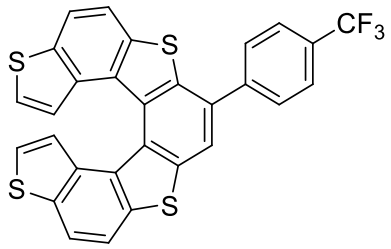

143.6 (Cq), 138.5 (Cq), 137.2 (Cq), 137.1 (Cq), 136.9 (Cq), 136.8 (Cq), 136.2 (Cq), 136.1 (Cq), 133.2 (Cq), 131.0 (Cq), 130.7 (Cq), 130.6 (Cq), 130.4 (m, J = 130 Hz, C-CF_3), 129.6 (Cq), 129.0 (2CH), 125.9 (m, J = 15 Hz, 2CH), 125.2 (CH), 125.1 (CH), 124.6 (2CH), 124.2 (m, J = 1084 Hz, CF_3), 121.7 (CH), 121.6 (CH), 120.3 (CH), 118.7 (CH), 118.4 (CH). ^{19}F NMR (300 MHz, $CDCl_3$): δ = − 62.49. IR: (neat) $\tilde{\nu}$ = 3088, 2921, 2848, 1923, 1859, 1614, 1573, 1448, 1409, 1382, 1320, 1262, 1190, 1165, 1130, 1108, 1070, 1041, 1014, 969, 886, 840, 821, 788, 767, 747, 731, 703, 663, 637, 613, 597, 576, 541, 519, 505, 492, 474, 456 cm^{-1}. HRMS (EI) calcd for $C_{29}H_{13}F_3S_4$ [M]$^+$: 545.9852, found 545.9851.

General Procedure for the synthesis of dimers 65a–c. A deaerated mixture of bromide **53** (0.1 mmol), (hetero)arylboronic acid **69** (0.2 mmol), Pd(dppf)Cl_2 (7.3 mg, 0.01 mmol), KF (17 mg, 0.3 mmol) in toluene (5 mL) and methanol (5 mL) was stirred at 70 °C for 9 hours under a nitrogen atmosphere. The outcome of the reaction was monitored by TLC analysis. After completion of the reaction, the mixture was cooled to room temperature and the solvent was removed under reduced pressure. The residue was taken up with CH_2Cl_2 and poured into water (10 mL). The aqueous phase was extracted with CH_2Cl_2 (4 × 5 mL), and the collected organic phases were dried over Na_2SO_4, and concentrated under reduced pressure. The crude was purified by column chromatography on silica gel to provide the required product **65**.

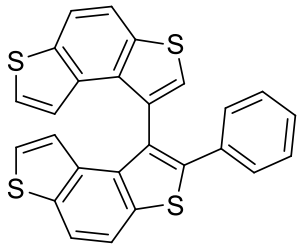

Dimer 65a. The crude product obtained from the Suzuki reaction between bromide **53a** and phenylboronic acid (**69a**) was purified by column chromatography on silica gel with hexane as the eluent to give **65a** (41 mg, 91%) as colourless solid. M.p. (heptane) 240–242 °C. ^{1}H NMR (400 MHz, $CDCl_3$): δ = 7.94–7.85 (m, 4H, Ar), 7.42 (s, 1H, thiophene), 7.33–7.30 (m, 2H, phenyl), 7.15–7.12 (m, 3H phenyl + 1H thiophene), 7.05 (d, J = 5.5 Hz, 2H, thiophene), 6.69 (d, J = 5.5 Hz, 1H, thiophene), 6.21 (d, J = 5.5 Hz, 1H, thiophene). ^{13}C NMR (125 MHz, $CDCl_3$): δ = 141.9 (Cq), 137.8 (Cq), 137.6 (Cq), 136.9 (Cq), 135.6 (Cq), 135.1 (Cq), 134.6 (2Cq), 134.4 (Cq), 134.0 (Cq), 132.4 (Cq), 128.8 (2CH), 128.5 (2CH), 128.2 (Cq), 127.9 (CH), 126.5 (CH), 125.97 (CH), 125.95 (CH), 121.5 (CH), 121.2 (CH), 119.6 (CH), 119.4 (CH), 119.1 (CH), 118.4 (CH). IR (neat): ν̃ = 1463, 1386, 1335, 1193, 1160, 1144, 1085, 930, 884, 853, 819, 783, 775, 763, 744, 711, 702, 693, 671, 603, 534, 516, 495, 477, 461 cm^{-1}. HRMS (EI): calcd for $C_{26}H_{14}S_4$ [M]$^+$: 453.9978, found 453.9979.

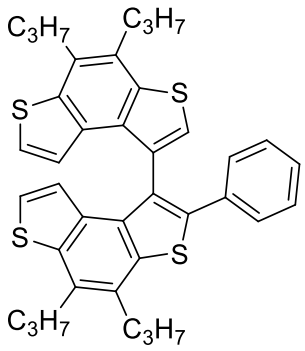

Dimer 65b. The crude product obtained from the Suzuki reaction between bromide **53b** and phenylboronic acid (**69a**) was purified by column chromatography on silica gel with hexane as the eluent to give **65b** (53 mg, 86%) as colourless solid. M.p. (hexane) 68–72 °C. ^{1}H NMR (300 MHz, $CDCl_3$): δ = 7.36–7.33 (m, 2H, phenyl), 7.31 (s, 1H, thiophene), 7.14–7.11 (m, 3H, phenyl), 7.03 (d, J = 5.6 Hz, 1H, thiophene), 6.96 (d, J = 5.5 Hz, 1H, thiophene), 6.72 (d, J = 5.6 Hz, 1H, thiophene), 6.19 (d, J = 5.6 Hz, 1H, thiophene), 3.11–

2.96 (m, 8H, CH_2), 1.99–1.77 (m, 8H, CH_2), 1.21–1.08 (m, 12H, CH_3). ^{13}C NMR (75 MHz, $CDCl_3$): δ = 140.2 (Cq), 140.0 (Cq), 139.8 (Cq), 139.2 (Cq), 137.2 (Cq), 134.4 (Cq), 133.9 (Cq), 133.2 (Cq), 132.9 (Cq), 132.8 (Cq), 132.6 (Cq), 130.8 (Cq), 130.7 (Cq), 130.2 (Cq), 129.7 (Cq), 129.1 (Cq), 128.8 (2CH), 128.4 (2CH), 127.5 (CH), 124.7 (CH), 124.4 (CH), 124.3 (CH), 122.3 (CH), 122.0 (CH), 34.52 (CH_2), 34.49 (CH_2), 34.2 ($2CH_2$), 23.3 (CH_2), 23.2 (CH_2), 23.1 ($2CH_2$), 14.7 ($4CH_3$). IR (neat): ν˜ = 2958, 2933, 2865, 1464, 1443, 1165, 1088, 932, 888, 854, 833, 822, 774, 755, 724, 713, 690, 644, 620, 600, 571, 522, 496, 425 cm^{-1}. HRMS (EI) calcd for $C_{38}H_{38}S_4$ $[M]^+$: 622.1856, found 622.1858.

Dimer 65c. The crude product obtained from the Suzuki reaction between bromide **53a** and 2-thienylboronic acid (**69b**) was purified by column chromatography on silica gel with hexane as the eluent to give **65c** (37 mg, 80%) as colourless solid. M.p. (heptane) 232–235 °C. ^1H NMR (500 MHz, $CDCl_3$): δ = 7.96 (d, *J* = 8.7 Hz, 1H, Ar) 7.90 (d, *J* = 8.7 Hz, 1H, Ar), 7.87–7.82 (m, 2H, Ar), 7.61 (s, 1H, thiophene), 7.18 (dd, *J* = 3.7, 1.1 Hz, 1H, thienyl), 7.11 (d, *J* = 5.5 Hz, 1H, thiophene), 7.09 (d, *J* = 5.6 Hz, 1H, thiophene), 7.04 (dd, *J* = 5.1, 1.2 Hz, 1H, thienyl), 6.85 (dd, *J* = 5.1, 3.7 Hz, 1H, thienyl), 6.65 (dd, *J* = 5.6, 0.7 Hz, 1H, thiophene), 6.35 (dd, *J* = 5.6, 0.6 Hz, 1H, thiophene). ^{13}C NMR (75 MHz, $CDCl_3$): δ = 138.0 (Cq), 137.5 (Cq), 137.4 (Cq), 136.1 (Cq), 135.7 (Cq), 135.4 (Cq), 134.59 (Cq), 134.55 (Cq), 134.2 (Cq), 133.6 (Cq), 131.7 (Cq), 127.5 (Cq), 127.1 (CH), 126.9 (CH), 126.8 (CH), 126.5 (CH), 126.4 (CH), 126.2 (CH), 121.4 (CH), 121.2 (CH), 119.69 (CH), 119.65 (CH), 119.0 (CH), 118.2 (CH). IR (neat): ν˜ = 1418, 1386, 1330, 1193, 1159, 1145, 1085, 880, 855, 823, 791, 773, 746, 694, 671, 645, 534, 463, 452 cm^{-1}. HRMS (EI): calcd for $C_{24}H_{12}S_5$ $[M]^+$: 459.9542, found 459.9549.

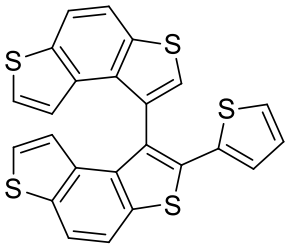

General Procedure for the synthesis of benzo fused helicenes 66a–c. A stirred solution of compound **65** (0.1 mmol) and a catalytic amount of iodine in toluene (750 mL) was irradiated at room temperature with a 125 W unfiltered medium-pressure Hg lamp. The outcome of the reaction was monitored by HPLC analysis (eluent: H2O/CH_3CN = 95:5). After completion of the reaction, the solvent was removed under reduced pressure, and the residue was purified by column chromatography on silica gel to provide the required product **66**.

Helicene 66a. The crude product obtained from the photocyclisation of **65a** was purified by column chromatography on silica gel with the mixture hexane/CH_2Cl_2 (9:1) as the eluent to give **66a** (44 mg, 99%) as colourless solid. M.p. (hexane/CH_2Cl_2) 293-294 °C. ^1H NMR (300 MHz, $CDCl_3$): δ = 8.33–8.30 (m, 2H, fused phenyl), 8.03 (s, 4H, Ar-7TH), 7.71–7.68 (m, 2H, fused phenyl), 6.90 (d, *J* = 5.6 Hz, 2H, thiophene-7TH), 6.83 (d, *J* = 5.6 Hz, 2H, thiophene-7TH). ^{13}C NMR (75 MHz, $CDCl_3$): δ = 137.3 (Cq), 136.9 (Cq), 135.9 (Cq), 135.7 (Cq), 132.0 (Cq), 127.9 (Cq), 127.5 (Cq), 127.2 (CH), 125.14 (CH), 125.07 (CH), 124.1 (CH), 120.9 (CH), 118.7 (CH). IR (neat): ν˜ = 1414,

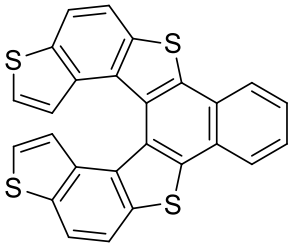

1382, 1372, 1330, 1300, 1282, 1226, 1190, 1157, 1095, 1033, 1015, 918, 897, 885, 827, 819, 787, 777, 766, 756, 740, 723, 702, 652, 620, 542, 466, 440 cm^{-1}. HRMS (EI): calcd for $C_{26}H_{12}S_4$ $[M]^+$: 451.9822, found 451.9822.

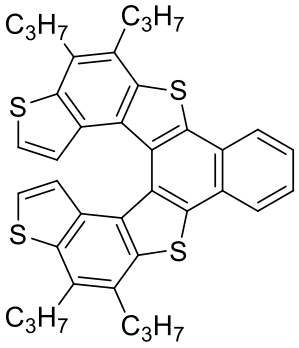

Helicene 66b. The crude product obtained from the photocyclisation of **65b** was purified by column chromatography on silica gel with the mixture hexane/ CH_2Cl_2 (9:1) as the eluent to give **66b** (56 mg, 91%) as colourless solid. M.p. (hexane) 244–247 °C. ^{1}H NMR (300 MHz, $CDCl_3$): δ = 8.35–8.31 (m, 2H, fused phenyl), 7.67–7.64 (m, 2H Ar-7TH), 6.81 (d, *J* = 5.7 Hz, 2H, thiophene-7TH), 6.78 (d, *J* = 5.5 Hz, 2H, thiophene-7TH), 3.20–3.00 (m, 8H, CH_2), 2.04–1.83 (m, 8H, CH_2), 1.24 (t, *J* = 7.3 Hz, 6H, CH_3), 1.16 (t, *J* = 7.3 Hz, 6H, CH_3). ^{13}C NMR (75 MHz, $CDCl_3$): δ = 139.0 (Cq), 137.8 (Cq), 136.0 (Cq), 134.1 (Cq), 132.4 (Cq), 130.3 (Cq), 129.8 (Cq), 128.7 (Cq), 127.4 (Cq), 126.6 (CH), 125.8 (CH), 124.9 (CH), 122.2 (CH), 34.6 ($2CH_2$), 23.4 ($2CH_2$), 14.9 (CH_3), 14.7 (CH_3). IR (neat): ν̃ = 2956, 2927, 2868, 1468, 1453, 1376, 1329, 1246, 1158, 1109, 1086, 1026, 939, 882, 818, 761, 743, 702, 673, 646, 622, 492, 420 cm^{-1}. HRMS (EI): calcd for $C_{38}H_{36}S_4$ $[M]^+$: 620.1700, found 620.1703.

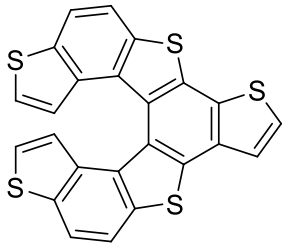

Helicene 66c. The crude product obtained from the photocyclisation of **65c** was purified by column chromatography on silica gel with the mixture hexane/CH_2Cl_2 (9:1) as the eluent to give **66c** (43 mg, 94%) as colourless solid. M.p. (heptane) 276–279 °C. ^{1}H NMR (500 MHz, $CDCl_3$): δ = 8.04–7.98 (m, 4H, Ar-7TH), 7.75 (d, *J* = 5.3 Hz, 1H, fused thiophene), 7.68 (d, *J* = 5.3 Hz, 1H, fused thiophene), 6.90 (d, *J* = 5.5 Hz, 1H, thiophene-7TH), 6.89 (d, *J* = 5.5 Hz, 1H, thiophene-7TH), 6.79 (dd, *J* = 5.6 Hz, 0.6 Hz, 1H, thiophene-7TH), 6.78 (dd, *J* = 5.6 Hz, 0.7 Hz, 1H, thiophene-7TH). ^{13}C NMR (125 MHz, $CDCl_3$): δ = 137.0 (Cq), 136.9 (Cq), 136.1 (Cq), 136.0 (Cq), 135.4 (Cq), 135.2 (Cq), 133.5 (Cq), 132.7 (Cq), 132.3 (Cq), 132.1 (Cq), 131.7 (Cq), 131.6 (Cq), 127.4 (2Cq), 127.1 (CH), 125.2 (2CH), 124.2 (CH), 124.1 (CH), 122.7 (CH), 121.0 (CH), 120.9 (CH), 118.72 (CH), 118.69 (CH). IR (neat): ν̃ = 3096, 2964, 2922, 2822, 1461, 1386, 1343, 1325, 1300, 1260, 1194, 1156, 1125, 1095, 1067, 1016, 934, 915, 896, 882, 855, 826, 816, 789, 776, 767, 749, 721, 701, 688, 639, 627, 586, 541, 507, 490, 479, 472, 459, 421 cm^{-1}. HRMS (EI): calcd for $C_{24}H_{10}S_5$ $[M]^+$: 457.9386, found 457.9384.

Chapter 2

Synthesis of thia[6]helicene derivatives through palladium-catalysed annulation of biaryl intermediates

This chapter describes a preliminary study for the synthesis of a novel class of thiaheterohelicenes exploiting the palladium-catalysed annulation reaction of iodobi(hetero)aryls, through a synthetic methodology very similar than that reported in *Chapter 1* for the synthesis of functionalised tetrathia[7]helicenes. This early-stage study aims to demonstrate the general and versatile character of this procedure that can be extended for the synthesis of other classes of heterohelicenes.

2.1 Novel class of thiaheterohelicenes through metal-catalysed annulation reactions

As previously reported in the *Introduction*, heterohelicenes find potential applications in manifold fields,[3,36] due to the presence of different heteroatoms in the helical backbone, that confer peculiar physical and chemical properties to the entire molecule. On the other hand, the number of aromatic rings as well as their orientation within the helical skeleton also play a pivotal role in determining the final photophysical and electronic properties of the helicene. However, the synthetic methodologies so far described generally provide a specific class of heterohelicenes, and often lack versatility to yield different helical skeletons. In this context, the versatility of the transition metal promoted methodologies reported in *Chapter 1* for the synthesis of 7-TH derivatives has been investigated to prepare different heterohelicenes, containing different heteroaromatic frameworks. In particular, we envisaged to prepare a novel class of thia[6]helicenes through a three-step procedure that involves the palladium-catalysed annulation of internal alkynes and iodides **70**, which in turn can be obtained by regioselective iodination of intermediates **71** exploiting the acidity of the α-position of the terminal thiophene ring (*Scheme 42*).

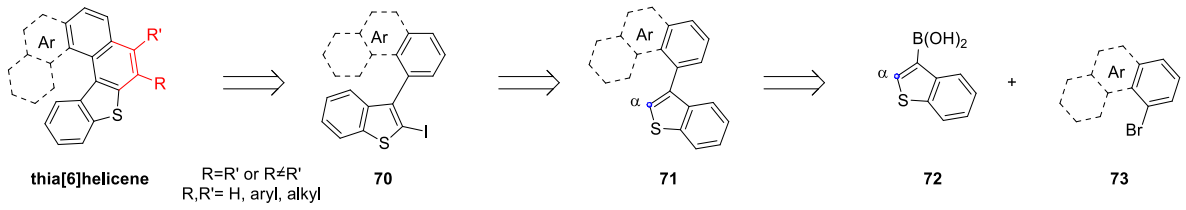

Scheme 42: General retrosynthetic pathway for thia[6]helicenes.

The latter diheteroaryl derivatives **71** can be synthesized through a Suzuki reaction between commercially available boronic acid **72** and polyaromatic scaffolds **73**, including bromides reported in *Figure 21*.

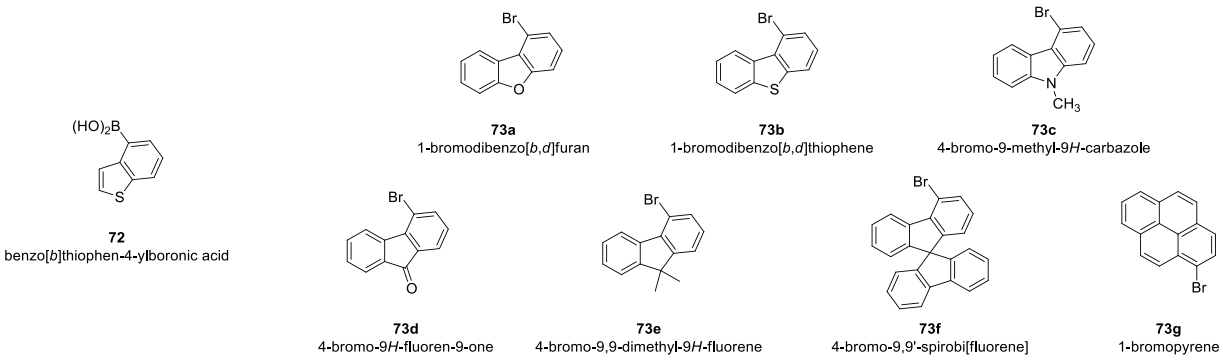

Figure 21: Commercially available building blocks used in this study.

The selected polycyclic bromides represent interesting moieties to be inserted within the helical skeleton since most of them are very attractive chromophore thanks to their peculiar photophysical and electronic properties, that in principle can be transferred in the helicene skeleton. For example, fluorene-based helicenes exhibit promising CPL properties and fluorescence quantum yields (Φ_F),[58,183] while pyrene-based helicenes present reduced band gaps[28] and show large Stokes shift[184,185] as well as bathochromic effects.[186] On the other hand, carbazole-based helicenes are known to be electroluminescent materials that display interesting CPL phenomena[187] and fluorescence quantum yields,[40] and found application in optoelectronics[188-190] as well as in sensors.[191]

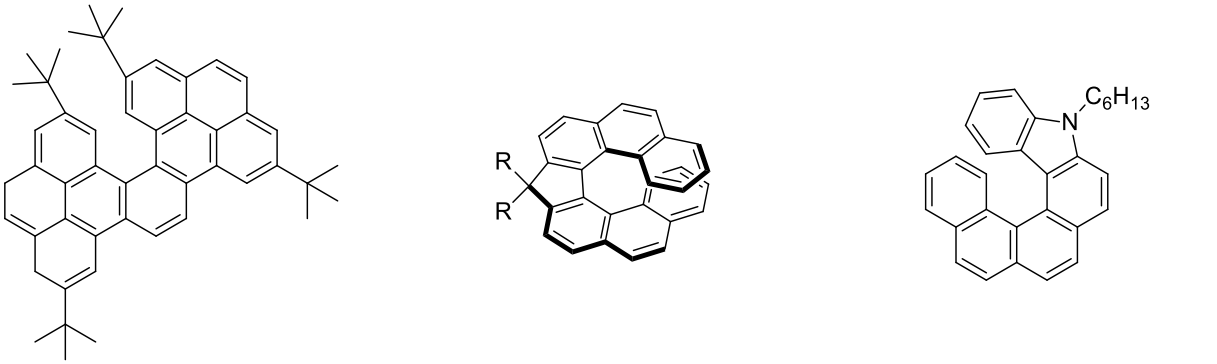

Pyrene-based helicenes[28] **Fluorene-based helicenes[58]** **Carbazole-based helicenes[40]**

Figure 22: Examples of pyrene-, fluorene- and carbazole-based helicenes.

2.2 Synthesis of diheteroaryl derivatives 70 and 71

According to the retrosynthetic pathway reported in *Scheme 42*, we initially focused our attention on the synthesis of diheteroaryl derivatives **71** through a palladium-catalysed Suzuki reaction between benzothiophene-3-boronic acid (**72**) and bromides **73** (*Scheme 43*).

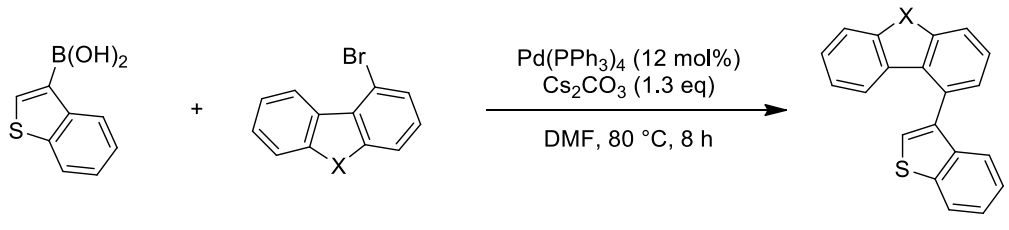

72
1.4 eq

73a: X= O
73b: X= S
73c: X= NCH_3
73d: X= CO
73e: X= $C(CH_3)_2$
73f: X=

71a–f

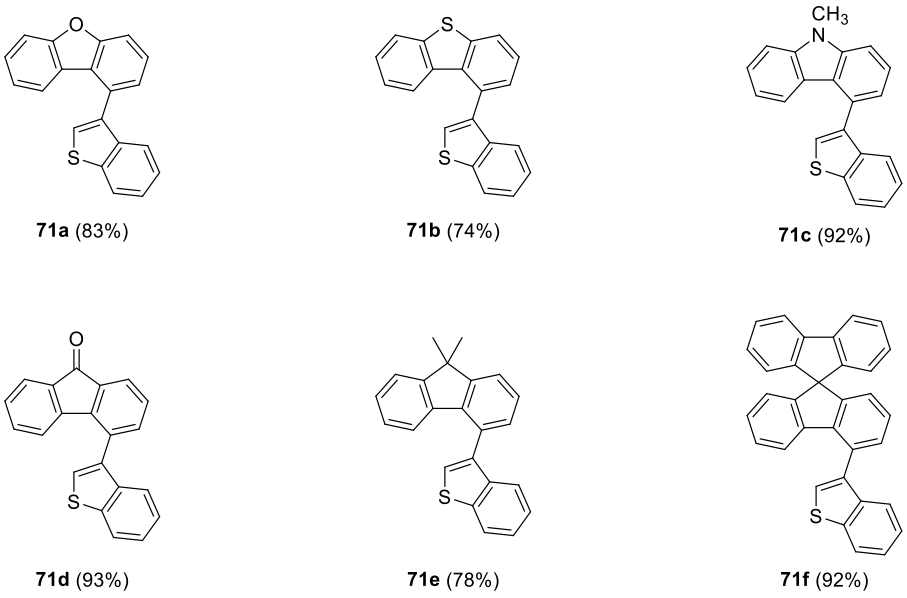

Scheme 43: Synthesis of intermediates **71a**–**f** via Suzuki coupling between bromides **73** and boronic acid **72**.

In particular, the Suzuki reactions were performed using $Pd(PPh_3)_4$ as catalyst and Cs_2CO_3 as base in DMF at 80 °C, according to some literature procedures previously reported for the Suzuki coupling involving boronic acid **72**.[192] As reported in *Scheme 43*, these experimental conditions afforded the required products **71a–f** in good to excellent yields (74–93%), demonstrating the effectiveness of all bromides **73a–f** in these coupling reactions.

With these di(hetero)aryls **71** in hand, we focused on their regioselective iodination through the deprotonation with a strong base, such as *n*BuLi, and the reaction of the formed monoanion with iodine (*Scheme 44*).

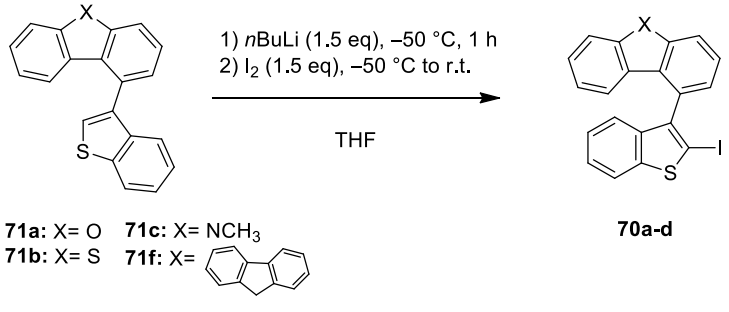

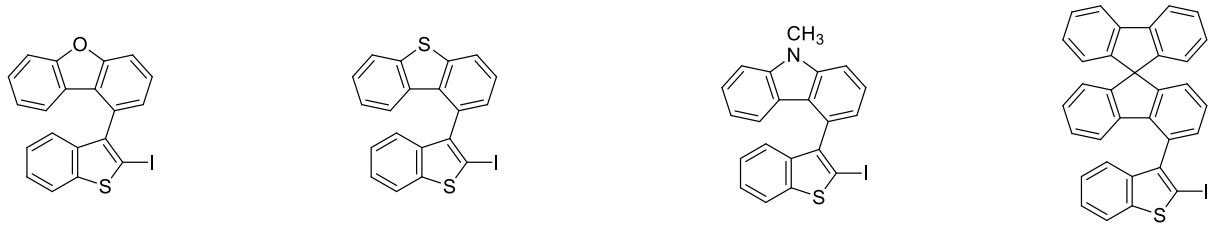

70a (86%) **70b** (92%) **70c** (80%) **70d** (88%)

Scheme 44: Iodination of diheteroaryls **71**.

According to Górski's procedure[193] previously reported for the iodination of bis(benzothiophene) derivatives, a solution of compound **71** in dry THF was reacted with 1.5 equiv. of *n*BuLi at −50 °C to give the corresponding monoanion in α-position of the terminal thiophene ring, which, by reaction with a solution of iodine in THF (1.5 eq), provided iodides **70a–d** in good to excellent yields (up to 92%).

Noteworthy, the same experimental conditions reported in *Schemes 43* and *44* were used for the preparation of pyrene-based diaryl **71g** and the corresponding iodide **70e** (*Scheme 45*).

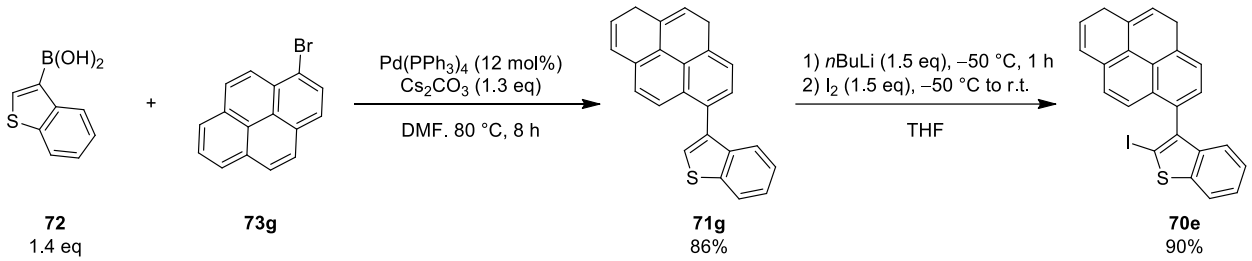

72
1.4 eq

73g

71g
86%

70e
90%

Scheme 45: Synthesis of pyrene-based derivatives **71g** and **70e**.

Also in this case, the $Pd(PPh_3)_4$-catalysed Suzuki reaction between commercially available bromide **73g** and 1.4 equiv. of boronic acid **72** gave the desired pyrene-based diaryl **71g** in 86% yield. Next, the regioselective iodination of **71g** was accomplished by deprotonation with *n*BuLi (1.5 eq) followed by the reaction with iodine (1.5 eq), and the required iodide **70e** was isolated in 90% yield.

Overall, we set up a general and highly efficient two-step procedure for the synthesis of di(hetero)aryl iodides **70a**–**e** that involves a Suzuki coupling between commercially available building blocks **72** and **73a**–**g**, followed by a regioselective iodination of intermediates **71**.

2.3 Preliminary study of the palladium-catalysed carboannulation of iodides 70

With iodides **70** in hand, we then turned our attention on the study of their palladium-catalysed carboannulation with internal alkynes to give the corresponding functionalised thia[6]helicenes **74**. As previosuly highlighted in *Chapter 1* for the synthesis of 7,8-disubstituted 7-TH derivatives **62**, this annulation reaction could provide straightforward access to a wide class of functionalised thia[6]helicenes,

taking advantage from the plethora of internal alkynes easily available from commercial sources or form well-established synthetic procedures. We started this study performing the carboannulation of carbazole-based iodide **70c** with diphenylacetylene (**67a**) through two different experimental procedures (*Table 6*).

Table 6. Pd-catalysed carboannulation of iodide **70c** and diphenylacetylene (**67a**).

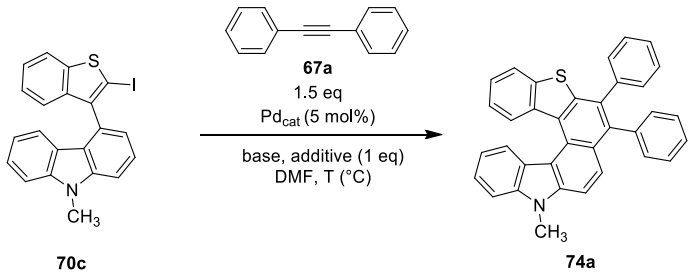

Entry[a]	Pd_{cat}	Additive	Base (eq)	T (°C)	t (h)[b]	Yield of **74a** (%)[c]
1	$Pd(dppf)Cl_2$	LiBr	K_2CO_3 (3 eq)	130	24	65[d]
2	$Pd(OAc)_2$	LiCl	NaOAc (2 eq)	100	9	79[d]

[a] Rection conditions: 0.1 mmol of **70c**, 1.5 equiv of **67a**, 5 mol% of Pd_{cat}, 1 equiv of additive, 2 or 3 equiv. of base in DMF under nitrogen. [b] The reactions were stopped when they did not further progress. [c] Isolated yield. [d] The reduced by-product **71c** was also recovered (ca. 10%).

The first selected procedure involved the optimised experimental conditions used for the carboannulation of bis(benzodithiophene) bromides **53** to give 7-TH derivatives **62** (see *Scheme 36*, *Chapter 1*). More in detail, iodide **70c** was reacted with 1.5 equiv. of diphenylacetylene (**67a**) in the presence of $Pd(dppf)Cl_2$ as catalyst, K_2CO_3 as base and LiBr as additive in DMF at 130 °C (*Table 6*, entry 1). After 24 hours, the desired helicene **74a** was isolated in 65% yield along with small amount of de-halogenated side-product **71c** (12%). Since the experimental conditions reported in entry 1 were optimised for the annulation of bromides **53**, we though to try alternative conditions, previously reported by Larock and co-workers[159] for the palladium annulation of 2-iodobiaryls with internal acetylenes. Thus, iodide **70c** was treated with 1.5 equiv. of diphenylacetylene (**67a**) in the presence of $Pd(OAc)_2$ as catalyst, NaOAc as base and LiCl as additive in DMF at 100 °C (*Table 6*, entry 2). We were pleased to find that after 9 hours the reaction mixture did not contain the starting iodide **70c** and the desired helicene **74a** was isolated in higher yield (79% vs 65%).

On the base of this result, we preliminary investigated two further annulation reactions involving two different iodides **70**, such as the dibenzofuran- and dibenzothiophene-based iodide **70a** and **70b**, and the heteroaryl-containing alkyne **67b** (*Scheme 46*).

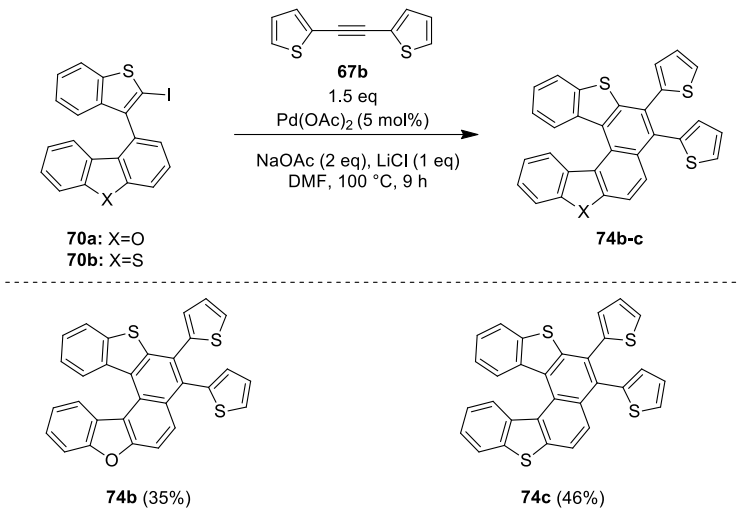

Scheme 46: Synthesis of helicenes **74b**,**c** through Pd-catalysed annulation of **70a**,**b** with **67b**.

The iodides **70a** and **70b** were reacted with 1.5 equiv. of alkyne **67b** under the experimental conditions reported in *Scheme 46*, and after 9 hours the corresponding thiahelicenes **74b** and **74c** were isolated in similar moderate yields (35 and 46%, respectively). Trace of starting iodides **70a** and **70b** were found in the reaction mixture, while reduced by-products **71a** and **71b** (ca. 20%) were also recovered.

Although this study is in its early stage, the results so far obtained look very promising, because they demonstrate that a novel class of iodobi(hetero)aryl derivatives **70** is able to undergo the palladium promoted annulation with internal alkynes to provide the corresponding thia[6]helicenes.

2.4 Conclusions and perspectives

In summary, the Pd-catalysed annulation of bis(benzodithiophene) bromides **53** set up for the synthesis of 7,8-disubstituted tetrathia[7]helicenes **62** has also proved effective for the synthesis of a novel class of functionalised thia[6]helicenes **74**. Indeed, a set of biheteroaryls **71** has been synthesized in good yields and their regioselective iodination has been successfully accomplished to obtain the corresponding key intermediates **70**. First attempts to prepare disubstituted thia[6]helicenes **74** through the carboannulation of two diaryl acetylenes with some iodides **70** provided promising results, though the efficiency of this reaction should be improved as well as its substrate scope should be further investigated.

According to the synthetic approach designed for the synthesis of functionalised tetrathia[7]helicenes, in perspective, iodides **70** could represent useful intermediates not only to get access to helicenes **74** but also for the synthesis of diverse thia[6]helicene scaffolds, including derivatives **75** and **76** (*Scheme 47*).

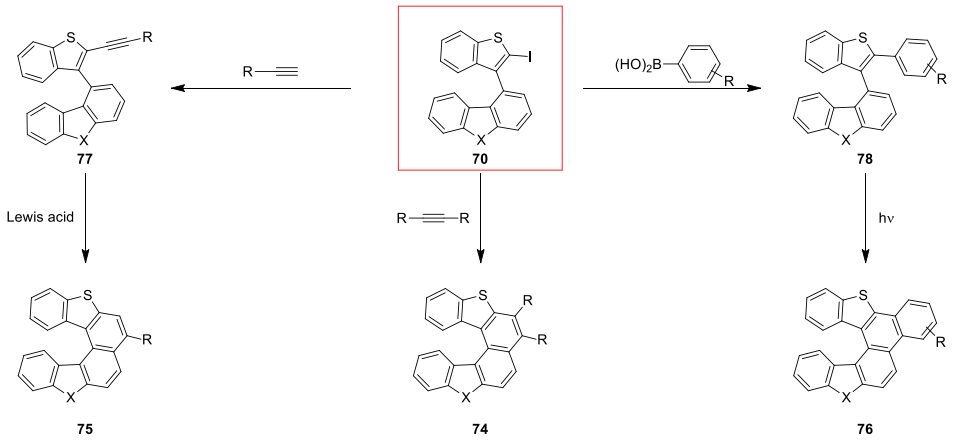

Scheme 47: Synthesis of diverse classes of thia[6]helicenes.

In particular, monosubstituted thia[6]helicenes **75** could be prepared by a Sonogashira coupling with terminal alkynes, followed by metal-promoted intramolecular hydroarylation of intermediates **77**, while benzo fused helicenes **76** could be synthesized by a Suzuki coupling with arylboronic acids, followed by an oxidative photochemical cyclisation of intermediates **78**.

Furthermore, chiroptical, photophysical and electrochemical properties of these new classes of thia[6]helicenes and the biaryl intermediates will be investigated in order to evaluate their configurational stability and potentialities for applications in material science.

2.5 Experimental part

2.5.1 General methods.

The reactions were run under inert atmosphere (nitrogen or argon atmosphere) by means of standard Schlenk technique for manipulating air-sensitive compounds. All commercially available reagents and solvents were purchased from Sigma-Aldrich and used without further purification. Anhydrous solvents (THF and DMF) were purchased from Sigma-Aldrich 250 mL bottles on molecular sieves with crown cap. Solutions of *n*BuLi (1.6 M in hexane) were purchased from Sigma-Aldrich and titrated prior to use. Bromides **73** and boronic acid **72** were purchased from TCI and used as received. Thin-layer chromatography (TLC) was performed with Aldrich silica gel 60 F254 precoated plates, and plates were visualized with short-wave UV light (254 and 366 nm). Column chromatography was carried out with Aldrich silica gel (70-230 mesh). The ^{1}H NMR and ^{13}C NMR spectra were recorded in $CDCl_3$ at 25 °C using a Bruker AC-300 and AC-400 MHz spectrometer. Chemical shifts were reported relative to the residual protonated solvent resonances (^{1}H: δ = 7.26 ppm, ^{13}C: δ = 77.00 for $CDCl_3$, ^{1}H: δ = 5.32 ppm for CD_2Cl_2). The chemical shifts are given in ppm and coupling constants in Hz. High Resolution Electron Ionization (HR EI) mass spectra were recorded on a FISONS - Vg Autospec- M246 spectrometer.

2.5.2 Synthesis and characterization of compounds 70a–e, 71a–g and 74a–c

General procedure for the synthesis of diheteroaryls species 71a–g. To a flame-dried vessel bromide **73** (0.4 mmol), boronic acid **72** (0.56 mmol, 1.4 eq), $Pd(PPh_3)_4$ (0.048 mmol, 12 mol%), Cs_2CO_3 (0.56 mmol, 1.4 eq) were added. The reaction vessel was fitted with a silicon septum, evacuated and back-filled with argon, and this sequence was repeated twice. Deareated dry DMF (0.5 mL) was added and the mixture was stirred at 80 °C for 8 hours under argon atmosphere. After cooling to room temperature, 10 mL of H_2O was added. The aqueous phase was extracted with CH_2Cl_2 (5 × 10 mL), and the collected organic phases were washed with water, dried over Na_2SO_4 and the solvent was removed under reduced pressure. The crude product was purified by chromatography on silica gel to provide the desired compound **71**.

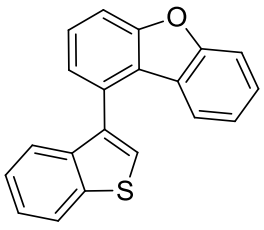

Diheteroaryl 71a. The crude product obtained from the Pd-catalysed Suzuki reaction between bromide **73a** and boronic ester **72** was purified by column chromatography on silica gel (hexane/CH_2Cl_2 95:5) to give **71a** (100 mg, 83%) as colourless oil. ^{1}H NMR (300 MHz, $CDCl_3$): δ = 8.01 (d, J = 8.1 Hz, 1H), 7.66 (dd, J = 8.3, 0.8 Hz, 1H), 7.59 (s, 1H), 7.58–7.50 (m, 3H), 7.45–7.35 (m, 3H), 7.32–7.26 (m, 1H), 7.06–6.98 (m, 2H). ^{13}C NMR (75 MHz, $CDCl_3$): δ = 156.3 (Cq), 140.1 (Cq), 138.3 (Cq), 135.6 (Cq), 130.8 (Cq), 127.0 (CH), 127.0 (CH), 124.7 (2CH), 124.5 (CH), 124.4 (CH), 123.7 (Cq), 123.4 (Cq), 122.8 (CH), 122.6 (CH), 122.4 (CH), 111.4 (CH), 111.1 (CH). HRMS (EI): calcd for $C_{20}H_{12}OS$ $[M]^+$: 300.0609, found 300.0597.

Diheteroaryl 71b. The crude product obtained from the Pd-catalysed Suzuki reaction between bromide **73b** and boronic ester **72** was purified by column chromatography on silica gel (hexane/CH_2Cl_2 95:5) to give **71b** (94 mg, 74%) as colourless solid. ^{1}H NMR (300 MHz, $CDCl_3$): δ = 8.00 (d, J = 8.1 Hz, 1H), 7.96 (dd, J = 1.0, 8.0 Hz, 1H), 7.82 (d, J = 8.0 Hz, 1H), 7.53 (t, J = 7.7 Hz, 1H), 7.48 (s, 1H, Th), 7.42–7.36 (m, 2H), 7.33–7.27 (m, 2H), 7.25–7.19 (m, 1H), 7.00–6.90 (m, 2H). ^{13}C NMR (75 MHz, $CDCl_3$): δ = 140.1 (Cq), 139.9 (Cq), 139.6 (Cq), 138.9 (Cq), 136.9 (Cq), 135.1 (Cq), 133.9 (Cq), 132.3 (Cq), 127.7 (CH), 126.3 (CH), 126.0 (CH), 124.8 (CH), 124.7 (CH), 124.5 (CH), 124.1 (2CH), 123.3 (CH), 122.8 (CH), 122.6 (CH), 122.4 (CH). HRMS (EI): calcd for $C_{20}H_{12}S_2$ $[M]^+$: 316.0380, found 316.0389.

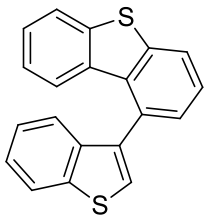

Diheteroaryl 71c. The crude product obtained from the Pd-catalysed Suzuki reaction between bromide **73c** and boronic ester **72** was purified by column chromatography on silica gel (hexane/CH_2Cl_2 95:5) to give **71c** (109 mg, 92%) as colourless solid. ^{1}H NMR (300 MHz, $CDCl_3$): δ = 8.00 (d, J = 8.1 Hz, 1H), 7.60–7.54 (m, 2H), 7.50 (dd, J = 1.1, 8.2 Hz, 1H), 7.45 (d, J = 8.1 Hz, 1H), 7.42–7.34 (m, 4H), 7.26–7.20 (m, 2H), 7.07 (d, J = 8.0 Hz, 1H), 6.87 (ddd, J = 2.3, 5.9, 8.1 Hz, 1H), 3.93 (s, 3H, CH_3). ^{13}C NMR (75 MHz, $CDCl_3$): δ = 141.3 (Cq), 141.2 (Cq), 140.0 (Cq), 138.9 (Cq), 137.0 (Cq), 130.5 (Cq), 125.5 (CH), 125.4 (CH), 124.5 (CH), 124.2 (CH), 124.0 (CH), 123.6 (CH), 122.7 (CH), 122.6 (CH), 122.2 (Cq), 121.4 (Cq), 121.3 (CH), 118.7 (CH), 108.1 (CH), 108.0 (CH), 29.2 (CH_3). HRMS (EI): calcd for $C_{21}H_{15}NS$ $[M]^+$: 313.0925, found 313.0925.

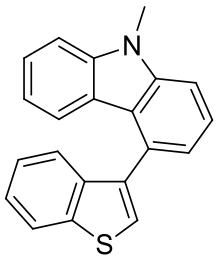

Diheteroaryl 71d. The crude product obtained from the Pd-catalysed Suzuki reaction between bromide **73d** and boronic ester **72** was purified by column chromatography on silica gel (hexane/AcOEt 98:2) to give **71d** (113 mg, 93%) as orange solid. ^{1}H NMR (300 MHz, $CDCl_3$): δ = 7.99 (d, J = 8.1 Hz, 1H), 7.77 (dd, J = 1.5, 6.4 Hz, 1H), 7.65 (d, J = 7.3 Hz, 1H), 7.49 (s, 1H, Th), 7.46–7.38 (m, 4H), 7.32 (t, J = 7.3 Hz, 1H), 7.17 (t, J = 7.3 Hz, 1H), 7.07 (t, J = 7.5 Hz, 1H), 6.43 (d, J = 7.5 Hz, 1H). ^{13}C NMR (75 MHz, $CDCl_3$): δ = 193.7 (C=O), 144.1 (Cq), 142.7 (Cq), 140.0 (Cq), 138.2 (Cq), 137.4 (CH), 134.9 (Cq), 134.6 (CH), 134.4 (Cq), 131.1 (Cq), 128.9 (CH), 128.8 (CH), 124.9 (CH), 124.6 (2CH), 124.1 (CH), 123.9 (CH), 123.2 (CH), 123.1 (CH), 122.9 (CH). HRMS (EI): calcd for $C_{21}H_{12}OS$ $[M]^+$: 312.0610, found 312.0610.

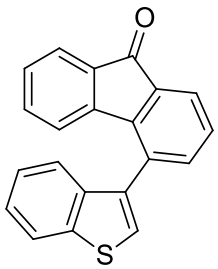

Diheteroaryl 71e. The crude product obtained from the Pd-catalysed Suzuki reaction between bromide **73e** and boronic ester **72** was purified by column chromatography on silica gel (hexane/CH_2Cl_2 95:5) to give **71e** (102 mg, 78%) as colourless solid. ^{1}H NMR (300 MHz, $CDCl_3$): δ = 8.01 (d, J = 8.0 Hz, 1H), 7.56 (d, J = 7.4 Hz, 1H), 7.49 (s, 1H), 7.47–7.38 (m, 4H), 7.32–7.28 (m, 2H), 7.21 (t, J = 7.3 Hz, 1H), 6.94 (t, J = 7.5 Hz, 1H), 6.63 (d, J = 7.7 Hz, 1H), 1.61 (s, 3H, CH_3), 1.58 (s, 3H, CH_3). ^{13}C

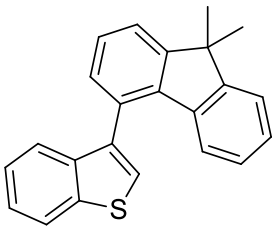

NMR (75 MHz, $CDCl_3$): δ = 154.5 (Cq), 154.0 (Cq), 140.0 (Cq), 138.9 (Cq), 138.7 (Cq), 137.7 (Cq), 136.9 (Cq), 130.5 (Cq), 129.7 (CH), 127.0 (CH), 126.9 (CH), 126.7 (CH), 124.5 (CH), 124.3 (CH), 123.9 (CH), 123.5 (CH), 123.0 (CH), 122.7 (CH), 122.2 (2CH), 46.4 ($Cq(CH_3)_2$), 27.6 (CH_3), 27.4 (CH_3). HRMS (EI): calcd for $C_{23}H_{18}S$ $[M]^+$: 326.1129, found 326.1129.

Diheteroaryl 71f. The crude product obtained from the Pd-catalysed Suzuki reaction between bromide **73f** and boronic ester **72** was purified by column chromatography on silica gel (hexane/CH_2Cl_2 95:5) to give **71f** (186 mg, 92%) as colourless solid. ^1H NMR (300 MHz, $CDCl_3$): δ = 8.03 (d, J = 8.0 Hz, 1H), 7.88 (d, J = 7.5 Hz, 2H), 7.59 (s, 1H), 7.57 (d, J = 7.5 Hz, 1H), 7.46–7.28 (m, 5H), 7.22–7.13 (m, 3H), 6.99–6.92 (m, 2H), 6.87–6.78 (m, 3H), 6.70–6.67 (m, 2H). ^{13}C NMR (75 MHz, $CDCl_3$): δ = 149.5 (Cq), 149.0 (Cq), 148.9 (Cq), 148.9 (Cq), 141.9 (Cq), 141.8 (Cq), 141.2 (Cq), 140.2 (Cq), 140.0 (Cq), 138.9 (Cq), 136.7 (Cq), 130.5 (CH), 127.9 (3CH), 127.8 (2CH), 127.6 (CH), 127.5 (CH), 127.4 (CH), 124.7 (CH), 124.5 (CH), 124.1 (CH), 124.0 (CH), 123.7 (CH), 123.7 (CH), 123.4 (CH), 123.0 (CH), 122.9 (CH), 120.1 (CH), 120.0 (CH), 65.8 (Cq). HRMS (EI): calcd for $C_{33}H_{20}S$ $[M]^+$: 448.1286, found 448.1277.

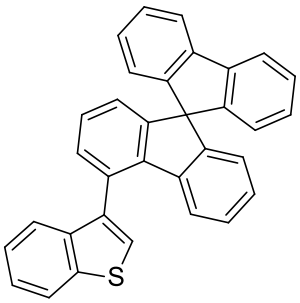

Diheteroaryl 71g. The crude product obtained from the Pd-catalysed Suzuki reaction between bromide **73g** and boronic ester **72** was purified by column chromatography on silica gel (hexane/CH_2Cl_2 95:5) to give **71g** (115 mg, 86%) as colourless solid. ^1H NMR (300 MHz, $CDCl_3$): δ = 8.28–8.14 (m, 5H), 8.08–7.97 (m, 5H), 7.61 (s, 1H), 7.47–7.40 (m, 2H), 7.32–7.27 (m, 1H). ^{13}C NMR (75 MHz, $CDCl_3$): δ = 140.1 (Cq), 139.8 (Cq), 136.8 (Cq), 131.4 (Cq), 131.1 (Cq), 131.0 (Cq), 129.8 (Cq), 128.2 (CH), 127.7 (CH), 127.5 (CH), 127.4 (CH), 126.1 (CH), 125.5 (2CH), 125.3 (CH), 125.1 (CH), 125.0 (Cq), 124.8 (Cq), 124.7 (CH), 124.5 (CH), 124.4 (CH), 123.6 (CH), 123.4 (Cq), 122.8 (CH). HRMS (EI): calcd for $C_{24}H_{14}S$ $[M]^+$: 334.0816, found 334.0815.

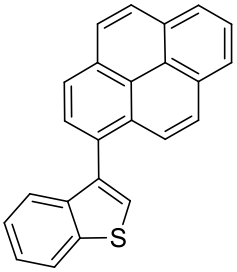

General procedure for the synthesis of iodides 70a–e. A solution of *n*BuLi (0.48 mmol, 1.5 eq) was added dropwise to a stirring solution of diheteroaryl **71** (0.32 mmol) in dry THF (1 mL) at – 50 °C under argon atmosphere. The resulting mixture was stirred for 1 hour at –50 °C and then the solution was treated with a solution of I_2 (0.48 mmol, 1.5 eq) in dry THF. After 10 min at –50 °C, the mixture was warmed at room temperature, and slowly added to a saturated aqueous solution of $N_2S_2O_3$ (10 mL). The aqueous phase was extracted with CH_2Cl_2 (3 × 10 mL), and the collected organic phases were dried over Na_2SO_4, and concentrated under reduced pressure. The crude product was purified by chromatography on silica gel to provide the required iodide **70**.

Iodide 70a. The crude product obtained from the iodination of **71a** was purified by column chromatography on silica gel (hexane) to give **70a** (112 mg, 82%) as colourless solid. ^{1}H NMR (300 MHz, $CDCl_3$): δ = 7.89 (d, J = 8.2 Hz, 1H), 7.71 (d, J = 8.4 Hz, 1H), 7.63–7.55 (m, 2H), 7.40–7.15 (m, 5H), 7.03 (t, J = 7.6 Hz, 1H), 6.81 (d, J = 8.0 Hz, 1H). ^{13}C NMR (75 MHz, $CDCl_3$): δ = 156.4 (Cq), 156.3 (Cq), 143.9 (Cq), 141.2 (Cq), 138.7 (Cq), 130.6 (Cq), 127.2 (CH), 127.1 (CH), 125.0 (CH), 124.9 (2CH), 123.4 (2CH), 123.1 (CH), 122.8 (CH), 122.5 (CH), 121.6 (CH), 111.7 (CH), 111.4 (CH), 82.1 (Cq). HRMS (EI): calcd for $C_{20}H_{11}OSI$ $[M]^+$: 425.9575, found 425.9574.

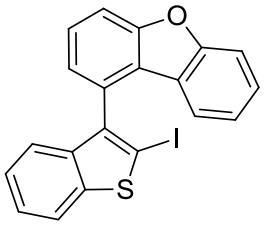

Iodide 70b. The crude product obtained from the iodination of **71b** was purified by column chromatography on silica gel (hexane) to give **70b** (130 mg, 92%) as colourless solid. ^{1}H NMR (300 MHz, $CDCl_3$): δ = 8.00 (d, J = 8.0 Hz, 1H), 7.88 (d, J = 8.2 Hz, 1H), 7.82 (d, J = 8.0 Hz, 1H), 7.59 (t, J = 7.6 Hz, 1H), 7.35–7.28 (m, 3H), 7.16–7.14 (m, 2H), 7.02 (t, J = 8.1 Hz, 1H), 6.84 (d, J = 8.3 Hz, 1H). ^{13}C NMR (75 MHz, $CDCl_3$): δ = 143.8 (Cq), 142.6 (Cq), 140.3 (Cq), 139.6 (Cq), 138.9 (Cq), 134.8 (Cq), 133.8 (Cq), 132.3 (Cq), 127.6 (CH), 126.4 (CH), 126.3 (CH), 124.9 (2CH), 124.5 (CH), 124.1 (CH), 123.1 (2CH), 122.5 (CH), 121.6 (CH), 82.3 (Cq). HRMS (EI): calcd for $C_{20}H_{11}S_2I$ $[M]^+$: 441.9347, found 441.9341.

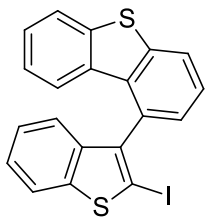

Iodide 70c. The crude product obtained from the iodination of **71c** was purified by column chromatography on silica gel (hexane/AcOEt 9:1) to give **70c** (113 mg, 80%) as colourless solid. ^{1}H NMR (400 MHz, $CDCl_3$): δ = 7.88 (d, J = 8.1 Hz, 1H), 7.64–7.60 (m, 1H), 7.55 (d, J = 7.7 Hz, 1H), 7.41–7.36 (m, 2H), 7.31 (dt, J = 1.1,7.0 Hz, 1H), 7.21 (d, J = 8.0 Hz, 1H), 7.15–7.10 (m, 2H), 6.92–6.89 (m, 2H), 3.94 (s, 3H, CH_3). ^{13}C NMR (75 MHz, $CDCl_3$): δ = 143.8 (Cq), 142.7 (Cq), 141.3 (Cq), 141.1 (Cq), 139.0 (Cq), 130.3 (Cq), 125.7 (CH), 125.5 (CH), 124.6 (2CH), 123.3 (CH), 122.2 (CH), 121.9 (Cq), 121.5 (CH), 121.3 (CH), 119.0 (CH), 108.5 (CH), 108.2 (CH), 29.2 (CH_3). HRMS (EI): calcd for $C_{21}H_{14}INS$ $[M]^+$: 438.9892, found 438.9888.

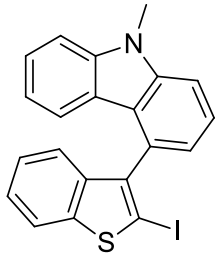

Iodide 70d. The crude product obtained from the iodination of **71f** was purified by column chromatography on silica gel (hexane) to give **70d** (162 mg, 88%) as colourless solid. ^{1}H NMR (300 MHz, $CDCl_3$): δ = 7.94–7.86 (m, 3H), 7.46 (t, J = 7.8 Hz, 1H), 7.39 (t, J = 7.7 Hz, 3H), 7.32–7.29 (m, 1H), 7.24–7.12 (m, 4H), 6.99–6.96 (m, 2H), 6.87–6.79 (m, 3H), 6.71–6.60 (m, 2H). ^{13}C NMR (75 MHz, $CDCl_3$): δ = 149.7 (Cq), 149.0 (Cq), 148.6 (Cq), 143.9 (Cq), 142.3 (Cq), 142.0 (Cq), 141.7 (Cq), 141.0 (Cq), 140.5 (Cq), 138.9 (Cq), 130.5 (Cq), 130.2 (CH),

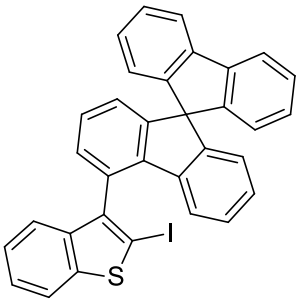

128.0 (CH), 127.9 (2CH), 127.8 (4CH), 124.9 (CH), 124.9 (CH), 124.1 (3CH), 123.7 (CH), 123.2 (CH), 122.5 (CH), 121.7 (CH), 120.1 (2CH), 82.5 (Cq), 65.8 (Cq). HRMS (EI): calcd for $C_{33}H_{19}SI$ $[M]^+$: 574.0252, found 574.0252.

Iodide 70e. The crude product obtained from the iodination of **71g** was purified by column chromatography on silica gel (hexane) to give **70e** (133 mg, 90%) as colourless solid. ^1H NMR (300 MHz, $CDCl_3$): δ = 8.31 (d, J = 7.9 Hz, 1H), 8.26–8.16 (m, 4H), 8.08–7.89 (m, 4H), 7.68 (d, J = 9.2 Hz, 1H), 7.37–7.32 (m, 1H), 7.21–7.14 (m, 2H). ^{13}C NMR (75 MHz, $CDCl_3$): δ = 143.8 (Cq), 142.6 (Cq), 140.0 (Cq), 131.5 (Cq), 131.3 (Cq), 131.0 (Cq), 130.9 (Cq), 129.8 (Cq), 128.4 (CH), 128.0 (CH), 127.9 (CH), 127.4 (CH), 126.2 (CH), 125.4 (CH), 125.4 (CH), 125.2 (CH), 125.0 (Cq), 124.8 (CH), 124.7 (CH), 124.7 (CH), 123.4 (CH), 121.6 (CH), 83.3 (Cq). HRMS (EI): calcd for $C_{24}H_{14}SI$ $[M]^+$: 459.9783, found 459.9783.

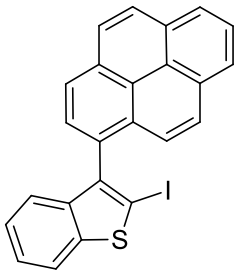

General Procedure for the synthesis thia[6]helicenes 74a–c. To a flame-dried reaction vessel iodide **70** (0.10 mmol), $Pd(OAc)_2$ (1.1 mg, 0.005 mmol, 5 mol%), LiCl (4.2 mg, 0.10 mmol), NaOAc (16.4 mg, 0.20 mmol) and alkyne **67** (0.15 mmol) were added. The reaction vessel was fitted with a silicon septum, evacuated and back-filled with argon, and this sequence was repeated twice. Deaerated DMF (5 mL) was then added successively under a stream of argon at room temperature. The resulting mixture was stirred at 100 °C under argon and the outcome of the reaction was monitored by TLC analysis. After 9 hours, the mixture was cooled to room temperature and poured into water (20 mL). The aqueous phase was extracted with CH_2Cl_2 (4 × 10 mL), and the collected organic phases were washed with brine (2 × 20 mL), dried over Na_2SO_4, and concentrated under reduced pressure. The residue was purified by column chromatography on silica gel to provide the required product **74**.

Helicene 74a. The crude product obtained from the Pd-catalysed annulation reaction between iodide **70c** and alkyne **67a** was purified by column chromatography on silica gel (hexane/CH_2Cl_2 95:5) to give **74a** (39 mg, 79%) as yellow solid. ^1H NMR (300 MHz, $CDCl_3$): δ = 8.02 (d, J = 8.1 Hz, 1H), 7.95 (d, J = 7.9 Hz, 1H), 7.84 (d, J = 9.1 Hz, 1H), 7.62–7.23 (m, 14H), 7.16–7.11 (m, 2H), 4.05 (s, 3H). ^{13}C (75 MHz, $CDCl_3$): δ = 142.5 (Cq), 140.7 (Cq), 140.1 (Cq), 140.0 (Cq), 139.4 (Cq), 139.2 (Cq), 137.7 (Cq), 137.0 (Cq), 131.7 (CH), 131.3 (CH), 130.3 (2CH), 128.0 (2CH), 127.7 (CH), 127.4 (2CH), 127.2 (CH), 127.0 (Cq), 126.7 (2CH), 126.5 (CH), 125.1 (CH), 124.2 (CH), 124.1 (Cq), 123.8 (Cq), 122.7 (CH), 122.1 (CH), 118.1 (CH), 114.8 (Cq), 109.2 (CH), 108.5 (CH), 29.5 (CH_3). HRMS (EI): calcd for $C_{35}H_{23}NS$ $[M]^+$: 489.1551, found 489.1533.

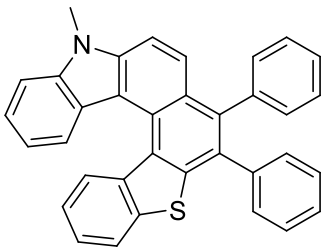

Helicene 74b. The crude product obtained from the Pd-catalysed annulation reaction between iodide **70a** and alkyne **67b** was purified by column chromatography on silica gel (hexane/CH_2Cl_2 95:5) to give **74b** (19 mg, 35%) as yellow solid. 22% of de-iodinated di(hetero)aryl **71a** was also recovered. ^{1}H NMR (300 MHz, CD_2Cl_2): δ = 8.08–8.01 (m, 2H), 7.97 (d, J = 8.1 Hz, 1H), 7.85 (d, J = 9.2 Hz, 1H), 7.75 (d, J = 8.2 Hz, 1H), 7.56–7.46 (m, 3H), 7.44–7.33 (m, 3H), 7.29–7.21 (m, 2H), 7.14–7.08 (m, 2H). ^{13}C (75 MHz, $CDCl_3$): δ = 156.7 (Cq), 156.1 (Cq), 143.3 (Cq), 140.0 (Cq), 139.8 (Cq), 139.1 (Cq), 136.4 (Cq), 131.7 (Cq), 130.5 (CH), 129.8 (Cq), 129.4 (Cq), 129.0 (CH), 128.4 (CH), 127.9 (CH), 127.8 (Cq), 127.1 (2CH), 126.7 (2CH), 126.7 (CH), 126.2 (CH), 126.1 (CH), 125.1 (Cq), 123.7 (Cq), 123.4 (CH), 122.5 (CH), 121.7 (CH), 117.0 (Cq), 112.0 (CH), 111.4 (CH). HRMS (EI): calcd for $C_{30}H_{16}OS_3$ $[M]^+$: 488.0363, found 488.0342.

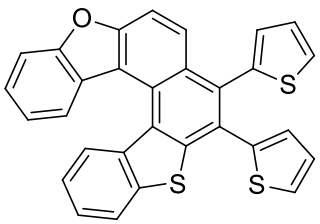

Helicene 74c. The crude product obtained from the Pd-catalysed annulation reaction between iodide **70b** and alkyne **67b** was purified by column chromatography on silica gel (hexane/CH_2Cl_2 95:5) to give **74c** (23 mg, 46%) as yellow solid. 20% of de-iodinated di(hetero)aryl **71b** was also recovered. ^{1}H NMR (300 MHz, $CDCl_3$): δ = 8.00 (d, J = 8.2 Hz, 1H), 7.96–7.92 (m, 3H), 7.54 (t, J = 8.6 Hz, 2H), 7.45–7.36 (m, 4H), 7.31 (dd, J = 3.5, 1.1 Hz, 1H), 7.16–7.07 (m, 5H). ^{13}C (75 MHz, $CDCl_3$): δ = 143.0 (Cq), 140.8 (Cq), 140.0 (Cq), 139.2 (Cq), 139.0 (Cq), 138.7 (Cq), 136.5 (Cq), 136.3 (Cq), 131.0 (2Cq), 130.4 (CH), 129.2 (Cq), 128.8 (CH), 128.7 (Cq), 128.3 (Cq), 127.8 (CH), 127.7 (CH), 127.1 (2CH), 126.6 (CH), 126.5 (CH), 126.4 (CH), 125.7 (CH), 125.5 (CH), 124.4 (Cq), 123.0 (2CH), 122.5 (CH), 122.2 (CH), 120.6 (CH). HRMS (EI): calcd for $C_{30}H_{16}S_4$ $[M]^+$: 504.0135, found 504.0126.

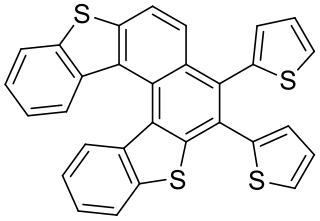

Chapter 3

Stereochemical and chiroptical studies of bis(benzo[1,2-*b*:4,3-*b*']dithiophene) atropisomers

This chapter describes the experimental and theoretical studies performed to evaluate the stereochemical and chiroptical properties of axially chiral bis(benzo[1,2-*b*:4,3-*b*']dithiophene) derivatives synthesised in the *Chapter 1*. The configurational stability of these intermediates by means of dynamic HPLC and kinetic studies has been carried out in collaboration with Dr. Roberta Franzini and Prof. Claudio Villani (Università di Roma, *La Sapienza*). The chiroptical properties of single enantiomers by experimental and theoretical electronic and vibrational circular dichroism spectra, as well as CPL phenomena for some derivatives have been studied in collaboration with Dr. Giuseppe Mazzeo, Prof. Giovanna Longhi and Prof. Sergio Abbate (Università degli Studi di Brescia).

3.1 Atropisomers: general concepts

Conformational chirality in a molecule is due to the presence of a stereogenic element other than the stereogenic centre. In this case, the inversion of configuration can occur without breaking a bond, and usually has lower energetic barriers. In particular axial chirality is owing to the hindered rotation around a single bond, which corresponds to the stereogenic axis, and so two different enantiomers exist (*Figure 23*).

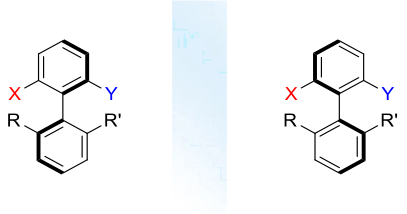

Figure 23: Mirror images of axially chiral biaryls.

In 1933, Khun[194] defined the conformers resulting from the limited rotation around a single bond as *atropisomers*. The rotational energy that controls the rate of interconversion of one enantiomer into the other one depends on steric effect and electronic influences, even if on a minor scale. The bond rotation is time-dependent and the half-live time of racemization ($t_{1/2}$) can be in a range between seconds and years, and this value can change according to the temperature and the solvent.[195]

Compounds can be considered atropisomers if their enantiomerization barrier is equal or above 22 kcal/mol, and so their half-live time allows to isolate them at room temperature.[196] In case of rotational energies lower than 22 kcal/mol, the half-live time of interconversion is too short and it is impossible to isolate the single enantiomer at room temperature, thus the rotation may be considered as free. To study the stereochemical stability of this kind of stereoisomers, very low temperatures are required. When the rotational energy is higher than 29 kcal/mol, no interconversion can be observed at room temperature even after very long time and molecules are considered stable atropisomers (*Figure 24*).

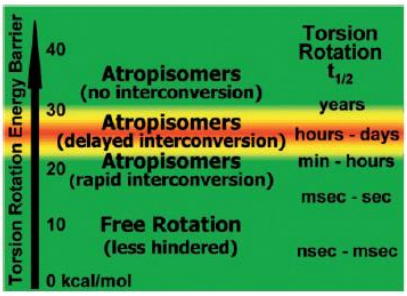

Figure 24: Qualitative guide to help correlate calculated torsion rotation energy barriers ($t_{1/2}$).[197]

The most suitable techniques to study the stereochemical stability of atropisomers are the nuclear magnetic resonance spectroscopy or chromatographic methods that make use of chiral stationary phases. Dynamic-NMR and dynamic-HPLC are complementary methodologies that allow to measure free energy interconversion barrier values ($\Delta G^{\neq}$), although dynamic-HPLC requires significantly smaller amounts of compounds than dynamic-NMR.[198] Moreover, the key experimental parameters for the dynamic-HPLC can be easily controlled and changed (temperature, eluent and flow rate), and the separation of the racemic material into the single enantiomers is also possible.

Concerning the study of the chiroptical properties of atropisomers, beside the X-ray diffraction analysis, by which it is possible to assign unambiguously the absolute configuration of the enantiomers, the spectroscopic techniques such as the Electronic Circular Dichroism (ECD) and Vibrational Circular Dichroism (VCD), in combination with DFT and TD-DFT calculations, are emerging as valuable tools.[199]

Moreover, several chiral poly(hetero)aromatic compounds also show interesting emission properties in solution, so CPL properties of these molecules are being widely studied, and this has proved very useful in identifying promising molecules for diverse applications especially in optoelectronics.[200]

In this context, we selected four bis(benzo[1,2-*b*:4,3-*b*']dithiophene) derivatives **54b**, **53b**, **63b** and **65b** (*Figure 25*) to study the stereochemical and chiroptical properties of this novel class of atropisomers. In particular, dynamic HPLC analyses in combination with kinetic studies were performed to evaluate their configurational stability as well as their absolute configuration was determined by means of experimental and theoretical ECD and VCD spectra. Furthermore, a preliminary study on the CPL properties of these systems was also carried out.

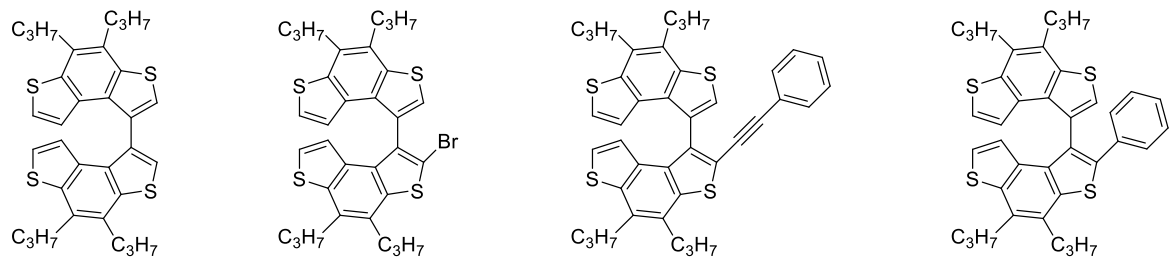

Figure 25: Selected bis(benzodithiophene) derivatives for stereochemical studies.

3.2 Studies of the configurational stability by dynamic HPLC

First studies to evaluate the configurational stability of bis(benzodithiophene) derivatives **54b**, **53b**, **63b** and **65b** were performed through temperature dependent dynamic HPLC. At the onset of this study, these compounds were initially separated into the corresponding enantiomers by HPLC at 20 °C using chiral stationary phases based on cellulose and amylose (Chiralpack IA or IB or Chiralcel OD-H) along with a mobile phase composed by hexane and a small percentage of isopropyl alcohol (0.05–0.1%) at a flow rate of 1 mL min^{-1}. As shown in *Figure 26*, all compounds were found to be configurationally stable at 20 °C since their chromatograms displayed two well separated peaks related to the enantiomers generated by the hindered rotation around the single β-β' bond.

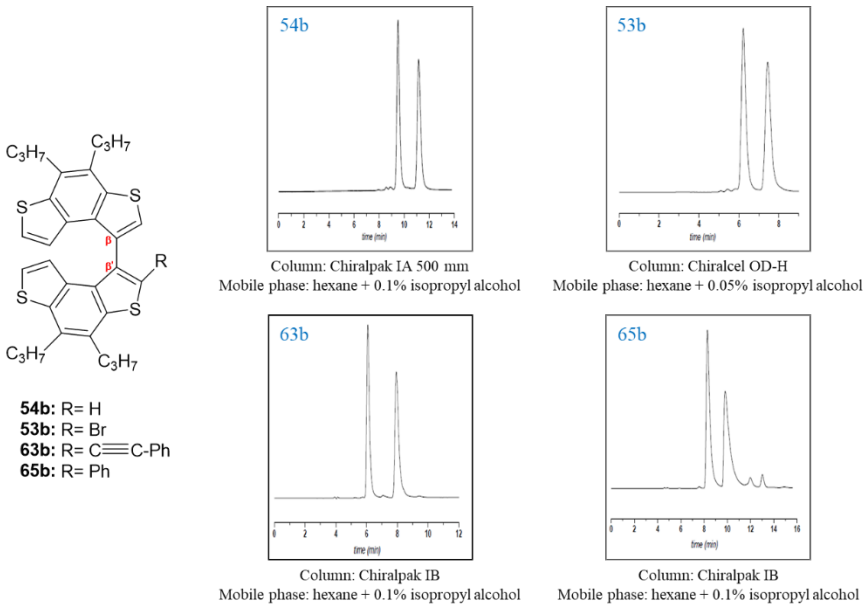

Figure 26: Elution profiles of **54b**, **53b**, **63b** and **65b** registered at 20 °C.

With these optimised HPLC analytical conditions in hands, we then carried out temperature dependent dynamic HPLC experiments at temperatures between 15 and 60 °C in 5 or 10 °C steps. For compound **54b**, which lacks a substituent in the *ortho* position, we observed that a gradually increase of the column temperature provided a progressive coalescence of the chromatographic peaks (*Figure 27*). In particular, a plateau between the peaks related to the interconversion process was observed at 40 °C, and this phenomenon was notable at 60 °C, thus suggesting that single enantiomers of **54b** are not stereochemically stable at temperature slightly above the room temperature.

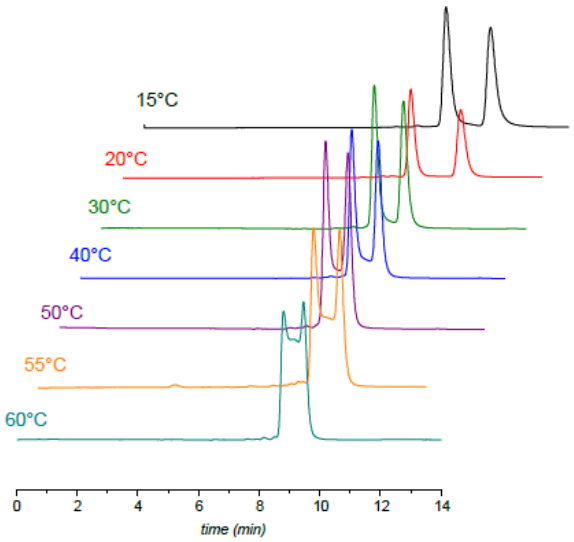

Figure 27: Temperature dependent dynamic-HPLC elution profiles of **54b**.

On the contrary, no evidence of on-column interconversion was observed up to 55 °C for the *ortho*-substituted derivatives **53b**, **63b** and **65b**, thus demonstrating that these compounds are configurationally stable at this temperature due to the steric hindrance of the substituents in the *ortho* position. On the base of the different stability of these compounds, diverse experiments were performed to estimate the free energy of rotation $\Delta G^{\neq}$ around the C-C bond of the bis(benzodithiophene) system. As for the more labile derivative **54b**, the dynamic chromatographic profiles obtained at column temperature of 40, 50 and 55 °C were simulated using a stochastic model based on *Unified Equation of Trapp*[201] (*Figure 28*) in order to obtain the kinetic parameters of the interconversion between the two enantiomers (*Table 7*).

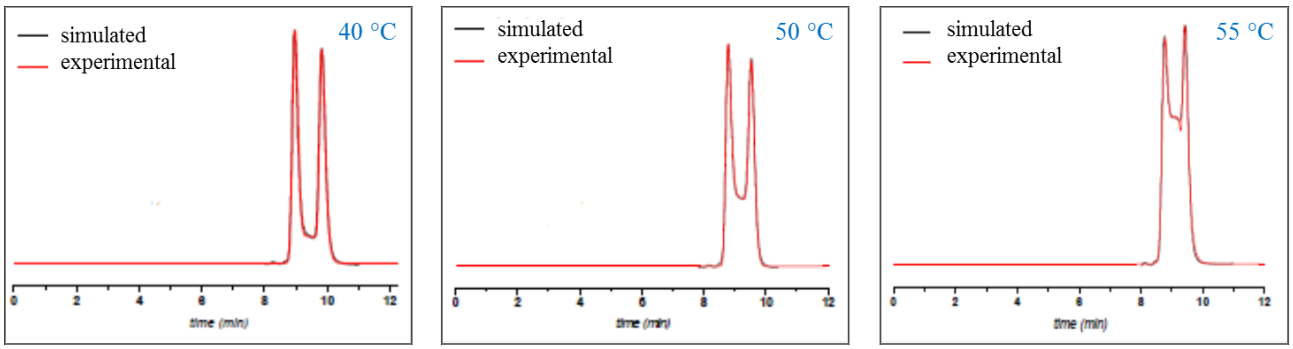

Figure 28: Superimposed chromatographic profiles of simulated and experimental chromatograms of **54b**.

As reported in *Figure 28*, the simulated profiles at different temperatures perfectly matched with the experimental ones, and this similarity allowed us to obtain the kinetic and thermodynamic parameters for the on-column enantiomerization of compound **54b** (*Table 7*).

Table 7. Kinetic rate constants (k) and energetic barrier of the on-column enantiomerization ($\Delta G^{\neq}$) of **54b**.

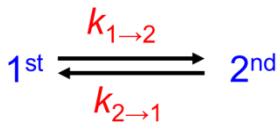

T (°C)[a]	$k_{1\rightarrow2}$ (min^{-1})	$\Delta G^{\neq}{}_{1\rightarrow2}$ (kcal/mol)[b]	$k_{2\rightarrow1}$ (min^{-1})	$\Delta G^{\neq}{}_{2\rightarrow1}$ (kcal/mol) [b]	k (min^{-1})[c]	$\Delta G^{\neq}$ (kcal/mol)[b,c]
40	0.024	23.23	0.022	23.29	0.023	23.26
50	0.056	23.44	0.052	23.49	0.054	23.47
55	0.095	23.47	0.088	23.52	0.092	23.50

[a] Column temperatures are intended ± 0.1 °C. [b] Errors in $\Delta G^{\neq}$ ± 0.02 kcal/mol. [c] Average value.

Since the $\Delta G^{\neq}$ values are in the range 23.26–23.50 kcal/mol, compound **54b** can be considered an atropisomer, even if the interconversion of the enantiomers was observed above room temperature, with a calculated $t_{1/2}$ of 30 minutes at 40 °C. To further confirm this data, the kinetic of racemization of the two enantiomers of **54b** was studied in off-column experiments. Single enantiomers of **54b** were isolated upscaling the analytical method to semipreparative level, and stored at 0 °C. Their kinetic of racemization off-column was determined incubating a solution of the first eluted enantiomer in hexane/isopropyl alcohol (0.025%) as mobile phase for 90 minutes at 35.5 °C, and the decay of enantiomeric excess (*ee*) was measured over time by HPLC (*Figure 29a*).

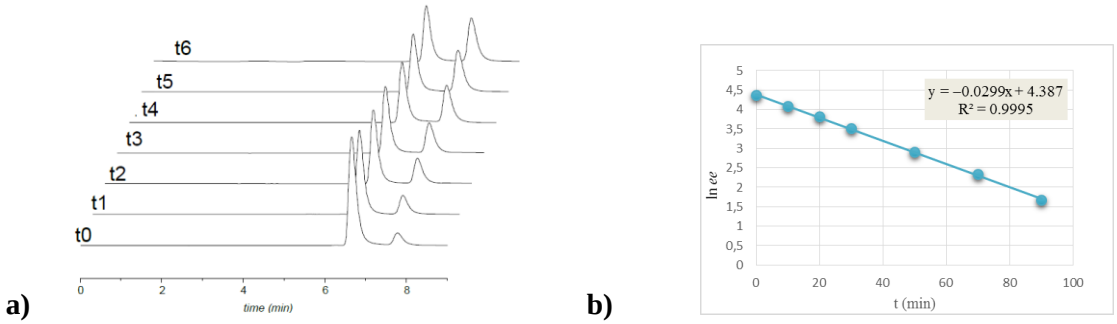

Figure 29: a) thermal racemization of **54b** monitored over time by chiral HPLC. t_0= 0 min, t_1= 10 min, t_2= 20 min, t_3= 30 min, t_4= 50 min, t_5= 70 min, t_6= 90 min. b) rate constant for the racemization of **54b**.

Plotting the logarithm of *ee* against the time (*Figure 29b*), the rate constant for the racemization of **54b** was found to be 0.0299 min^{-1}, and through the Eyring equation the $\Delta G^{\neq}$ resulted 22.75 kcal/mol, in agreement with that obtained with on-column experiment. For stereochemically stable compounds **53b**, **63b** and **65b**, kinetic experiments in decalin at 150 °C were carried out. More in detail, single enantiomers of **53b**, **63b** and **65b** have been isolated upscaling the analytical method to semipreparative level, with an enantiomeric excess

higher than 95%. The latter were dissolved in decalin and the solution was heated up at 150 °C. The reaction was controlled over time checking the decay of *ee* by HPLC (*Figure 30*).

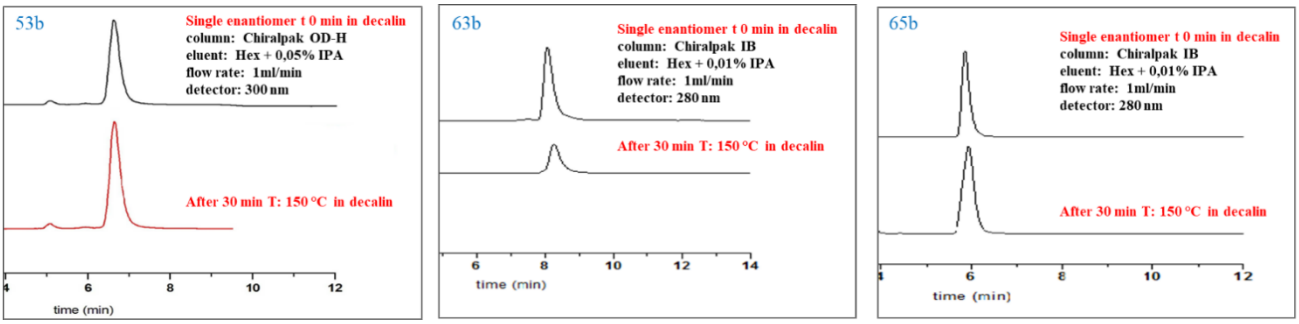

Figure 30: Kinetic studies in decalin for compounds **53b**, **63b** and **65b**.

After 30 minutes at 150 °C, no sign of racemization was observed for all samples, and their interconversion barrier $\Delta G^{\neq}$ value was estimated higher than 34 kcal/mol considering that this value would be 34 kcal/mol in case of $t_{1/2}$= 45 minutes. We could assume that the rotation around the stereogenic axis in **53b**, **63b** and **65b** was too slow to be observed at room temperature, so the two conformations of these atropisomers are considered locked.

3.3 Experimental and theoretical ECD and VCD spectra

The low configurational stability of unsubstituted derivative **54b** did not allow us to thoroughly study the stereochemical properties of its enantiomers, including the assignment of the absolute configuration, and only the ECD spectra of both enantiomers of **54b** could be registered at 5 °C (*Figure 31*).

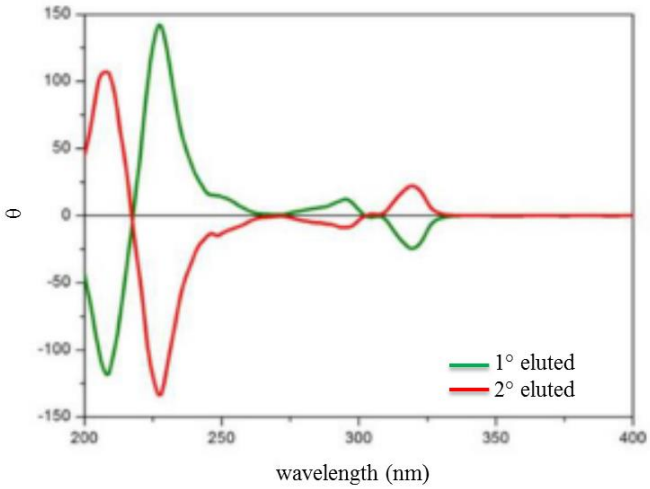

Figure 31: ECD spectra of the enantiomers of **54b** at 5 °C (solvent: hexane).

On the contrary, the stereochemical properties of the three configurationally stable dimers **53b**, **63b** and **65b** were investigated by means of chiroptical spectroscopic techniques such as Electronic Circular Dichroism (ECD) and Vibrational Circular Dichroism (VCD), in combination with DFT and TD-DFT calculations.

We initially separated the two enantiomers of (±)-**53b**, (±)-**63b** and (±)-**65b** by HPLC using semipreparative chiral columns with a binary mobile phase (hexane-isopropyl alcohol) under isocratic conditions, obtaining the two enantiomers of each compound in high optical purity (*ee* up to 99%). The earlier eluting fractions of **63b** and **65b** consisted of the enantiomers exhibiting a negative optical rotation, while for derivative **53b** the first eluted enantiomer showed a positive optical rotation value (see *Experimental part* for the optical rotation values, *Table 8*).

Since we were not able to obtain suitable crystals for X-ray diffraction of both enantiomers of **53b**, **63b** and **65b**, we could assign the absolute configuration through ECD and VCD spectroscopy along with theoretical calculations.

The ECD and UV absorption spectra of **53b**, **63b** and **65b** are showed in *Figure 32*. All compounds were characterized by a vibronically resolved structure, typical of rigid π-conjugated systems, with two distinct regions: a high energy region (185–285 nm) and a low energy region (285–390 nm). The absorption spectra of **63b** and **65b** significantly redshifted compared to **53b** (by ca. 25 nm in case of **65b** and by ca. 35 nm in compound **63b**), as consequence of the higher conjugation due to the presence of aryl and alkynyl pendant, respectively.[171] Moreover, the spectral shape, especially for alkynyl derivative **63b**, remarkable changed being dominated by the transitions of the aryl-acetylene modes as described in literature for diphenylacetylene derivatives.[202,203]

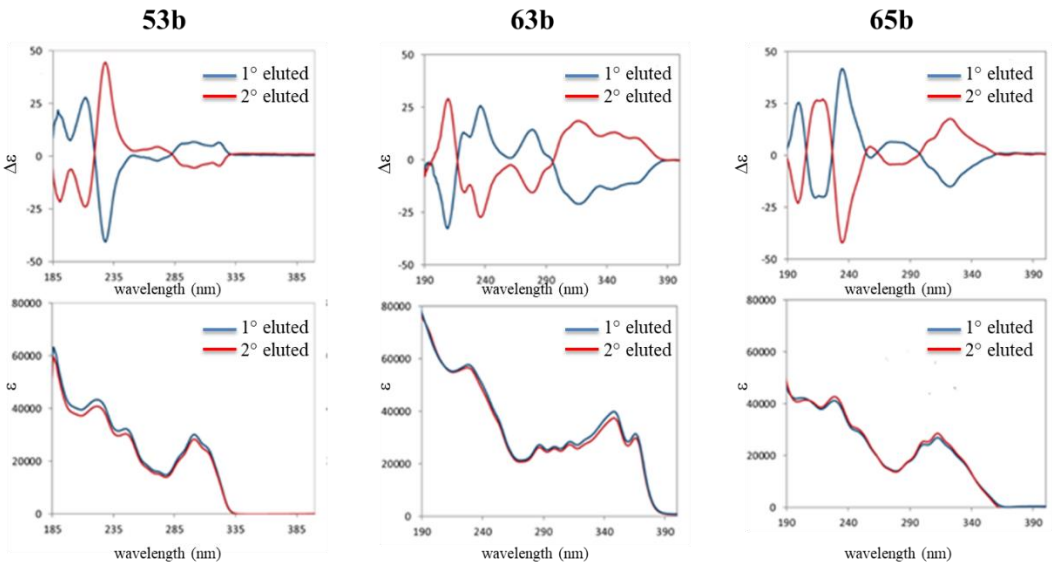

Figure 32: Experimental ECD (top panels) and UV (lower panels) spectra of **53b**, **63b** and **65b** in the two enantiomeric forms eluted through the HPLC experiments.

While the low lying ECD allied band was negative for first eluted enantiomer in case of **63b** and **65b**, this band was positive for first eluted fraction of **53b**. In particular, there were two diagnostic bands in the range of 230–290 nm (ca. 235 and 280 nm) that were positive for the first eluted fractions of **63b** and **65b**, while they were negative for the first eluted fraction of **53b**. Thus, ECD features also indicated that axial chirality

of first eluted enantiomer of **53b** was opposite to the axial chirality of the first eluted enantiomers of **63b** and **65b**, in agreement with their optical rotation value. VCD and IR spectra of dimers **53b**, **63b** and **65b** are showed in *Figure 33*.

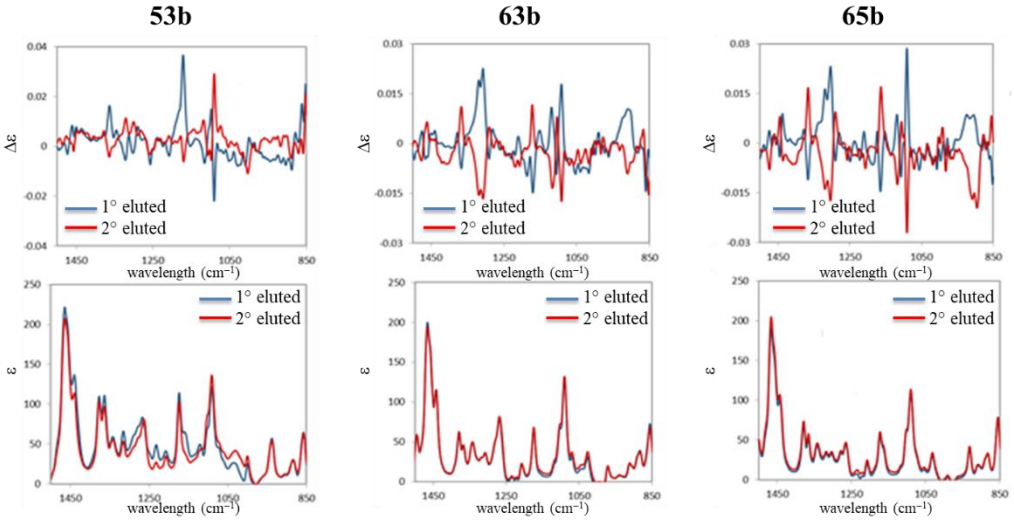

Figure 33: Experimental VCD (top panels) and IR (lower panels) spectra of the two enantiomers of **53b**, **63b** and **65b.**

While the IR spectra of both enantiomers of **53b**, **63b** and **65b** were quite similar, VCD spectra showed different profiles. Indeed, the earlier eluting enantiomers of **63b** and **65b** showed a (+,–,+) triplet in the range of 1090–1116 cm^{-1}, whereas an opposite sequence of signs was observed for the first eluted fraction of **53b**. The same attitude was observed in the range 1300–1370 cm^{-1}. Furthermore, dimers **63b** and **65b** had a common VCD signed band at 910 cm^{-1} with positive band for the first eluted enantiomers, while **53b** did not show good experimental correlation in that region. So, VCD features were in agreement with the results obtained by ECD spectroscopy (*Figure 32*) and the optical rotation values.

Having no similar compounds in literature with which to compare the obtained ECD and VCD spectra (*Figures 32 and 33*), we simulated them to compare the latter with the experimental ones and assign the absolute configuration of each enantiomer. The models of *P* and *M* enantiomers for each compound were then constructed by Gaussian16 in vacuum.

In consequence of the presence of the four propyl chains in the structures, the conformational search involves many conformers with different orientation of flexible propyl group and with very close relative energies. These alkyl chains can be important especially for VCD–IR calculation, which is quite sensitive to configuration and conformational structures. Oppositely, orientations of propyl groups may not influence ECD–UV spectra that are sensitive to aromatic chromophores. Based on these considerations, ECD–UV[204] (*Figure 34*) and VCD–IR[205] (*Figure 35*) calculations were performed not only for dimers **53b**, **63b** and **65b**, but also for model dimers obtained replacing each propyl group of dimers with a methyl group in order to simplify the simulations.

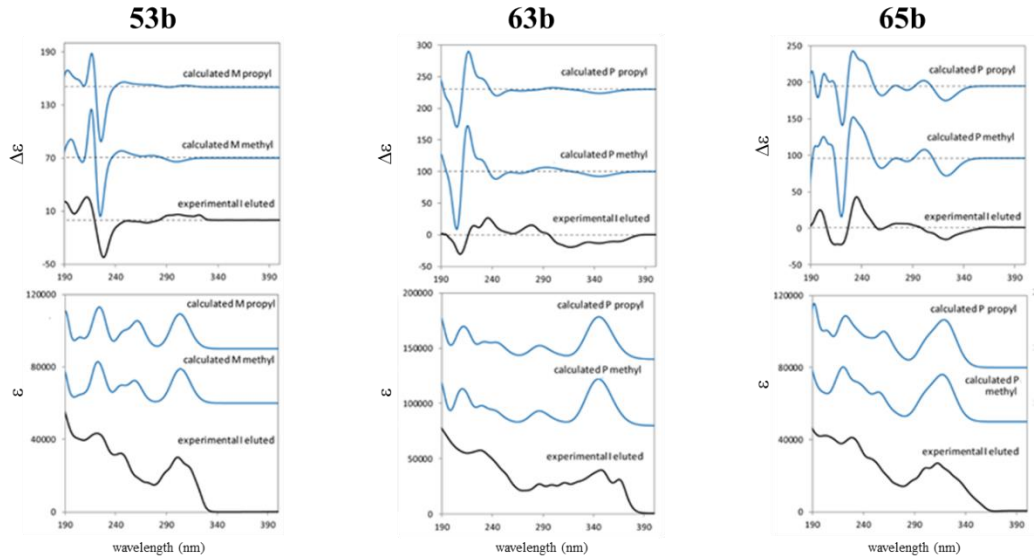

Figure 34: ECD (top panels) and UV (bottom panels) spectra: comparison of experimental (black lines) of the first eluted fractions of **53b**, **63b** and **65b** with the calculated spectra (blue lines) for (*M*)–**53b** isomer, (*P*)–**63b** and (*P*)–**65b** isomers.

As reported in *Figure 34*, the calculated ECD and UV spectra for model dimers with methyl groups showed a nice correlation with experimental spectra in position, intensity and sign of principal bands. A correct prediction was observed in experimental doublet at ca. 200 nm; in particular, we found a negative-positive doublet in case of (*M*)–**53b** and a positive-negative one for (*P*)–**63b** and (*P*)–**65b**. These doublets permitted the assignment of absolute configurations associated to the first eluted fractions of dimers **53b**, **63b** and **65b**. More in detail, *R* in case of **53b** (*M* torsion) and *S* for **63b** and **65b** (*P* torsion). So, these approximate models with methyl chains may be considered good enough for configuration assignment based on ECD.

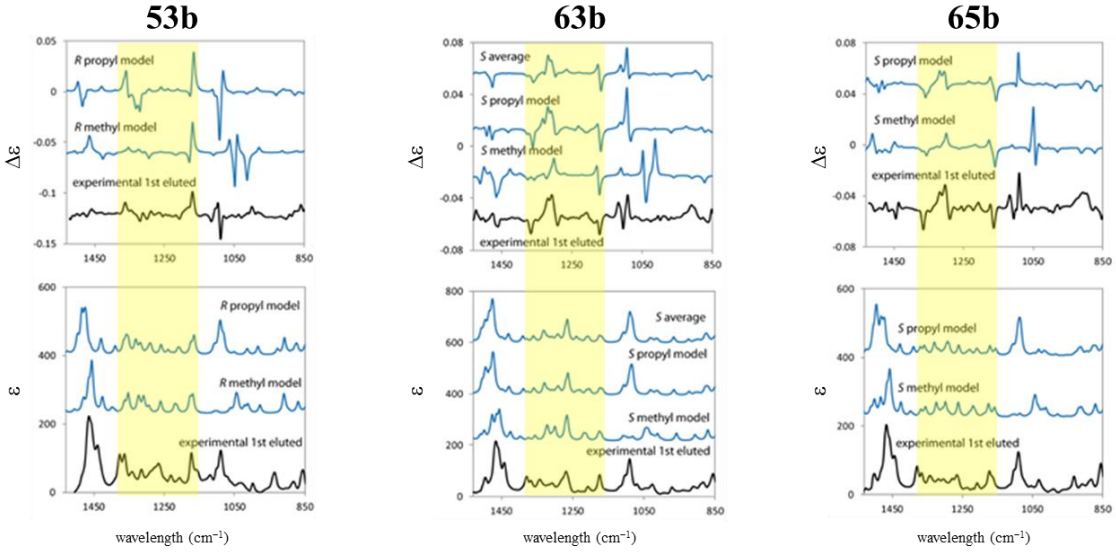

Figure 35: VCD (top panels) and IR (bottom panels) spectra: comparison of experimental (black lines) of the first eluted fractions of **53b**, **63b** and **65b** with the calculated (blue lines) for (*R*)–**53b** isomer, (*S*)–**63b** and (*S*)–**65b** isomers. For (*S*)–**65b** a more complete conformational average model for propyl has also been considered.

Concerning VCD and IR data, a comparison between experimental and calculated spectra of **53b**, **63b** and **65b** (with both propyl and methyl groups) have been performed (*Figure 35*). Regarding the IR absorption, experimental and calculated spectra showed a nice correlation. On the contrary, calculated VCD spectra were less satisfactory considering the methyl models. More in detail, the bands sign sequence was nicely predicted for all dimers in 1300–1370 cm^{-1}, provided that propyl groups are explicitly introduced, even in just one conformation. Next, the band at 1170 cm^{-1} (positive for **53b** and negative for **63b** and **65b**) was predicted for both methyl and propyl approximated models in each case. Besides, the experimental triplet (+,–,+) at ca. 1100 cm^{-1} seems to be correctly predicted for methyl model of **63b**, even if only at low wavenumber. Thus, this triplet seems to be quite sensitive to propyl group conformations. Furthermore, the region 1150–1400 cm^{-1} (evidenced in yellow in *Figure 35*) is well reproduced also without average over possible propyl structures. This permitted the assignment of axial absolute configurations associated to the first eluted fractions of dimers **53b**, **63b** and **65b**. More in detail, *R* in case of **53b** (*M* torsion) and *S* for **63b** and **65b** (*P* torsion), in agreement with the conclusions deduced by ECD.

3.4 Circularly Polarized Luminescence (CPL) properties of dimer 63b

To complete the study on the chiroptical properties of these new atropisomers, we evaluated their emission, and we observed that the presence of alkynyl pendant in *ortho* position promoted appreciable emission in compound **63b**. For this reason, the CPL^{200} spectra of both enantiomers of **63b** were registered (*Figure 36*).

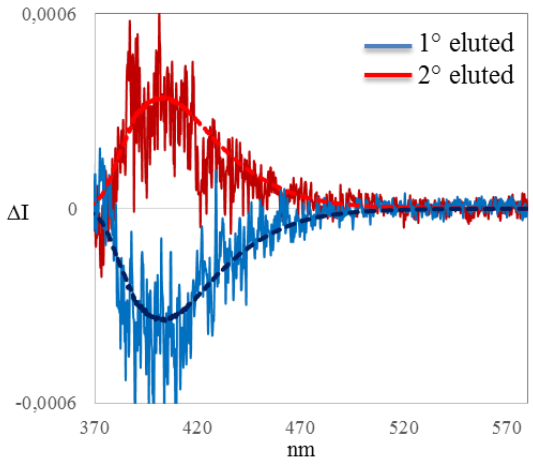

Figure 36: CPL spectra of two eluted fractions of compound **63b** after normalising to one the corresponding fluorescence signal. The superimposed red and blue dashed traces are the corresponding fluorescence spectra.

The fluorescence band was centred at ca. 400 nm, and it was reported superimposed on the CPL traces, which showed a similar shape. The sign of CPL band was the same as the sign of low frequency/high wavelength ECD band of the corresponding enantiomer (*Figure 32* vs. *Figure 36*). The dissymmetry ratio

g_{lum} was ca. 3.5×10^{-4}. Optimisation of the ground and first excited state permitted to compare the structures for the two states (which are superimposed in *Figure 37*, left), and to check that they were quite different in the central dihedral angle.[206,207]

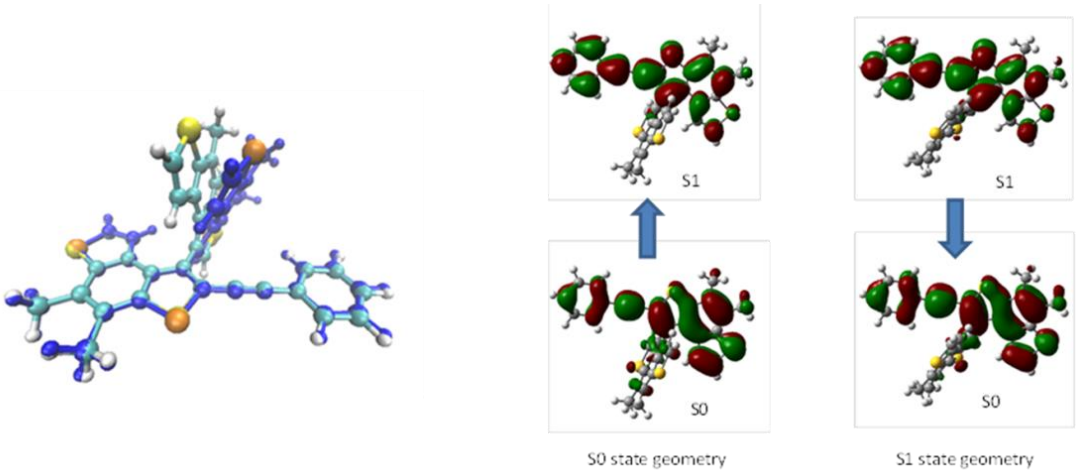

Figure 37: Superposition of ground (light blue) and excited (dark blue) structures for compound with methyl groups (left). Kohn-Sham HOMO-LUMO orbitals of methyl model for compound **63b** for the ground and first excited state structure (right).

As reported in *Figure 37* (right), the HOMO and LUMO orbitals involved in the first transition were quite similar in the two cases and were localized on the extended flat moiety comprising benzodithiophene and alkynyl pendant. *Table 9* reports the calculated spectroscopic characteristics.

Table 9. Comparison of ground (G) and first excited (E) state characteristics from TD-DFT calculations: central dihedral angle (CCCC) value, transition wavelength (λ), dipole strength (D), rotational strength (R), calculated *g* dissymmetry factor.

	CCCC	λ (nm)	D	R	$g = 4R/D$
G	81	323.6	7.3×10^5	−28	-1.5×10^{-4}
E	116	393.6	8.3×10^5	−149	-7.2×10^{-4}

Rotational forces calculations from ground state geometry and excited state geometry were the correct sign of the observed CPL and ECD bands, but the g_{lum} value (-7.2×10^{-4}) was overestimated while the g_{abs} value (-1.5×10^{-4}) was underestimated. This fact was probably due to the fact that vibronic contributions were not considered.

3.5 Conclusions

The racemic mixture of dimers **53b**, **54b**, **63b** and **65b** have been successfully resolved into the corresponding antipodes by HPLC using chiral stationary phases based on cellulose and amylose.

The unsubstituted dimer **54b** was found to be configurationally unstable at temperature above 40 °C ($\Delta G^{\neq}$ ca. 23.3 kcal/mol). On the other hand, *ortho*-substituted compounds **53b**, **63b** and **65b** were found to be configurationally stable, with an estimated value of $\Delta G^{\neq} > 34$ kcal/mol (*Figure 38*).

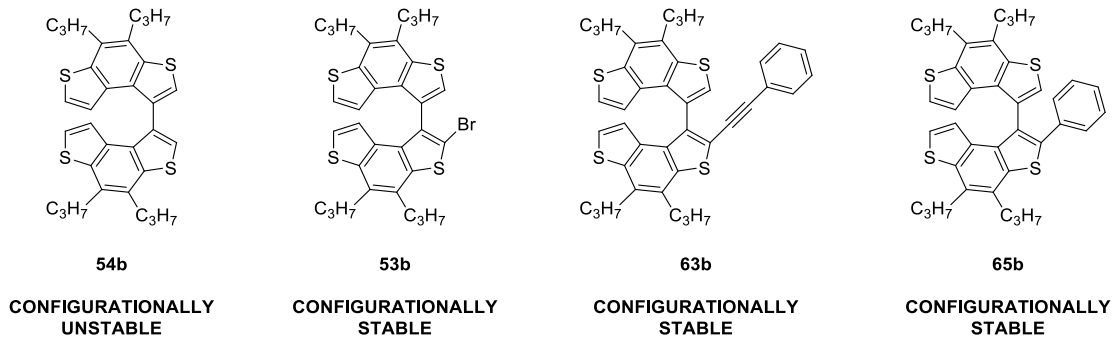

Figure 38: Configurational stability of selected atropisomers.

Furthermore, the absolute configuration of the enantiomers of **53b**, **63b** and **65b** has been assigned through the comparison between ECD–VCD experimental spectra and DFT calculation, which are in agreement with the (*P*)-helicity for (+)-**53b**, (+)-**63b** and (+)-**65b**, and then (*M*)-helicity for (–)-**53b**, (–)-**63b** and (–)-**65b**.

Finally, due to the good conjugation, compound **63b** has been characterized in its emissive chiral properties recording CPL spectrum, which presents the same shape as the fluorescence band and exhibits a g_{lum} value of 3.5×10^{-4}.

Thanks to the fully elucidation of the chiroptical properties of dimeric intermediates, asymmetric version of the protocols reported and discussed in *Chapter 1* could be envisage. In particular, in *Chapter 4* a preliminary study for the synthesis of enantioenriched 7-THs by asymmetric Au(I)-catalysed hydroarylation of alkynes **63** has been discussed.

3.6 Experimental part

3.6.1 Dynamic HPLC studies

All reagents and solvents (HPLC grade) were purchased from Sigma Aldrich and were used without further purification.

Analytical chromatography was performed on a Jasco (Tokyo, Japan) HPLC system with a universal Rheodyne 20 μL injector, a pump Jasco PU 980 and a second CO_2 pump Jasco PU 1580. Detection is provided by a Jasco UV 975 detector a Jasco UV/CD 995 detector. During dynamic HPLC experiments low temperatures were maintained using a home-made cooling device. Preparative chromatography was performed with a chromatographic apparatus composed by Waters with a pump Waters Millipore Model 590 and a Waters Millipore Lambda-Max model 481 LC spectrophotometer detector. Chiral resolution of the racemic mixtures by HPLC was performed by polysaccharide-based chiral stationary phases: Chiralpak IA (250 × 4.6 mm, 5 μm particle size), Chiralpak IB (250 × 4.6 mm, 5 μm particle size), Chiralcel OD-H (250 × 4.6 mm, 5 μm particle size), purchased from Chiral technologies at flow rates of 1.0 ml min^{-1}. Separation of the enantiomers was performed by semipreparative chiral column: Chiralpak IA (250 × 10 mm, 10 μm particle size), Chiralpak IB (250 × 10 mm, 10 μm particle size), Chiralcel OD-H (250 × 10 mm, 10 μm particle size), purchased from Chiral technologies at flow rates of 4.0 ml min^{-1}.

Specific optical rotation measurements were performed at room temperature on a Jasco P 1030 polarimeter, with Na and Hg light sources and filters at different wavelength for studying ORD. A 10 mm cylindrical cuvette was used for the samples. CD spectra were recorded on a Jasco J-700 spectropolarimeter, using 1 cm cell.

3.6.2 Experimental ECD and VCD spectra

ECD and UV spectra were measured in a 2 mm quartz cuvette at ca. 10^{-4} M in hexane on a Jasco815SE spectrometer. CPL and fluorescence spectra have been recorded on the same solutions used for ECD measurements on a home-built apparatus;[200,208] with 350 nm excitation wavelength. VCD and IR spectra were measured in a 500 μm BaF_2 cell, at a concentration of ca. 0.05 M in CCl_4 solvent on a FVS6000 FTIR spectrometer, equipped with a ZnSe Photo-Elastic Modulator and an MCT liquid N_2-cooled detector.

3.6.3 Computational study

Simulation of variable temperature experimental chromatograms presenting a dynamic profile were performed by Auto DHPLC y2k (Auto Dynamic HPLC), using the stochastic model. Both chromatographic and kinetic parameters can be automatically optimised by simplex algorithm until the best agreement between experimental and simulated dynamic chromatograms is obtained.

Preliminary conformational search was performed by means of Molecular Mechanics (MM) retaining only the conformers within a 10 kcal/mol energy interval with respect to the most stable one. The geometries found in this way were fully optimised at Density Functional Theory (DFT) B3LYP/6-31G* level and the

conformers within 5 kcal/mol in electronic energies were further optimised at B3LYP/TZVP level.[209] Frequency, dipole and rotational strength calculations were performed for the conformers within 2.5 kcal/mol at B3LYP/TZVP level in the harmonic approximation for VCD-IR[205] and CAM-B3LYP/TZVP for ECD-UV.[204] Also the first excited state has been optimised and compared to the ground state, in order to calculate also CPL spectra.[206,210] ECD spectra were simulated by assigning to each electronic calculated transition 0.2 eV wide Gaussian bands. All calculated ECD and UV absorption transitions were shifted by 10 nm. The first 100 excited states were considered in setting up the calculation Lorentzian band-shapes were assigned to calculated IR and VCD transitions (with 10 cm^{-1} bandwidth) and the frequencies of all calculated bands were scaled by a 0.98 scaling factor, as usually done in VCD spectroscopy.[211-214]

3.6.4 Resolution HPLC and optical rotations

Table 8. Chiral HPLC resolution of dimers **53**, **63** and **65**.

	Column	**Eluent**	**t_R(min)**	**$[\alpha]_D$[a]**	***ee (%)***
(+)-53b	Chiralcel OD-H	Hexane + 0.05% IPA	6.4	+69[b]	99
(–)-53b	Chiralcel OD-H	Hexane + 0.05% IPA	7.5	–63[b]	94
(–)-63b	Chiralpak IB	Hexane + 0.1% IPA	8.3	–318[c]	99
(+)-63b	Chiralpak IB	Hexane + 0.1% IPA	9.3	+305[c]	96
(–)-65b	Chiralpak IB	Hexane + 0.1% IPA	6.1	–166[d]	99
(+)-65b	Chiralpak IB	Hexane + 0.1% IPA	7.9	+156[c]	94

[a] Measured in $CHCl_3$ at 20 °C. [b] C= 2.1×10^{-4} g/mL. [c] C= 1.7×10^{-3} g/mL. [d] C= 1.6×10^{-3} g/mL.

Chapter 4

Synthesis of tetrathia[7]helicenes by gold catalysis also in enantioenriched form

This chapter describes the studies conducted in the synthesis of monosubstituted 7-THs also in enantioenriched form using Au(I)-complexes. This study was performed during a period in the laboratories of Prof. Manuel Alcarazo (Georg-August-Universität Göttingen). X-ray analyses were performed by Dr. Christopher Golz (Georg-August-Universität Göttingen), while HPLC analyses were carried out by Mr. Martin Simon (Georg-August-Universität Göttingen).

4.1 Asymmetric gold catalysis

Catalytic applications of gold developed much slower than other transition metals. Although exhibiting a rich coordination chemistry, gold was considered to be largely catalytically inactive by the scientific community[215] and was appreciated to make coins, jewellery and, more recently, medical implants and electronic parts. Fortunately, this view gradually started to change thanks the reports of heterogeneous gold catalysts in the hydrogenation of olefins in 1973,[216] the hydrochlorination of alkynes[217] and the oxidation of CO[218] where gold outperformed other catalysts. The first report of asymmetric gold catalysis was published in 1986 by Ito and co-workers.[219] Despite the rapid acceleration of research activity in field of gold catalysis, the enantioselective gold catalysis progressed at a slower race and the first communication about it was reported in 2005.[220]

4.1.1 Gold catalysts

In the periodic table, Gold is located in group 11 and exists most commonly in the oxidation states +1 and +3. More in detail, gold(III) complexes tend to have a square planar geometry, while gold(I) complexes a predominantly linear geometry.

Gold is a chemically soft, carbophilic Lewis acid, thanks to its low lying, large and polarizable empty orbitals. Furthermore, gold(I) compounds present a high stability towards redox processes. Due to these properties, gold has been widely applied in field of π-acid catalysis alongside metals such as platinum.[221-225] Nowadays, gold(I) complexes are widely exploited owing to the linear geometry of these gold species, for which any chiral information on the ligand is constrained to lie at the opposite side of the gold to the substrate. Besides, the mono-coordination permits an ample degree of freedom in the subsidiary ligand, with the possibility of free rotation around the single bonds[226] (*Figure 39*).

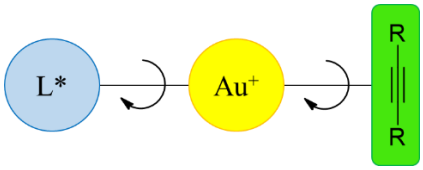

***Figure 39*:** Linear coordination mode.

In this context, a frequently used gold(I) complex is the type **L·AuX** thanks to their stability and tunability through the auxiliary ligand L, while the gold(III) catalyst $AuCl_3$ is most popular in gold catalysis when higher Lewis acidity may be required.

Concerning **L·AuX** complexes, when X is a non-coordinating counterion (e.g., triflamide), these complexes can be directly applied in catalysis, as the gold has a coordination vacancy. The corresponding cationic gold(I) complex can also be stabilized through neutral donors which are then easily displaced under catalytic conditions such as acetonitrile or toluene. Another method is the removal of X *in situ*. This approach is generally achieved either by deprotonation with 1 equiv. of Brønsted acid, for instance when X = CH_3, or by silver-mediated abstraction when X = Cl. In the latter case, a silver salt is used, which forms an insoluble silver chloride and the active gold species.[227] Subsequently, the coordination vacancy of gold is filled by formation of a π-complex with a suitable donor as allene, alkene or alkyne.[228]

4.1.2 Ligands

An important aspect about these complexes toward asymmetric gold catalysis is the choice of the ligands, depending on the nature of the reaction. Indeed, the electronic aspect of the ligand allows control over the reaction outcome in some cases. Moreover, when there is the necessity of a large distance between the substrate and ligand to effectively transfer the chiral information, a steric "wall" must be designed to enclose the gold center and it can be reach using bulky substituents.

For example, chiral disphosphanes represent useful class of ligands for gold(I) complexes. They form linear, binuclear species on coordination to gold, and the most widely used catalyst from this class are derivatives of BINAP[229,230], MeO-BIPHEP[231] and SEGPHOS[232] scaffolds (*Figure 40*, a–c).

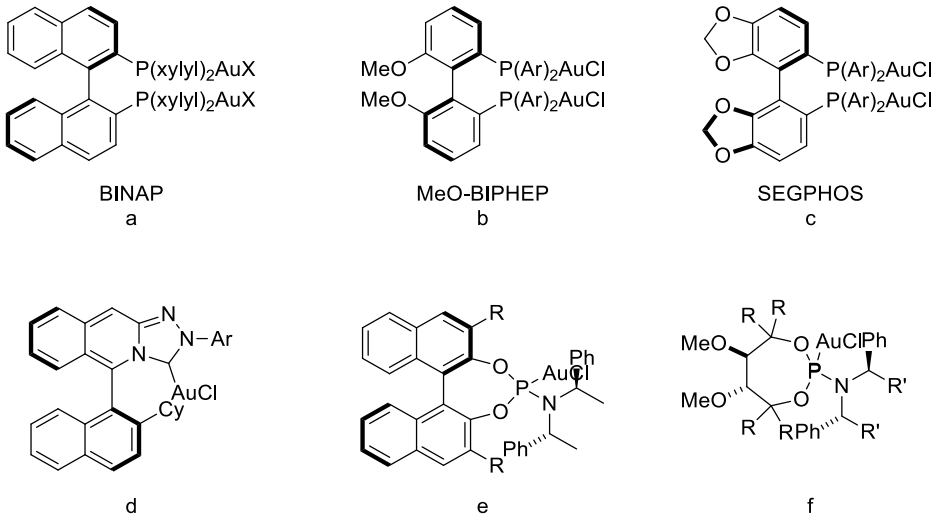

***Figure 40*:** Examples of L·AuX complexes.

Also chiral carbenes[233,234] are used as ligands (*Figure 40*, d). In particular, they are strong electron donor ligands and a variety of chiral carbene-gold complexes have been reported when an electronic rich gold(I) is beneficial for the outcome of the asymmetric and regiodivergent transformations.

Another fascinating tool in asymmetric gold catalysis is the emergence of monodentate phosphoramidites,[235-237] that don't require the presence of two gold centre *per* catalyst unlike bidentate phosphines (*Figure 40*, e–f). Furthermore, they are extremely electron poor ligands and are perfect for transformations in which an electron-poor gold(I) centre can influence the selectivity or the rate of the reaction. The majority of ligands are either anionic or neutral, because of their higher ability in coordination of electropositive metal centers and stabilization of metal complexes. Nevertheless, α-cationic ligands have recently emerged as a class of exceptionally strong π-acceptor ligands, especially phosphines and phosphonites, due to their modular syntheses[238-246] and high stability compared with other strong electron withdrawing ligands. Even though their electron poor nature, many of them exhibit a rich coordination chemistry.[247] Thanks to their increased polarity and high stability, α-cationic phosphine-containing complexes initially found numerous applications in phase-transfer catalysis and in a variety of these reactions the recyclability of cationic phosphines had been demonstrated.[248] However, the applications of their electronic abilities in catalysis have not been widely explored yet. In this context, Alcarazo's group has recently and actively investigated the application of cationic ligands,[248] with an interest in π-acid-catalysed intramolecular hydroarylation reaction of *ortho*-alkynyl-substituted biaryls.

4.1.3 Applications in intramolecular hydroarylation

As previously mentioned, an on-going topic of interest of Alcarazo and co-workers is the π- acid-catalysed intramolecular hydroarylation reaction of *ortho*-alkynyl-substituted biaryls. Initially, the synthesis of phenanthrene **79** starting from alkyne **80** was tested and polycationic ligands proved to be excellent catalyst using gold(I) complexes (*Scheme 48*).[245]

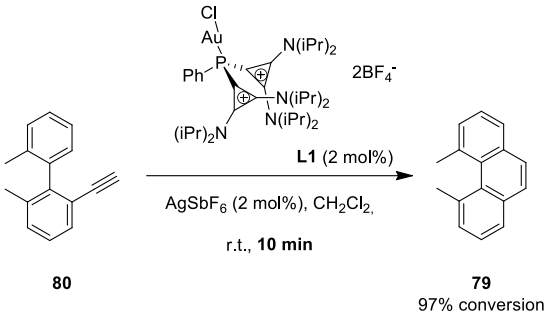

Scheme 48: Synthesis of phenanthrene **79** using gold(I) complexes.

Interestingly, the formation of 5-*exo* side-product[55] was not observed, but only of the 6-*endo* desired product **79**. With this knowledge in hand, Alcarazo's group applied this methodology for the synthesis of natural products such as *Monbarbatain A*[249] (*Figure 41*).

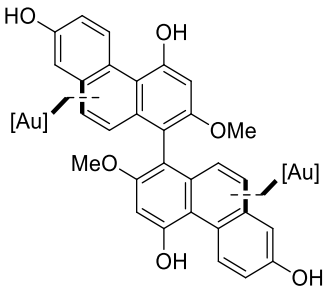

Figure 41: *Monbarbatain A.*

In light of Alcarazo and co-workers' successful results, it was recognised the possibility to apply this methodology for the synthesis of helicenes also in enantiopure form. In particular, they were able to prepare [4]-,[91] [5]-[90] and [6]-carbohelicenes[92,93,250] using different cationic ligands in gold(I) complexes (*Scheme 49*).

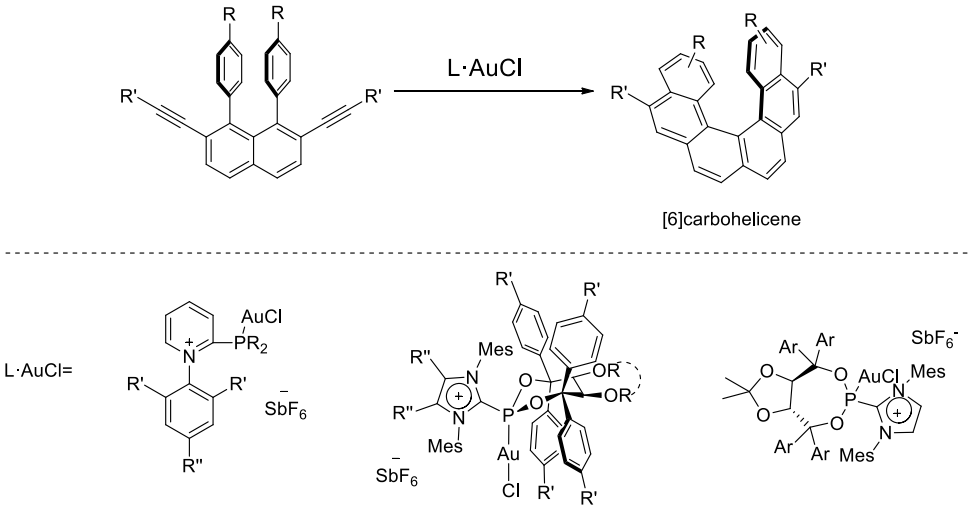

Scheme 49: Synthesis of [6]carbohelicenes using cationic ligands in gold(I) complexes.

Within this context, and in view of potential advantages, cationic ligands in gold(I) complexes have been used for the synthesis of 7-TH systems (*Chapter 1*) by an intramolecular hydroarylation of the key intermediates **63**. Taking into account the configurational stability of atropisomeric alkynes **63**, a preliminary investigation of the cycloisomerisation of (±)-**63** with chiral Au(I)-catalyst to obtain enantioenriched 7-monosubstituted derivatives **64** through a kinetic resolution has been carried out.

4.2 Intramolecular hydroarylation of alkynes 63 promoted by Au(I)-catalyst

This study was initiated by examining the reaction of dimer **63a** as model starting material with different Au(I)-pre-catalysts **L2–6** in the presence of $AgSbF_6$ under experimental conditions very similar to those used by Alcarazo and co-workers[250] (*Table 10*) in order to evaluate the efficacy of this kind of pre-catalyst for the synthesis of 7-THs **64**.

Table 10. Optimisation of intramolecular hydroarylation of alkyne **63a** promoted by Au(I)-catalyst.

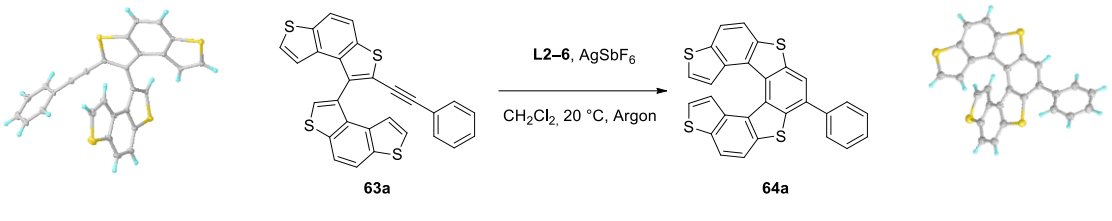

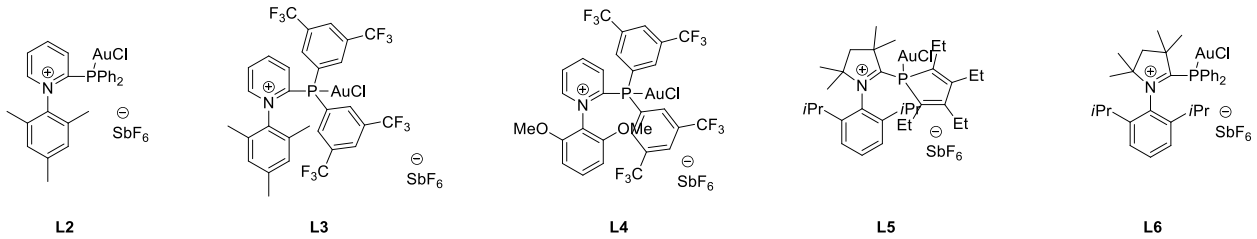

Entry[a]	**L**	mol% **L**/$AgSbF_6$	Time (h)	Ratio **63a**:**64a**[b]	Yield (%)[c]
1	**L2**	5	24	0:1	92
2	**L2**	1	24	1:3	-[d]
3	**L2**	5	2	1:1	-[d]
4	**L2**	5	4	0:1	92
5	**L3**	5	4	0:1	68
6	**L4**	5	4	0:1	73
7	**L5**	5	4	0:1	85
8	**L6**	5	4	0:1	47

[a] Reaction conditions: 25.1 μmol of **63a** in 1 mL CH_2Cl_2 at room temperature, under argon. [b] The ratio was evaluated by ^{1}H-NMR. [c] Isolated yield. [d] The crude was not purified.

Thus, dimer **63a** was reacted in CH_2Cl_2 (1 mL) at room temperature in presence of 5 mol% of pre-catalyst **L2** and 5 mol% of $AgSbF_6$. After 24 hours, the conversion was complete, and the expected product **64a** was isolated in 92% yield (*Table 10*, entry 1). When the loading of **L2** was decreased from 5 mol% to 1 mol%, the ratio of **63a**:**64a** was 1:3 (*Table 10*, entry 2). Next, the time of the reaction using 5 mol% of **L2** was investigated. While after 2 hours the ratio of **63a**:**64a** was 1:1 (*Table 10*, entry 3), a complete conversion was observed after 4 hours and the desired helicene **64a** was isolated in 92% yield (*Table 10*, entry 4). At this point, different pre-catalysts were used in 5 mol% loading to evaluate the most effective for this kind of substrates. After 4 hours, complete conversions and good yields were achieved in case of pyridinium pre-catalysts **L3** (*Table 10*, entry 5) and **L4** (*Table 10*, entry 6) and the desired helicene **64a** was isolated in 68% and 73% yields, respectively. Moreover, **64a** was obtained in 85% yield with pre-catalyst **L5** that is more

active than **L2-4**, but also more difficult and expensive to prepare (*Table 10*, entry 7). Finally, **L6** was used and a complete conversion was observed after 4 hours, but the final helicene **64a** was isolated in only 47% yield (*Table 10*, entry 8). In conclusion, the higher yield was achieved with **L2**, that represents the easiest and cheapest pre-catalyst to prepare. Interestingly, colourless needles of the atropisomeric intermediate **63a** and the tetrathia[7]helicene **64a** were achieved by a slow evaporation of a warm solution of $CDCl_3$ and by layering acetonitrile over a dichloromethane solution, respectively. The X-ray diffraction analysis confirmed the structure of the molecules.

With these conditions in hand, this process was extended by exploring the substrate scope of the reaction with diverse alkynes **63a–g**, containing various (hetero)aryl and alkyl pendants (*Scheme 50*).

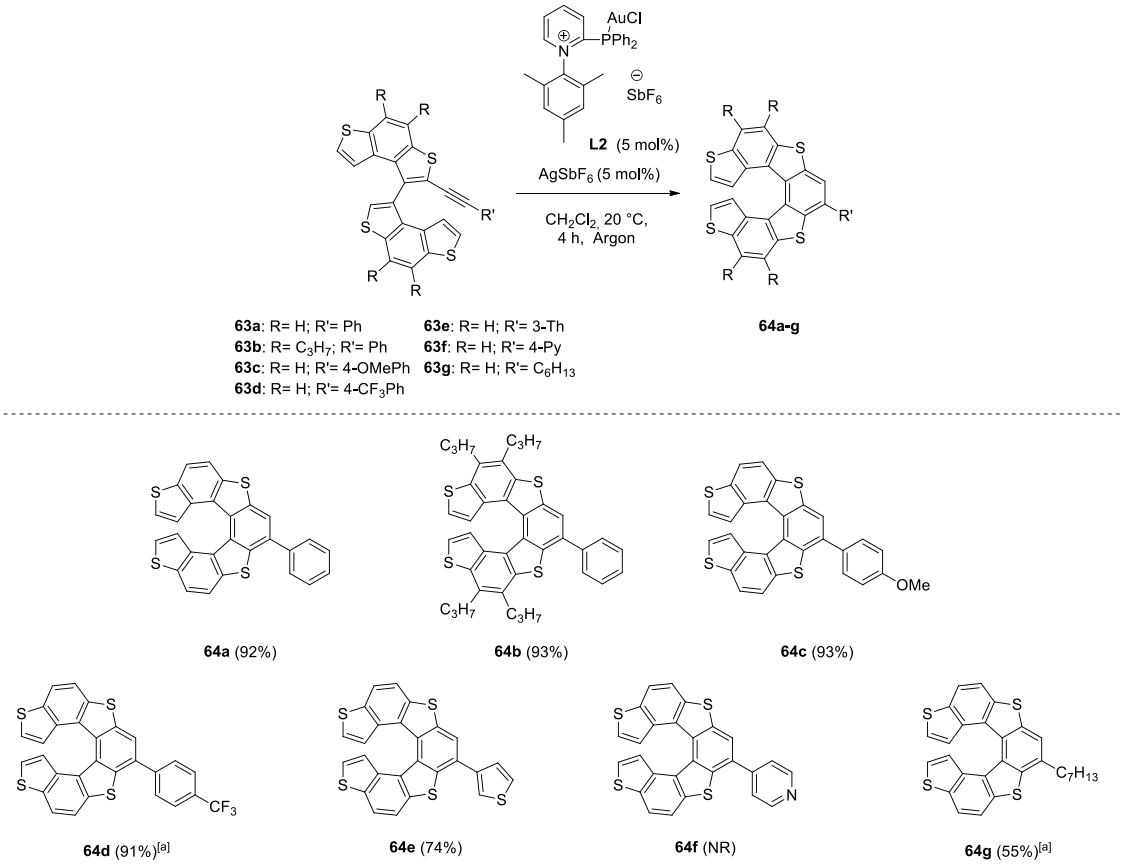

Scheme 50: Synthesis of 7-THs **64a–g** using gold(I) complex **L2**. [a] The complete conversion was observed after 24 h.

As shown in *Scheme 50*, both alkynes **63a,b** were extremely effective in the ring closing process thereby delivering the expected products **64a,b** in 92% and 93% yield, respectively. The same good result was observed in the presence of electron-donor groups such as OMe (**63c**) and electron-withdrawing group such as CF_3 (**63d**). Indeed, the 7-THs **64c** and **64d** were isolated in 93% and 91% yield, respectively. The latter reaction was not finish in 4 hours, and a complete conversion was observed after 24 hours. Good yield was also achieved with the electron rich heteroaryl such as 3-thienyl (**63e**) which gave the desired product **64e** in

74% yield. Unfortunately, no conversion was observed using alkyne **63f**, probably because of the presence of the pyridine ring which could poison the Au(I) catalyst. In this case the starting material was quantitatively recovered. Finally, also the alkyl-substituted alkyne **63g** was moderately reactive leading to the helicene **64g** in 55% yield after 24 hours. Furthermore, the crystals of some of these new molecules have been obtained and X-ray diffraction analysis confirmed the structure of the compounds (*Figure 42*).

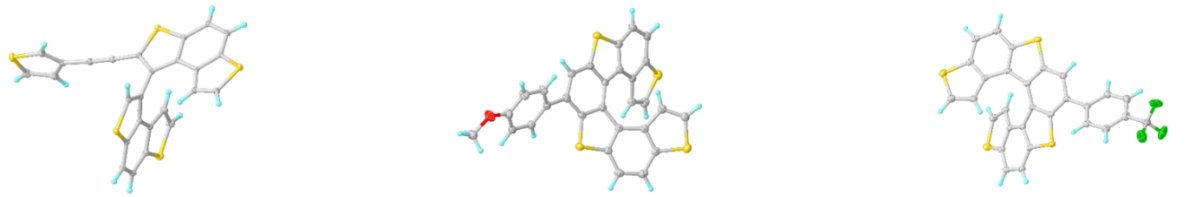

63e
$CDCl_3$ (warm solution)

64c
CH_3CN + 10% CH_2Cl_2

64d
CH_3CN + 10% CH_2Cl_2

Figure 42: ORTEP view of the molecules **63e**, **64c** and **64d**.

In conclusion, this kind of Au(I) catalysts is extremely effective in intramolecular hydroarylation of alkynes **63**. Indeed, these yields are much higher than those obtained with commercially available Lewis acids previously tested and reported in *Scheme 38* of *Chapter 1*.
In light of these promising results, a preliminary study of kinetic resolution of atropisomeric intermediates **63** promoted by chiral Au(I)-catalysts has been faced.

4.3 Kinetic resolution of alkyne dimers 63 promoted by chiral Au(I)-catalyst

This study was initiated by examining the reaction of dimer **63a** as model starting material with the chiral Au(I)-pre-catalyst **L7** with TADDOL-base ligand in presence of $AgSbF_6$ under experimental conditions very similar to those used by Alcarazo and co-workers[91,92] (*Table 11*).

Table 11. Optimisation of the intramolecular hydroarylation of alkyne **63a** promoted by chiral Au(I)-catalyst **L7**.

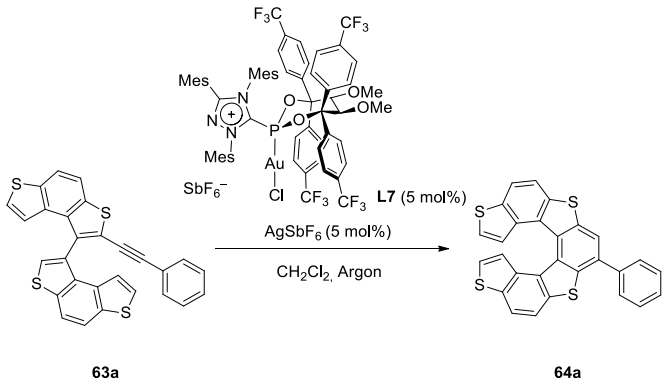

63a **64a**

Entry[a]	T (°C)	Time (h)	Ratio **63a**:**64a** [b]	*ee* (%)[c]	Yield (%)[d]
1	–20	24	0:1	-[e]	84
2	–20	1	1:0.8	23 (2nd enantiomer)	-[f]
3	–40	24	0.2:1	-[e]	-[f]
4	–40	1	1:0.02	-[e]	-[f]
5	–40	8	1:0.65	4 (1st enantiomer)	-[f]
6	–10	1	1:0.8	43 (2nd enantiomer)	-[f]
7	0	1	1:0.36	52 (2nd enantiomer)	-[f]
8	10	1	0:1	-[e]	83
9	10	0.25	0.31:1	-[e]	-[f]
10	10	0.10	1:0.18	37 (2nd enantiomer)	-[f]

[a] Reaction conditions: 25.1 μmol of **63a** in 1 mL CH_2Cl_2, 5 mol% of **L7**, 5 mol% of $AgSbF_6$, under argon. [b] The ratio was evaluated by ^{1}H-NMR and HPLC. [c] The *ee* was evaluated by CSP-HPLC. [d] Isolated yield. [e] The *ee* was not measured because the ratio **63a**:**64a** was >1:1. [f] The crude was not purified.

Initially, dimer **63a** was reacted in CH_2Cl_2 at −20 °C in the presence of 5 mol% of pre-catalyst **L7** and 5 mol% of $AgSbF_6$. In literature this kind of reaction requires 48 hours, but we stopped the reaction after 24 hours, because it is a kinetic resolution. However, after this time a complete conversion of the starting material **63a** was observed and the expected product **64a** was isolated in 84% yield (*Table 11*, entry 1). Decreasing the time up to 1 hour, the ratio **63a**:**64a** was 1:0.8 and an enantioselectivity was observed (helicene **64a** was obtained in 23% *ee*, *Table 11*, entry 2). Although the *ee* was not so high, this result is incredible promising because it represented the first example of the use of this class of chiral catalysts for kinetic resolution. To increase the *ee*, we repeated the reaction at −40 °C (*Table 11*, entries 3–5). Unexpectedly, we obtained a lower *ee* (4% vs. 23%, *Table 11*, entries 5 and 2, respectively). Interestingly, the major enantiomer in this case was the first eluted (1st enantiomer) with the CSP-HPLC (*Table 11*, entry 5), while the second enantiomer was the major product at −20 °C (*Table 11*, entry 2). Then the same reaction was tested at higher temperatures. The same reaction rate of the reaction was observed at −10 °C with higher *ee* (43% vs. 23%, *Table 11*, entries 6 and 2, respectively). With this promising result in hand, the reaction was performed also at 0 °C (52% *ee*, *Table 11*, entry 7) and 10 °C (37% *ee*, *Table 11*, entry 10). The best *ee* was obtained at 0 °C.

Next, the chiral Au(I)-pre catalysts with BINOL-ligand **L8** was tested in the same model reaction under experimental conditions used by Alcarazo and co-workers[90] (*Scheme 51*).

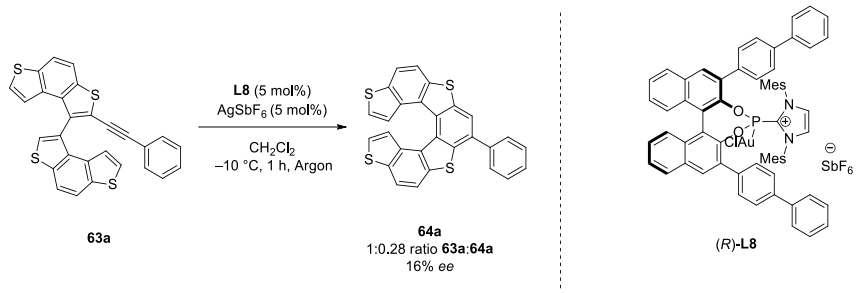

Scheme 51: Synthesis of **64a** using chiral Au(I)-catalyst **L8**.

After 1 hour at –10 °C, the ratio **63a**:**64a** was 1:0.28, but unfortunately the *ee* was only 16%. So, the Au(I)-pre catalysts **L8** resulted to be less effective than **L7** with this class of substrate.

Finally, a preliminary study of kinetic resolution to obtain other helicenes **64** in enantioenriched form was started using the optimised conditions reported in entry 7 of *Table 11* (*Scheme 52*).

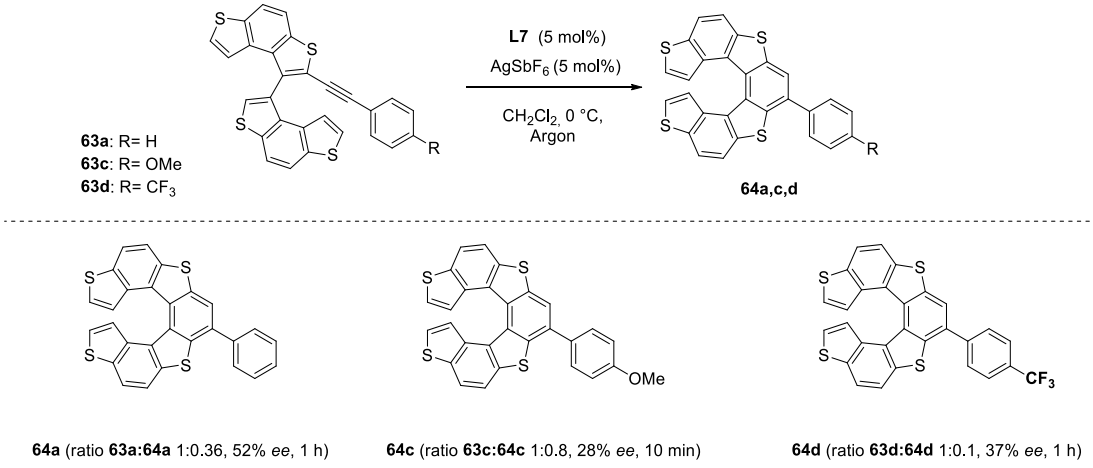

Scheme 52: Preliminary study of kinetic resolution.

In particular, the effect in the outcome of the reaction of the nature of *para*-substituent in the phenyl pendant was evaluated. As shown in *Scheme 52*, the presence of an electron-donor group such as OMe (**63c**) significantly increased the reaction rate. Indeed, a ratio of 1:0.8 between dimer **63c** and helicene **64c** was observed after only 10 minutes. Unfortunately, the *ee* was lower than that obtained in case of **64a** (28% *vs.* 52%). On the other hand, the presence of an electron-withdrawing group such as CF_3 (**63d**) considerably decreased the reaction rate and the *ee* of the desired helicene **64d** was 37%. This result was expected considering the longer time required for the synthesis of **64d** also with the non-chiral Au(I)-pre catalyst **L2** (see *Scheme 50*).

This was a preliminary study, but the obtained results are very interesting because they represent the first examples of the use of cationic chiral Au(I)-pre catalysts in kinetic resolution, demonstrating their moderate efficiency also in case of configurationally stable atropisomers as starting materials.

4.4 Conclusions and perspective

In summary, 7-monosubstituted tetrathia[7]helicenes **64** have been prepared in good to excellent yields by an intramolecular hydroarylation using Au(I)-complexes with cationic phosphine ligands. Towards this goal, a screening of the experimental conditions has been carried out and diverse ligands have been tested.

In an effort to envisage an asymmetric version of this protocol, a preliminary study of kinetic resolution of some of these helicenes has been started using chiral Au(I)-complexes containing TADDOL- and BINOL-base ligands (*Figure 43*).

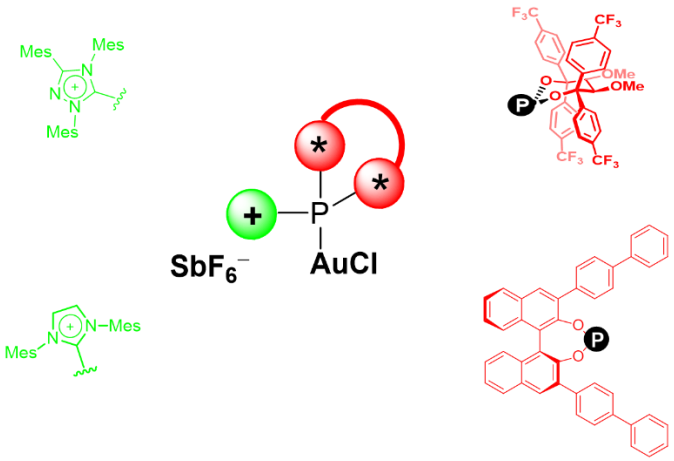

Figure 43: Chiral Au(I)-complexes.

In particular, these chiral catalysts provided enantiomerical excesses up to 52%.

In perspective, an extensive screening of the experimental conditions will be performed to improve the enantioselectivity of the kinetic resolution with these atropisomeric starting materials.

4.5 Experimental part

4.5.1 General methods. All reactions were carried out under inert atmosphere by means of standard techniques for manipulating air-sensitive compounds. Dry and degassed CH_2Cl_2 was obtained with MBraun Solvent Purification System (MB-SPS-800). Silver hexafluoroantimonate ($AgSbF_6$) was purchased from Sigma Aldrich, transferred into a glovebox and finely ground using a pestle and mortar. The cationic non-chiral Au(I)-pre catalysts **L2–6**[250,251] and the chiral Au(I) complexes with TADDOL[92]- and BINOL[90] -base ligands **L7–8** were prepared as reported in literature. Thin-layer chromatography (TLC) was performed with polygram SIL G/UV254 from Macherey Nagel, and plates were visualized with short-wave UV light (254 and 366 nm). Melting points were determined with a Büchi Melting Point M-560 apparatus and are uncorrected. The IR spectra were recorded FT/IR-4100 (Jasco), wavenumbers ($\tilde{\nu}$) in cm^{-1}. The ^1H and ^{13}C NMR spectra were recorded in $CDCl_3$ or CD_2Cl_2 at 25 °C using a Bruker DPX300, AV-500 and AC-600 MHz spectrometer. Chemical shifts were reported relative to the residual protonated solvent resonances (^1H: δ = 7.26 ppm, ^{13}C: δ = 77.0 for $CDCl_3$, ^1H: δ = 5.33 ppm, ^{13}C: δ = 53.5 ppm for CD_2Cl_2). The chemical shifts are given in ppm and coupling constants in Hz. High Resolution Electron Ionization (HR EI) mass spectra were recorded on Finnigan MAT 95 (70 *e*v, EI), Bruker Daltonic (HRMS).

X-ray studies. The X-ray data collection was done on two dual source equipped Bruker D8 Venture four-circle-diffractometer from Bruker AXS GmbH. Used X-ray sources: microfocus IμS 2.0 Cu/Mo and microfocus IμS 3.0 Ag/Mo from Incoatec GmbH with mirror optics HELIOS and single-hole collimator from Bruker AXS GmbH. Used detector: Photon III CE14 (Cu/Mo) and Photon III HE (Ag/Mo) from Bruker AXS GmbH. Used programs: APEX3 Suite (v2019.1-0) for data collection and therein integrated programs SAINT V8.38A (Integration) and SADABS 2016/2 (Absorption correction) from Bruker AXS GmbH; structure solution was done with SHELXT[252], refinement with SHELXL-2018/3[252]; OLEX[2] was used for data finalization[253]. Special Utilities: SMZ1270 stereomicroscope from Nikon Metrology GmbH was used for sample preparation; crystals were mounted on MicroMounts or MicroLoops from MiTeGen in NVH oil; for sensitive samples the X-TEMP 2 System was used for picking of crystals; crystals were cooled to given temperature with Cryostream 800 from Oxford Cryosystems.

HPLC studies. HPLC analyses were performed using a Waters Acquity multidimensional high-performance liquid chromatograph (MD-UPLC), custom configuration with column switching in both separation dimensions. Detection via PDA-UV, trap-and-elute transfer to second dimension with separate PDAUV coupled with fluorescence or single-quad MS detection. System comprised of Waters Acquity Sample Manager FT-N, Quaternary Solvent Manager, Column Manager with 2 additional CM-Aux modules, PDA Detector for fast single dimension method screening. Separation was carried out on: Agilent ZORBAX SB-C18, 4.6x250 mm, 3.5μm column; Daicel Chiral Technologies 3.0x100 mm, 1.6 or 3μm columns. Specific

conditions such as column type used, eluent mixtures, flow rates and temperatures are stated for each compound.

4.5.2 Synthesis and characterization of tetrathia[7]helicenes 64

General procedure for racemic cycloisomerisations.[92] To a flame-dried reaction vessel, alkyne **63** (25 µmol) and the gold pre-catalyst **L2** (1 mg, 5 mol%) were added. The reaction vessel was fitted with a silicon septum, evacuated and back-filled with argon, and this sequence was repeated twice. Deaerated CH_2Cl_2 (0.025 M) was added and the stirred mixture $AgSbF_6$ (5 mol%, 0.05 M in CH_2Cl_2) was added dropwise. After stirring overnight at room temperature, the mixture was filtered through a silica plug eluting with CH_2Cl_2. Evaporation of the solvent yielded a crude product which was purified by recrystallization.

Helicene 64a. The crude product obtained from the cyclomerisation of **63a** (12 mg, 25 µmol) was purified by recrystallization (dichloromethane/hexane) to afford the product **64a** (11.1 mg, 92%) as yellow solid. ^{1}H NMR (500 MHz, $CDCl_3$): δ = 8.06–8.02 (m, 3H), 7.99 (d, *J* = 8.5 Hz, 1H), 7.94 (d, *J* = 8.5 Hz, 1H), 7.86–7.84 (m, 2H), 7.60–7.57 (m, 2H), 7.52–7.49 (m, 1H), 6.94–6.91 (m, 2H), 6.78–6.76 (m, 2H). Spectroscopic data are in agreement with those reported in *Chapter 1*.

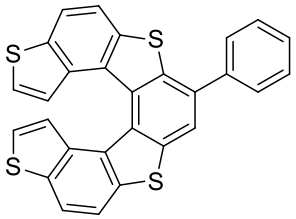

Helicene 64b. The crude product obtained from the cyclomerisation of **63b** (16.2 mg, 25 µmol) was purified by recrystallization (heptane) to afford the product **64b** (15.0 mg, 93%) as yellow solid. ^{1}H NMR (300 MHz, $CDCl_3$): δ = 7.97 (s, 1H), 7.87–7.85 (m, 2H), 7.62–7.58 (m, 2H), 7.53–7.49 (m, 1H), 6.82–6.79 (m, 2H,), 6.75 (d, *J* = 5.6 Hz, 2H), 3.20–2.99 (m, 8H), 1.98–1.81 (m, 8H), 1.23–1.12 (m, 12H). Spectroscopic data are in agreement with those reported in *Chapter 1*.

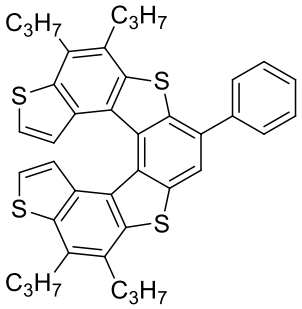

Helicene 64c. The crude product obtained from the cyclomerisation of **63c** (12.7 mg, 25 µmol) was purified by recrystallization (dichloromethane/hexane) to afford the product **64c** (11.8 mg, 93%) as yellow solid**.** ^{1}H NMR (300 MHz, $CDCl_3$): δ = 8.05–7.92 (m, 5H), 7.78 (d, *J* = 8.6 Hz, 2H), 7.12 (d, *J* = 8.6 Hz, 2H), 6.93–6.91 (m, 2H), 6.77 (d, *J* = 5.6 Hz, 2H), 3.93 (s, 3H). Spectroscopic data are in agreement with those reported in *Chapter 1*.

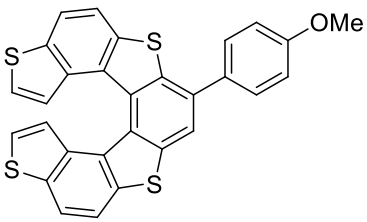

Helicene 64d. The crude product obtained from the cyclomerisation of **63d** (13.6 mg, 25 µmol) was purified by recrystallization (dichloromethane/heptane) to afford the product **64d** (12.4 mg, 91%) as yellow solid**.** M.p. (dichloromethane/heptane) 150–153 °C. ^{1}H NMR (500 MHz, $CDCl_3$): δ = 8.08–8.04 (m, 3H), 8.00–7.97 (m, 4H), 7.94 (d, *J* = 8.5 Hz, 1H), 7.85 (d, *J* = 8.1 Hz, 2H), 6.94 (t, *J* = 5.4 Hz, 2H), 6.76 (ddd, *J* = 5.6, 2.5, 0.6 Hz, 2H). Spectroscopic data are in agreement with those reported in *Chapter 1*.

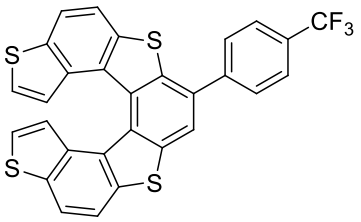

Helicene 64e. The crude product obtained from the cyclomerisation of **63e** (12.1 mg, 25 µmol) was purified by recrystallization (warm dichloromethane) to afford the product **64e** (8.9 mg, 74%) as yellow solid. M.p. (dichloromethane) 322–325 °C. ^{1}H NMR (500 MHz, CD_2Cl_2): δ = 8.17 (s, 1H), 8.09 (dd, *J* = 2.6, 0.8 Hz, 1H), 8.07 (dd, *J* = 2.6, 0.8 Hz, 1H), 8.02 (dt, *J* = 8.6, 0.7 Hz, 2H), 7.92 (dd, *J* = 2.9, 1.4 Hz, 1H), 7.69 (dd, *J* = 5.0, 1.4 Hz, 1H), 7.61 (dd, *J* = 5.0, 2.9 Hz, 1H), 6.95 (d, *J* = 5.5 Hz, 2H), 6.74 (ddd, *J* = 8.0, 5.5, 0.8 Hz, 2H). ^{13}C NMR (125 MHz, CD_2Cl_2): δ = 140.4 (Cq), 138.5 (Cq), 137.0 (Cq), 137.0 (Cq), 136.9 (Cq), 136.9 (2Cq), 136.1 (2Cq), 131.0 (Cq), 130.7 (Cq), 130.6 (Cq), 129.5 (Cq), 129.0 (Cq), 127.8 (CH), 126.7 (CH), 125.1 (CH), 125.1 (CH), 124.6 (CH), 124.6 (CH), 123.6 (CH), 121.6 (CH), 121.5 (CH), 119.8 (CH), 118.7 (CH), 118.5 (CH). IR: (neat) ν̃ = 3104, 3082, 2962, 2907, 2853, 1779, 1587, 1564, 1525, 1482, 1396, 1326, 1300, 1258, 1194, 1149, 1132, 1078, 1044, 1014, 947, 937, 855, 784, 767, 744, 731, 704, 665, 627, 596, 579, 564, 537, 514, 490, 452 cm^{-1}. HRMS: calcd m/z. for; $C_{26}H_{12}S_5$ $[M]^+$: 483.9537; found (EI) 483.9536.

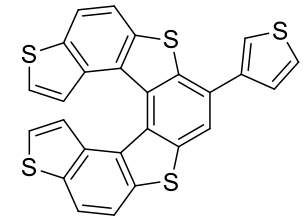

Helicene 64f. The crude product obtained obtained from the cyclomerisation of **63f** (12.1 mg, 25 µmol) was purified by recrystallization (warm dichloromethane) to afford the product **64f** (6.6 mg, 55%) as colourless solid. M.p. (dichloromethane/hexane) 85–86 °C. ^{1}H NMR (600 MHz, $CDCl_3$): δ = 8.03 (dd, *J* = 8.5, 0.8 Hz, 1H), 8.01 (dd, *J* = 8.5, 0.8 Hz, 1H), 7.99 (dd, *J* = 8.5, 0.5 Hz, 1H), 7.95 (dd, *J* = 8.5, 0.5 Hz, 1H), 7.86 (m, 1H), 6.90 (ddd, *J* = 5.6, 2.7, 0.5 Hz, 2H), 6.75 (ddd, *J* = 9.4, 5.6, 0.8 Hz, 2H), 3.13–3.08 (m, 2H), 1.97–1.89 (m, 2H), 1.55–1.48 (m, 2H), 1.42–1.32 (m, 4H), 0.91 (t, *J* = 7.1 Hz, 3H). ^{13}C NMR (150 MHz, $CDCl_3$): δ = 138.4 (Cq), 138.1 (Cq), 136.6 (Cq), 136.6 (Cq), 136.3 (Cq), 136.2 (Cq), 136.2 (Cq), 136.0 (Cq), 134.9 (Cq), 131.4 (Cq), 130.9 (Cq), 129.9 (Cq), 128.3 (Cq), 125.3 (CH), 125.3 (CH), 124.2 (CH), 124.1 (CH), 121.2 (CH), 120.9 (CH), 119.5 (CH), 118.7 (CH), 118.6 (CH), 35.0 (CH_2), 31.7 (CH_2), 29.4 (CH_2), 29.3 (CH_2), 22.6 (CH_2), 14.1 (CH_3). IR: (neat) ν̃ = 3091, 2949, 2919, 2850, 1855, 1779, 1693, 1564, 1533, 1480, 1455, 1410, 1397, 1378, 1322, 1298, 1259, 1193, 1147, 1087, 1049, 1017, 896, 846, 817, 784, 767, 742, 700, 654, 635, 531, 509, 472, 454, 406 cm^{-1}. HRMS: calcd m/z. for; $C_{28}H_{22}S_4$ $[M]^+$: 486.0599; found (EI) 486.0598.

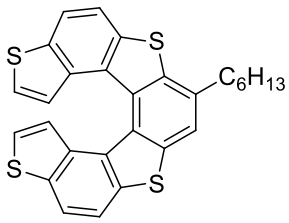

General procedure for enantioselective cycloisomerisations.[92] To a flame-dried reaction vessel, dialkynes **63** (25 µmol) and the chiral gold pre-catalyst **L7** (2 mg, 5 mol%) were added. The reaction vessel was fitted with a silicon septum, evacuated and back-filled with argon, and this sequence was repeated twice. Deaerated CH_2Cl_2 (0.025 M) was added and to the stirred mixture $AgSbF_6$ (5 mol%, 0.05 M in CH_2Cl_2) was added dropwise. After stirring for 10-60 minutes at 0 °C, the mixture was filtered through a silica plug eluting with CH_2Cl_2. Evaporation of the solvent yielded a crude product which was purified by recrystallization. The product ratios and the enantiomeric excesses were determined by CSP-HPLC.

Chapter 5

Enantioselective synthesis of thia[5]helicenes by gold catalysis

This chapter is insert in a larger study on the synthesis of enantiomerically pure helicenes using Au(I)-complexes with chiral ligands. More in detail, the preparation of novel thiahelicenes by asymmetric gold(I)-catalysis is described. This study was performed during a period in the laboratories of Prof. Manuel Alcarazo (Georg-August-Universität Göttingen). X-ray analyses were performed by Dr. Christopher Golz, while HPLC analyses were carried out by Mr. Martin Simon (Georg-August-Universität Göttingen).

5.1 Preamble

As previously reported in *Chapter 4*, Au(I) complexes with α-cationic ligands are extremely effective for the preparation of different carbohelicenes[90-93,250] and the first example of the synthesis of heterohelicenes using these catalysts is reported in this thesis (see *Chapter 4*). Although the great importance of carbohelicenes, the introduction of heteroatoms in the backbone adds additional physical and chemical properties and improves the possibility of functionalisations.[36] For this reason and in order to demonstrate the versatility of these complexes for the synthesis of diverse heterohelicenes, novel promising compounds containing BDT frameworks have been designed as key starting molecules for thiahelicenes. In particular, two potential intermediates **81** and **82** have been thought up (*Figure 44*) that could be converted into the corresponding heterohelicenes **83** and **84** by a double Au(I)-catalysed intramolecular hydroarylation.

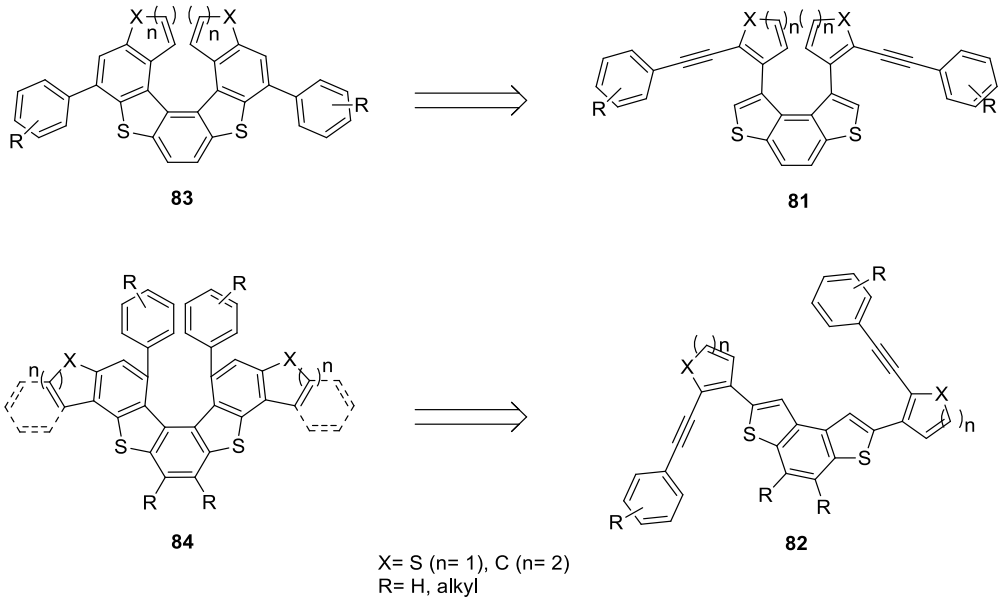

83 81 84 82

Figure 44: New designed intermediates for the synthesis of thiahelicenes **83** and **84**.

5.2 Synthesis of dialkynes 81

To prepare dialkynes **81**, a procedure that involved a Suzuki reaction between dibromoBDT **85** and boronic acids **86**[90] have been studied (*Scheme 53*).

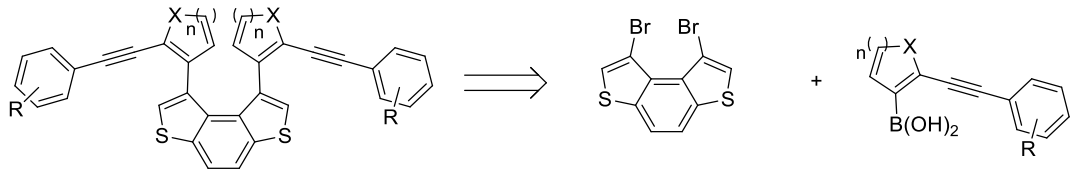

Scheme 53: Retrosynthesis of dialkynes **81**.

More in detail, dibromide **85** was prepared through the two-step procedure reported in *Scheme 54*.

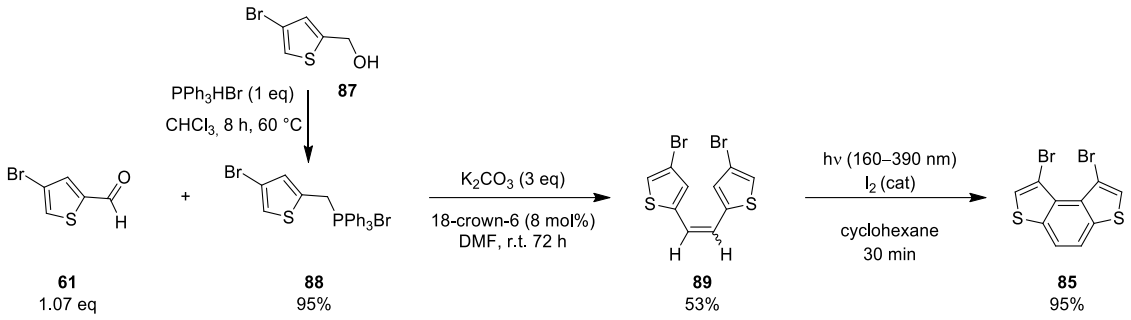

Scheme 54: Synthesis of dibromoBDT **85**.

A solution of alcohol **87** in $CHCl_3$ was treated with 1 equiv. of PPh_3·HBr. The reaction mixture was stirred at 60 °C for 8 hours and the phosphonium salt **88** was isolated in 95% yield. Then, a solution of phosphonium salt **88** and aldehyde **61** in DMF was treated with K_2CO_3 to form the phosphorus ylide in the presence of 18-crown-6 as phase transfer, and then the mixture was stirred at room temperature. After 72 hours, the alkene **89** was isolated in 53% yield as a mixture of (*E*)/(*Z*) isomers in ca 1:1 molar ratio calculated by RP-HPLC. Finally, the alkene **89**, obtained as pale-yellow solid, was converted into the corresponding brominated BDT **85** through an oxidative photochemical reaction. At the beginning, the reaction was performed in the presence of a catalytic amount of I_2 using a medium-pressure Hg lamp with a 125-watt generator in cyclohexane solution (6.4×10^{-4} M) under air, but the yields of **85** were not satisfactory (max. 21%) because of the formation of debrominated side-products (BDT **56a** and **55a**). Likely, the yield significantly increased using a 160–390 nm lamp, in place of medium-pressure Hg lamp. Indeed, after 30 minutes of irradiation of the cyclohexane solution (2.8×10^{-3} M) under air, **85** was isolated in 95% yield and the formation of debrominated side-products was not observed. Besides, a crystal of **85** has been obtained by layering hexane over a dichloromethane solution and the X-ray has been performed (*Figure 45*).

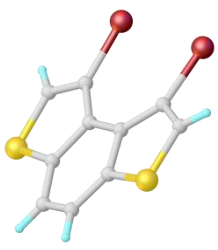

Figure 45: ORTEP view of **85**.

As it can be noted in *Figure 45*, dibrominated BDT **85** is not perfectly planar as parent BDT **56a**, but has a slight distortion due to the two substituents in β-positions.

At this point, bromide **85** was reacted with diverse boronic acids **86** in the presence of $Pd(PPh_3)_2Cl_2$ as catalyst, KF as base in a mixture of toluene:methanol in 1:1 ratio at 70 °C (*Scheme 55*), but the final products **81** were not isolated because of the large amount of side-products in the crude.

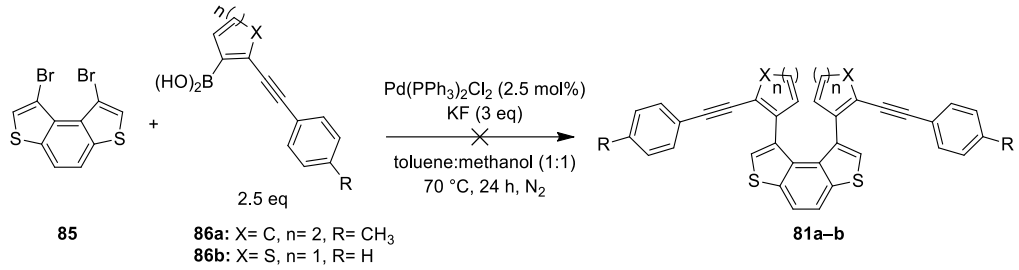

Scheme 55: Suzuki reaction for the synthesis of **81a,b**.

The same result was achieved using $Pd(PPh_3)_4$ in place of $Pd(PPh_3)_2Cl_2$. Other conditions reported in literature for the preparation of helicenes' intermediates[90-92] were tested (*Scheme 56*).

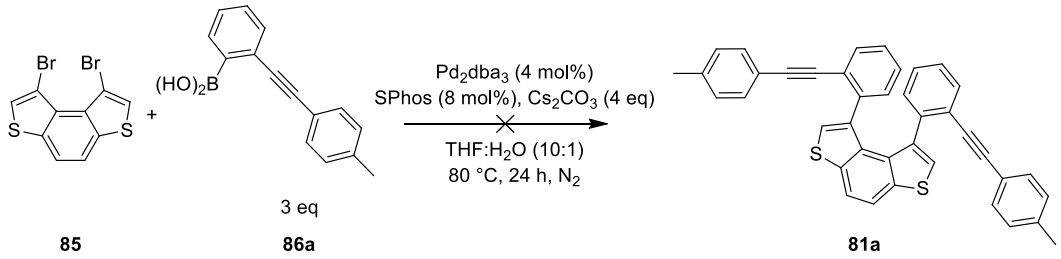

Scheme 56: Suzuki reaction for the synthesis of **81a**.

More in detail, Pd_2dba_3 (4 mol%) was used with SPhos (8 mol%) and 4 equiv. of Cs_2CO_3 in a mixture of THF:H_2O in 10:1 ratio at 80 °C (*Scheme 56*), but also in this case the final product **81a** was not isolated because of the large amount of side-products. These results were unexpected and to evaluate the reactivity of this specific brominated BDT **85**, a test reaction using phenyl boronic acid **69a** in the common conditions for these substrates[175] was carried out (*Scheme 57*).

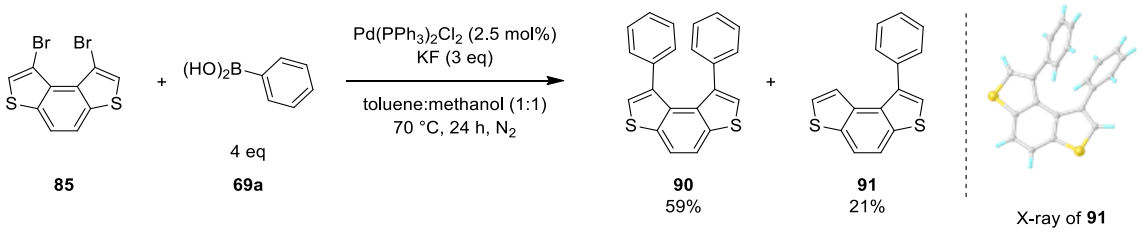

Scheme 57: Suzuki reaction to evaluate the reactivity of **85**.

After 24 hours, the disubstituted BDT **90** was isolated in 59% along with a 21% of the monosubstituted **91**. This result demonstrated the possibility to obtain the desired Suzuki reaction's product, but also the easily debromination of the starting material. Similar result was also achieved using 2.5 equiv. of **69a**. CSP-HPLC analysis of **90** showed only one sharp pick at 10 °C, so there is enough space for the rotation of the phenyl rings. Due to the obtained unsatisfactory results in the synthesis of dialkynes **81**, different experimental conditions and/or alternative procedures (e.g., Negishi reaction) will be investigated.

5.3 Synthesis of dialkynes 82

Next, the preparation of dialkynes **82** was studied. Also for **82**, a procedure that involved a Suzuki coupling was investigated. More in detail, the reaction was performed between either dihalide **92** and boronic acids **86** or boronic ester of BDT **93**[254] and bromides **94** (*Scheme 58*) using the experimental conditions previously tested for the synthesis of **81**.

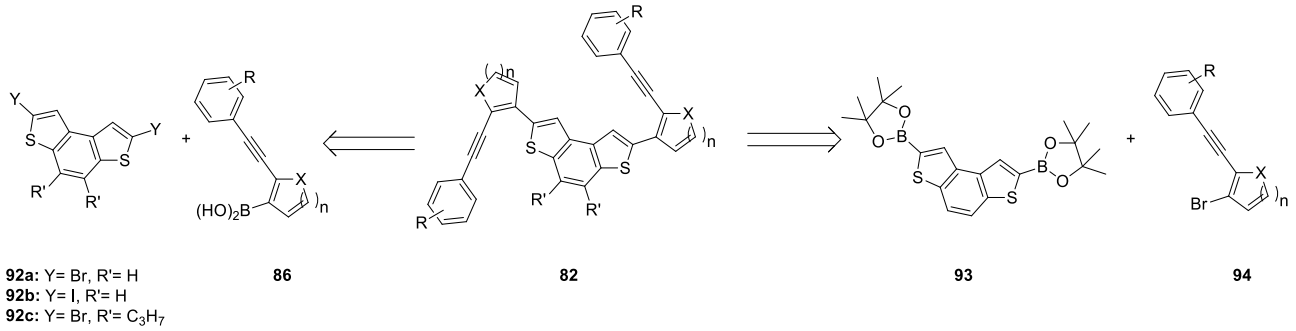

Scheme 58: Retrosynthesis of dialkynes **82**.

Initially, we performed the reactions to obtain dialkynes **82a-e** using both routes under the experimental conditions previously reported for benzodithiophene derivatives[175] (*Scheme 59*).

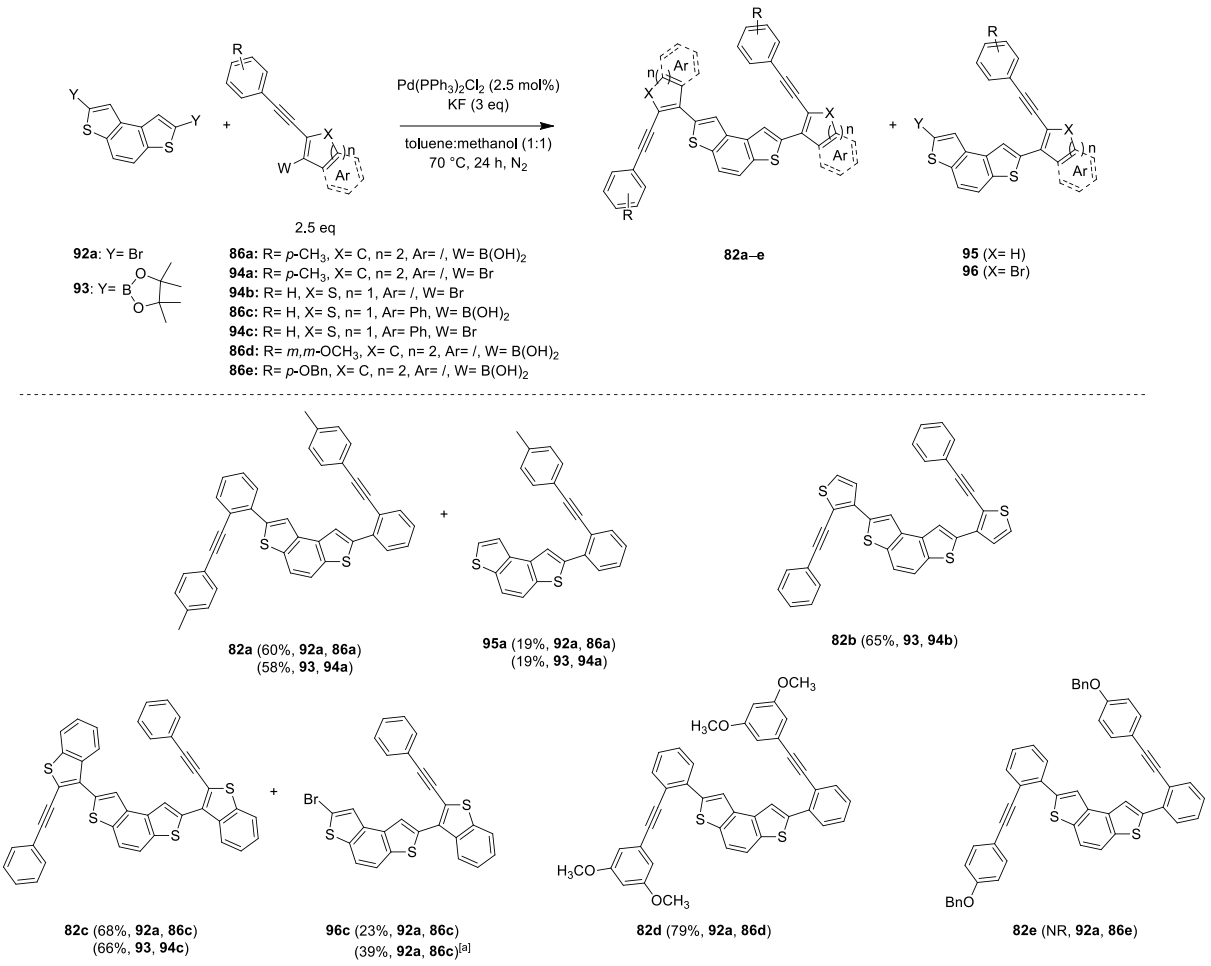

Scheme 59: Synthesis of dialkynes **82**. [a] The reaction was performed with only 1.1 eq of boronic acid **86c**.

As it can be seen in *Scheme 59*, both strategies are equally effective in the coupling process thereby delivering the expected products **82a** in similar yields (58–60%) along with a 19% of monosubstituted derivative **95a**. Starting from boronic ester of BDT **93**, the desired products **82b** and **82c** were obtained in good yields (65% and 66%, respectively), and the formation of monosubstituted side-products was not observed. Similar yield of **82c** was achieved starting from bromide **92a** and boronic acid **86c** (68%), with a 23% of brominated monocoupling product **96c**, that could represent a very interesting starting material for the preparation of helicenes with different substituents in α-positions of the terminal thiophene rings. In order to increase the yield of this promising molecule **96c**, the latter reaction was performed with only 1.1 equiv. of boronic acid **86c** and the desired **96c** was isolated in 39% yield, and a 30% of BDT **56a** was also recovered. Next, in the presence of two electron-donor group in *meta*-positions as -OMe in the partner **86d**, the desired dialkyne **82d** was isolated in 79% yield. On the contrary, the presence of a very bulky substituent as -OBn in boronic acid **86e** completely disfavoured the reaction and the starting bromide **92a** was quantitatively recovered.

In order to obtain the desired dialkyne **82e**, different conditions were tested[92] (*Scheme 60*).

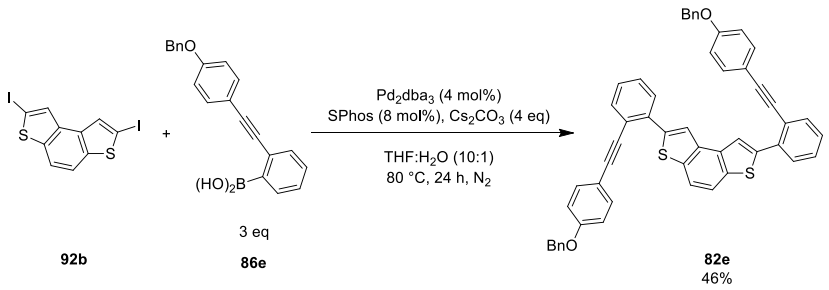

Scheme 60: Synthesis of dialkyne **82e**.

More in detail, iodinated BDT **92b**[160] was reacted with 3 equiv. of boronic acid **86e** in presence of Pd_2dba_3 (4 mol%), SPhos (8 mol%) and Cs_2CO_3 (4 eq) in a mixture of THF:H_2O in 10:1 ratio at 80 °C, and the final product **82e** was isolated in 46% yield. With this result in hand, these conditions could be exploit for the synthesis of different dialkynes **82** starting from bromide **92c** or iodide **92b** (*Scheme 61*).

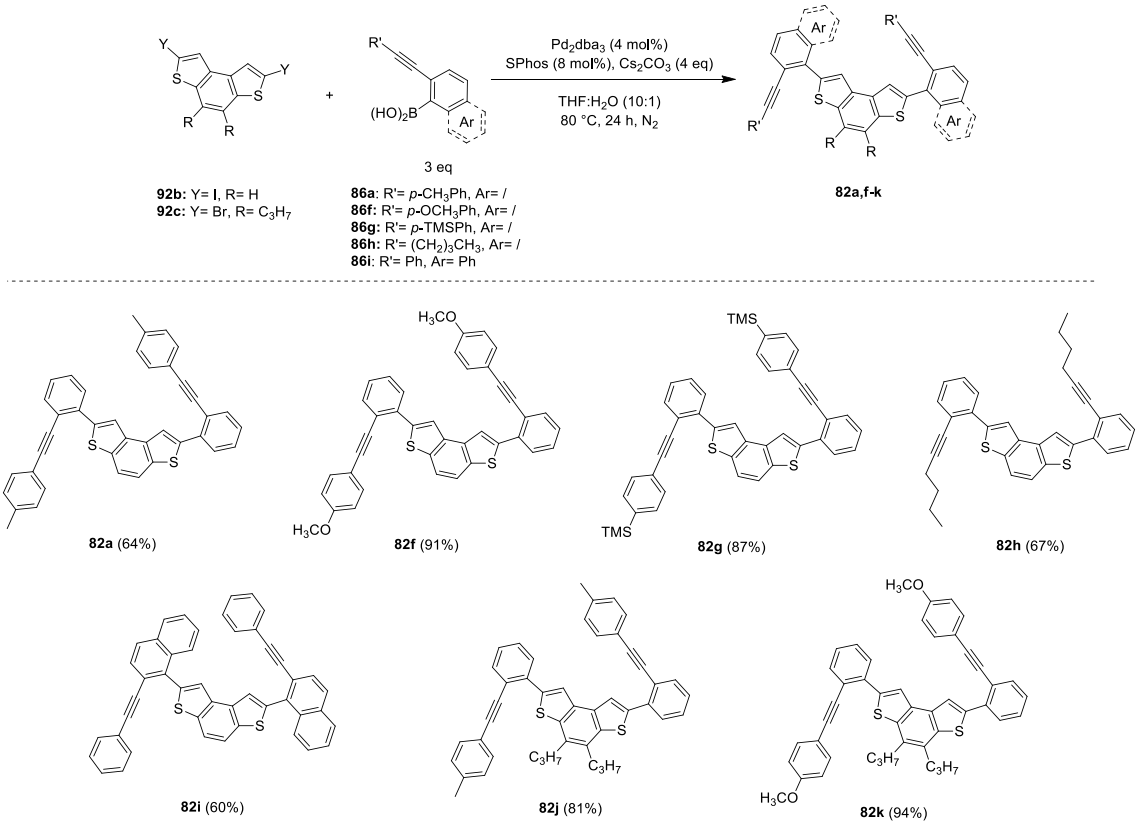

Scheme 61: Synthesis of dialkynes **82**.

Initially, these conditions were tested for the preparation of **82a** in order to evaluate their efficacy in comparison with the conditions reported in *Scheme 59*. As can be noticed, the yield obtained with the new conditions was comparable to that achieved in *Scheme 59* (64% vs. 60%). At this point, small library of dialkynes **82** were prepared taking advantage of these conditions with a set of synthetised boronic acid **86** (*Scheme 61*). In particular, good results were obtained in the presence of electron-donor group as -OMe and electron-withdrawing group as -TMS. Indeed, **82f** was isolated in 91% yield, while **82g** in 87% yield.

Moderate results were achieved in the presence of an alkyl chain (**82h**, 67%) and a more conjugated aryl ring as naphthyl (**82i**, 60%). Besides, good yields were also obtained starting from a more electron-rich BDT as **92c**. In particular, **82j** and **82k** were isolated in 81% and 94% yield, respectively.

Finally, as a proof of concept, these latter conditions were also used for the synthesis of the first dialkyne **82** with two different substituents in α-positions of the terminal thiophene rings starting from the monobrominated side-product **96c** (*Scheme 62*).

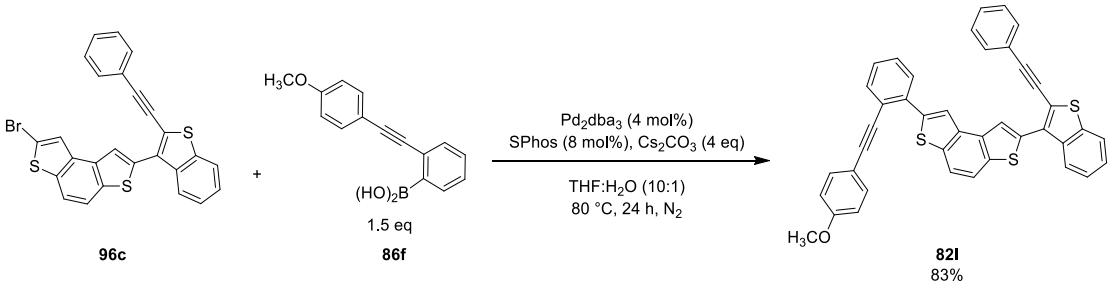

Scheme 62: Synthesis of mixed dialkyne **82l**.

More in detail, the bromide **96c** was reacted with 1.5 equiv. of boronic acid **86f**, that gave the best results in *Scheme 61*, and the final mixed dialkyne **82l** was isolated in 83% yield.

In conclusion, two different valid experimental conditions have been found for the preparation of a set of dialkynes **82** in good to excellent yields. Some of these new compounds were analysed by CSP-HPLC and sharp peaks at 10 °C were observed in each case, thus demonstrating that these dialkynes **82** were not configurationally stable at this temperature and so there was the possibility to prepare the corresponding helicenes **84** also in enantioenriched way by an intramolecular hydroarylation promoted by chiral Au(I)-catalyst (*Scheme 63*).

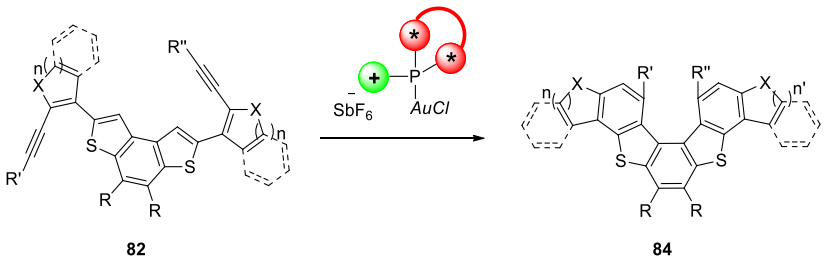

Scheme 63: Synthesis of novel thia[5]helicenes **84**.

5.4 Synthesis of a new class of helicenes 84

In order to evaluate the efficacy of this kind of catalysts for these particular substrates, dialkynes **82a-l** were first reacted in CH_2Cl_2 at room temperature in the presence of 5 mol% of non-chiral Au(I)-complex **L2**[92] (see *Chapter 4* for the choice of the catalyst) and 5 mol% of $AgSbF_6$ (*Scheme 64*).

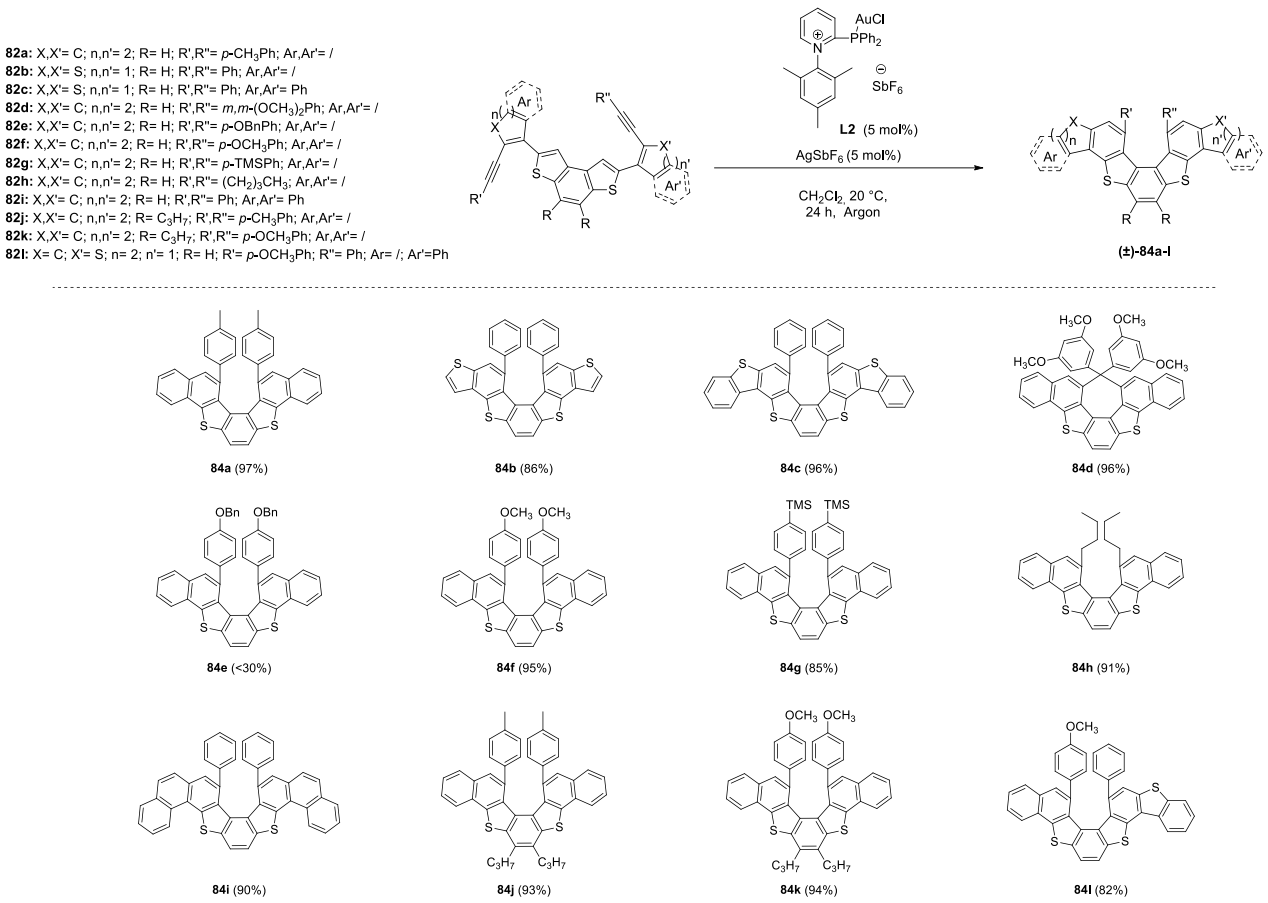

Scheme 64: Synthesis of novel thia[5]helicenes **84** in racemic form.

After 24 hours, no starting material was found in the reaction mixture, and the expected products (±)–**84a–d,f–k** were isolated in excellent yields (up to 97%). On the contrary, the crude of **84e** was very complicated, and the final helicene **84e** was isolated non completely purified. These new helicenes **84** were analysed by CSP-HPLC and two peaks were observed for each compound. No on-column interconversion was observed at 37 °C, and this suggested that these new helicenes were configurationally stable at this temperature.

5.5 Enantioselective synthesis of helicenes 84

Based on the good results achieved in the preparation of (±)–**84**, the enantioselective intramolecular hydroarylation of dialkynes **82** promoted by chiral catalyst **L7** was performed using experimental conditions very similar than those reported in literature for the enantioselective synthesis of carbohelicenes[91,92] (*Scheme 65*).

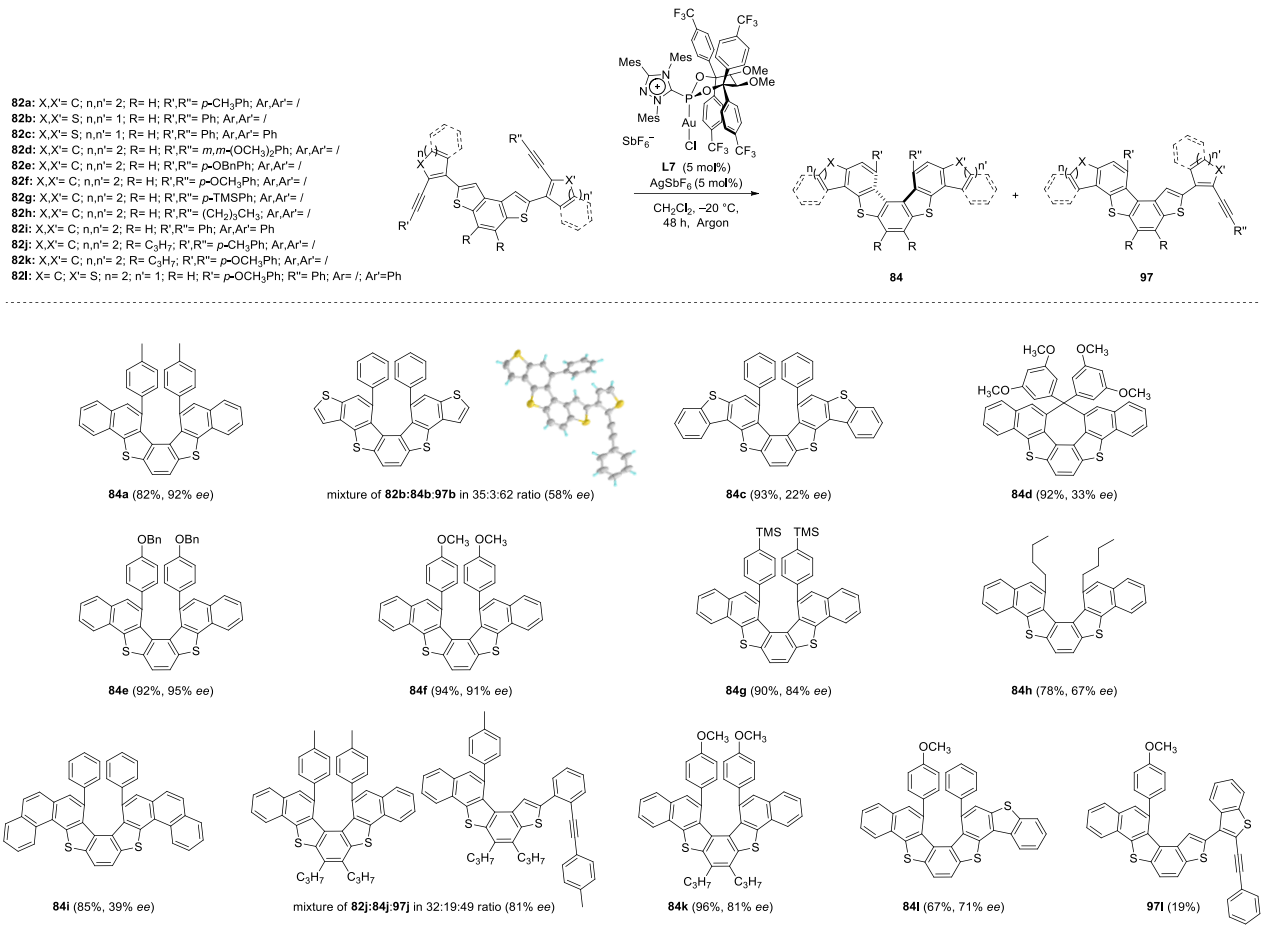

Scheme 65: Synthesis of novel thia[5]helicenes **84** in enantioenriched form.

Dialkynes **82** were reacted in CH_2Cl_2 at –20 °C in the presence of 5 mol% of pre-catalyst **L7** and 5 mol% of $AgSbF_6$ under argon for 48 hours, and excellent yields and very good *ee* were achieved with electron-rich and electron-withdrawing substituents in the *para*-position of the phenyl ring **84a,e–g,k** (82–96%, 81–95% *ee*). For compounds **84b** and **84j**, no complete conversion of the starting material was observed and the side-products **97b** and **97j** were also found in the reaction mixture. A single crystal of compound **97b** was obtained, and the X-ray analysis confirmed its structure. Moreover, **97b** was a single sharp peak at 37 °C in CSP-HPLC, while **84b** had two different peaks. This data suggested that the second ring-closing gave the enantioselectivity because **84b** existed as a pair of enantiomers, while **97b** was not chiral. Next, moderate yield and *ee* were obtained in case of **84h** (78% yield and 67% *ee*). Noteworthy, X-ray studies on the enantioenriched mixture of **84h** suggested that the enantiomer of **L7** used as catalyst in these reactions favoured the formation of the thiahelicene with the right-handed helicity (the *P*-configuration). Lower *ee* were obtained in case of substituents in *meta*-positions of the phenyl ring **84d** (33% *ee*) and more conjugated (hetero)aryl systems, such as **84c** and **84i** (22% and 39% *ee*, respectively), although they were isolated in very good yield (up to 93%). Finally, the first example of mixed enantioenriched helicene **84l** was obtained in moderate yield and good *ee*, along with a small amount of the side-product **97l** (19%).

In summary, a small library of novel thiahelicenes **84** was prepared in good to excellent yields and with moderate to very good *ee* using chiral Au(I)-catalyst. Furthermore, diverse X-ray structures of dithialkynes **82** and helicenes **84** were obtained (see *Section 5.7.3*).

5.6 Conclusions and perspectives

In conclusion, a set of novel thia[5]helicenes **84** has been prepared in good to excellent yields and in moderate to very good enantiomerical excesses by a double intramolecular hydroarylation using Au(I)-complexes with cationic phosphine TADDOL-base ligand, thus demonstrating the efficacy of these complexes for the synthesis not only of carbohelicenes, but also for the preparation of heterohelicenes.

Interestingly, X-ray studies suggested that the (*R*)-enantiomer of **L7** used as catalyst in these reactions favoured the formation of the thia[5]helicene with the right-handed helicity (the *P*-configuration).

In perspective, chiroptical, photophysical and electrochemical properties of this new class of thia[5]helicenes will be investigated in order to evaluate their potentialities in material science.
Furthermore, these stimulating Au(I)-complexes will be applied for the development of novel heterohelicenes containing diverse heteroatoms such as oxygen and nitrogen.

5.7 Experimental part

5.7.1 General methods. All reactions were carried out under inert atmosphere by means of standard techniques for manipulating air-sensitive compounds. All reagents were purchased from Sigma-Aldrich and used without further purification. Silver hexafluoroantimonate ($AgSbF_6$) was purchased from Sigma Aldrich, transferred into a glovebox and finely ground using a pestle and mortar. Dry and degassed solvent (CH_2Cl_2, THF and toluene) was obtained with MBraun Solvent Purification System (MB-SPS-800). The boronic acids **86**,[90] bromides **94**,[90] benzo[1,2-*b*:4,3-*b'*]dithiophene derivatives **92a**,[181] **92b,**[160] **92c**[161] and **93**[254] were synthesised as reported in literature. Phosphonium salt **88** was prepared according to literature.[162] The cationic non-chiral Au(I)-pre catalysts **L2**[92] and the chiral Au(I) complexes with TADDOL-base ligands **L7**[250] were prepared as previously reported. Thin-layer chromatography (TLC) was performed with polygram SIL G/UV254 from Macherey Nagel, and plates were visualized with short-wave UV light (254 and 366 nm). Melting points were determined with a Büchi Melting Point M-560 apparatus and are uncorrected. The ^1H and ^{13}C NMR spectra were recorded in $CDCl_3$ or CD_2Cl_2 at 25 °C using a Bruker DPX300, AV-400, AV-500 and AC-600 MHz spectrometer. Chemical shifts were reported relative to the residual protonated solvent resonances (^1H: δ = 7.26 ppm, ^{13}C: δ = 77.0 for $CDCl_3$, ^1H: δ = 5.33 ppm, ^{13}C: δ = 53.5 ppm for CD_2Cl_2). The chemical shifts are given in ppm and coupling constants in Hz. High Resolution Mass (HRMS) spectra were recorded on Finnigan MAT 95 (70 eV, EI), Finnigan LCQ (ESI) and APEX IV 7T FTICR, Bruker Daltonic. The IR spectra were recorded FT/IR-4100 (Jasco), wavenumbers ($\tilde{\nu}$) in cm^{-1}. Specific rotations were collected using Jasco P-2000 polarimeters at the stated temperature under a Na/Hg lamp, λ = 589 nm (*c* in g/100 ml).

X-ray studies. The X-ray data collection was done on two dual source equipped Bruker D8 Venture four-circle-diffractometer from Bruker AXS GmbH. Used X-ray sources: microfocus IμS 2.0 Cu/Mo and microfocus IμS 3.0 Ag/Mo from Incoatec GmbH with mirror optics HELIOS and single-hole collimator from Bruker AXS GmbH. Used detector: Photon III CE14 (Cu/Mo) and Photon III HE (Ag/Mo) from Bruker AXS GmbH. Used programs: APEX3 Suite (v2019.1-0) for data collection and therein integrated programs SAINT V8.38A (Integration) and SADABS 2016/2 (Absorption correction) from Bruker AXS GmbH; structure solution was done with SHELXT[252] refinement with SHELXL-2018/3[252]; OLEX^2 was used for data finalization[253]. Special Utilities: SMZ1270 stereomicroscope from Nikon Metrology GmbH was used for sample preparation; crystals were mounted on MicroMounts or MicroLoops from MiTeGen in NVH oil; for sensitive samples the X-TEMP 2 System was used for picking of crystals; crystals were cooled to given temperature with Cryostream 800 from Oxford Cryosystems.

HPLC studies. HPLC analyses were performed using a Waters Acquity multidimensional high-performance liquid chromatograph (MD-UPLC), custom configuration with column switching in both separation dimensions. Detection via PDA-UV, trap-and-elute transfer to second dimension with separate PDAUV

coupled with fluorescence or single-quad MS detection. System comprised of Waters Acquity Sample Manager FT-N, Quaternary Solvent Manager, Column Manager with 2 additional CM-Aux modules, PDA Detector for fast single dimension method screening. Separation was carried out on: Agilent ZORBAX SB-C18, 3.0x100 nm or 4.6x250 mm, 3.5µm column; Daicel Chiral Technologies 3.0x100 mm, 1.6 or 3µm columns. Specific conditions such as column type used, eluent mixtures, flow rates and temperatures are stated for each compound.

5.7.2 Synthesis and characterization of new compounds

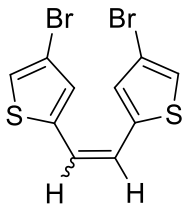

Synthesis of 89. A mixture of phosphonium salt **88** (0.8 g, 1.54 mmol), K_2CO_3 (0.5 g, 3.5 mmol, 2.3 eq), 18-crown-6 ether (65 mg, 0.2 mmol, 0.16 eq) and aldehyde **61** (0.3 g, 1.64 mmol, 1.07 eq) in DMF (10 mL) was stirred at room temperature. After 72 hours, the solvent was removed under reduced pressure, and the residue was poured into water (10 mL). The aqueous phase was extracted with CH_2Cl_2 (4 × 10 mL), and the collected organic phases were washed with H_2O (2 × 10 mL), dried over Na_2SO_4, and concentrated under reduced pressure. The residue was purified by column chromatography on silica gel with hexane as the eluent to afford **89** (0.29 g, 0.82 mmol, 52%) as a mixture of *E/Z* isomers in 1:1 molar ratio. ^{1}H NMR (300 MHz, $CDCl_3$): δ = 7.10 (m, 4H, *E*+*Z*), 6.98–6.97 (m, 4H, *E*+*Z*), 6.94 (s, 4H, *E*+*Z*). HRMS: calcd m/z. for; $C_{10}H_6S_2Br_2$ $[M]^+$: 347.8278; found (EI) 347.8209.

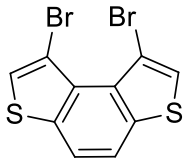

Synthesis of 1,1′-bromobenzo[1,2-b:4,3-b']dithiophene 85. A stirred solution of alkene **89** (200 mg, 0.57 mmol) and a catalytic amount of iodine in cyclohexane (200 mL) was irradiated at room temperature with a 160-390 nm lamp. After 30 minutes, a complete conversion was observed, the solvent was removed under reduced pressure, and the residue was purified by column chromatography on silica gel with hexane as eluent to give **85** (189 mg, 95%) as colourless solid. M.p. (dichloromethane/hexane) 116–117 °C. ^{1}H NMR (300 MHz, $CDCl_3$): δ = 7.79 (s, 2H), 7.76 (s, 2H). ^{13}C NMR (300 MHz, $CDCl_3$): δ = 139.4 (Cq), 131.5 (Cq), 126.7 (CH), 120.2 (CH), 106.1 (Cq). HRMS: calcd m/z. for; $C_{10}H_4S_2Br_2$ $[M]^+$: 345.8121; found (EI) 345.8116.

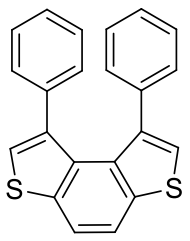

Synthesis of 1,1′-diphenylbenzo[1,2-b:4,3-b']dithiophene 90. To bromide **85** (83 mg, 0.24 mmol, 1 eq), phenylboronic acid **69a** (35 mg, 0.96 mmol, 4 eq), $Pd(PPh_3)_2Cl_2$ (4.5 mg, 0.006 mmol, 5 mol%), KF (42 mg, 0.72 mmol, 3 eq) was added 12 mL of toluene/methanol (1:1) mixture as solvent and the mixture was stirred at 70 °C for 24 hours under a nitrogen atmosphere. After cooling to room temperature, the aqueous phase was extracted with CH_2Cl_2 (3 × 10 mL), and the organic phases were dried with Na_2SO_4, and the solvent was removed under reduced pressure to afford the crude products. The crude reaction product was purified by chromatography on silica gel with a mixture of hexane and CH_2Cl_2 (9:1) as eluent to afford **90** (48 mg, 0.14 mmol, 59%) as colourless solid along with 21% of side-product **91** (see

Chapter 6 for the characterization of **91**). ^{1}H NMR (300 MHz, $CDCl_3$): δ = 7.86 (s, 1H), 7.23 (s, 1H), 6.99–6.90 (m, 5H). ^{13}C NMR (400 MHz, $CDCl_3$): δ = 140.1 (Cq), 139.5 (Cq), 138.8 (Cq), 132.1 (Cq), 128.0 (2CH), 127.8 (2CH), 126.3 (CH), 125.6 (CH), 119.5 (CH). HRMS: calcd m/z. for; $C_{22}H_{13}S_2$ $[M]^+$: 341.0453; found (EI) 341.0453.

General procedure A for Suzuki cross-couplings. A deaerated mixture of bromide **92a** or boronic ester **93** (0.18 mmol), the boronic acid **86** or bromide **94** (2.5 eq), $Pd(PPh_3)_2Cl_2$ (2.5 mol%) and KF (3 eq) in toluene and MeOH (1:1, 0.02 M) was heated at 70 °C under nitrogen for 24 hours. The outcome of the reaction was monitored by TLC analysis. After completion of the reaction, the mixture was cooled to room temperature and poured into water (10 mL). The aqueous phase was extracted with CH_2Cl_2 (4 × 5 mL), and the collected organic phases were dried over Na_2SO_4, and concentrated under reduced pressure. The residue was purified by column chromatography on silica gel to provide the required product **82**.

General procedure B for Suzuki cross-couplings. A deaerated mixture of bromide **92c** or iodide **92b** (0.18 mmol), the boronic acid **86** (3 eq), Pd_2dba_3 (8 mol%), SPhos (16 mol%) and Cs_2CO_3 (4 eq) in THF and H_2O (10:1, 0.02 M) was heated at 80 °C under nitrogen for 24 hours. The outcome of the reaction was monitored by TLC analysis. After completion of the reaction, the mixture was cooled to room temperature and poured into water (10 mL). The aqueous phase was extracted with CH_2Cl_2 (4 × 5 mL), and the collected organic phases were dried over Na_2SO_4, and concentrated under reduced pressure. The residue was purified by column chromatography on silica gel to provide the required product **82**.

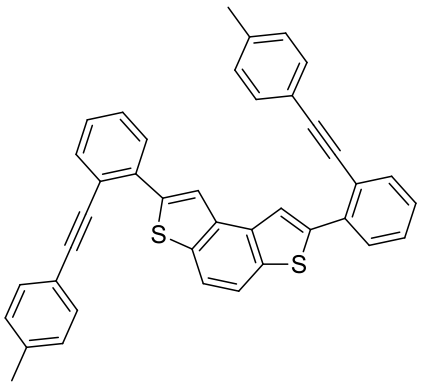

Dialkyne 82a. The crude product obtained according to *General procedure B* between iodide **92b** (80 mg, 0.18 mmol) and boronic acid **86a** (115 mg, 0.54 mmol) was purified by column chromatography on silica gel (hexane:dichloromethane 9:1) to afford the product **82a** (66 mg, 64%) as yellow solid. M.p. (dichloromethane/acetonitrile) 140–142 °C. ^{1}H NMR (300 MHz, $CDCl_3$): δ = 8.30 (s, 2H), 7.81 (s, 2H), 7.73–7.67 (m, 4H), 7.43–7.32 (m, 8H), 7.10 (d, *J* = 8.0 Hz, 4H). ^{13}C NMR (100 MHz, $CDCl_3$): δ = 142.8 (Cq), 138.7 (Cq), 136.9 (Cq), 135.7 (Cq), 135.1 (Cq), 133.7 (CH), 131.4 (2CH), 129.3 (CH), 129.2 (2CH), 128.4 (CH), 127.6 (CH), 121.6 (CH), 121.3 (Cq), 120.2 (Cq), 118.6 (CH), 94.8 (C≡C), 88.9 (C≡C), 21.5 (CH_3). IR: (neat) $\tilde{\nu}$ = 3048, 2914, 2856, 2210, 1902, 1694, 1589, 1508, 1475, 1438, 1279, 1181, 1164, 1145, 1101, 1037, 947, 913, 827, 813, 782, 751, 694, 578, 531, 512, 494, 455, 413 cm^{-1}. HRMS: calcd m/z. for; $C_{40}H_{26}S_2^+$ $[M+H]^+$: 571.1549; found (ESI) 571.1547.

Alkyne 95a. The crude product obtained according to *General procedure A* between bromide **92a** (63 mg, 0.18 mmol) and boronic acid **86a** (95 mg, 0.45 mmol) was purified by column chromatography on silica gel (hexane: dichloromethane 9:1) to afford the product **82a** (62 mg, 60%) as yellow solid along with 19% (13 mg) of monocoupling side-product **95a** as yellow solid. M.p. (dichloromethane/acetonitrile) 128–129 °C. ^{1}H NMR (600 MHz, $CDCl_3$): δ = 8.37 (d, *J* = 0.7 Hz, 1H), 7.84–7.80 (m, 2H), 7.74–7.72 (m, 1H), 7.70–7.67 (m, 2H), 7.57 (dd, *J* = 5.5, 0.8 Hz, 1H), 7.43–7.38 (m, 3H), 7.34 (dt, *J* = 7.6, 1.3 Hz, 1H), 7.15–7.12 (m, 2H), 2.36 (s, 1H). ^{13}C NMR (150 MHz, $CDCl_3$): δ = 142.6 (Cq), 138.7 (Cq), 136.7 (Cq), 136.6 (Cq), 135.7 (Cq), 135.1 (Cq), 134.7 (Cq), 133.7 (CH), 131.4 (2CH), 129.5 (CH), 129.2 (2CH), 128.5 (CH), 127.7 (CH), 126.6 (CH), 121.9 (CH), 121.6 (CH), 121.3 (Cq), 120.2 (Cq), 118.9 (CH), 118.4 (CH), 94.3 (C≡C), 88.9 (C≡C), 21.5 (CH_3). IR: (neat) ṽ = 3053, 2955, 2918, 2845, 2207, 1632, 1589, 1557, 1509, 1476, 1439, 1404, 1338, 1261, 1182, 1164, 1145, 1092, 1019, 948, 914, 872, 813, 754, 737, 704, 579, 535, 518, 495, 470 cm^{-1}. HRMS: calcd m/z. for; $C_{25}H_{16}S_2$ $[M]^+$: 380.0688; found (EI) 380.0684.

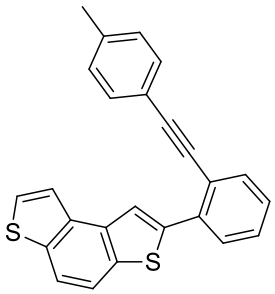

Dialkyne 82b. The crude product obtained according to *General procedure A* between boronic ester **93** (80 mg, 0.18 mmol) and bromide **94b** (118 mg, 0.45 mmol) was purified by column chromatography on silica gel (hexane:dichloromethane 9:1) to afford the product **82b** (65 mg, 65%) as yellow solid. M.p. (dichloromethane/acetonitrile) 179–182 °C. ^{1}H NMR (300 MHz, $CDCl_3$): δ = 8.23 (s, 1H), 7.78 (s, 1H), 7.62–7.58 (m, 2H), 7.40–7.37 (m, 4H), 7.32 (d, *J* = 5.3 Hz, 1H). ^{13}C NMR (100 MHz, $CDCl_3$): δ = 138.4 (Cq), 137.9 (Cq), 136.4 (Cq), 134.7 (Cq), 131.3 (2CH), 128.7 (CH), 128.6 (2CH), 128.2 (Cq), 127.0 (CH), 126.8 (CH), 123.0 (Cq), 119.9 (CH), 118.8 (CH), 98.7 (C≡C), 83.4 (C≡C). IR: (neat) ṽ = 3098, 3058, 2922, 2850, 2193, 1661, 1597, 1507, 1487, 1442, 1427, 1405, 1378, 1339, 1321, 1277, 1254, 1186, 1150, 1126, 1083, 1070, 1041, 1018, 907, 873, 852, 828, 807, 779, 748, 720, 683, 642, 575, 562, 521, 492, 444, 406 cm^{-1}. HRMS: calcd m/z. for; $C_{34}H_{18}S_4^+$ $[M+H]^+$: 555.0354; found (ESI) 555.0364.

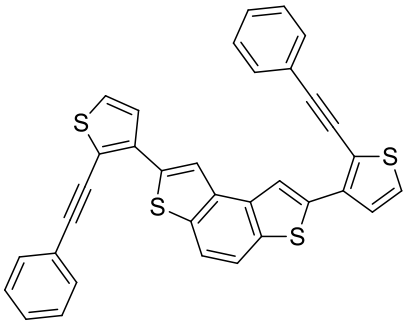

Dialkyne 82c. The crude product obtained according to *General procedure A* between boronic ester **93** (80 mg, 0.18 mmol) and bromide **94c** (56 mg, 0.45 mmol) was purified by column chromatography on silica gel (hexane:dichloromethane 9:1) to afford the product **82c** (78 mg, 66%) as yellow solid. M.p. (dichloromethane/acetonitrile) 218–220 °C. ^{1}H NMR (300 MHz, $CDCl_3$): δ = 8.21–8.17 (m, 2H), 7.92 (s, 1H), 7.86–7.83 (m, 1H), 7.54–7.38 (m, 4H), 7.34–7.28 (m, 3H). ^{13}C NMR (100 MHz, $CDCl_3$): δ = 139.5 (Cq), 137.7 (Cq), 137.1

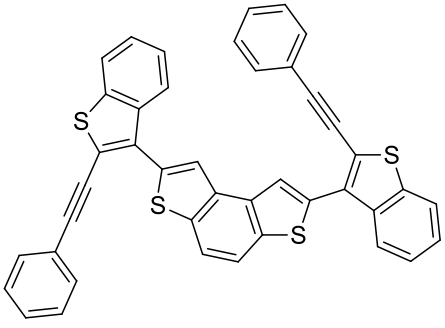

(Cq), 136.3 (Cq), 134.7 (Cq), 133.4 (Cq), 131.5 (2CH), 128.9 (CH), 128.5 (2CH), 126.0 (CH), 125.3 (CH), 123.6 (CH), 122.6 (Cq), 122.4 (CH), 122.3 (CH), 121.3 (Cq), 118.8 (CH), 98.8 (C≡C), 83.4 (C≡C). IR: (neat) ṽ = 3054, 2920, 2848, 2359, 2341, 2195, 1939, 1866, 1696, 1596, 1564, 1551, 1501, 1475, 1455, 1436, 1428, 1399, 1338, 1321, 1300, 1263, 1248, 1181, 1139, 1127, 1067, 1022, 982, 942, 897, 834, 814, 794, 774, 747, 722, 686, 646, 624, 552, 526, 512, 495, 458, 439, 409 cm^{-1}. HRMS: calcd m/z. for; $C_{42}H_{22}S_4^+[M+H]^+$: 655.0677; found (ESI) 655.0671.

Dialkyne 82d. The crude product obtained according to *General procedure A* between bromide **92a** (63 mg, 0.18 mmol) and boronic acid **86d** (127 mg, 0.45 mmol) was purified by column chromatography on silica gel (hexane:dichloromethane 7:3) to afford the product **82d** (94 mg, 79%) as yellow gel. ^{1}H NMR (300 MHz, $CDCl_3$): δ = 8.37 (s, 1H), 7.81 (s, 1H), 7.72–7.67 (m, 2H), 7.45–7.32 (m, 2H), 6.57 (d, *J* = 2.3 Hz, 2H), 6.39 (t, *J* = 2.3 Hz, 1H), 3.60 (s, 6H). ^{13}C NMR (100 MHz, $CDCl_3$): δ = 160.5 (2Cq), 142.8 (Cq), 136.8 (Cq), 135.8 (Cq), 135.1 (Cq), 133.7 (CH), 129.5 (CH), 128.8 (CH), 127.7 (CH), 124.4 (Cq), 121.6 (CH), 121.0 (Cq), 118.6 (CH), 109.0 (2CH), 102.2 (CH), 94.3 (C≡C), 88.9 (C≡C), 55.2 ($2OCH_3$). IR: (neat) ṽ = 3055, 2996, 2954, 2932, 2834, 2360, 2341, 2210, 1583, 1480, 1449, 1417, 1354, 1343, 1315, 1280, 1265, 1249, 1202, 1151, 1097, 1052, 988, 961, 943, 925, 907, 827, 784, 753, 729, 700, 676, 640, 624, 577, 562, 536, 514, 474, 449, 429 cm^{-1}. HRMS: calcd m/z. for; $C_{42}H_{30}O_4S_2^+$ $[M+H]^+$: 663.1658; found (ESI) 663.1653.

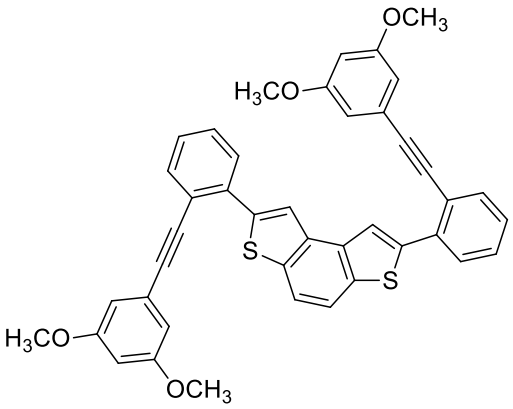

Dialkyne 82e. The crude product obtained according to *General procedure B* between iodide **92b** (80 mg, 0.18 mmol) and boronic acid **86e** (177 mg, 0.54 mmol) was purified by column chromatography on silica gel (hexane:dichloromethane 7:3) to afford the product **82e** (62 mg, 46%) as orange gel. ^{1}H NMR (300 MHz, CD_2Cl_2): δ = 8.41 (s, 1H), 7.89 (s, 1H), 7.79 (d, *J* = 7.7 Hz, 1H), 7.72 (dd, *J* = 7.1, 1.0 Hz, 1H), 7.49–7.36 (m, 9H), 6.95–6.92 (m, 2H), 5.03 (s, 2H). ^{13}C NMR (100 MHz, CD_2Cl_2): δ = 159.2 (Cq), 142.9 (Cq), 136.9 (Cq), 136.8 (Cq), 135.4 (Cq), 135.1 (Cq), 133.6 (CH), 133.0 (2CH), 129.4 (CH), 128.6 (2CH), 128.5 (CH), 128.1 (CH), 127.9 (CH), 127.6 (2CH), 121.6 (CH), 121.3 (CH), 118.7 (CH), 115.5 (Cq), 115.1 (2CH), 94.6 (C≡C), 88.3 (C≡C), 70.0 (CH_2). IR: (neat) ṽ = 3056, 2921, 2848, 1698, 1586, 1504, 1486, 1453, 1436, 1404, 1337, 1276, 1233, 1196, 1184, 1165, 1145, 1098, 1072, 1049, 1023, 1014, 974, 933, 905, 886, 869, 846, 833, 803, 781, 751,

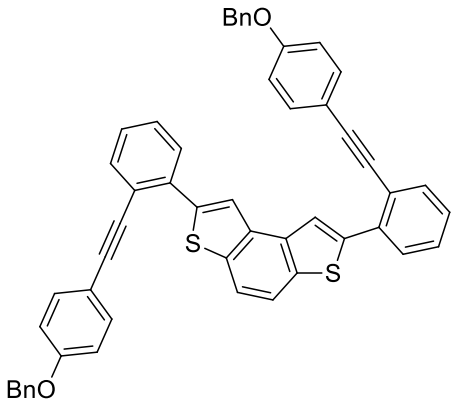

723, 688, 664, 646, 597, 574, 529, 512, 472, 445 cm^{-1}. HRMS: calcd m/z. for; $C_{52}H_{34}O_2S_2^+$ $[M+H]^+$: 755.2073; found (ESI) 755.2052.

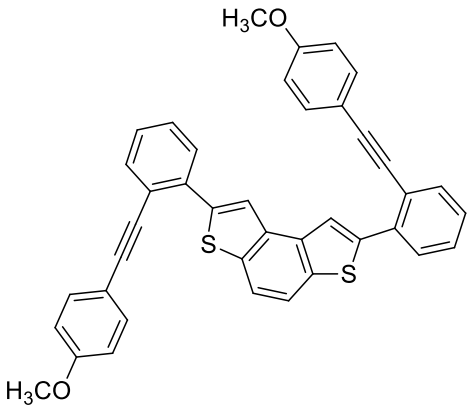

Dialkyne 82f. The crude product obtained according to *General procedure B* between iodide **92b** (80 mg, 0.18 mmol) and boronic acid **86f** (136 mg, 0.54 mmol) was purified by column chromatography on silica gel (hexane: dichloromethane 9:1) to afford the product **82f** (99 mg, 91%) as yellow solid. M.p. (dichloromethane/acetonitrile) 140–142 °C. ^{1}H NMR (300 MHz, $CDCl_3$): δ = 8.33 (s, 1H), 7.81 (s, 1H), 7.73–7.65 (m, 2H), 7.44–7.30 (m, 2H), 6.84–6.79 (m, 2H), 3.74 (s, 3H). ^{13}C NMR (100 MHz, $CDCl_3$): δ = 159.8 (Cq), 142.8 (Cq), 136.8 (Cq), 135.5 (Cq), 135.1 (Cq), 133.5 (CH), 133.0 (2CH), 129.3 (CH), 128.3 (CH), 127.6 (CH), 121.5 (CH), 121.4 (Cq), 118.6 (CH), 115.3 (Cq), 114.1 (2CH), 94.7 (C≡C), 88.3 (C≡C), 55.3 (OCH_3). IR: (neat) ṽ = 3056, 3008, 2960, 2923, 2853, 2835, 2208, 1604, 1567, 1508, 1462, 1438, 1406, 1345, 1289, 1245, 1173, 1145, 1105, 1024, 988, 948, 914, 833, 822, 783, 746, 692, 642, 619, 567, 532, 502, 456 cm^{-1}. HRMS: calcd m/z. for; $C_{40}H_{26}O_2S_2^+$ $[M+H]^+$: 603.1447; found (ESI) 603.14432.

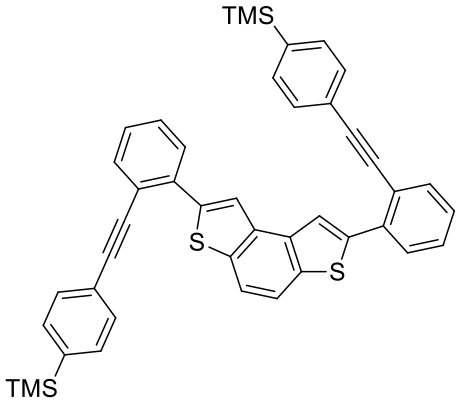

Dialkyne 82g. The crude product obtained according to *General procedure B* between iodide **92b** (80 mg, 0.18 mmol) and boronic acid **86g** (143 mg, 0.54 mmol) was purified by column chromatography on silica gel (hexane: dichloromethane 8:2) to afford the product **82g** (104 mg, 87%) as yellow solid. M.p. (dichloromethane/acetonitrile) 121–124 °C. ^{1}H NMR (300 MHz, $CDCl_3$): δ = 8.37 (s, 1H), 7.82 (s, 1H), 7.74 (dd, *J* = 5.5, 1.0 Hz, 1H), 7.69 (dd, *J* = 5.7, 1.0 Hz, 1H), 7.43–7.38 (m, 5H), 7.34 (dt, *J* = 5.6, 1.0 Hz, 1H), –0.22 (s, 9H). ^{13}C NMR (100 MHz, $CDCl_3$): δ = 142.7 (Cq), 141.3 (Cq), 136.9 (Cq), 135.8 (Cq), 135.1 (Cq), 133.8 (CH), 133.2 (2CH), 130.5 (2CH), 129.4 (CH), 128.7 (CH), 127.7 (CH), 123.4 (Cq), 121.6 (CH), 121.1 (Cq), 118.6 (CH), 94.6 (C≡C), 89.9 (C≡C), –1.3 ($3CH_3$). IR: (neat) ṽ = 3059, 3019, 2951, 2922, 2893, 2848, 1593, 1501, 1471, 1403, 1341, 1303, 1245, 1183, 1145, 1106, 950, 913, 835, 815, 751, 631, 575, 450 cm^{-1}. HRMS: calcd m/z. for; $C_{44}H_{38}S_2Si_2^+$ $[M+H]^+$: 687.2026; found (ESI) 687.2024.

Dialkyne 82h. The crude product obtained according to *General procedure B* between iodide **92b** (80 mg, 0.18 mmol) and boronic acid **86h** (129 mg, 0.54 mmol) was purified by column chromatography on silica gel (hexane:dichloromethane 9:1) to afford the product **82h** (60 mg, 67%) as yellow gel. ^{1}H NMR (300 MHz, $CDCl_3$): δ = 8.22 (s, 1H), 7.78 (s, 1H), 7.66 (d, *J* = 7.8 Hz, 1H), 7.57 (d, *J* = 7.7 Hz, 1H), 7.38–7.28 (m, 2H), 2.45 (t, *J* = 7.1 Hz, 2H), 1.65–1.54 (m, 2H), 1.47–1.35 (m, 2H), 0.81 (t, *J* = 7.4 Hz, 3H). ^{13}C NMR (100 MHz, CD_2Cl_2): δ = 143.0 (Cq), 136.8 (Cq), 135.6 (Cq), 135.0 (Cq), 134.0 (CH), 129.4 (CH), 128.0 (CH), 127.8 (CH), 122.1 (Cq), 121.4 (CH), 118.5 (CH), 96.0 (C≡C), 80.1 (C≡C), 30.6 (CH_2), 22.2 (CH_2), 19.4 (CH_2), 13.4 (CH_3). IR: (neat) ṽ = 3057, 2954, 2927, 2857, 2226, 1698, 1592, 1560, 1509, 1478, 1466, 1438, 1426, 1403, 1377, 1339, 1294, 1282, 1244, 1217, 1184, 1159, 1145, 1105, 1046, 944, 909, 832, 782, 753, 715, 670, 608, 580, 512, 474, 450 cm^{-1}. HRMS: calcd m/z. for; $C_{34}H_{30}S_2$ $[M]^+$: 502.1783; found (EI) 502.1783.

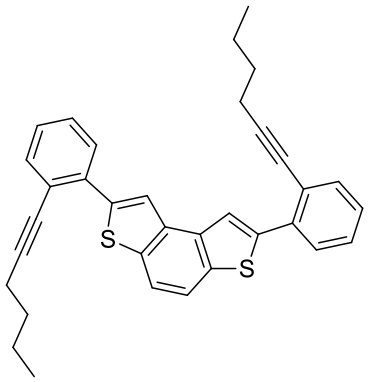

Dialkyne 82i. The crude product obtained according to *General procedure B* between iodide **92b** (80 mg, 0.18 mmol) and boronic acid **86i** (147 mg, 0.54 mmol) was purified by column chromatography on silica gel (hexane:dichloromethane 8:2) to afford the product **82i** (81 mg, 70%) as colourless solid. M.p. (dichloromethane) 136–139 °C. ^{1}H NMR (300 MHz, $CDCl_3$): δ = 8.00 (d, *J* = 8.0 Hz, 1H), 7.95 (s, 1H), 7.91–7.86 (m, 3H), 7.71 (d, *J* = 8.5 Hz, 1H), 7.54–7.42 (m, 2H), 7.26–7.09 (m, 5H). ^{13}C NMR (100 MHz, $CDCl_3$): δ = 140.2 (Cq), 137.8 (Cq), 134.9 (Cq), 134.8 (Cq), 133.0 (2Cq), 131.5 (2CH), 128.8 (CH), 128.4 (CH), 128.2 (3CH), 128.0 (CH), 127.1 (CH), 126.7 (CH), 126.5 (CH), 124.0 (CH), 123.1 (Cq), 122.2 (Cq), 118.5 (CH), 96.6 (C≡C), 89.4 (C≡C). IR: (neat) ṽ = 3054, 2955, 2928, 2853, 1596, 1570, 1500, 1490, 1441, 1404, 1372, 1339, 1258, 1179, 1140, 1087, 1068, 1024, 944, 900, 865, 837, 816, 783, 747, 747, 687, 670, 648, 626, 587, 538, 517, 479, 457, 426 cm^{-1}. HRMS: calcd m/z. for; $C_{46}H_{26}S_2^+$ $[M+H]^+$: 643.1549; found (ESI) 643.1537.

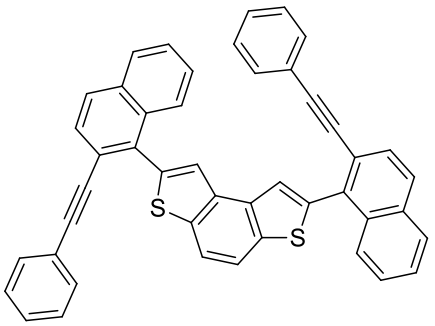

Dialkyne 82j. The crude product obtained according to *General procedure B* between bromide **92c** (78 mg, 0.18 mmol) and boronic acid **86a** (114 mg, 0.54 mmol) was purified by column chromatography on silica gel (hexane:dichloromethane 8:2) to afford the product **82j** (95 mg, 81%) as yellow solid. M.p. (dichloromethane/acetonitrile) 157–159 °C. ^{1}H NMR (300 MHz, $CDCl_3$): δ = 8.28 (s, 1H), 7.75–7.72 (m, 1H), 7.69–7.66 (m, 1H), 7.43–7.29 (m, 4H), 7.10 (d, *J* = 7.8 Hz, 2H), 3.04–2.98 (m, 2H), 2.32 (s, 3H), 1.91–1.78 (m, 2H), 1.11 (t, *J* = 7.3 Hz, 3H). ^{13}C NMR (100 MHz, $CDCl_3$): δ = 141.2 (Cq),

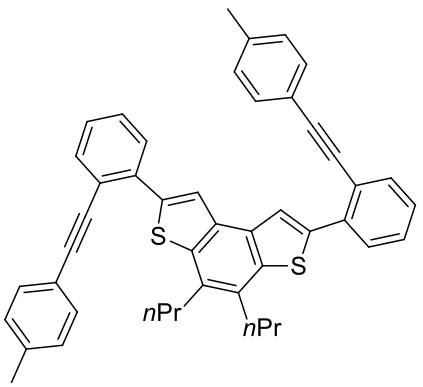

139.0 (Cq), 138.6 (Cq), 137.7 (CH), 136.0 (Cq), 133.3 (Cq), 131.3 (2CH), 130.3 (Cq), 129.2 (2CH), 129.1 (CH), 128.4 (CH), 127.3 (CH), 122.1 (CH), 121.0 (CH), 120.3 (Cq), 94.7 (C≡C), 89.1 (C≡C), 34.4 (CH_2), 23.2 (CH_2), 21.5 (CH_2), 14.8 (CH_3). IR: (neat) ṽ = 3053, 2955, 2925, 2867, 2207, 1887, 1590, 1554, 1509, 1477, 1468, 1434, 1407, 1319, 1273, 1258, 1204, 1182, 1159, 1145, 1091, 1047, 1020, 947, 919, 881, 860, 830, 812, 749, 703, 680, 648, 634, 566, 534, 516, 507, 482, 433, 412 cm^{-1}. HRMS: calcd m/z. for; $C_{46}H_{38}S_2^+$ $[M+H]^+$: 655.2488; found (ESI) 655.2472.

Dialkyne 82k. The crude product obtained according to *General procedure B* between bromide **92c** (78 mg, 0.18 mmol) and boronic acid **86f** (136 mg, 0.54 mmol) was purified by column chromatography on silica gel (hexane: dichloromethane 8:2) to afford the product **82k** (116 mg, 94%) as yellow solid. M.p. (dichloromethane/acetonitrile) 140–141 °C. ^{1}H NMR (300 MHz, $CDCl_3$): δ = 8.30 (s, 1H), 7.75–7.72 (m, 1H), 7.66 (dd, *J* = 7.5, 1.6 Hz, 1H), 7.47–7.41 (m, 2H), 7.40–7.28 (m, 2H), 6.83–6.80 (m, 2H), 3.74 (s, 3H), 3.04–2.99 (m, 2H), 1.91–1.78 (m, 2H), 1.11 (t, *J* = 7.3 Hz, 3H). ^{13}C NMR (100 MHz, $CDCl_3$): δ = 159.8 (Cq), 141.2 (Cq), 138.9 (Cq), 135.8 (Cq), 133.5 (CH), 133.3 (Cq), 132.9 (2CH), 130.3 (Cq), 129.2 (CH), 128.3 (CH), 127.4 (CH), 122.0 (CH), 121.1 (Cq), 115.5 (Cq), 114.1 (2CH), 94.6 (C≡C), 88.5 (C≡C), 55.3 (OCH_3), 34.4 (CH_2), 23.2 (CH_2), 14.8 (CH_3). IR: (neat) ṽ = 3056, 3003, 2956, 2930, 2867, 2835, 2210, 1604, 1567, 1509, 1463, 1439, 1287, 1246, 1201, 1174, 1146, 1105, 1092, 1029, 950, 920, 829, 782, 754, 701, 537 cm^{-1}. HRMS: calcd m/z. for; $C_{46}H_{38}O_2S_2^+$ $[M+H]^+$: 687.2386; found (ESI) 687.2375.

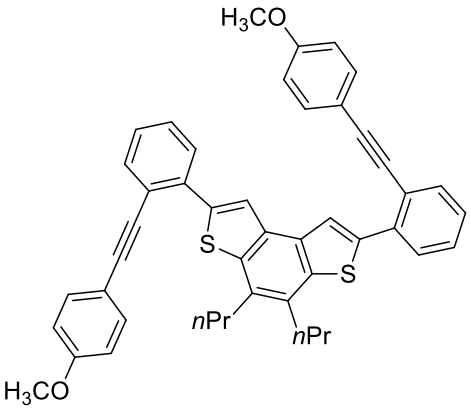

Brominated alkyne 96c. A deaerated mixture of bromide **92a** (63 mg, 0.18 mmol), the boronic acid **86c** (141 mg, 0.20 mmol, 1.1 eq), $Pd(PPh_3)_2Cl_3$ (3 mg, 2.5 mol%) and KF (16 mg, 1.5 eq) in toluene and MeOH (1:1, 0.02 M) was heated at 70 °C under nitrogen for 24 hours. The outcome of the reaction was monitored by TLC analysis. After completion of the reaction, the mixture was cooled to room temperature and poured into water (10 mL). The aqueous phase was extracted with CH_2Cl_2 (4 × 5 mL), and the collected organic phases were dried over Na_2SO_4, and concentrated under reduced pressure. The residue was purified was purified by column chromatography on silica gel (hexane: dichloromethane 9:1) to afford the product **96c** (35 mg, 39%) as yellow solid along with 30% of BDT **56a**. M.p. (dichloromethane/acetonitrile) 171–173 °C. ^{1}H NMR (300 MHz, $CDCl_3$): δ = 8.22–8.18 (m, 1H), 8.07 (s, 1H), 7.87–7.82 (m, 2H), 7.74 (s, 1H), 7.71 (d, *J* = 6.5 Hz, 1H), 7.53–7.45 (m, 4H), 7.36–7.33 (m, 3H). ^{13}C NMR (100 MHz, $CDCl_3$): δ = 139.5 (Cq), 137.7 (Cq), 137.6 (Cq), 137.3 (Cq), 136.5 (Cq), 134.4 (Cq), 133.7 (Cq), 133.1 (Cq), 131.5 (2CH), 129.0 (CH), 128.5 (CH), 126.1 (CH), 125.3 (CH), 124.9 (CH), 123.5 (CH),

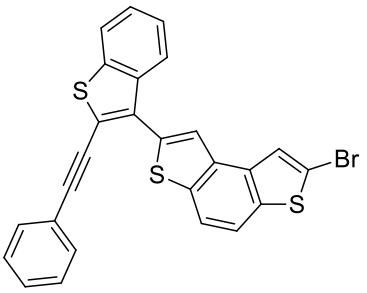

122.5 (Cq), 122.3 (CH), 122.1 (CH), 121.4 (Cq), 118.7 (CH), 118.0 (CH), 115.5 (Cq), 98.8 (C≡C), 83.4 (C≡C). IR: (neat) ṽ = 3057, 3021, 2359, 2341, 2201, 1599, 1573, 1490, 1479, 1455, 1429, 1399, 1358, 1320, 1245, 1178, 1159, 1140, 1069, 1024, 906, 817, 795, 768, 754, 746, 733, 725, 684, 652, 608, 594, 539, 528, 516, 499, 461, 444, 416 cm^{-1}. HRMS: calcd m/z. for; $C_{26}H_{13}S_3Br^+$ $[M+H]^+$: 501.9337; found (ESI) 501.9331.

Dialkyne 82l. A deaerated mixture of bromide **96c** (30 mg, 0.06 mmol), the boronic acid **86f** (30 mg, 2 equiv), Pd_2dba_3 (2 mg, 4 mol%), SPhos (2 mg, 8 mol%) and Cs_2CO_3 (39 mg, 2 equiv.) in THF and H_2O (10:1, 0.02 M) was heated at 80 °C under nitrogen for 24 hours. The outcome of the reaction was monitored by TLC analysis. After completion of the reaction, the mixture was cooled to room temperature and poured into water (5 mL). The aqueous phase was extracted with CH_2Cl_2 (4 × 5 mL), and the collected organic phases were dried over Na_2SO_4, and concentrated under reduced pressure. The residue was purified by column chromatography on silica gel (hexane:dichloromethane 9:1) to provide product **82l** (31 mg, 83%) as yellow solid. ^{1}H NMR (300 MHz, $CDCl_3$): δ = 8.43 (s, 1H), 8.16–8.13 (m, 1H), 8.12 (s, 1H), 7.87–7.82 (m, 2H), 7.76–7.73 (m, 1H), 7.69–7.66 (m, 1H), 7.52–7.29 (m, 11H), 6.80–6.74 (m, 2H), 3.69 (s, 3H). ^{13}C NMR (100 MHz, $CDCl_3$): δ = 159.8 (Cq), 143.1 (Cq), 139.5 (Cq), 137.7 (Cq), 137.0 (Cq), 136.8 (Cq), 136.1 (Cq), 135.4 (Cq), 135.1 (Cq), 134.7 (Cq), 133.6 (CH), 133.4 (Cq), 132.9 (2CH), 131.5 (2CH), 129.4 (CH), 128.9 (CH), 128.4 (2CH), 128.4 (CH), 127.7 (CH), 126.0 (CH), 125.3 (CH), 123.6 (CH), 122.5 (Cq), 122.3 (CH), 122.3 (CH), 121.5 (CH), 121.4 (Cq), 121.2 (Cq), 118.8 (CH), 118.6 (CH), 115.3 (Cq), 114.2 (2CH), 98.9 (C≡C), 94.6 (C≡C), 88.4 (C≡C), 88.3 (C≡C), 55.2 (OCH_3). IR: (neat) ṽ = 3051, 2949, 2921, 2851, 2359, 2332, 2213, 1941, 1699, 1606, 1589, 1570, 1508, 1480, 1465, 1440, 1404, 1288, 1242, 1172, 1143, 1095, 1071, 1033, 939, 908, 819, 796, 779, 747, 736, 723, 687, 667, 646, 530, 517, 490, 437, 409 cm^{-1}. HRMS: calcd m/z. for; $C_{41}H_{24}OS_3^+$ $[M+H]^+$: 629.1062; found (ESI) 629.1046.

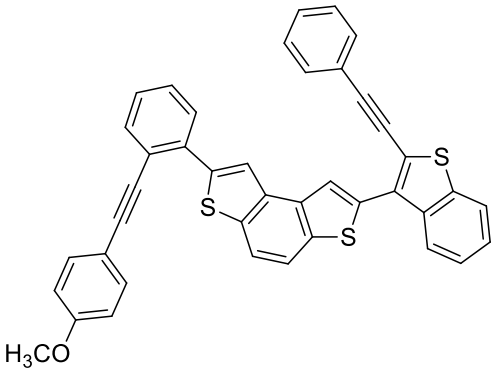

General procedure for racemic cycloisomerisations.[92] To a flame-dried reaction vessel, dialkyne **82** (1 eq, 25 µmol) and the gold precatalyst **L2** (1 mg, 5 mol%) were added. The reaction vessel was fitted with a silicon septum, evacuated and back-filled with argon, and this sequence was repeated twice. Deaerated CH_2Cl_2 (0.025 M) was added and to the stirred mixture $AgSbF_6$ (5 mol%, 0.05 M in CH_2Cl_2) was added dropwise. After stirring overnight at room temperature, the mixture was filtered through a silica plug eluting with CH_2Cl_2. Evaporation of the solvent yielded a crude product which was purified by recrystallization.

General procedure for enantioselective cycloisomerisations.[92] To a flame-dried reaction vessel, dialkynes **82** (1 eq, 25 µmol) and the chiral gold pre-catalyst **L7** (2 mg, 5 mol%) were added. The reaction vessel was fitted with a silicon septum, evacuated and back-filled with argon, and this sequence was repeated twice. Deaerated CH_2Cl_2 (0.025 M) was added and to the stirred mixture $AgSbF_6$ (5 mol%, 0.05 M in CH_2Cl_2) was

added dropwise. After stirring for 48 hours at –20 °C, the mixture was filtered through a silica plug eluting with CH_2Cl_2. Evaporation of the solvent yielded a crude product which was purified by recrystallization or by preparative HPLC. The product ratios and the enantiomeric excesses were determined by CSP-HPLC.

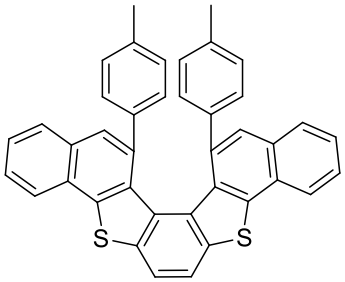

Helicene 84a. The crude product obtained from the racemic cycloisomerisation starting from **82a** (14.2 mg, 25 µmol) was purified by recrystallization (dichloromethane/hexane) to afford the product **84a** (13.7 mg, 97%) as yellow solid. *According to general procedure for the enantioselective cycloisomerisation*, the product **84a** was isolated in 82% yield (11.6 mg), + 92% *ee*. M.p. (dichloromethane/acetonitrile) 268–270 °C. ^{1}H NMR (600 MHz, $CDCl_3$, –50 °C): δ = 8.11–8.09 (m, 1H), 7.98 (s, 1H), 7.87 (dd, *J* = 7.9, 1.7 Hz, 1H), 7.84–7.82 (m, 1H), 7.57–7.51 (m, 2H), 7.36 (s, 1H), 6.91 (d, *J* = 7.3 Hz, 1H), 6.21 (dd, *J* = 7.3, 2.0 Hz, 1H), 5.95 (d, *J* = 7.4 Hz, 1H), 1.42 (s, 3H). ^{13}C NMR (150 MHz, $CDCl_3$, –50 °C): δ = 137.0 (Cq), 136.4 (Cq), 135.5 (Cq), 135.1 (Cq), 134.8 (Cq), 132.3 (Cq), 131.8 (Cq), 131.1 (Cq), 128.3 (CH), 128.2 (CH), 128.1(CH), 127.9 (CH), 126.4 (Cq), 126.2 (CH), 126.1 (CH), 125.6 (CH), 124.4 (CH), 123.6 (CH), 119.7 (CH), 19.8 (CH_3). IR: (neat) ṽ = 3042, 2914, 2853, 2243, 1512, 1488, 1445, 1395, 1336, 1318, 1296, 1259, 1185, 1162, 1133, 1112, 1020, 1000, 944, 907, 887, 846, 813, 790, 771, 745, 726, 647, 624, 606, 573, 550, 522, 498, 477, 456 cm^{-1}. HRMS: calcd m/z. for; $C_{40}H_{26}S_2^+$[M+H]$^+$: 571.1549; found (ESI) 571.1539. [α]^D: (92% *ee*) + 1054° (in $CHCl_3$).

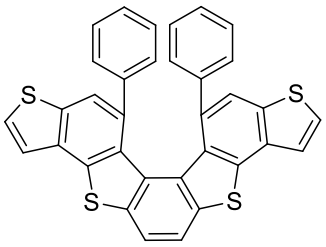

Helicene 84b. The crude product obtained from the racemic cycloisomerisation starting from **82b** (13.8 mg, 25 µmol) was purified by recrystallization (dichloromethane/hexane) to afford the product **84b** (11.8 mg, 86%) as yellow solid. *According to general procedure for the enantioselective cycloisomerisation*, the crude was obtained as mixture (11.7 mg) of the **84b** with the starting material **82b** and the monoclosed intermediate **97b** (**84b**:**82b**:**97b** 3:35:62), + 58% *ee*. M.p. (dichloromethane/acetonitrile) 328–329 °C. ^{1}H NMR (600 MHz, CD_2Cl_2, –50 °C): δ = 7.98 (s, 1H), 7.91 (d, *J* = 7.9 Hz, 1H), 7.56 (d, *J* = 5.3 Hz, 1H), 7.52 (dd, *J* = 5.3, 0.7 Hz, 1H), 7.42 (s, 1H), 7.19 (dt, *J* = 7.6, 1.4 Hz, 1H), 6.54 (tt, *J* = 7.3, 1.2 Hz, 1H), 6.26 (d, *J* = 7.9 Hz, 1H), 6.21–6.18 (m, 1H). ^{13}C NMR (150 MHz, CD_2Cl_2, –50 °C): δ = 138.8 (Cq), 137.1 (Cq), 134.7 (Cq), 134.3 (Cq), 133.3 (Cq), 131.2 (Cq), 130.9 (Cq), 130.9 (Cq), 127.6 (CH), 127.4 (CH), 127.3 (CH), 126.8 (CH), 125.8 (CH), 125.4 (CH), 121.0 (CH), 119.5 (2CH). IR: (neat) ṽ = 3102, 3052, 3020, 2961, 2922, 2853, 1597, 1570, 1538, 1520, 1492, 1472, 1445, 1434, 1393, 1360, 1318, 1296, 1257, 1206, 1179, 1157, 1073, 1023, 956, 906, 846, 792, 767, 735, 715, 694, 654, 628, 603, 586, 542, 527, 499, 479 cm^{-1}. HRMS: calcd m/z. for; $C_{34}H_{18}S_4$ [M]$^+$: 555.0354; found (EI) 554.0283.

Helicene 84c. The crude product obtained from the racemic cycloisomerisation starting from **82c** (16.3 mg, 25 µmol) was purified by recrystallization (dichloromethane/hexane) to afford the product **84c** (15.6 mg, 96%) as yellow solid. *According to general procedure for the enantioselective cycloisomerisation*, the product **84c** was isolated in 93% yield (15.1 mg), + 22% *ee*. M.p. (dichloromethane/acetonitrile) 363–366 °C. ^{1}H NMR (600 MHz, CD_2Cl_2, –50 °C): δ = 8.50 (d, *J* = 7.9 Hz, 1H), 8.13 (s, 1H), 7.99–7.96 (m, 2H), 7.69–7.66 (m, 1H), 7.57–7.54 (m, 1H), 7.51 (s, 1H), 7.24 (dt, *J* = 7.5, 1.3 Hz, 1H), 6.53 (t, *J* = 7.3 Hz, 1H), 6.33 (d, *J* = 7.8 Hz, 1H), 6.20–6.16 (m, 1H). ^{13}C NMR (150 MHz, CD_2Cl_2, –50 °C): δ = 139.1 (Cq), 138.5 (Cq), 137.2 (Cq), 136.2 (Cq), 134.7 (Cq), 134.0 (Cq), 133.0 (Cq), 131.6 (Cq), 130.0 (Cq), 127.7 (CH), 127.6 (CH), 127.5 (CH), 126.3 (CH), 125.9 (Cq), 125.7 (CH), 125.6 (CH), 124.4 (CH), 123.2 (CH), 122.4 (CH), 119.8 (CH), 119.7 (CH). IR: (neat) ṽ = 3080, 3054, 3032, 2922, 2851, 2248, 1591, 1566, 1516, 1492, 1446, 1396, 1338, 1320, 1300, 1260, 1213, 1159, 1132, 1063, 1027, 1006, 926, 902, 864, 851, 838, 801, 788, 759, 722, 695, 658, 632, 600, 584, 544, 533, 484, 429 cm^{-1}. HRMS: calcd m/z. for; $C_{42}H_{22}S_4$ $[M]^+$: 655.0677; found (EI) 654.0598.

Helicene 84d. The crude product obtained from the racemic cycloisomerisation starting from **82d** (16.6 mg, 25 µmol) was purified by recrystallization (dichloromethane/hexane) to afford the product **84d** (15.9 mg, 96%) as yellow solid. *According to general procedure for the enantioselective cycloisomerisation*, the product **84d** was isolated in 92% yield (15.2 mg), + 33% *ee*. M.p. (dichloromethane/acetonitrile) 289–290 °C. ^{1}H NMR (500 MHz, $CDCl_3$, –50 °C): δ = 8.12 (d, *J* = 8.1 Hz, 1H), 7.97 (s, 1H), 7.85 (d, *J* = 7.8 Hz, 1H), 7.60–7.51 (m, 2H), 7.50 (s, 1H), 7.23 (bs, 1H), 5.46 (bs, 1H), 5.43 (t, *J* = 2.3 Hz, 1H), 3.62 (s, 3H), 2.91 (s, 3H). ^{13}C NMR (125 MHz, $CDCl_3$, –50 °C): δ = 159.4 (Cq), 158.5 (Cq), 140.7 (Cq), 137.3 (Cq), 135.7 (Cq), 135.0 (Cq), 132.4 (Cq), 132.1 (Cq), 131.3 (Cq), 128.1 (CH), 126.9 (Cq), 126.4 (CH), 126.2 (CH), 124.7 (CH), 123.8 (CH), 119.9 (CH), 108.9 (CH), 105.2 (CH), 97.3 (CH), 55.2 (OCH_3), 54.6 (OCH_3). IR: (neat) ṽ = 3048, 2984, 2918, 2849, 2236, 1733, 1590, 1554, 1492, 1454, 1421, 1393, 1336, 1317, 1259, 1220, 1203, 1192, 1152, 1063, 1047, 1024, 998, 946, 926, 904, 862, 831, 792, 773, 751, 724, 701, 690, 648, 634, 614, 593, 548, 530, 489, 473, 452 cm^{-1}. HRMS: calcd m/z. for; $C_{42}H_{30}O_4S_2^+$ $[M+H]^+$: 663.1658; found (ESI) 663.1655.

Helicene 84e. The crude obtained from the racemic cycloisomerisation starting from **82e** (18.8 mg, 25 μmol) was purified by recrystallization and column chromatography on silica gel (hexane:dichloromethane 10:1), but the product **84e** was not isolated clean (the purity was evaluated with HPLC and evaluated yield was <30%). *According to general procedure for the enantioselective cycloisomerisations*, the product **84e** was isolated in

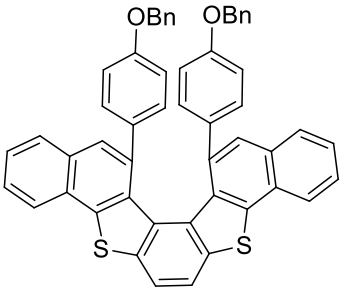

92% yield (17.3 mg), + 95% *ee*. M.p. (dichloromethane/acetonitrile) 221–222 °C. ^{1}H NMR (500 MHz, CD_2Cl_2, –35 °C): δ = 8.16–8.13 (m, 1H), 8.04 (s, 1H), 7.93–7.88 (m, 2H), 7.60–7.52 (m, 2H), 7.41 (s, 1H), 7.35–7.28 (m, 3H), 7.03–7.00 (m, 2H), 6.76 (dd, *J* = 8.3, 2.6 Hz, 1H), 6.26 (dd, *J* = 8.8, 2.2 Hz, 1H), 5.70 (dd, *J* = 8.5, 2.6 Hz, 1H), 4.17 (d, *J* = 10.2 Hz, 1H), 3.87 (d, *J* = 10.2 Hz, 1H). ^{13}C NMR (125 MHz, CD_2Cl_2, –35 °C): δ = 157.2 (Cq), 137.0 (Cq), 136.2 (Cq), 135.0 (Cq), 134.9 (Cq), 132.3 (Cq), 131.7 (Cq), 131.2 (Cq), 131.1 (Cq), 129.5 (2CH), 128.0 (2CH), 127.9 (CH), 127.7 (2CH), 127.6 (CH), 126.3 (CH), 126.2 (Cq), 125.6 (CH), 123.9 (CH), 123.5 (CH), 119.7 (CH), 114.1 (CH), 110.7 (CH), 69,3 ($2CH_2$). IR: (neat) ν̃ = 3033, 2952, 2921, 2848, 1695, 1604, 1570, 1508, 1490, 1453, 1392, 1377, 1314, 1293, 1258, 1240, 1173, 1108, 1073, 1020, 944, 914, 881, 859, 823, 784, 770, 732, 694, 646, 610, 572, 550, 528, 515, 479, 462 cm^{-1}. HRMS: calcd m/z. for; $C_{52}H_{34}O_2S_2^+$ $[M+H]^+$: 755.2073; found (ESI) 755.2062. $[\alpha]^D$: (92% *ee*) + 852° (in $CHCl_3$).

Helicene 84f. The crude product obtained from the racemic cycloisomerisation starting from **82f** (15.0 mg, 25 μmol) was purified by recrystallization (dichloromethane/hexane) to afford the product **84f** (14.3 mg, 95%) as yellow solid. *According to general procedure for the enantioselective cycloisomerisation*, the product **84f** was isolated in 94% yield (14.1 mg), + 91% *ee*. M.p. (dichloromethane/acetonitrile) 238–240 °C. ^{1}H NMR (500 MHz, $CDCl_3$, –35 °C): δ = 8.11–8.08 (m, 1H), 8.00 (s,

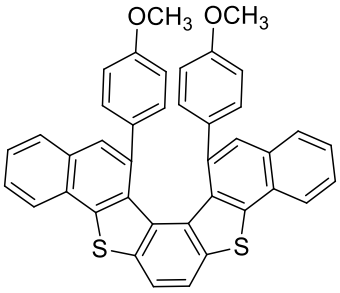

1H), 7.89–7.81 (m, 2H), 7.57–7.50 (m, 2H), 7.37 (s, 1H), 6.69 (d, *J* = 8.4 Hz, 1H), 6.28 (d, *J* = 8.5 Hz, 1H), 5.63 (d, *J* = 8.5 Hz, 1H), 2.95 (s, 3H). ^{13}C NMR (125 MHz, $CDCl_3$, –35 °C): δ = 157.7 (Cq), 137.2 (Cq), 135.0 (Cq), 134.9 (Cq), 132.3 (Cq), 131.9 (Cq), 131.3 (Cq), 131.1 (Cq), 129.8 (CH), 129.6 (CH), 128.0 (CH), 126.5 (Cq), 126.3 (CH), 125.7 (CH), 124.1 (CH), 123.6 (CH), 119.8 (CH), 113.9 (CH), 109.9 (CH), 54.7 (OCH_3). IR: (neat) ν̃ = 3046, 3000, 2955, 2924, 2851, 2831, 1605, 1509, 1489, 1460, 1437, 1394, 1319, 1293, 1243, 1199, 1174, 1108, 1029, 944, 904, 882, 860, 824, 792, 768, 733, 672, 650, 625, 606, 548, 514, 461 cm^{-1}. HRMS: calcd m/z. for; $C_{40}H_{26}O_2S_2^+$ $[M+H]^+$: 603.1447; found (ESI) 603.1440. $[\alpha]^D$: (91% *ee*) + 1862° (in $CHCl_3$).

Helicene 84g. The crude product obtained from the racemic cycloisomerisation starting from **82g** (16.7 mg, 25 µmol) was purified by recrystallization (dichloromethane/hexane) to afford the product **84g** (14.2 mg, 85%) as yellow solid. *According to general procedure for the enantioselective cycloisomerisation*, the product **84g** was isolated in 90% yield (15.0 mg), + 84% *ee*. M.p. (dichloromethane/acetonitrile) 170–171 °C.

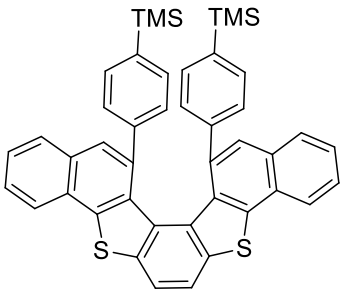

^{1}H NMR (600 MHz, CD_2Cl_2, –35 °C): δ = 8.07 (d, *J* = 8.1 Hz, 1H), 8.04–8.00 (m, 2H), 7.79 (d, *J* = 8.1 Hz, 1H), 7.54–7.51 (m, 1H), 7.49–7.46 (m, 1H), 7.35 (s, 1H), 7.30 (d, *J* = 7.3 Hz, 1H), 6.30 (dd, *J* = 7.6, 1.3 Hz, 1H), 6.27 (d, *J* = 8.0, 1.8 Hz, 1H), – 0.33 (s, 9H). ^{13}C NMR (150 MHz, CD_2Cl_2, –35 °C): δ = 138.9 (Cq), 137.9 (Cq), 137.1 (Cq), 135.4 (Cq), 135.2 (Cq), 132.3 (CH), 131.9 (Cq), 131.8 (Cq), 131.0 (Cq), 130.4 (CH), 128.1 (CH), 127.1 (CH), 127.1 (CH), 126.5 (Cq), 126.2 (CH), 125.9 (CH), 125.2 (CH), 123.4 (CH), 119.6 (CH), –2.5 ($3CH_3$). IR: (neat) ṽ = 3055, 2951, 2916, 2892, 2850, 2359, 2339, 1596, 1488, 1396, 1318, 1293, 1259, 1243, 1162, 1101, 1051, 1020, 944, 915, 883, 835, 814, 772, 751, 741, 724, 686, 649, 626, 613, 579, 550, 523, 502, 480, 455 cm^{-1}. HRMS: calcd m/z. for; $C_{44}H_{38}S_2Si_2^+$ $[M+H]^+$: 687.2026; found (ESI) 687.2019.

Helicene 84h. The crude product obtained from the racemic cycloisomerisation starting from **82h** (12.5 mg, 25 µmol) was purified by recrystallization (dichloromethane/hexane) to afford the product **84h** (11.4 mg, 91%) as yellow solid. *According to general procedure for the enantioselective cycloisomerisation*, the product **84h** was isolated in 78% yield (9.8 mg), + 67% *ee*. M.p. (dichloromethane/acetonitrile) 224–225 °C. ^{1}H NMR (300 MHz, $CDCl_3$): δ = 8.24–8.20 (m, 1H), 8.00 (s, 1H), 7.95–7.90 (m, 1H), 7.63–7.55 (m, 3H), 3.09–2.98 (m, 1H), 2.79–2.69 (m, 1H), 1.09–0.94 (m, 1H), 0.92–0.77 (m, 1H), 0.64–0.43 (m, 2H), 0.24 (t, *J* = 7.3 Hz, 3H). ^{13}C NMR (100 MHz, $CDCl_3$): δ = 140.3 (Cq), 137.7 (Cq), 137.0 (Cq), 134.9 (Cq), 132.1 (Cq), 131.9 (Cq), 127.8 (CH), 127.4 (Cq), 126.5 (CH), 125.7 (CH), 124.1 (CH), 123.8 (CH), 120.0 (CH), 35.3 (CH_2), 32.4 (CH_2), 21.9 (CH_2), 13.1 (CH_3). IR: (neat) ṽ = 2946, 2918, 2866, 2848, 1583, 1490, 1455, 1439, 1391, 1317, 1294, 1262, 1222, 1158, 1140, 1008, 944, 870, 842, 781, 771, 740, 685, 647, 605, 573, 527, 506, 477, 466 cm^{-1}. HRMS: calcd m/z. for; $C_{34}H_{30}S_2$ $[M]^+$: 502.1783; found (EI) 502.1784.

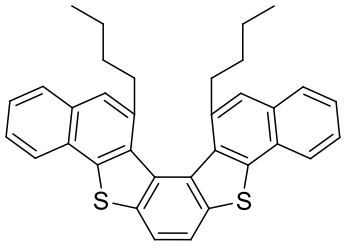

Helicene 84i. The crude product obtained from the racemic cycloisomerisation starting from **82i** (16.0 mg, 25 µmol) was purified by recrystallization (dichloromethane/hexane) to afford the product **84i** (14.4 mg, 90%) as yellow solid. *According to general procedure for the enantioselective cycloisomerisation*, the product **84i** was isolated in 85% yield (13.6 mg), + 39% *ee*. M.p. (dichloromethane) 398–400 °C. ^{1}H NMR (500 MHz, CD_2Cl_2, –35 °C): δ = 9.31 (dd, *J* = 8.2, 0.7 Hz, 1H), 8.15 (s, 1H), 8.08–

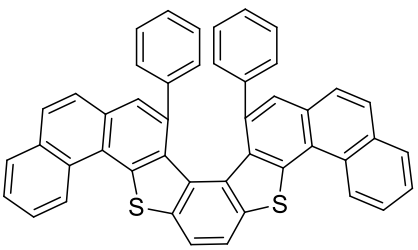

8.04 (m, 2H), 7.92–7.88 (m, 1H), 7.85 (d, *J* = 8.5 Hz, 1H), 7.82 (d, *J* = 8.8 Hz, 1H), 7.74–7.68 (m, 1H), 7.06 (dt, *J* = 8.0, 1.3 Hz, 1H), 6.32 (tt, *J* = 7.3, 1.3 Hz, 1H), 6.28–6.26 (m, 1H), 6.23–6.20 (m, 1H). ^{13}C NMR (125 MHz, CD_2Cl_2, –35 °C): δ = 139.2 (Cq), 136.6 (Cq), 135.4 (Cq), 134.9 (Cq), 133.8 (Cq), 132.3 (Cq), 131.1 (Cq), 130.0 (Cq), 129.1 (Cq), 128.8 (CH), 127.9 (CH), 127.7 (CH), 127.7 (CH), 127.3 (CH), 126.9 (CH), 126.8 (CH), 126.7 (CH), 126.2 (CH), 125.8 (CH), 125.5 (CH), 125.3 (CH), 123.1 (CH), 119.6 (CH). IR: (neat) ṽ = 3045, 1800, 1597, 1573, 1547, 1478, 1447, 1418, 1398, 1353, 1308, 1268, 1219, 1188, 1164, 1140, 1113, 1076, 1024, 1009, 979, 961, 950, 913, 880, 850, 813, 808, 789, 767, 749, 728, 693, 672, 635, 608, 580, 564, 538, 498, 485, 437, 416 cm^{-1}. HRMS: calcd m/z. for; $C_{46}H_{26}S_2^+$ $[M+H]^+$: 643.1549; found (ESI) 643.1525.

Helicene 84j. The crude product obtained from the racemic cycloisomerisation starting from **82j** (16.3 mg, 25 µmol) was purified by recrystallization (dichloromethane/hexane) to afford the product **84j** (15.1 mg, 93%) as yellow solid. *According to general procedure for the enantioselective cycloisomerisation*, the crude was obtained as mixture (15.0 mg) of the **84j** with the starting material **82j** and the monoclosed intermediate **97j** (**84j**:**82j**:**97j** 19:32:49), + 81% *ee*. M.p. (dichloromethane) 244–245 °C. ^{1}H NMR (300 MHz, CD_2Cl_2): δ = 8.14–8.10 (m, 1H), 7.85–7.79 (m, 1H), 7.56–7.48 (m, 2H), 7.32 (s, 1H), 7.17–6.25 (m, 4H), 3.25–3.09 (m, 2H), 2.03–1.90 (m, 2H), 1.45 (s, 3H), 1.22 (t, *J* = 7.3 Hz, 3H). ^{13}C NMR (100 MHz, CD_2Cl_2): δ = 137.6 (Cq), 136.6 (2Cq), 136.2 (Cq), 135.8 (Cq), 133.4 (Cq), 131.6 (2Cq), 130.5 (Cq), 128.5 (2CH), 128.1 (CH), 127.4 (2CH), 127.1 (Cq), 126.0 (CH), 125.8 (CH), 124.6 (CH), 123.6 (CH), 34.4 (CH_2), 23.6 (CH_2), 19.6 (CH_2), 14.6 (CH_3). IR: (neat) ṽ = 3036, 2956, 2925, 2866, 1511, 1488, 1468, 1445, 1375, 1349, 1319, 1257, 1216, 1182, 1150, 1089, 1023, 940, 917, 883, 862, 844, 811, 766, 740, 724, 660, 632, 604, 573, 550, 531, 500, 478, 432 cm^{-1}. HRMS: calcd m/z. for; $C_{46}H_{38}S_2^+$ $[M+H]^+$: 655.2488; found (ESI) 655.2471.

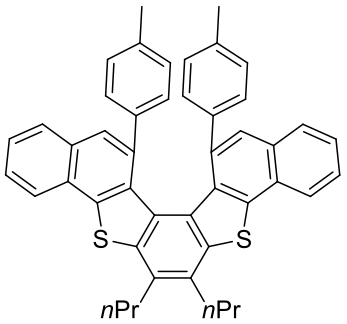

Helicene 84k. The crude product obtained from the racemic cycloisomerisation starting from **82k** (17.1 mg, 25 µmol) was purified by recrystallization (dichloromethane/hexane) to afford the product **84k** (16.1 mg, 94%) as yellow solid. *According to general procedure for the enantioselective cycloisomerisation*, the product **84k** was isolated in 96% yield (16.4 mg), + 81% *ee*. M.p. (dichloromethane/acetonitrile) 283–284 °C. ^{1}H NMR (600 MHz, CD_2Cl_2, –35 °C): δ = 8.11 (d, *J* = 8.0 Hz, 1H), 7.85–7.80 (m, 2H), 7.56–7.48 (m, 2H), 7.32 (s, 1H), 6.67 (d, *J* = 8.5 Hz, 1H), 6.25 (d, *J* = 8.5 Hz, 1H), 5.58 (d, *J* = 8.5 Hz, 1H), 3.13–3.10 (m, 2H), 2.94 (s, 3H), 1.93–1.87 (m, 2H), 1.20 (t, *J* = 7.2 Hz, 3H). ^{13}C NMR (150 MHz, CD_2Cl_2, –35 °C): δ = 157.4 (Cq), 136.8 (Cq), 135.8 (Cq), 134.5 (Cq), 132.6 (Cq), 131.0 (Cq), 130.8 (Cq), 130.8 (Cq), 129.6 (Cq), 129.3 (2CH), 127.6 (CH), 126.1 (Cq), 125.6 (CH), 125.3 (CH), 123.6 (CH),

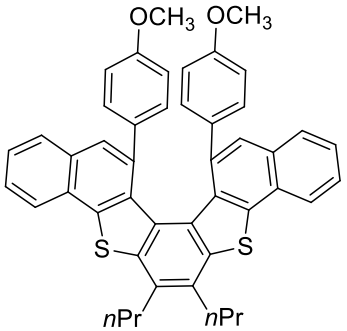

123.0 (CH), 113.4 (CH), 109.5 (CH), 54.2 (OCH_3), 33.9 (CH_2), 23.1 (CH_2), 14.4 (CH_3). IR: (neat) $\tilde{\nu}$ = 3052, 2957, 2928, 2863, 2834, 1605, 1509, 1488, 1469, 1434, 1376, 1347, 1299, 1244, 1173, 1142, 1108, 1083, 1026, 979, 950, 917, 883, 862, 825, 767, 747, 729, 711, 631, 616, 602, 573, 548, 534, 513, 454, 405 cm^{-1}. HRMS: calcd m/z. for; $C_{46}H_{38}O_2S_2^+$ $[M+H]^+$: 687.2386; found (ESI) 687.2376.

The crude product obtained from the racemic cycloisomerisation starting from **82l** (15.4 mg, 25 µmol) was purified by recrystallization (dichloromethane/hexane) to afford the product **84l** (12.6 mg, 82%) as yellow solid. *According to general procedure for the enantioselective cycloisomerisation*, the product **84l** was isolated by HPLC in 67% yield (10.3 mg, + 71% *ee*) along with 19% of monoclosed intermediate **97l** (2.9 mg).

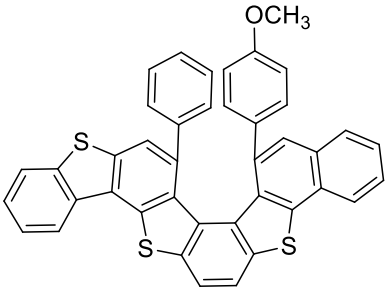

Helicene 84l. M.p. (dichloromethane/acetonitrile) 323–324 °C. ^{1}H NMR (500 MHz, CD_2Cl_2, –35 °C): δ = 8.52 (d, *J* = 7.8 Hz, 1H), 8.09–8.06 (m, 3H), 8.00 (d, *J* = 7.8 Hz, 1H), 7.95–7.93 (m, 2H), 7.81 (d, *J* = 7.6 Hz, 1H), 7.70–7.67 (m, 1H), 7.59–7.49 (m, 3H), 7.48 (s, 1H), 7.39 (s, 1H), 7.14 (d, *J* = 7.5 Hz, 1H), 7.79 (dd, *J* = 8.6, 2.6 Hz, 1H), 6.47 (t, *J* = 7.3 Hz, 1H), 6.36 (d, *J* = 7.9 Hz, 1H), 6.23 (t, *J* = 7.3 Hz, 1H), 6.17 (dd, *J* = 8.6, 2.0 Hz, 1H), 5.59 (dd, *J* = 8.6, 2.5 Hz, 1H). ^{13}C NMR (125 MHz, CD_2Cl_2, –35 °C): δ = 157.8 (Cq), 139.3 (Cq), 138.3 (Cq), 137.5 (Cq), 137.3 (Cq), 136.1 (Cq), 135.5 (Cq), 135.4 (Cq), 134.4 (Cq), 134.1 (Cq), 132.8 (Cq), 132.1 (Cq), 131.8 (Cq), 131.7 (Cq), 131.3 (Cq), 131.0 (Cq), 130.2 (Cq), 129.2 (CH), 129.1 (CH), 128.2 (CH), 127.8 (CH), 127.6 (CH), 126.2 (Cq), 126.1 (CH), 125.9 (CH), 125.7 (CH), 125.6 (CH), 125.5 (CH), 124.6 (CH), 124.3 (CH), 123.4 (CH), 123.2 (CH), 122.6 (CH), 120.2 (Cq), 119.6 (CH), 119.4 (CH), 112.8 (CH), 110.5 (CH), 54.3 (OCH_3). IR: (neat) $\tilde{\nu}$ = 3046, 2952, 2926, 2831, 1606, 1567, 1509, 1489, 1450, 1437, 1394, 1321, 1290, 1263, 1244, 1217, 1201, 1176, 1161, 1133, 1107, 1071, 1033, 996, 969, 933, 881, 857, 828, 787, 771, 758, 745, 728, 699, 654, 622, 605, 577, 560, 539, 519, 458, 431 cm^{-1}. HRMS: calcd m/z. for; $C_{41}H_{24}OS_3^+$ $[M+H]^+$: 629.1062; found (ESI) 629.1054.

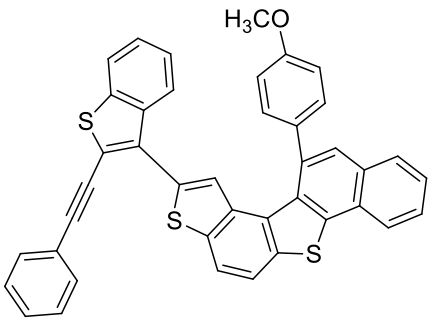

Partially closed 97l. Yellow solid. ^{1}H NMR (600 MHz, CD_2Cl_2, –35 °C): δ = 8.28–8.26 (m, 1H), 8.04–7.99 (m, 3H), 7.88–7.86 (m, 1H), 7.32 (s, 1H), 7.81–7.79 (m, 2H), 7.67–7.61 (m, 2H), 7.51–7.44 (m, 4H), 7.33–7.30 (m, 3H), 7.26–7.23 (m, 2H), 6.57–6.54 (m, 2H), 6.28 (s, 1H), 3.13 (s, 3H). ^{13}C NMR (150 MHz, CD_2Cl_2, –35 °C): δ = 158.3 (Cq), 138.6 (Cq), 138.5 (Cq), 137.9 (Cq), 136.5 (Cq), 136.1 (2Cq), 134.9 (Cq), 133.9 (Cq), 133.1 (Cq), 132.3 (2Cq), 131.0 (Cq), 130.9 (2CH), 130.5 (Cq), 130.5 (Cq), 129.6 (2CH), 128.6 (CH), 128.1 (2CH), 128.0 (CH), 127.1 (CH), 127.0 (Cq), 126.7 (CH), 126.6 (CH), 126.2 (CH), 125.7 (CH), 124.7 (CH), 123.7 (CH), 123.6 (CH), 121.8 (CH), 120.2 (CH), 119.0 (CH), 119.0 (Cq), 114.0 (2CH), 97.8 (C≡C), 82.9 (C≡C),

54.4 (OCH_3). IR: (neat) $\tilde{\nu}$ = 2960, 2913, 1606, 1510, 1487, 1439, 1395, 13221, 1265, 1243, 1175, 1156, 1141, 1071, 1028, 844, 829, 786, 760, 729, 698, 653, 542, 519 cm^{-1}. HRMS: calcd m/z. for; $C_{41}H_{23}OS_3$ $[M]^+$: 628.0989; found (EI) 628.0978.

5.7.3 X-Ray structure of intermediates 82 and thia[5]helicenes 84

The crystals were obtained by layering acetonitrile over a dichloromethane solution.

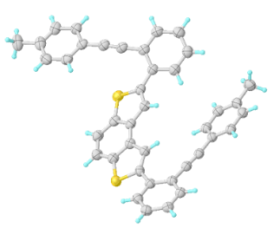

82a

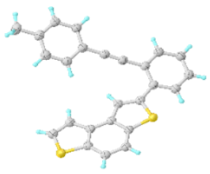

95a

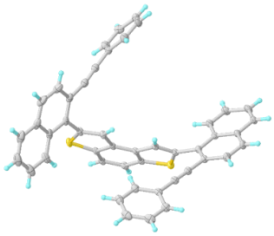

82i

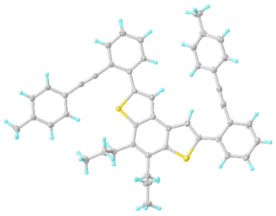

82j

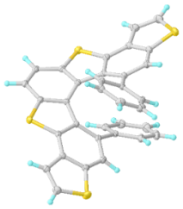

84b

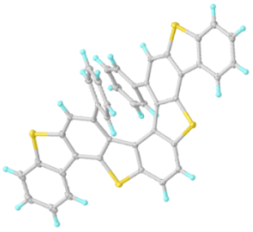

84c

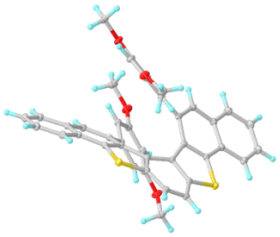

84d

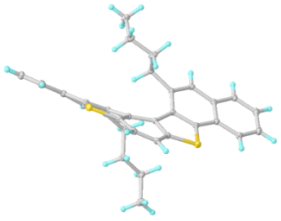

84h

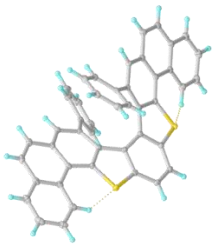

84i

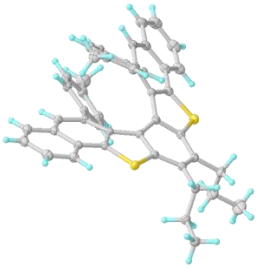

84j

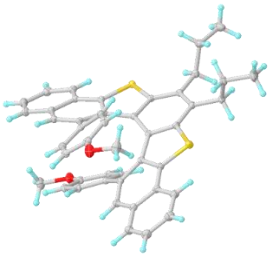

84k

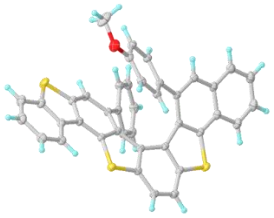

84l

Chapter 6

A route to benzodithiophene systems by ligand-free Suzuki-Miyaura coupling reaction in Deep Eutectic Solvents

This chapter describes the synthesis of functionalised benzo[1,2-*b*:4,3-*b*']dithiophenes in more eco-friendly conditions by ligand-free Suzuki-Miyaura cross-coupling reaction in *Deep Eutectic Solvents* (*DESs*), and their photophysical and electrochemical characterization. This work was performed during a period in the laboratories of Prof. Vito Capriati (Università degli Studi di Bari). Emission properties of some derivatives obtained in this study were analysed by Dr. Alessandro Aliprandi (Universitè de Strasbourg). Electrochemical studies were performed by Dr. Serena Arnaboldi and Dr. Sara Grecchi (Università degli Studi di Milano).

6.1 Introduction

6.1.1. Benzodithiophenes: structure and properties

Thiophene-fused polyaromatic compounds represent a valuable class of organic π-conjugated materials in organic electronics.[255-258] Tricyclic β-fused benzodithiophenes have received notable attention owing to their extensive π-conjugation, rigid and planar molecular structure, high charge-carrier mobility in the solid state under the effect of a field and good conductivity, mostly because of the thienyl S/S interactions.[259] The different position of two sulphur atoms in the benzodithiophene core provides structural isomers (*Figure 46*), which are characterised by diverse degrees of curvature and electronic properties.

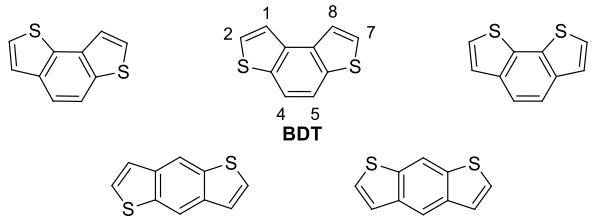

Figure 46: Structure of benzodithiophenes.

Among them, we are interested in the synthesis and functionalisation of benzo[1,2-*b*:4,3-*b*']dithiophene (BDT) and its derivatives,[161,260] which have stimulating a lot of interest due to the fact that they are convenient precursors of thiahelicenes[152,182,261,262] as previously reported in *Chapters 1, 4 and 5*. These systems also found several applications as functional materials to use in electronic devices. For example, BDTs have been used as π-spacers[263-265] in metal-free organic dyes for solar cells, while 1,2-diarylethylene derivatives containing BDT units were employed for the construction of organic light emitting diodes (OLEDs)[266] and as *p*-type semiconductors for organic thin-film transistors (OFETs).[267] Moreover, polymers based on BDT units have been reported as good donor units in donor-acceptor (D-A) copolymers for polymer solar cells (PSCs),[268] and their charge-carrier mobility have been widely studied for potential applications in OFET.[181,269,270] In 2013, Zade *et al.*[175] reported that a BDT-based polymer displayed particular behaviour in neutral and oxidised state, showing an electrochromic switching ability, that represents an interesting aspect for potential applications in electronic identification tags, smart cards as well as switching

element in flat panel displays.[271] Thus, BDTs can be considered key starting molecules that, through a judicious functionalisation, can allow access to more complex and interesting systems.

6.1.2. General synthetic procedures of BDTs and their functionalisation

The most common procedure for the synthesis of the parent BDT and 4,5-disubstituted derivatives involves the oxidative photocyclization of di(thiophen-2-yl)ethenes,[160] which can be prepared by the intermolecular McMurry reductive coupling of 2-thiophenecarboxaldehyde or ketone derivatives[272] (*Scheme 66*).

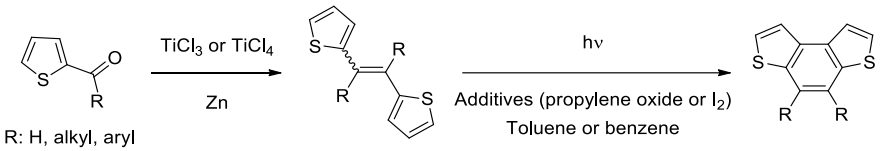

Scheme 66: Synthesis of parent BDT and 4,5-disubstituted derivatives.

Exploiting this strategy, parent BDT and derivatives functionalised in 4 and 5 positions with alkyl, alkoxy or aryl substituents can be easily obtained in good yields (89–95%). Further modifications, especially in 2 and 7 position, of the BDT scaffold can be accomplished by electrophilic aromatic substitution[180] as well as deprotonation of the alpha positions with *n*BuLi followed by reaction with proper electrophiles.[152]

Alternatively, the oxidative photocyclisation reaction can also be used to directly prepare 2,7-disubstituted BDTs, such as the 2,7-dibromo BDT **92a** (*Scheme 67*).[181]

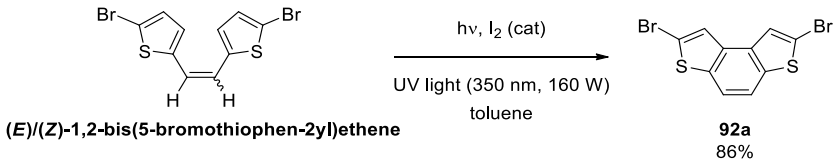

Scheme 67: Synthesis of bromide **92a**.

More recently, the Licandro's group developed an alternative strategy to obtain 2,7-disubstituted BDTs, by means of the $FeCl_3$-mediated cyclization of functionalised (*Z*)-olefins[161] (*Scheme 68*).

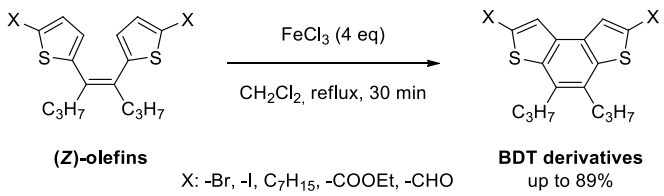

Scheme 68: Synthesis of 2,7-disubstituted BDTs by $FeCl_3$-mediated cyclisation.

On the other hand, the presence of appropriate functional groups in the 2 and 7 position of the BDT scaffold, such as halogen atoms, allows further functionalisation of the BDT, for example to synthesise the BDT-based polymers and oligomers through chemical or electrochemical polymerisation. To date, these compounds are generally prepared by palladium catalysed Stille[181,269] and Suzuki reactions[175,269,273,274] starting from the corresponding BDT dihalides. As example, the Suzuki coupling between the dibromide reported in *Scheme 69* with arylboronic acids provided the coupling products that are important monomers to get access to the corresponding oligomers.

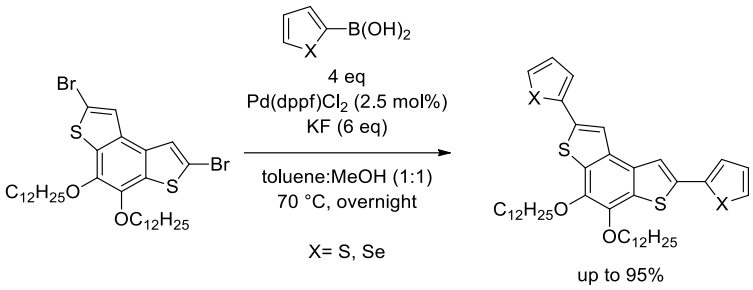

Scheme 69: Synthesis of 2,7-disubstituted BDT by Suzuki reaction.

In spite of the great potential of 2,7-disubstituted BDTs as key building blocks for BDT-based polymers, an eco-friendly procedure to introduce aryl, alkenyl or alkynyl pendants onto the BDT scaffolds has not been developed yet.

6.1.3. Deep Eutectic Solvents (DESs)

In last decade, green reaction media have been emerged to carry out transition metal catalysed cross coupling reactions. Among them, Deep Eutectic Solvents (DESs) represent a rising class of environmentally responsible solvents.[275-277] Abbott[278] first introduced this word in 2003 to describe sustainable solvents (*Figure 47*). *DESs* are composed by two or more natural compounds. These components are cheap, safe and include at least one hydrogen bond donor and one hydrogen bond acceptor, that when mixed at a determined molar ratio form a mixture with a melting point much lower than the individual compounds, owing to an extended hydrogen-bond network between the components.

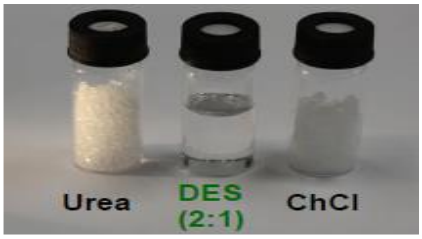

Figure 47: First reported DES.[278]

Typical DES components come from renewable sources such as ammonium salts, sugars, amino acids and vitamins (*Figure 48*).

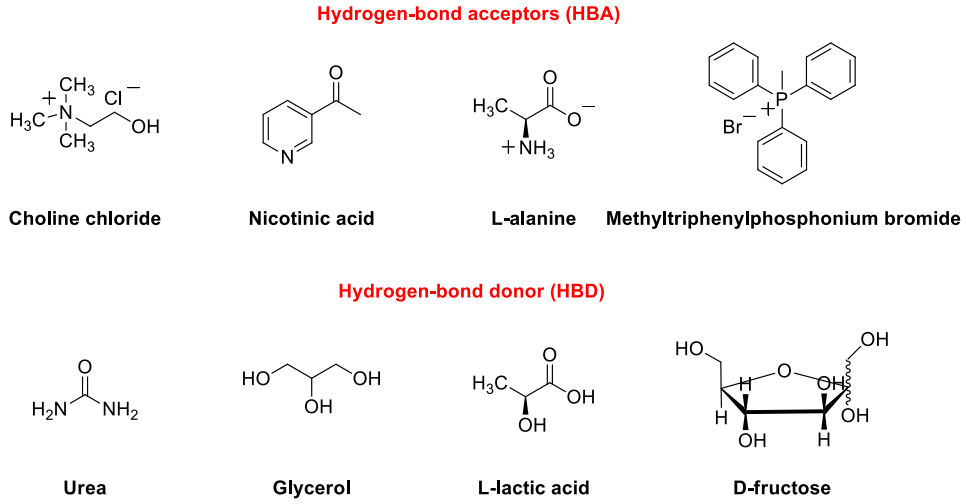

Figure 48: Typical DES components.

Hence, they exhibit significant biocompatibility, and their toxicity is very low.[279,280] On the contrary, their biodegradability is extraordinarily high[281,282] and they have neglectable vapour pressures, high thermal stability, and no flammability. Furthermore, the atom economy of the preparation of DESs is higher than other green reaction media. For all these reasons, their ecological footprint is minimum. The polarity of DESs allows the easy solution of many organic and inorganic reagents and catalysts.[283] Besides, the partial solubility of less polar organic reagents is favoured by the formation of microemulsion.[284,285] Finally, one of their most appreciated advantages is their easy preparation. Indeed, DESs can be formed by simply mixing the starting materials at suitable temperatures with no need of further purification, and they can be easily recycled. One disadvantage can be the high density and viscosity of some DESs,[286] especially for application in continuous flow reactions and in industrial scale. However, the introduction of components such as water, organic/inorganic halides and carboxylic acids significantly decreases the viscosity and density.[287]

Consequently, DESs are emerged as useful reaction media and find several applications in different fields, whereby organometallics,[288,289] electrochemistry,[290] metal-,[177,291-294] bio-[291,295-297] and organocatalysis,[298-300] solar technology[301,302] and photosynthesis.[303] Recently, Capriati and co-workers[177] have reported that the eutectic mixture glycerol/choline chloride in 2/1 ratio is an effective medium to prepare a variety of biaryl and terphenyl derivatives (up to 50 compounds) by Suzuki coupling reactions using aryltrifluoroborates as nucleophilic partners in air under ligandless and mild conditions.

Within this context, simple and eco-friendly ligandless Suzuki-Miyaura cross-coupling reaction between halogenated BDT derivatives and (hetero)aryl-, alkenyl- and alkynyl boronic species in DES was studied. Moreover, the electrochemical and photophysical properties of the newly 2,7-disubstituted BDTs obtained in this study were investigated, including electrochemical oligomerization behaviour of some properly functionalised BDTs.

6.2 Synthesis of 2,7-disubstituted BDTs through Suzuki reaction in DESs

6.2.1. Study of the Suzuki coupling between dihalides 92 and phenylboronic species in DESs

Our study on the functionalisation of BDT halides through Suzuki reaction in DESs was initiated by examining the reaction of 2,7-dibromobenzo[1,2-*b*:4,3-*b'*]dithiophene[181] (**92a**) with potassium phenyltrifluoroborate salt (**69c**) as model reaction (*Table 12*).

Table 12. Screening of the Suzuki coupling in DES between dibromide **92a** and borate salt **69c**.

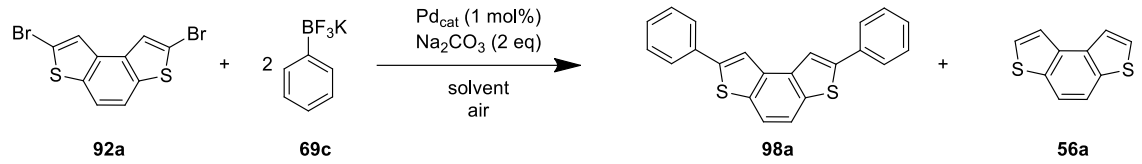

92a **69c** **98a** **56a**

Entry[a]	Pd_{cat}	Solvent	T (°C)/t (h)	Ratio **92a**:**98a**:**56a**[b]	Yield of **98a** (%)[c]
1	**$Pd(OAc)_2$**	**Gly/ChCl**	**60 / 72**	**0:100:0**	**79**
2	$Pd(OAc)_2$	Gly/ChCl	60 / 24	20:80:0	70
3	$Pd(OAc)_2$	Gly/ChCl	25 / 72	100:0:0	-
4	$Pd(OAc)_2$	Gly/ChCl	75 / 15	0:100:0	58
5	$Pd(OAc)_2$	Gly/ChCl	90 / 15	50:50:0	-
6	$Pd(OAc)_2$	Gly/ChCl	90 / 24	0:100:0	44
7[d]	$Pd(OAc)_2$	Gly/ChCl	60 / 0.5	56:20:24	-
8[d]	$Pd(OAc)_2$	Gly/ChCl	60 / 2	38:16:46	-
9[d]	$Pd(OAc)_2$	Gly/ChCl	75 / 0.5	49:17:34	-
10[d]	$Pd(OAc)_2$	Gly/ChCl	90 / 0.5	37:7:56	-
11	$PdCl_2$	Gly/ChCl	60 / 72	22:78:0	-
12	$PdCl_2$	Gly/ChCl	75 / 15	44:56:0	-
13	$Pd_2(dba)_3$	Gly/ChCl	60 / 72	58:42:0	-
14	$Pd_2(dba)_3$	Gly/ChCl	75 / 15	63:37:0	-
15	$Pd(OAc)_2$	Urea/ChCl	60 / 72	51:49:0	-
16	$Pd(OAc)_2$	Urea/ChCl	75 / 15	48:52:0	-
17[e]	$Pd(OAc)_2$	Toluene/MeOH	60 / 10	35:65:0	58%

[a] Reaction conditions: 0.1 mmol of **92a**, 0.2 mmol of **69c**, 2 equiv. of Na_2CO_3, 1 mol% of $Pd(OAc)_2$, Gly/ChCl in 2:1 ratio (1.0 g) under air. [b] The normalised ratio was evaluated by RP-HPLC (eluent: CH_3CN) on the crude reaction mixture. [c] Isolated yield. [d] Reactions were run under MW irradiation. [e] A mixture of toluene and methanol (1:1) was used as solvent.

We initially performed this reaction under experimental conditions very similar to those used by Capriati and co-workers[177] for the synthesis of bi(hetero)aryl systems (*Table 12*, entry 1). In particular, bromide **92a** was reacted with 2 equiv. of borate salt **69c** in the eutectic mixture formed by glycerol and choline chloride (Gly/ChCl) in 2:1 ratio at 60 °C in the presence of 1 mol% of $Pd(OAc)_2$ as catalyst and 2 equiv. of Na_2CO_3 as base. After 72 hours, the conversion was complete, and the expected product **98a** was isolated in 79% yield. No by-products,[304] including the reduced BDT **56a**, the monohalogenated compound **49b**, the homocoupling product **99**, the monobromide **100** or the derivative **101** (*Figure 49*), were found in the final reaction mixture, thus suggesting a good selectivity in the formation of the disubstituted product **98a**.

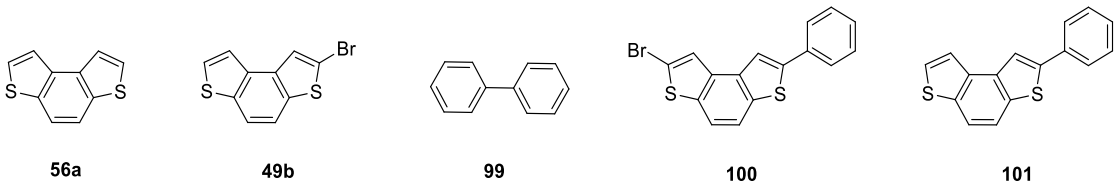

***Figure 49**:* Potential by-products from the Suzuki reaction between bromide **92a** and borate **69c**.

In order to improve the efficiency of this reaction, the effects of some parameters such as the reaction temperature, the palladium catalyst and the nature of DESs were examined. As far as the temperature is concerned, while the reaction did not work at room temperature (*Table 12*, entry 3), and the starting dibromide **92a** was quantitatively recovered, when the reaction was carried out at 60 °C the product **98a** was isolated in 70% and 79% after 24 hours and 72 hours, respectively (*Table 12*, entries 2 and 1). On the other hand, when the mixture was warmed at 75 and 90 °C, a complete conversion of the dibromide **92a** was observed after 15 and 24 hours, respectively (*Table 12*, entries 4 and 6), but **98a** was isolated in lower yields (58 and 44%) than those obtained at 60 °C (70–79%) (*Table 12*, entries 1–2). Indeed, the higher temperatures provided more complex reaction mixtures containing several by-products which were not isolated. The microwave oven was also used in place of the oil bath to warm the reaction mixture, with the aim to decrease the reaction time, but unsatisfactory results were obtained (*Table 12*, entries 7–10). Indeed, the formation of the dehalogenated substrate **56b** significantly occurred along with the formation of the required product **98a**. Concerning the palladium catalyst, when $PdCl_2$ or $Pd_2(dba)_3$ were used in place of $Pd(OAc)_2$ the conversion of dibromide **92a** was not complete after 72 hours (*Table 12*, entries 11–14), thus $Pd(OAc)_2$ seemed to be the best catalyst for this reaction. The use of an alternative DES, such as the mixture of urea and ChCl in 2:1 ratio did not provide better results, since after 72 hours the reaction mixture contained the starting dibromide **92a** and the desired product **98a** in *ca.* 1:1 ratio (*Table 12*, entries 15–16). Finally, to evaluate the advantage of using DES as reaction media in place of common organic solvents, we performed the reaction in the presence of a mixture of organic solvents, such as toluene and methanol (*Table 12*, entry 17). Indeed, this mixture has been previously used in Suzuki coupling involving similar BDT bromides (see *Scheme 70*).[175] In this case, compound **98a** was isolated in a significantly lower yield (58%) than that obtained in DES (79%,

Table 12, entry 1), so demonstrating a better performance of the catalytic system in DES than that in common organic solvents.

Of note, when the reaction was carried out in a mixture of toluene and MeOH (70 °C, 9 hours) in the presence of $Pd(dppf)Cl_2$ (2.5 mol%) and KF (6 eq), following a previously reported procedure for the Suzuki coupling of similar BDT bromides,[175] target compound **98a** was obtained in 53% yield (*Scheme 70*).

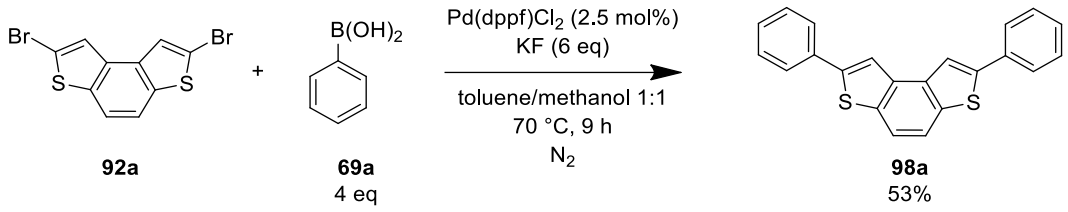

Scheme 70: Suzuki reaction between **92a** and phenylboronic acid (**69a**) under literature conditions.[175]

This result further confirmed the use of DES as an advantage reaction media for this reaction. With these results in hand, we evaluated the nature of the halide and boronic species in the outcome of the reaction (*Table 13*).

Table 13. Suzuki coupling in DES between dihalides **92a**,**b** and phenyl boron species **69a,c,e**.

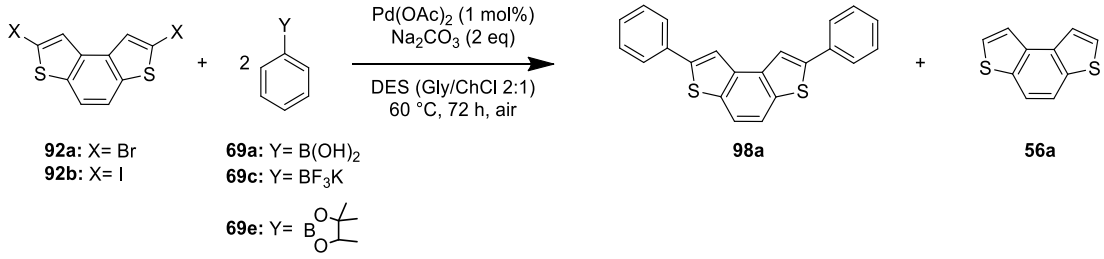

Entry[a]	**92**	**69**	Ratio **92**:**98a**:**56a**[b]	Yield of **98a** (%)[c]
1	**92a**	**69c**	0:100:0	79
2	**92b**	**69c**	0:100:0	54
3	**92a**	**69a**	0:100:0	70
4	**92b**	**69a**	0:100:0	53
5	**92a**	**69e**	0:100:0	75

[a] Reaction conditions: 0.1 mmol of **92a**, 0.2 mmol of **69**, 2 equiv. of Na_2CO_3, 1 mol% of $Pd(OAc)_2$, Gly/ChCl in 2:1 ratio (1.0 g) under air. [b] The normalised ratio was evaluated by RP-HPLC (eluent: CH_3CN) on the crude reaction mixture. [c] Isolated yield.

As shown in *Table 13*, while the reaction was carried out using the diiodide **92b**[305] as electrophile in place of dibromide **92a**, the required product **98a** was isolated in lower yield (54% *vs.* 79%, entry 1 and entry 2,

Table 13), when **69c** was replacing with the corresponding phenylboronic acid **69a** or phenylboronic acid pinacol ester **69e**, the product **98a** was isolated in similar yields (*Table 13*, entries 1, 3 and 5). The same trend was recognised when the reaction was performed using the diiodide **92b** and the phenylboronic acid **69a**. Indeed, **98a** was isolated in lower yield compared to one obtained using **92a** (53% *vs.* 70%, entry 3 and entry 4, *Table 13*), but similar yield was obtained than one achieved using **69c** (*Table 13*, entry 2 and entry 4).

6.2.2. Substrate scope: synthesis of a set of functionalised BDTs

Having successfully demonstrated the viability of the $Pd(OAc)_2$-catalysed Suzuki coupling between dibromide **92a** or diiodide **92b** with boron species **69** in the presence of Na_2CO_3 as base and a mixture of Gly/ChCl as reaction media at 60 °C, the scope and limitations of this procedure were tested, evaluating the nature of the (hetero)aryl moiety of the boron species. More in detail, this process was extended by exploring the scope and limitations of the reaction with benzodithiophene dihalides **92a**,**b** and some commercially available (hetero)arylboronic species **69b–d**,**f–l** as nucleophilic partners (*Scheme 71*).

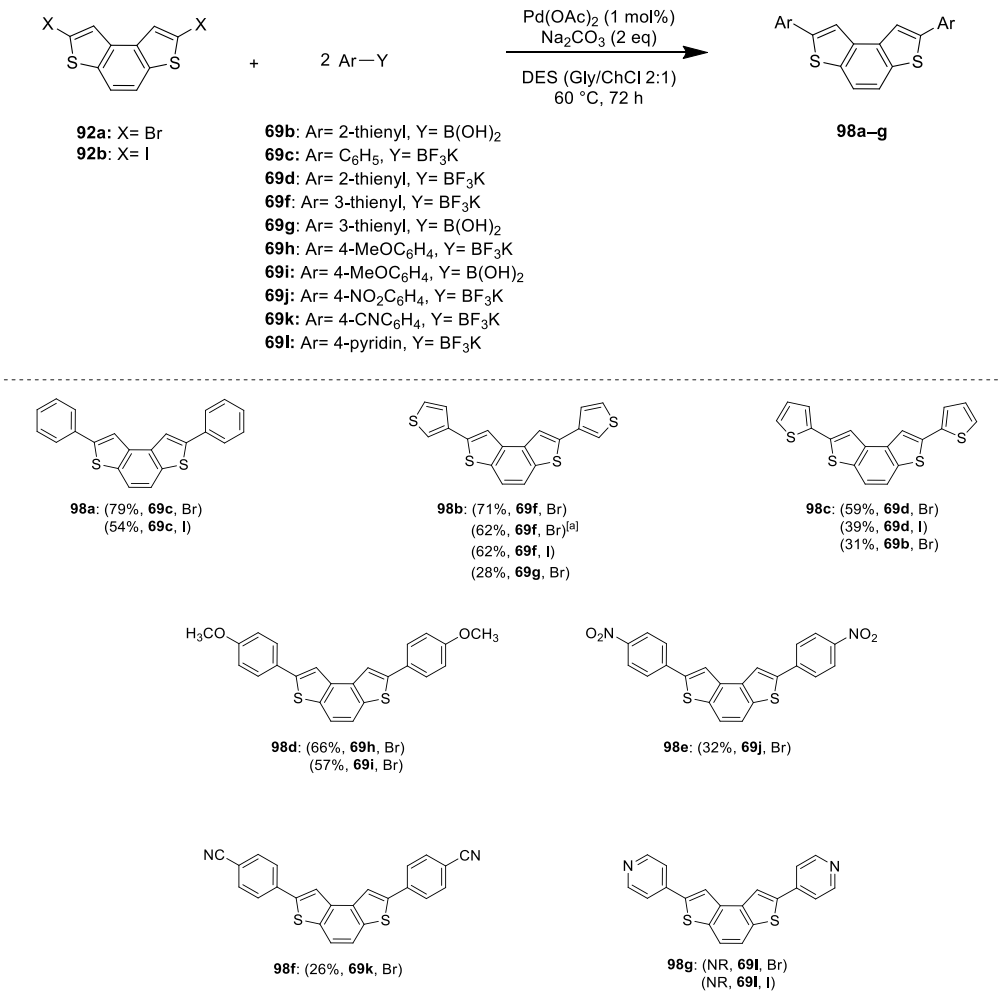

Scheme 71: Synthesis of bis(hetero)arylsubstituted benzodithiophenes **98a–g** via Suzuki coupling between dihalides **92a**–**b** and (hetero)arylboronic species **69**.

Dibromide **92a** participated more effective than the corresponding diiodide **92b** in the coupling process hereby delivering the expected products **98a**–**c** in 59–79% yield. In the presence of electron-donor group such as -OMe in the nucleophilic partners **69h**, product **98d** was obtained in 66% yield after 72 hours, but the starting material **92a** was also recovered in 17%. Moreover, the performance of (hetero)aryltrifluoroborates were found to be superior than that of the corresponding (hetero)arylboronic acids in all cases, as also ascertained in previous studies.[177] On the other hand, the presence of electron-withdrawing groups in the nucleophilic partners **69j–k** dramatically hindered the coupling process , and the expected products **98e–f** were obtained in only 26–32% yield. Moreover, no traces of compound **98g** were obtained in the Suzuki coupling with electron-withdrawing heteroarylboron species **69l**, and dihalides **92a**,**b** were quantitatively recovered. These low yields could be rationalised taking into account the formation of several by-products during these reactions. Unfortunately, the isolation and the identification of these side-products was not possible due to the complexity of the reaction mixtures. Finally, when a scale up of the reaction was performed under our optimised conditions, compound **98b** was isolated in 62% yield after 72 hours and the starting bromide **92a** was recovered in 8%. To further extend the scope of this procedure, especially to investigate the reactivity of alkenyltrifluoroborate salts towards Suzuki reaction of dihalides **92a**,**b** in DES, we carried out a brief screening of the experimental conditions for the Suzuki reaction of **92a**,**b** with alkenyltrifluoroborate **102** (*Table 14*).

Table 14. Suzuki coupling in Gly/ChCl between benzodithiophene dihalides **92a**,**b** and alkenyltrifluoroborate **102**.

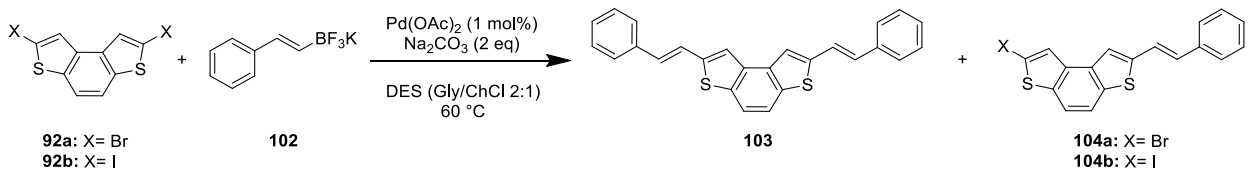

92a: X= Br
92b: X= I

102

103

104a: X= Br
104b: X= I

Entry[a]	**92**	Eq of **102**	t (h)	Yield **103** (%)[b]	Yield **104** (%)[b]
1	**92a**	2	24	62	27
2	**92b**	2	24	74	-[c]
3	**92a**	2	6	35	43
4[d]	**92a**	1	72	8	46

[a] Reaction conditions: 0.1 mmol of **92**, 0.2 or 0.1 mmol of **102**, 1 mol% of $Pd(OAc)_2$, 2 equiv. of Na_2CO_3, 1.0 g of Gly/ChCl (2:1 ratio) under air. Unless otherwise stated, the conversion of **92** was quantitative. [b] Isolated yield. [c] Monosubstituted compound **104b** was not observed in the reaction mixture. [d] Dibromide **92a** was recovered in 36% yield.

Unlike the results obtained for the synthesis of di(hetero)aryl substituted BDT **98**, in this case diiodide **92b** provided best results than those obtained with dibromide **92a** (compare entries 2 and 1, *Table 14*). Indeed, the bis(styryl) derivative **103** was isolated in 74% yield from the reaction involving the iodide **92b**, and in

62% yield from the reaction performed with bromide **92a**. However, a complete conversion of the starting material after 24 hours was observed in both reactions. Of note, when **92a** was used as electrophile, the mono-substituted adduct **104a** was also isolated from the reaction mixture in 27% yield after 24 hours (*Table 14*, entry 1). As this compound represents a useful intermediate for the synthesis of BDTs with different substituents in the alpha-positions, efforts were made to improve its yield. At the beginning, the reaction time was decreased, and **104a** was obtained as major product (43%) along with 35% yield of **103** after 6 hours (*Table 14*, entry 3). Again, using only one equivalent of **102**, **104a** was isolated as main product (46%) and only traces of **103** (8%) were obtained after 72 hours, although a significant amount of starting material **92a** (36%) was recovered (*Table 14*, entry 4).

Finally, as proof of concept, **104a** was reacted with one equiv. of **69c** under our optimised conditions, affording compound **105** in 27% yield after 72 hours (*Scheme 72*). The starting bromide **104a** was also recovered in 40% yield.

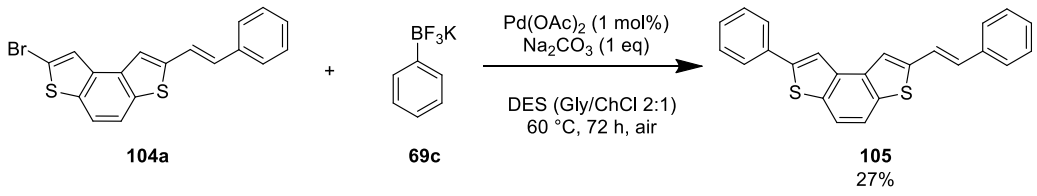

Scheme 72: Synthesis of disubstituted benzodithiophene **105**.

It also appeared to be of interest to investigate the possibility of performing Pd-catalysed C(sp^2)–C(sp) Suzuki reactions using our protocol. As shown in *Scheme 73*, the reaction between diiodide **92b** and 2 equiv. of potassium trifluorophenylethynylborate **106** gave the dialkynyl substituted BDT **107** in 44% yield.

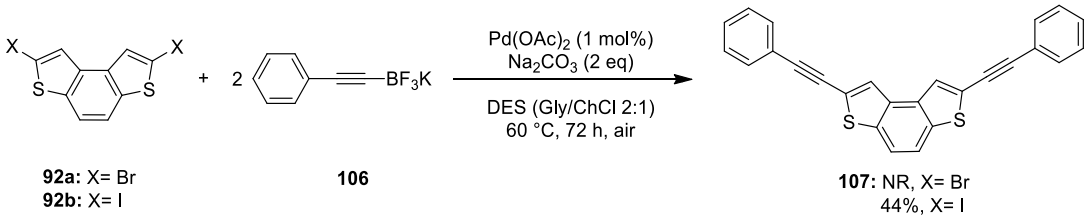

Scheme 73: Synthesis of dialkynyl substituted BDT **107**.

Unfortunately, when the same reaction was carried out using dibromide **92a** in place of diiodide **92b**, the starting material was quantitatively recovered. Finally, a second commercially available acetylenes **108** was selected (*Scheme 74*). Unfortunately, the product **109** was not isolated since the final reaction mixture contained several side-products.

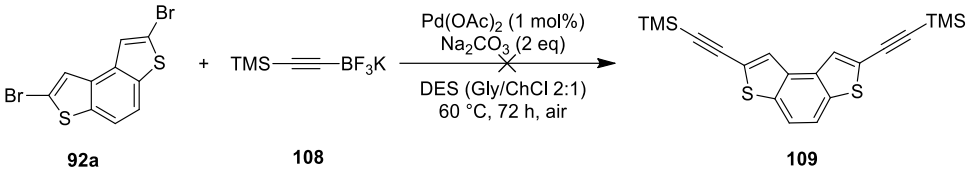

Scheme 74: Attempt to synthesise BDT **109**.

6.2.3. First studies on the recycling of the catalyst

The recycling of the catalyst was also preliminary investigated taking into account the diverse solubility of $Pd(OAc)_2$ in the eutectic mixture Gly/ChCl and in different organic solvents. The model reaction used for the recycling study was the Suzuki coupling between bromide **92a** and the borate salt **69c** under the experimental conditions reported in entry 1 of *Table 12* (1 mol% of $Pd(OAc)_2$, 2 equiv. of Na_2CO_3 in 1 g of DES at 60 °C under air). After 24 hours, the reaction mixture was washed with ethyl acetate (6 x 1 mL), and the product **98a** was isolated in 70% yield, and no starting bromide **92a** was detected in the reaction mixture. Next, after the addition of fresh reagents **98a** and **69c** to the DES mixture, containing the catalyst and base, the reaction was run for 24 hours. After the second cycle, the reaction mixture contained bromide **92a** and the product **98a** in 54:46 NMR ratio (*Figure 50*), so demonstrating that the catalyst efficiency decreased. After the third cycle we found a similar result than that observed after the second cycle, since the reaction mixture contained **92a** and **98a** in 62:38 NMR ratio. From this preliminary study, the experimental conditions used for the Suzuki coupling in DES of **92a** seem not to allow an efficient recovery of the catalyst, which significantly loses its catalytic activity after the first cycle.

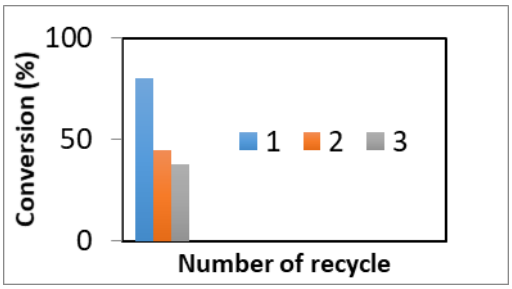

Figure 50: Recycling of the catalyst in the Suzuki coupling between **92a** and **69c**.

6.2.4. Miscellaneous

In order to further evaluate the versatility of this procedure, we compared the use of diverse halogenated benzodithiophene species: a) monohalogenated BDT **49** *vs.* dihalide **92**; b) α-bromoBDT **49b** *vs.* β-bromoBDT **55a**; c) different polycyclic thiophene-based halides.

*a) monohalogenated BDT **49** vs. dihalide **92***

As shown in *Scheme 75*, α-halides **49b**[180] and **49a**[152] were reacted with 1 equiv. of borate salt **69c** in 1 g of Gly/ChCl in 2/1 ratio at 60 °C in the presence of 1 mol% of $Pd(OAc)_2$ as catalyst and 1 equiv. of Na_2CO_3 as

base. After 72 hours, the expected product **101** was isolated in 61% yield in case of bromide **49b**, while 59% with iodide **49a**, and in both cases the starting halides were recovered (ca. 26%).

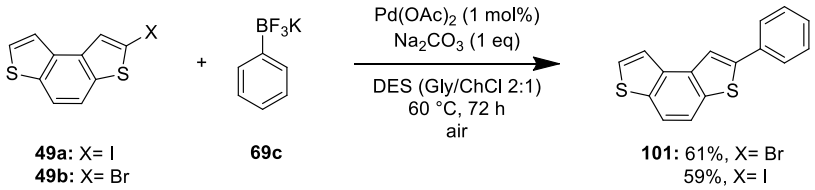

Scheme 75: Synthesis of 2-phenylbenzodithiophene **101**.

Thus, the nature of halide did not influence the efficiency of these reactions since comparable yields were obtained. On the contrary, in the case dihalides **92a**,**b** dibromide **92a** was found significantly more reactive than the iodide **92b** (*Table 13*, entry 1 vs. entry 2). Interestingly, monosubstituted BDT **101** could represent a key intermediate for the preparation of BDT derivatives with different substituents in α-positions.

*b) α-bromoBDT **49b** vs. β-bromoBDT **55a***

Starting from β-bromide **55a**, previously reported in *Chapter 1*, the desired product **91** was isolated in 65% yield after 72 hours (*Scheme 76*).

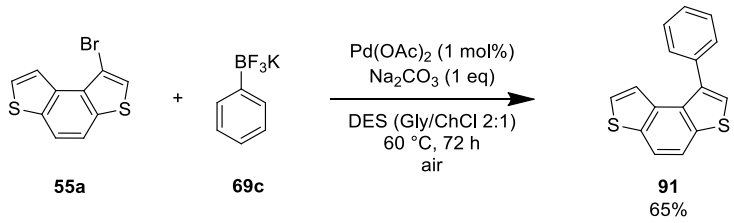

Scheme 76: Synthesis of 1-phenylbenzodithiophene **91**.

The β-bromide **55a** gave similar results to α-bromide **49b** (*Scheme 75*), showing that the position of the halide seems not to affect the final yield. Besides, this yield (*Scheme 76*) is completely comparable to that obtained using "classical" Suzuki conditions for benzodithiophene structures[175] (67%) and this result demonstrates the utility and the convenience of this protocol.

As proof of concept, we tried a preliminary experiment to prepare dimeric intermediate **54a** through the MBSC coupling previously reported in *Chapter 1*. In particular, β-bromide **55a** were reacted with 0.65 equiv. of bis(pinacolato)diboron in 1 g of Gly/ChCl in 2/1 ratio at 60 °C in the presence of 1 mol% of $Pd(OAc)_2$ as catalyst and 2 equiv. of Na_2CO_3 as base (*Scheme 77*).

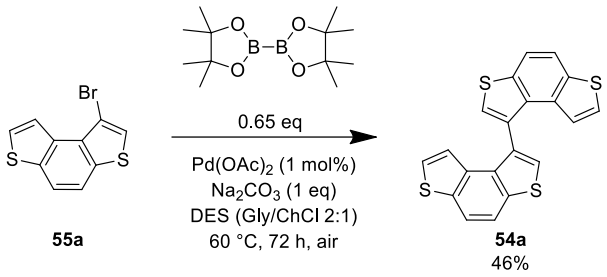

Scheme 77: Synthesis of dimer **54a** in DES.

After 72 hours, the expected dimer **54a** was isolated in 46% yield and the starting material was recovered (ca. 32%). The yield was lower than that obtained using the experimental conditions reported in entry 11 of *Table 1* (86%, see *Chapter 1*), but this result is very promising, because it is the first example of MBSC coupling in DESs.

c) different polycyclic thiophene-based halides

Because of the good results obtained with this specific BDT isomer, Pd-catalysed Suzuki procedure in DES was performed with different polycyclic thiophene-based bromides, such as compounds **92c**[161] and two commercially available dibromides **110** and **111** (*Scheme 78*).

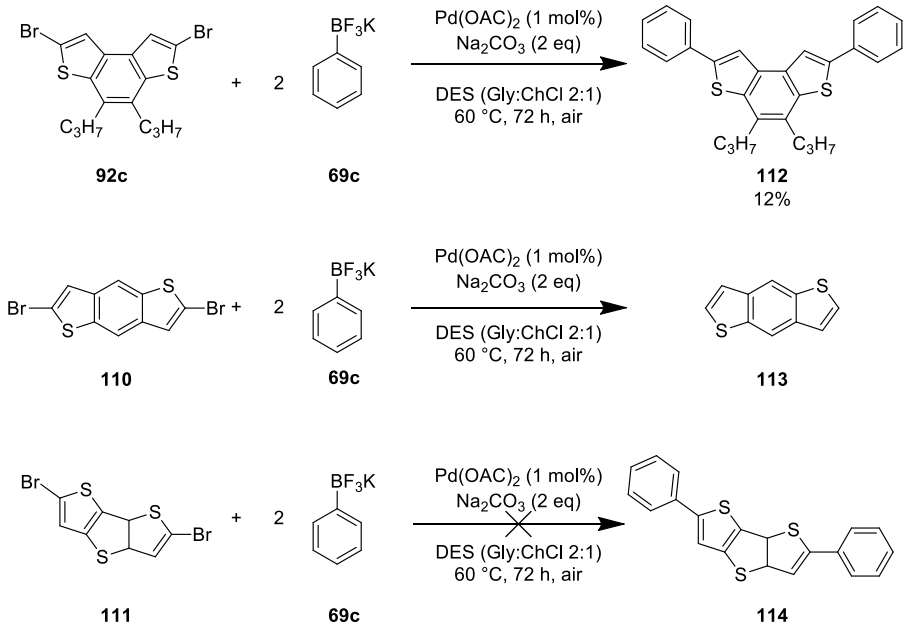

Scheme 78: Suzuki reaction in DES using thiophene-based bromides **92c**, **110** and **111**.

Starting from dibromide **92c**, the coupling product **112** was isolated in 12% yield and the starting material was recovered in 74% yield. In this case, the presence of two alkyl chains in the BDT scaffold significantly decreased the efficiency of this coupling, presumably due to the more lipophilic character of the substrate

that makes it less suitable for reaction in DES. On the contrary, the reaction with dibromide **110** gave the reduced product **113** as main compound, demonstrating that these experimental conditions were not selective in the formation of the desired product but they mainly favoured the debromination of **110**. Finally, bromide **111** was found to be unreacted under these conditions, providing the starting material.

6.3 Photophysical and electrochemical properties of BDT derivatives

6.3.1 Photophysical studies

The optical properties of novel BDT derivatives were initially investigated by UV-vis absorption spectroscopy in diluted DCM solution at room temperature and compared with those of the parent BDT (**56a**). The molar absorptivity spectra are represented in *Figure 51*, while the optical features (λ_{max} and molar absorptivities) are reported in *Table 15*. Three different series of compounds have been confronted and discussed: *i)* compounds with different phenyl pendants **98a**, **98d** and **98f** (*Figure 51a*); *ii)* compounds with thienyl pendants **98b** and **98c** (*Figure 51b*); *iii)* compounds bearing phenyl **98a**, alkenyl **103** and alkynyl pendants **107** (*Figure 51c*).

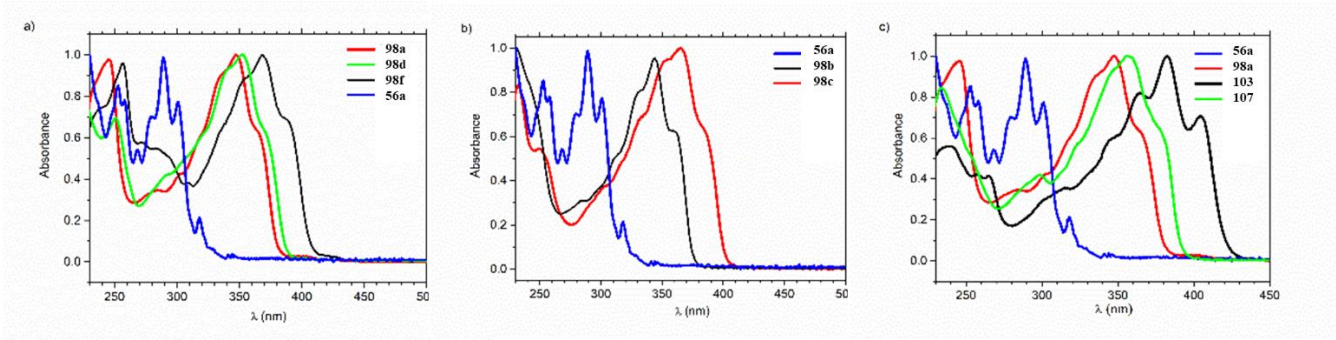

Figure 51: UV absorption spectra of **98a**, **98d** and **98f** (a), **98b** and **98c** (b), **98a**, **103** and **107** (c).

The introduction of aryl, alkenyl or alkynyl moiety on the BDT skeleton led to a consistent redshift (55−105 nm, *Table 15*) with respect to the parent BDT **56a** in all examined cases. This is a well-established effect because of the enhanced conjugation of the BDT-framework induced by the α-substituents. Furthermore, a significant change of the absorption shape of the peaks was observed, being remarkable less resolved than that of BDT **56a** (*Figure 51*). As reported in *Figure 51a*, diaryl substituted BDTs **98a**, **98d** and **98f** showed very similar absorption shape, though their absorption maxima were quite different. In case of **98d,** bearing the electron-rich methoxy substituent, the absorption spectrum was very similar than that of **98a**. On the contrary, the spectrum of **98f**, having the electron-withdrawing cyano group, was significantly red-shifted (21 nm) as consequence of a better conjugation through the BDT scaffold. Again, compound **98c**, having two 2-thienyl groups, showed a remarkable red-shift (23 nm) compared with **98b**, having two 3-thienyl groups (*Figure 51b*). Finally, comparing the set of compounds **98a**, **103** and **107**, we observed that a better conjugation resulted in the presence of alkenyl pendants, followed by alkynyl and aryl ones (*Figure 51c*).

Concerning the emission properties, we performed a preliminary study in diluted solution at room temperature of three representative compounds, such as **98a**, **98b** and **98c**. All derivatives showed a fluorescence emission in diluted DCM solutions due to the lowest excited state (*Figure 52*).

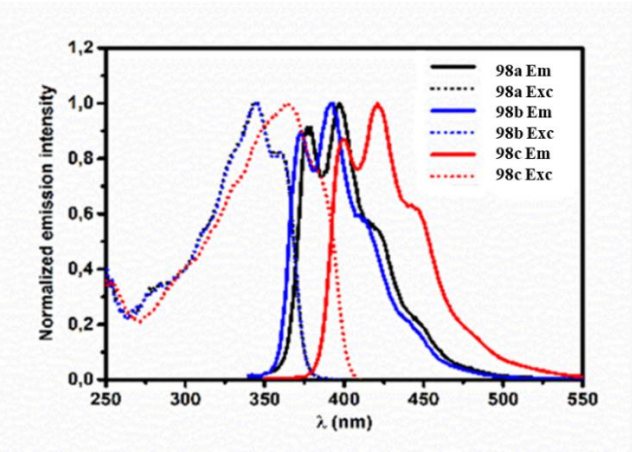

Figure 52: UV emission spectra. Normalised emission (solid lines, λ_{exc} = 310 nm) and excitation spectra (dotted lines) of **98a** (λ_{em} = 420 nm), **98b** (λ_{em} = 420 nm) and **98c** (λ_{em} = 433 nm) in DCM solution (10^{-5} M) at room temperature.

A small red Stokes shift was registered, suggesting that the excited state is very little distorted and the excited state emission lifetimes are mono-exponential for all the analysed compounds in the order of 1.1–1.8 ns. It is worth underlining that the photoluminescent quantum yields (PLQY) in solution of **98a**, **98b,** and **98c** were found to be 80, 49, and 71 %, respectively, that are remarkably high.

6.3.2 Electrochemical studies

The electrochemical properties of **98a**–**f**, **103**, **104a**, **105**, **107** and **112** were systematically investigated by cyclic voltammetry (CV) and were discussed comparing the CV features of the parent BDT (**56a**) reported in *Table 15*. The oxidation and reduction potential values provided information on the HOMO/LUMO levels of these molecules, from which the energy gap values were calculated according to the equations listed in *Table 15*. These compounds were found to be soluble in acetonitrile at 0.001 M concentration, so the CV measurements were carried out using this solvent along with tetrabutylammonium hexafluorophosphate ($TBAPF_6$) as supporting electrolyte.

Table 15. Spectroscopic and cyclovoltammetric features of **98a**–**f**, **103**, **104a**, **105**, **107** and **112** and BDT **56a** with corresponding HOMO/LUMO energy levels and gaps. CVs were recorded on GC electrode at 0.2 V s^{-1} potential scan rate in CH_3CN + $TBAPF_6$ 0.1 M. Potential values were referred to the intersolvental redox couple $Fc^+|Fc$.

	λ_{max} (nm) (log ε)[a]	$E_{p,\,Ia}$ /V	$E_{p,\,Ic}$ /V	[b]E_{HOMO} (max) / eV	[c]E_{LUMO} (max) / eV	E_G (max) /eV
56a[264]	289 (4.32)	1.10	–2.99	–5.90	–1.81	4.09
98a	347 (4.56)	0.94	–2.60	–5.74	–2.20	3.54
98b	344 (4.59)	1.26	–2.18	–6.06	–2.62	3.54
98c	367 (4.58)	1.18	–2.11	–5.98	–2.69	3.29
98d	352 (4.34)	0.64	–2.87	–5.44	–1.93	3.51
98e	394 (4.42)	1.34	–1.49	–6.14	–3.31	2.83
98f	368 (4.59)	1.02	–2.16	–5.82	–2.64	3.18
103	382 (4.71)	0.58	–2.19	–5.38	–2.61	2.77
104a	382 (4.54)	0.80	–2.24	–5.60	–2.56	3.04
105	369 (4.69)	0.75	–2.46	–5.55	–2.34	3.21
107	357 (4.57)	1.06	–2.36	–5.86	–2.44	3.42
112	353 (4.58)	0.73	–2.78	–5.53	–2.02	3.51

[a] Molar absorptivities in diluted DCM solutions (ca 2.5×10^{-5} M). [b] E_{LUMO}(eV) = –1e × [($E_{p,Ic}$/V(Fc^+|Fc) + 4.8 V(Fc^+|Fc *vs* zero)] (*maxima criterion*). [c] E_{HOMO} (eV) = –1e × [($E_{p,Ia}$ /V(Fc^+|Fc) + 4.8 V(Fc^+|Fc *vs* zero)] (*maxima criterion*).

All disubstituted BDTs showed energy gap values lower than that of parent BDT **56a**, in agreement with their optical behaviour. Indeed, the λ_{max} redshift and the subsequent decrease of the difference between HOMO/LUMO levels are ascribed to the better conjugation induced by the aryl, alkenyl or alkynyl substituents in the α-positions of the BDT skeleton. Compound **98a**, that have phenyl pendants, displayed the highest energy gap of the studied series, confirming worst conjugation related to the insertion of phenyl groups instead of thienyl ones. Besides, the electron withdrawing or donating substituents in the *para* position of the phenyl groups should tune the HOMO energy levels. More in detail, a linear relationship E_{HOMO} *vs* σ_{para} Hammett constants (*Figure 53*) for compounds **98a** (selected as reference), **98d** and **98f** was found. On the contrary, **98e** displayed a completely different reactivity according to the fact that the ingress of the electrons is on the nitro group.

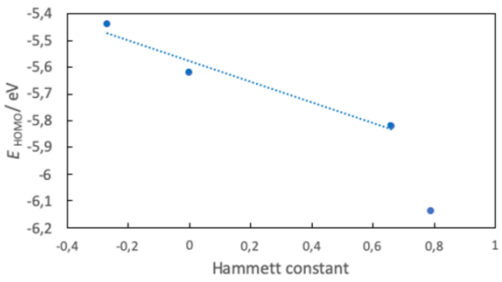

Figure 53: Correlation between E_{HOMO} values and Hammet constants for compounds **98a**, **98d**, **98f** and **98e**.

The reduction of these molecules became easier as the electron-withdrawing character of the substituent increases. On the other hand, oxidations resulted more difficult with related potential values following the sequence: OMe <Ph <CN< NO_2.

6.3.3 Preliminary electrooligomerization studies of 98b and 98c

The ability for electrooxidative deposition of monomers **98b** and **98c** was preliminary investigated by potentiodynamic electrodepositions, cycling around the first oxidation peak on glassy carbon electrode in CH_3CN + $TBAPF_6$ 0.1 M, in a three-electrode minicell. Performing preparative potentiodynamic electrodepositions cycling around the first oxidation peak of compound **98b**, a practically null formation of electroactive product was observed on the electrode surface. This behaviour could be attributed to the α–β connection between the thienyl ring and the BDT unit, that induces a more three-dimensional and rigidity character of the starting monomer **98b**. On the contrary, a virtually unlimited electrodeposition could be achieved using derivative **98c** (*Figure 54*, left). The electroactive layers appeared stable upon repeated *stability cycles*, performed cycling around the first oxidation peak in monomer free solution (*Figure 54*, *right*).

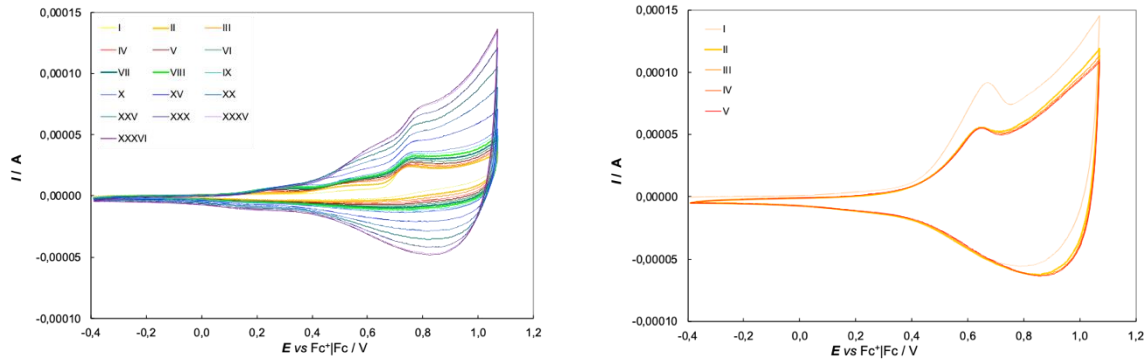

Figure 54: Electrodeposition experiments from **98c** by potential cycling on glassy carbon electrode, at constant 1 mM monomer concentration, with 0.1 M $TBPF_6$ supporting electrolyte and at 0.2 V s^{-1} potential scan rate, as a function of the total number of potential cycles (36) (left). Five stability cycles in monomer free solution for deposited film of **98c** (right).

The oligomeric pattern was similar to those obtained for the oligomerization of common conjugated polythiophenes. Indeed, the oligomerization of **98c** presumably occurs on the two α-homotopic positions of the thiophenes connected to the BDT unit.

A MALDI-TOF analysis of the material electrodeposited after the electrooligomerization of **98c** was performed, and it showed the presence of a mixture of oligomers including dimeric, trimeric, tetrameric and pentameric species in the film (*Figure 55*).

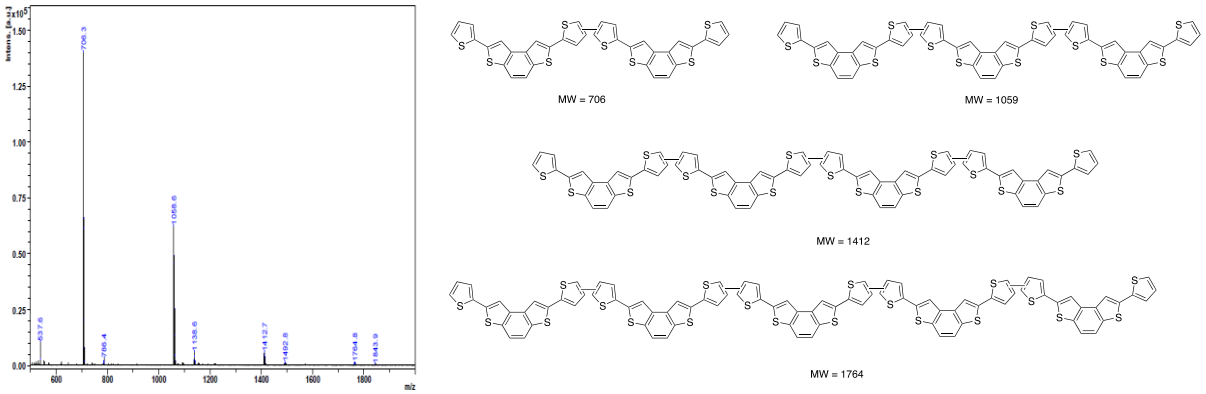

Figure 55: MALDI-TOF spectrum (left) and chemical structure of obtained homooligomers (right).

Finally, a preliminary investigation on the electrochromic switching ability of the oligomers obtained from **98c** was performed. In particular, we found that the colour of the solution of the oligomers changed from a yellow in the neutral state of the film (*Figure 56*, left) to blue when the applied potential was gradually increased from 0.5 V *vs* $Fc^+|Fc$ to 1.0 V *vs* $Fc^+|Fc$ (*Figure 56*, right), as consequence of the changes of the internal electronic structure of the film. Indeed, when the film was fully oxidised to 1.0 V the oligomer colour switched to blue.

Figure 56: Film of **98c** in neutral (yellow, left) and in oxidative (blue, right) phase.

This represents a striking feature of these systems since electroactive moieties with electrochromic switching ability between the oxidised and neutral states have potential applications in smart cards or electronic identification tags. Further studies will be carried out to investigate the optical contrast and the coloration efficiency of this polymer, and to evaluate its potentialities for applications in electronic identification tags, smart cards, and switching element in flat panel displays.

6.4 Conclusions and perspectives

In summary, a general procedure was developed for the synthesis of properly functionalised BDTs **98**, **101**, **91** and **112** (up to 79% yield) by palladium catalysed ligand-free Suzuki-Miyaura reaction between mono- or dihalide BDTs as electrophiles and (hetero)arylboron species as nucleophilic partners using eutectic mixture Gly/ChCl in 2/1 ratio as an environmentally benign and biodegradable unconventional reaction media, under air and mild conditions. Furthermore, alkenyl and alkynyl trifluoroborate salts were also used for the first time as nucleophilic partners in DES and alkenyl- and alkynyl substituted systems **103** and **107** were prepared in moderate to good yields (44–74% yield).

A systematic study on the optical and electronic properties of these molecules was performed by absorption measurements and cyclic voltammetry experiments, respectively, and the results were in agreement with those previously reported for similar functionalised BDTs, and it corroborated the peculiar features of BDT systems to use in organic electronics. Of note, some derivatives display photoluminescent quantum yields (PLQY) in solution significantly high (up to 80%).

On the other hand, these molecules are useful platform from which more complex structures could be prepared by conveniently modification of functional groups on the phenyl pendants (*e.g.* -OMe, -CN, -NO_2,) as well as by polymerisation of thienyl-substituted BDT. This latter study also confirmed that properly functionalised BDT scaffolds are suitable co-monomers for oligomers displaying electrochromic properties.

Finally, this work demonstrates that the use of DESs represents a valuable option in cross coupling reactions involving also π-conjugated (hetero)aryl systems of relevance in the field of the material sciences, and in the future palladium-catalysed cross coupling reactions (e.g. Suzuki coupling or carboannulation of internal alkynes) employed in the synthesis of thiahelicene scaffolds (see *Chapter 1*, *2* and *5*) will be studied in eco-friendly media such as DES.

6.5 Experimental part

6.5.1 General methods. All commercially available reagents and solvents were used without further purification. 2,7-Dibromo-benzo[1,2-*b*:4,3-*b'*]dithiophene (**92a**),[181] 2,7-diiodo-benzo[1,2-*b*:4,3-*b'*]dithiophene (**92b**),[160] 2,7-dibromo-4,5-disopropylbenzo[1,2-*b*:4,3-*b'*]ditiophene (**92c**),[161] 2-bromo-benzo[1,2-*b*:4,3-*b'*]dithiophene (**49b**),[180] 2-iodo-benzo[1,2-*b*:4,3-*b'*]dithiophene (**49a**)[160] were synthesized as previously reported. The Deep Eutectic Solvents urea/choline chloride (ChCl) (2:1 mol/mol) and glycerol (Gly)/ChCl (2:1 mol/mol)] were prepared by heating under stirring at 60 °C for 10 min the corresponding individual components until a clear solution was obtained.[276] Thin-layer chromatography (TLC) was performed with Aldrich silica gel 60 F254 precoated plates, and plates were visualized with short-wave UV light (254 and 366 nm). Column chromatography was carried out with Aldrich silica gel (70-230 mesh). Melting points were determined with a Büchi Melting Point B-540 apparatus and are uncorrected. UV spectra were recorded with a 500 Evolution Thermo Electron Corporation spectrophotometer. The ^{1}H and ^{13}C NMR spectra were recorded in $CDCl_3$ or CD_2Cl_2 at 25 °C using a Bruker AC-300 and Bruker AC-600 MHz spectrometer. Chemical shifts were reported relative to the residual protonated solvent resonances (^{1}H: δ = 7.26 ppm, ^{13}C: δ = 77.00 for $CDCl_3$; ^{1}H: δ = 5.32 ppm for CD_2Cl_2). The chemical shifts are given in ppm and coupling constants in Hz. High Resolution Electron Ionization (HR EI) mass spectra were recorded on a FISONS - Vg Autospec- M246 spectrometer. The purity of compounds was evaluated by Reverse-Phase RP-HPLC analyses that were performed on Agilent 1100 series system, equipped with DAD 300 analyzer, using the analytical column Zorbax Eclipse XDB-C18 (150 mm x 4.6 mm 5 µm).

Electrochemical studies. Cyclic voltammetry measurements were carried out in acetonitrile (CH_3CN) as solvent and tetrabutylammonium hexafluorophosphate ($TBAPF_6$) 0.1 M as supporting electrolyte in a three electrode minicell on a glassy carbon (GC) support as working electrode at potential scan rates of 0.2 Vs^{-1}, with ohmic drop compensation. The counter electrode was a platinum wire, and a saturated calomel electrode was used as reference one inserted in a jacket filled with solvent + supporting electrolyte 0.1 M to prevent water and chloride leakage. The experiments were carried out with an AUTOLAB PGSTAT 128 potentiostat of EcoChemie (Utrecht, The Netherlands) run by a PC with the GPES 4.9 software of the same manufacturer. Peak potential values have been normalised vs the Fc+|Fc redox couple (the intersolvental redox potential couple currently recommended by IUPAC), having a redox potential of 0.39 V (in CH_3CN) vs the operating SCE reference electrode. The matrix-assisted laser desorption/ionization (MALDI) spectrum of material electrodeposited by electrooligomerization of **98c** was recorded with a MALDI-TOF/TOF Autoflex III-Bruker Daltonics, using dithranol as matrix.

6.5.2 Synthesis and characterization of functionalised BDT derivatives.

General procedure for the synthesis of disubstituted BDT derivatives. To a mixture of boron species **69** (0.2 mmol, 2 eq) in Gly/ChCl in ratio 2/1 (1 g), were added dihalogenated benzodithiophenes **92a–c** (0.1

mmol, 1 eq), $Pd(OAc)_2$ (0.3 mg, 0.001 mmol, 1 mol%) as catalyst and Na_2CO_3 (22 mg, 0.2 mmol, 2 eq) as base. The resulting suspension, monitored by TLC and RP-HPLC of the reaction mixture diluted in CH_2Cl_2, was stirred at 60 ºC under air for 6 or 72 hours. After being cooled to room temperature, the reaction mixture was poured into water (10 mL) and the aqueous layer was extracted with CH_2Cl_2 (3 × 10 mL). The collected organic phases were dried over Na_2SO_4 and the solvent was removed under reduced pressure to afford the crude products. The latter were purified by column chromatography on silica gel (hexane/CH_2Cl_2) to provide the desired diarylsubstituted benzodithiophenes.

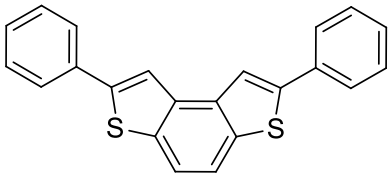

2,7-diphenylbenzo[1,2-*b*:4,3-*b'*]ditiophene (98a). The crude reaction product obtained from the Pd-catalysed Suzuki reaction of **92a** with **69c** was purified by column chromatography on silica gel with a mixture of hexane and CH_2Cl_2 (9:1) as eluent to afford **98a** (27 mg, 79%) as yellow solid. M.p. (pentane) 164–165 °C. UV/Vis (CH_2Cl_2) λ_{max} (log ε): 347 nm (4.56). ^{1}H NMR (600 MHz, $CDCl_3$): δ = 7.95 (s, 2H), 7.79 (d, *J* = 7.6 Hz, 4H), 7.75 (s, 2H), 7.46 (t, *J* = 7.4 Hz, 4H), 7.37 (t, *J* = 7.4 Hz, 2H). ^{13}C NMR (150 MHz, $CDCl_3$) δ: 144.7 (Cq), 136.3 (Cq), 135.5 (Cq), 134.3 (Cq), 129.0 (CH), 128.3 (CH), 126.5 (CH), 118.6 (CH), 117.5 (CH). HRMS-EI: calcd for $C_{22}H_{14}S_2$ $[M]^+$: 342.0537, found: 342.0520.

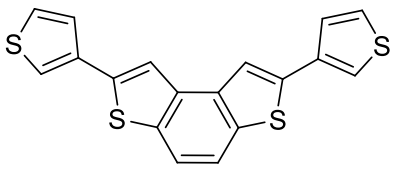

2,7-di(thiophen-3-yl)benzo[1,2-*b*:4,3-*b'*]ditiophene (98b). The crude reaction product obtained from the Pd-catalysed Suzuki reaction of **92a** with **69f** was purified by chromatography on silica gel with a mixture of hexane and CH_2Cl_2 (9:1) as eluent to afford **98b** (25 mg, 71%) as yellow solid. M.p. (hexane/CH_2Cl_2) 209–210 °C. UV/Vis (CH_2Cl_2) λ_{max} (log ε): 344 nm (4.59). ^{1}H NMR (600 MHz, $CDCl_3$) δ: 7.79 (s, 2H), 7.71 (s, 2H), 7.57 (bs, 2H), 7.49 (d, *J* = 4.9 Hz, 2H), 7.43 (m, 2H). ^{13}C NMR (75 MHz, $CDCl_3$) δ: 139.4 (Cq), 135.8 (Cq), 135.7 (Cq), 135.2 (Cq), 126.7 (CH), 126.1 (CH), 121.2 (CH), 118.4 (CH), 117.5 (CH). HRMS-EI: calcd for $C_{18}H_{10}S_4$ $[M]^+$: 353.9665, found: 353.9651.

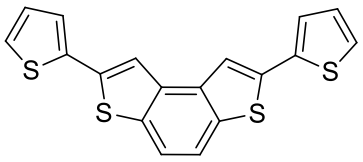

2,7-di(thiophen-2-yl)benzo[1,2-*b*:4,3-*b'*]ditiophene (98c). The crude reaction product obtained from the Pd-catalysed Suzuki reaction of **92a** with **69d** was purified by chromatography on silica gel with hexane as eluent to afford **98c** (21 mg, 59%) as yellow solid. M.p. (hexane/CH_2Cl_2) 185–187 °C. UV/Vis (CH_2Cl_2) λ_{max} (log ε): 367 nm (4.58). ^{1}H NMR (600 MHz, $CDCl_3$) δ: 7.75 (s, 2H), 7.68 (s, 2H), 7.34–7.32 (m, 4H), 7.10–7.08 (m, 2H). ^{13}C NMR (150 MHz, $CDCl_3$) δ: 137.8 (Cq), 137.4 (Cq), 136.0 (Cq), 135.1 (Cq), 128.0 (CH), 125.5 (CH), 125.1 (CH), 118.5 (CH), 117.9 (CH). HRMS-EI: calcd for $C_{18}H_{10}S_4$ $[M]^+$: 353.9665, found: 353.9656.

2,7-bis(4-methoxyphenyl)benzo[1,2-*b*:4,3-*b'*]ditiophene (98d). The crude reaction product obtained from the Pd-catalysed Suzuki reaction of **92a** with **69h** was purified by chromatography on silica gel with a mixture of hexane and CH_2Cl_2 (9:1) as eluent to afford **98d** (26 mg, 66%) as yellow solid. M.p. (hexane) 238–240 °C. UV/Vis (CH_2Cl_2) λ_{max} (log ε): 352 nm (4.34). ^{1}H NMR (300 MHz, $CDCl_3$) δ: 7.81 (s, 2H), 7.73–7.70 (m, 6H), 6.99 (d, *J* = 8.7 Hz, 4H), 3.88 (s, 6H, OCH_3). ^{13}C NMR (75 MHz, $CDCl_3$) δ: 159.8 (Cq), 144.5 (Cq), 135.9 (Cq), 135.5 (Cq), 127.7 (CH), 127.2 (Cq), 118.2 (CH), 116.4 (CH), 114.4 (CH), 55.4 (CH_3). HRMS-EI: calcd for $C_{24}H_{18}O_2S_2$ $[M]^+$: 402.0748, found: 402.0762.

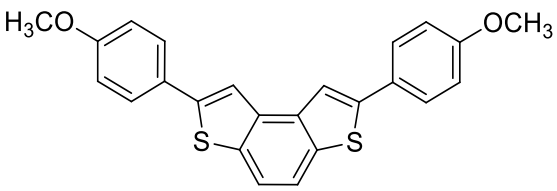

2,7-bis(4-nitrophenyl)benzo[1,2-*b*:4,3-*b'*]ditiophene (98e). The crude reaction product obtained from the Pd-catalysed Suzuki reaction of **92a** with **69j** was purified by chromatography on silica gel with CH_2Cl_2 as eluent to afford **98e** (14 mg, 32%) as orange solid. M.p. (hexane/CH_2Cl_2) 301 °C (dec.). UV/Vis (CH_2Cl_2) λ_{max} (log ε): 394 nm (4.42). ^{1}H NMR (300 MHz, $CDCl_3$) δ: 8.34 (d, *J* = 8.9 Hz, 4H), 8.13 (s, 2H), 7.94 (d, *J* = 8.9 Hz, 4H), 7.85 (s, 2H). HRMS-EI: calcd for $C_{22}H_{12}N_2O_4S_2$ $[M]^+$: 432.0238, found: 432.0260. The ^{13}C NMR spectrum was not recorded for **98e** because its low solubility in the common deuterated solvents.

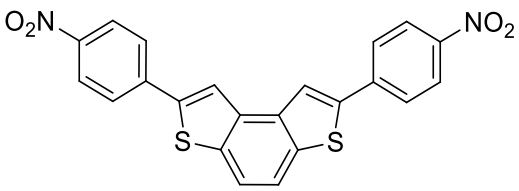

4,4'-(benzo[1,2-*b*:4,3-*b*']dithiophene-2,7-diyl)dibenzonitrile (98f). The crude reaction product obtained from the Pd-catalysed Suzuki reaction of **92a** with **69k** was purified by chromatography on silica gel with a mixture of hexane and CH_2Cl_2 (60:40) as eluent to afford **98f** (10 mg, 26%) as orange solid. M.p. (hexane/CH_2Cl_2) 291–293 °C. UV/Vis (CH_2Cl_2) λ_{max} (log ε): 368 nm (4.59). ^{1}H NMR (300 MHz, $CDCl_3$) δ: 8.06 (s, 2H), 7.88 (d, *J* = 8.4 Hz, 4H), 7.83 (s, 2H), 7.75 (d, *J* = 8.3 Hz, 4H). ^{13}C NMR (75 MHz, $CDCl_3$) δ: 142.7 (Cq), 138.5 (Cq), 137.4 (Cq), 135.5 (Cq), 132.9 (CH), 126.8 (CH), 119.6 (CH), 119.5 (CH), 118.6 (Cq), 111.6 (Cq). HRMS-EI: calcd for $C_{24}H_{12}N_2S_2$ $[M]^+$: 392.0442, found: 392.0442.

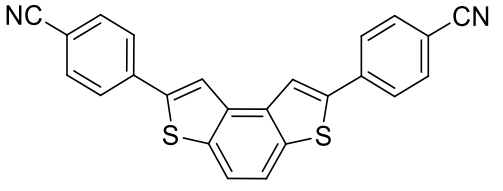

2,7-di((*E*)-styryl)benzo[1,2-*b*:4,3-*b'*]dithiophene (103). The crude reaction product obtained from the Pd-catalysed Suzuki reaction of **92b** with **102** was purified by chromatography on silica gel with a mixture of hexane and CH_2Cl_2 (90:10) as eluent to afford **103** (29 mg, 74%) as orange solid. M.p. (hexane/CH_2Cl_2) 253–254 °C. UV/Vis (CH_2Cl_2) λ_{max} (log ε): 382 nm (4.71). ^{1}H NMR

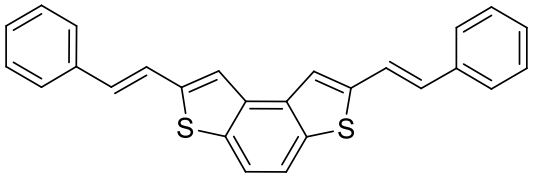

(600 MHz, $CDCl_3$) δ: 7.69 (s, 2H), 7.59 (s, 2H), 7.54 (d, *J* = 7.5 Hz, 4H), 7.40–7.37 (m, 6H), 7.29 (t, *J* = 7.2 Hz, 2H), 7.06 (d, *J* = 16 Hz, 2H, C=C). ^{13}C NMR (75 MHz, $CDCl_3$) δ: 143.5 (Cq), 136.6 (Cq), 135.8 (Cq), 134.9 (Cq), 130.8 (CH), 128.8 (CH), 128.1 (CH), 126.6 (CH), 122.2 (CH), 121.2 (CH), 118.9 (CH). HRMS-EI: calcd for $C_{26}H_{18}S_2$ $[M]^+$: 394.0850, found: 394.0835.

(*E*)-2-bromo-7-styrylbenzo[1,2-*b*:4,3-*b'*]dithiophene (104a). The crude reaction product obtained from the Pd-catalysed Suzuki reaction of **92a** with **102** was purified by chromatography on silica gel with a mixture of hexane and CH_2Cl_2 (90:10) as eluent to afford **104a** (17 mg, 46%) as colourless solid. M.p. (hexane/CH_2Cl_2) 177–179 °C. UV/Vis (CH_2Cl_2) λ_{max} (log ε): 382 nm (4.54). ^{1}H NMR (300 MHz, $CDCl_3$) δ: 7.69 (d, *J* = 8.5 Hz, 1H), 7.65 (s, 1H), 7.62 (d, *J* = 8.5 Hz, 1H), 7.53 (m, 3H), 7.40–7.35 (m, 3H), 7.30 (t, *J* = 7.3 Hz, 1H), 7.05 (d, *J* = 16 Hz, 1H, C=C). ^{13}C NMR (75 MHz, $CDCl_3$) δ: 137.4 (CH), 132.8 (CH), 131.1 (Cq), 129.2 (CH), 128.8 (CH), 128.6 (CH), 128.1 (Cq), 127.5 (CH), 126.6 (CH), 126.4 (CH), 124.8 (Cq), 122.0 (Cq), 120.8 (Cq), 118.7 (Cq), 118.1 (Cq). HRMS-EI: calcd for $C_{18}H_{11}BrS_2$ $[M]^+$: 369.9486, found: 369.9484.

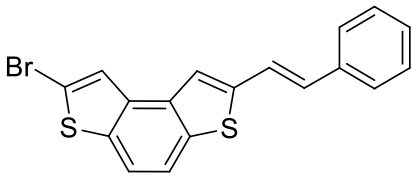

2,7-bis(phenylethynyl)benzo[1,2-*b*:4,3-*b*']dithiophene (107). The crude reaction product obtained from the Pd-catalysed Suzuki reaction of **92b** with **106** was purified by chromatography on silica gel with a mixture of hexane and CH_2Cl_2 (95:5) as eluent to afford **107** (17 mg, 44%) as a yellow solid. M.p. (hexane/CH_2Cl_2) 178–179 °C. UV/Vis (CH_2Cl_2) λ_{max} (log ε): 357 nm (4.57). ^{1}H NMR (300 MHz, CD_2Cl_2) δ: 7.89 (s, 2H), 7.79 (s, 2H), 7.62–7.56 (m, 4H), 7.43–7.38 (m, 6H). ^{13}C NMR (75 MHz, $CDCl_3$) δ: 137.5 (Cq), 134.0 (Cq), 131.6 (CH), 128.8 (CH), 128.5 (CH), 126.5 (CH), 124.0 (Cq), 122.5 (Cq), 119.3 (CH), 95.4 (C≡C), 82.9 (C≡C). HRMS-EI: calcd for $C_{26}H_{14}S_2$ $[M]^+$: 390.0537; found: 390.0534.

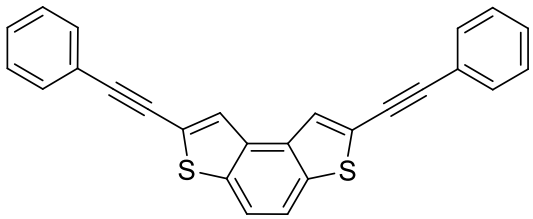

2,7-diphenyl-4,5-disopropylbenzo[1,2-*b*:4,3-*b'*]ditiophene (112). The crude reaction product obtained from the Pd-catalysed Suzuki reaction of **92c** with **69c** was purified by chromatography on silica gel with a mixture of hexane and CH_2Cl_2 (95:5) as eluent to afford **112** (5 mg, 12%) as a yellow solid. M.p. (pentane) 136–138 °C. UV/Vis (CH_2Cl_2) λ_{max} (log ε): 353 nm (4.58). ^{1}H NMR (300 MHz, CDC_3) δ: 7.91 (s, 2H, Het), 7.79 (d, *J* = 7.5 Hz, 4H, Ph), 7.45 (t, *J* = 7.8 Hz, 4H, Ph), 7.34 (t, *J* = 7.4 Hz, 2H, Ph), 2.99 (m, 4H, CH_2), 1.83 (m, 4H, CH_2), 1.13 (t, *J* = 7.3 Hz, 6H, CH_3). ^{13}C NMR (75 MHz, $CDCl_3$) δ: 143.1 (Cq), 138.5 (Cq), 134.6 (Cq), 133.7 (Cq), 130.3 (Cq), 128.9 (CH), 128.0 (CH), 126.3 (CH), 118.0 (CH), 34.4 (CH_2), 23.1 (CH_2), 14.7 (CH_3). HRMS-EI: calcd for $C_{28}H_{26}S_2$ $[M]^+$: 426.1476; found: 426.1477.

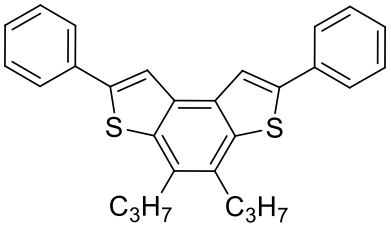

General procedure for the synthesis of 105, 101 and 91. To a mixture of boron species (0.1 mmol, 1 eq) in Gly/ChCl in ratio 2/1 (1 g), benzodithiophene **104a**, **49b** or **55a** (0.1 mmol, 1 eq), $Pd(OAc)_2$ (0.3 mg, 0.001 mmol, 1 mol%) and Na_2CO_3 (11 mg, 0.1 mmol, 1 eq) were added. The resulting suspension was stirred at 60 ºC under air for 72 hours. After being cooled to room temperature, the reaction mixture was poured into water (10 mL) and the aqueous layer was extracted with CH_2Cl_2 (3 × 10 mL). The combined organic phases were dried with Na_2SO_4 and the solvent was removed under reduced pressure. The crude product was purified by chromatography on silica gel (hexane/CH_2Cl_2) to provide the desired functionalised benzodithiophene **105**, **101** or **91**.

(*E*)-2-phenyl-7-styrylbenzo[1,2-*b*:4,3-*b'*]dithiophene (105). The crude reaction product obtained from the Pd-catalysed Suzuki reaction of **104a** with **69c** was purified by chromatography on silica gel with a mixture of hexane and CH_2Cl_2 (95:5) as eluent to afford **104a** (20 mg, 40%) and **105** (10 mg, 27%) as a yellow solid. M.p. (hexane/CH_2Cl_2) 192−194 °C. UV/Vis (CH_2Cl_2) λ_{max} (log ε): 369 nm (4.69). ^{1}H NMR (300 MHz, $CDCl_3$) δ: 7.87 (s, 1H), 7.79–7.68 (m, 2H), 7.65 (s, 1H), 7.54 (d, *J* = 7.4 Hz, 2H, Ph), 7.48–7.29 (m, 7H), 7.06 (d, *J* = 16 Hz, 1H, C=C).^{13}C NMR (75 MHz, $CDCl_3$) δ: 144.9 (Cq), 143.4 (Cq), 136.7 (Cq), 135.4 (Cq), 135.8 (Cq), 135.4 (Cq), 135.1 (Cq), 134.3 (Cq), 130.7 (CH), 129.0 (CH), 128.8 (CH), 128.3 (CH), 128.1 (CH), 126.6 (CH), 126.5 (CH), 122.2 (CH), 121.2 (CH), 119.0 (CH), 118.6 (CH), 117.5 (CH). HRMS-EI: calcd for $C_{24}H_{16}S_2$ $[M]^+$: 368.0693; found: 368.0692.

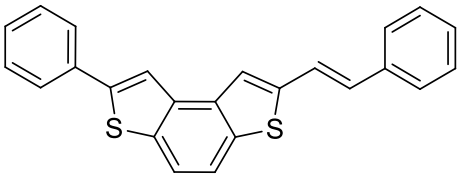

2-phenylbenzo[1,2-*b*:4,3-*b*']dithiophene (101). The crude product obtained from the Pd-catalysed Suzuki reaction of **49b** with **69c** was purified by chromatography on silica gel with a mixture of hexane and CH_2Cl_2 (95:5) as eluent to afford **101** (16 mg, 61%) as a colourless solid. ^{1}H NMR (300 MHz, CDC_3) δ: 7.93 (s, 1H), 7.83–7.75 (m, 4H), 7.73 (d, *J* = 5.4 Hz, 1H), 7.58 (d, *J* = 5.4 Hz, 1H), 7.46 (t, *J* = 7.5 Hz, 2H), 7.36 (t, *J* = 7.4 Hz, 1H). ^{13}C NMR (75 MHz, $CDCl_3$) δ: 145.7 (Cq), 136.7 (Cq), 136.1 (Cq), 135.6 (Cq), 134.5 (Cq), 134.4 (Cq), 129.0 (CH), 128.2 (CH), 126.6 (CH), 126.5 (CH), 121.8 (CH), 118.8 (CH), 118.5 (CH), 117.6 (CH).

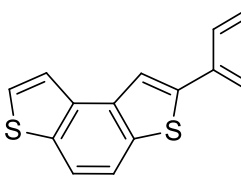

1-phenylbenzo[1,2-*b*:4,3-*b*']dithiophene (91). The crude reaction product obtained from the Pd-catalysed Suzuki reaction of **55a** with **69c** was purified by chromatography on silica gel with hexane as eluent to afford **91** (17 mg, 65%) as colourless solid. ^{1}H NMR (300 MHz, $CDCl_3$): δ = 8.69 (d, *J* = 5.5 Hz, 1H), 7.89 (d, *J* = 8.7 Hz, 1H), 7.79 (d, *J* = 8.6 Hz, 1H), 7.62 (d, *J* = 5.5 Hz, 1H), 7.54 (s, 1H). ^{13}C NMR (75 MHz, $CDCl_3$): δ = 138.8 (Cq), 137.8 (Cq), 137.6 (Cq), 137.3 (Cq), 134.5 (Cq), 133.1 (Cq), 129.8

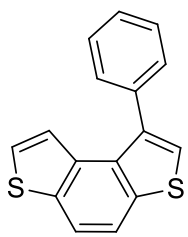

(CH), 128.4 (CH), 127.9 (CH), 125.5 (CH), 124.2 (CH), 122.3 (CH), 119.1 (CH), 119.1 (CH). HRMS-EI: calcd for $C_{16}H_{10}S_2$ $[M]^+$: 226.3806; found: 226.0229.

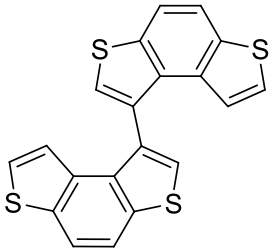

Synthesis of dimer 54a. To a mixture of bis(pinacolato)diboron (17 mg, 0.065 mmol, 0.65 eq) in Gly/ChCl in ratio 2/1 (1 g), bromide **55a** (27 mg, 0.1 mmol, 1 eq), $Pd(OAc)_2$ (0.3 mg, 0.001 mmol, 1 mol%) and Na_2CO_3 (22 mg, 0.2 mmol, 2 eq) were added. The resulting suspension was stirred at 60 ºC under air for 72 h and then cooled to room temperature. After the addition of water (10 mL), the aqueous layer was extracted with CH_2Cl_2 (3 × 10 mL), and the combined organic phases were dried over Na_2SO_4 and the solvent was removed under reduced pressure. The crude product was purified by chromatography on silica gel (hexane) to give **54a** (9 mg, 46%) as a colourless solid. ^{1}H NMR (300 MHz, $CDCl_3$): δ = 7.93 (d, J = 8.7 Hz, 2H), 7.89 (d, J = 8.7 Hz, 2H), 7.58 (s, 2H), 7.09 (d, J = 5.5 Hz, 2H), 6.49 (d, J = 5.5 Hz, 2H). ^{1}H NMR spectrum was in agreement with that previously reported in *Chapter 1*.

6.5.3 Cyclic voltammetry patterns of compounds 98a–f, 103, 104a, 105, 107 and 112.

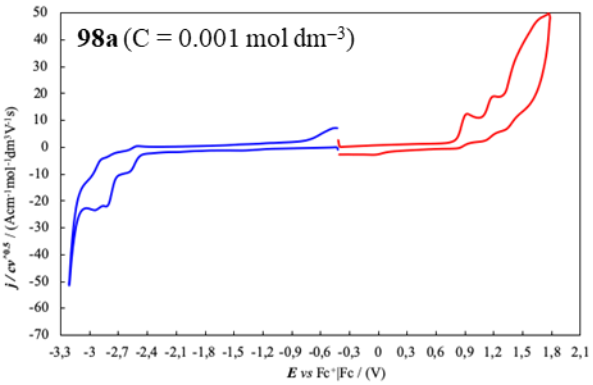

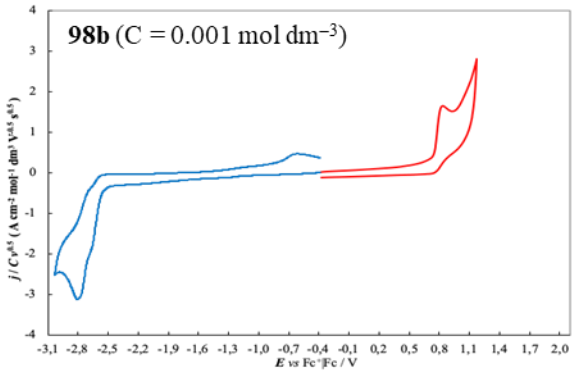

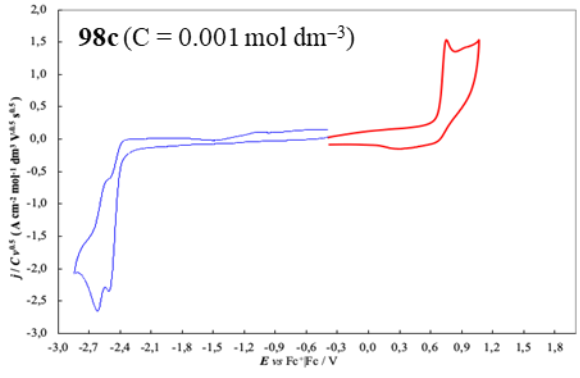

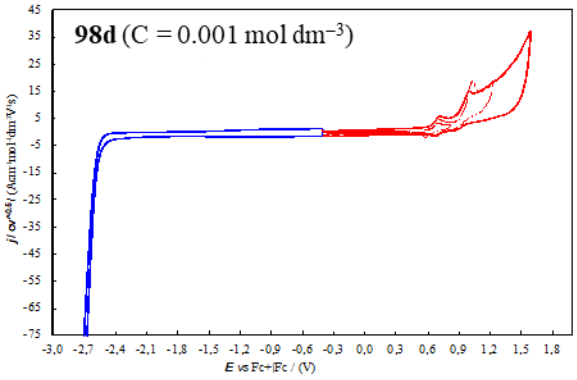

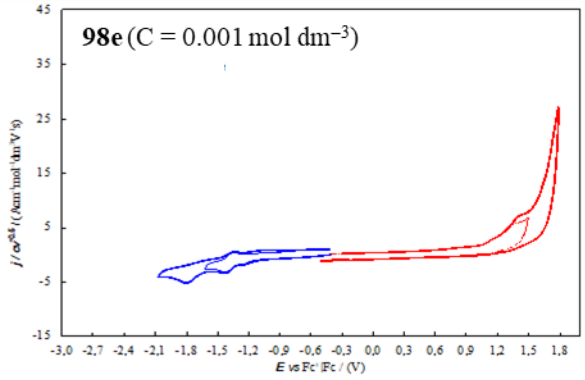

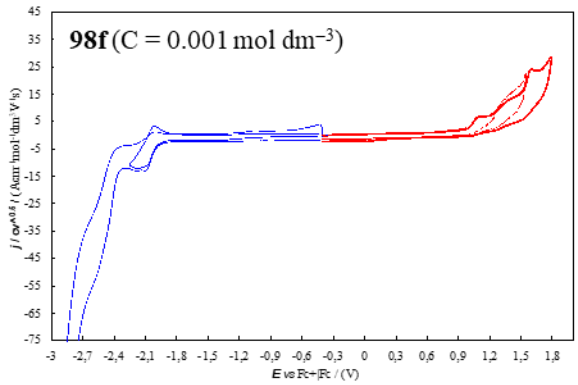

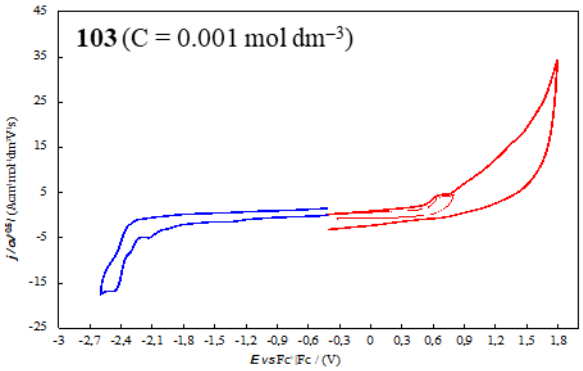

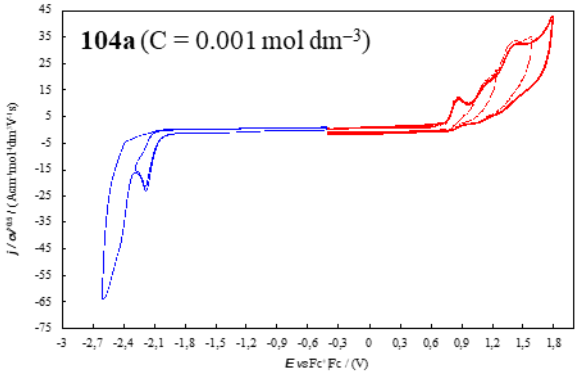

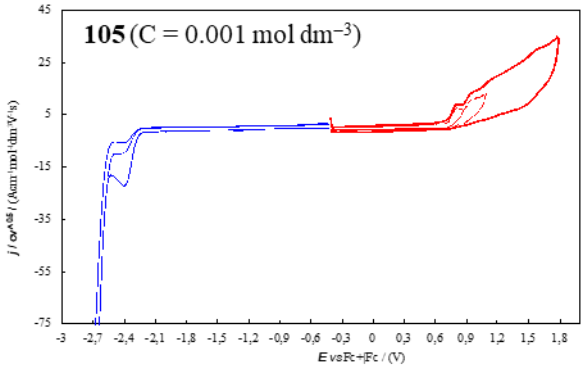
105 (C = 0.001 mol dm−3)
E vs Fc+|Fc / (V)

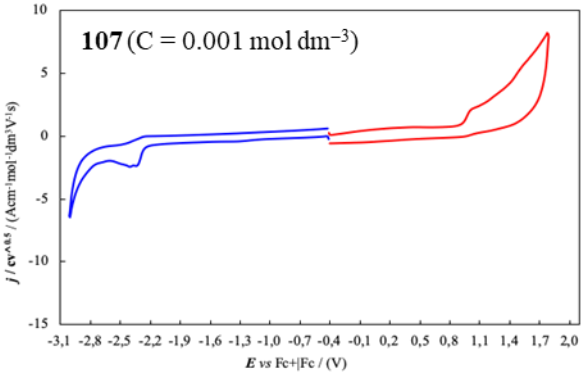
107 (C = 0.001 mol dm−3)
E vs Fc+|Fc / (V)

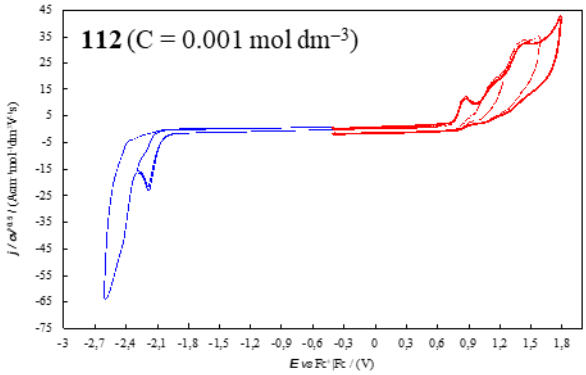
112 (C = 0.001 mol dm−3)
E vs Fc+|Fc / (V)

References

1 M. Stępień, E. Gońka, M. Żyła and N. Sprutta, *Chem. Rev.*, 2017, **117**, 3479–3716.
2 M. Ball, Y. Zhong, Y. Wu, C. Schenck, F. Ng, M. Steigerwald, S. Xiao and C. Nuckolls, *Acc. Chem. Res.*, 2015, **48**, 267–276.
3 Y. Shen and C. F. Chen, *Chem. Rev.*, 2012, **112**, 1463–1535.
4 N. Hoffmann, *J. Photochem. Photobiol. C Photochem. Rev.*, 2014, **19**, 1–19.
5 M. S. Newman and D. Lednicer, *J. Am. Chem. Soc.*, 1956, **78**, 4765–4770.
6 J. Meisenheimer and K. Witte, *Berichte der Dtsch. Chem. Gesellschaft*, 1903, **36**, 4153–4164.
7 R. H. Martin, *Angew. Chemie Int. Ed. English*, 1974, **13**, 649–660.
8 I. Sato, R. Yamashima, K. Kadowaki, J. Yamamoto, T. Shibata and K. Soai, *Angew. Chemie - Int. Ed.*, 2001, **40**, 1096–1098.
9 R. S. Cahn, C. Ingold and V. Prelog, *Angew. Chemie Int. Ed. English*, 1966, **5**, 385–415.
10 M. B. Groen and H. Wynberg, *J. Am. Chem. Soc.*, 1971, **93**, 2968–2974.
11 K. P. Meurer and F. Vögtle, in *Organic Chemistry*, 2006, 1–76.
12 D. A. Lightner, D. T. Hefelfinger, T. W. Powers, G. W. Frank and K. N. Trueblood, *J. Am. Chem. Soc.*, 1972, **94**, 3492–3497.
13 W. H. Laarhoven and W. J. C. Prinsen, *Top. Curr. Chem.*, 1984, **125**, 63–130.
14 F. H. Allen, O. Kennard, D. G. Watson, L. Brammer, A. G. Orpen and R. Taylor, *J. Chem. Soc. Perkin Trans. 2*, 1987, 1–19.
15 J. P. Gao, X. S. Meng, T. P. Bender, S. MacKinnon, V. Grand and Z. Y. Wang, *Chem. Commun.*, 1999, 1281–1282.
16 R. H. Martin and M. J. Marchant, *Tetrahedron Lett.*, 1972, **13**, 3707–3708.
17 R. H. Martin and M. J. Marchant, *Tetrahedron*, 1974, **30**, 343–345.
18 H. J. Lindner, *Tetrahedron*, 1975, **31**, 281–284.
19 M. C. Carreño, A. Enríquez, S. García-Cerrada, M. J. Sanz-Cuesta, A. Urbano, F. Maseras and A. Nonell-Canals, *Chem. - A Eur. J.*, 2008, **14**, 603–620.
20 C. Goedicke and H. Stegemeyer, *Tetrahedron Lett.*, 1970, **11**, 937–940.
21 H. Scherübl, U. Fritzsche and A. Mannschreck, *Chem. Ber.*, 1984, **117**, 336–343.
22 J. Barroso, J. L. Cabellos, S. Pan, F. Murillo, X. Zarate, M. A. Fernandez-Herrera and G. Merino, *Chem. Commun.*, 2017, **54**, 188–191.
23 H. Wynberg and M. B. Groen, *J. Chem. Soc. D Chem. Commun.*, 1969, 964–965.
24 J. M. Schulman and R. L. Disch, *J. Phys. Chem. A*, 1999, **103**, 6669–6672.
25 Y. H. Tian, G. Park and M. Kertesz, *Chem. Mater.*, 2008, **20**, 3266–3277.
26 A. Bossi, L. Falciola, C. Graiff, S. Maiorana, C. Rigamonti, A. Tiripicchio, E. Licandro and P. R. Mussini, *Electrochim. Acta*, 2009, **54**, 5083–5097.
27 D. Dova, S. Cauteruccio, N. Manfredi, S. Prager, A. Dreuw, S. Arnaboldi, P. R. Mussini, E. Licandro and A. Abbotto, *Dye. Pigment.*, 2019, **161**, 382–388.
28 C. Z. Wang, R. Kihara, X. Feng, P. Thuéry, C. Redshaw and T. Yamato, *ChemistrySelect*, 2017, **2**, 1436–1441.
29 J. Liu, J. Ma, K. Zhang, P. Ravat, P. Machata, S. Avdoshenko, F. Hennersdorf, H. Komber, W. Pisula, J. J. Weigand, A. A. Popov, R. Berger, K. Müllen and X. Feng, *J. Am. Chem. Soc.*, 2017, **139**, 7513–7521.
30 H. Kubo, T. Hirose and K. Matsuda, *Org. Lett.*, 2017, **19**, 1776–1779.
31 H. Oyama, K. Nakano, T. Harada, R. Kuroda, M. Naito, K. Nobusawa and K. Nozaki, *Org. Lett.*, 2013, **15**, 2104–2107.
32 Y. Ooyama, Y. Shimada, A. Ishii, G. Ito, Y. Kagawa, I. Imae, K. Komaguchi and Y. Harima, *J. Photochem. Photobiol. A Chem.*, 2009, **203**, 177–185.
33 W. L. Zhao, M. Li, H. Y. Lu and C. F. Chen, *Chem. Commun.*, 2019, **55**, 13793–13803.
34 G. Gingras, *Chem. Soc. Rev.*, 2013, **42**, 1051–1095.
35 M. Gingras, G. Félix and R. Peresutti, *Chem. Soc. Rev.*, 2013, **42**, 1007–1050.
36 C. F. Chen and Y. Shen, *Helicene chemistry: From synthesis to applications*, 2016.
37 M. Flammang-Barbieux, J. Nasielski and R. H. Martin, *Tetrahedron Lett.*, 1967, **8**, 743–744.
38 K. Mori, T. Murase and M. Fujita, *Angew. Chemie - Int. Ed.*, 2015, **54**, 6847–6851.
39 L. Liu, B. Yang, T. J. Katz and M. K. Poindexter, *J. Org. Chem.*, 1991, **56**, 3769–3775.

40 X. Y. Luo, Z. Liu, B. J. Zhang, W. M. Hua, Y. Feng, L. Li, D. C. Zhang and D. L. Cui, *ChemistrySelect*, 2018, **3**, 3426–3432.
41 L. Liu and T. J. Katz, *Tetrahedron Lett.*, 1990, **31**, 3983–3986.
42 E. J. Smutny and J. D. Roberts, *J. Am. Chem. Soc.*, 1955, **77**, 3420–3421.
43 K. Kamikawa, I. Takemoto, S. Takemoto and H. Matsuzaka, *J. Org. Chem.*, 2007, **72**, 7406–7408.
44 X. Xiang and L. T. Scott, *Org. Lett.*, 2007, **9**, 3937–3940.
45 M. Shimizu, I. Nagao, Y. Tomioka and T. Hiyama, *Angew. Chemie - Int. Ed.*, 2008, **47**, 8096–8099.
46 A. A. Ruch, S. Handa, F. Kong, V. N. Nesterov, D. R. Pahls, T. R. Cundari and L. M. Slaughter, *Org. Biomol. Chem.*, 2016, **14**, 8123–8140.
47 S. K. Collins, A. Grandbois, M. P. Vachon and J. Côté, *Angew. Chemie - Int. Ed.*, 2006, **45**, 2923–2926.
48 I. G. Stará, I. Starý, A. Kollárovič, F. Teplý, D. Šaman and M. Tichý, *J. Org. Chem.*, 1998, **63**, 4046–4050.
49 I. G. Stará, I. Starý, A. Kollárovič, F. Teplý, Š. Vyskočil and D. Šaman, *Tetrahedron Lett.*, 1999, **40**, 1993–1996.
50 F. Teplý, I. G. Stará, I. Starý, A. Kollárovič, D. Šaman, L. Rulíšek and P. Fiedler, *J. Am. Chem. Soc.*, 2002, **124**, 9175–9180.
51 I. G. Stará and I. Starý, *Acc. Chem. Res.*, 2020, **53**, 144–158.
52 J. Nejedlý, M. Šámal, J. Rybáček, I. G. Sánchez, V. Houska, T. Warzecha, J. Vacek, L. Sieger, M. Buděšínský, L. Bednárová, P. Fiedler, I. Císařová, I. Starý and I. G. Stará, *J. Org. Chem.*, 2020, **85**, 248–276.
53 P. M. Donovan and L. T. Scott, *J. Am. Chem. Soc.*, 2004, **126**, 3108–3112.
54 G. R. Kiel, S. C. Patel, P. W. Smith, D. S. Levine and T. D. Tilley, *J. Am. Chem. Soc.*, 2017, **139**, 18456–18459.
55 V. Mamane, P. Hannen and A. Fürstner, *Chem. - A Eur. J.*, 2004, **10**, 4556–4575.
56 J. Storch, J. Čermák, J. Karban, I. Císařová and J. Sýkora, *J. Org. Chem.*, 2010, **75**, 3137–3140.
57 M. Weimar, R. Correa Da Costa, F. H. Lee and M. J. Fuchter, *Org. Lett.*, 2013, **15**, 1706–1709.
58 H. Oyama, M. Akiyama, K. Nakano, M. Naito, K. Nobusawa and K. Nozaki, *Org. Lett.*, 2016, **18**, 3654–3657.
59 K. Yamamoto, M. Okazumi, H. Suemune and K. Usui, *Org. Lett.*, 2013, **15**, 1806–1809.
60 H.-E. Högberg, A. Hordvik, L.-Å. Smedman, I. Wennberg, A. H. Norbury and C.-G. Swahn, *Acta Chem. Scand.*, 1973, **27**, 2591–2596.
61 J. Areephong, N. Ruangsupapichart and T. Thongpanchang, *Tetrahedron Lett.*, 2004, **45**, 3067–3070.
62 J. F. Schneider, M. Nieger, K. Nättinen and K. H. Dötz, *Synthesis*, 2005, 1109–1124.
63 M. Miyasaka and A. Rajca, *J. Org. Chem.*, 2006, **71**, 3264–3266.
64 M. Miyasaka, M. Pink, S. Rajca and A. Rajca, *Angew. Chemie - Int. Ed.*, 2009, **48**, 5954–5957.
65 K. Y. Chernichenko, E. S. Balenkova and V. G. Nenajdenko, *Mendeleev Commun.*, 2008, **18**, 171–179.
66 Y. Masuya, Y. Kawashima, T. Kodama, N. Chatani and M. Tobisu, *Synlett*, 2019, **30**, 1995–1999.
67 X. Zheng, S. M. Baumann, S. M. Chintala, K. D. Galloway, J. B. Slaughter and R. D. McCulla, *Photochem. Photobiol. Sci.*, 2016, **15**, 791–800.
68 T. Zhang, G. Deng, H. Li, B. Liu, Q. Tan and B. Xu, *Org. Lett.*, 2018, **20**, 5439–5443.
69 S. Yasuike, T. Iida, K. Yamaguchi, H. Seki and J. Kurita, *Tetrahedron Lett.*, 2001, **42**, 441–444.
70 M. Murai, R. Okada, A. Nishiyama and K. Takai, *Org. Lett.*, 2016, **18**, 4380–4383.
71 A. Dore, D. Fabbri, S. Gladiali and O. De Lucchi, *J. Chem. Soc. Chem. Commun.*, 1993, 1124–1125.
72 K. Uematsu, K. Noguchi and K. Nakano, *Phys. Chem. Chem. Phys.*, 2018, **20**, 3286–3295.
73 S. Nishigaki, K. Murayama, Y. Shibata and K. Tanaka, *Mater. Chem. Front.*, 2018, **2**, 585–590.
74 D. E. Pereira, Neelima and N. J. Leonard, *Tetrahedron*, 1990, **46**, 5895–5908.
75 I. Yavari, M. T. Maghsoodlou and A. Pourmossavi, *J. Chem. Res. - Part S*, 1997, 212–213.
76 J. Klívar, A. Jančařík, D. Šaman, R. Pohl, P. Fiedler, L. Bednárová, I. Starý and I. G. Stará, *Chem. - A Eur. J.*, 2016, **22**, 14401–14405.
77 M. C. Carreno, R. Hernandez-Sanchez, J. Mahugo and A. Urbano, *J. Org. Chem.*, 1999, **64**, 1387–1390.
78 M. C. Carreño, S. García-Cerrada and A. Urbano, *Chem. Commun.*, 2002, **2**, 1412–1413.
79 A. Grandbois and S. K. Collins, *Chem. - A Eur. J.*, 2008, **14**, 9323–9329.
80 A. Jančařík, J. Rybáček, K. Cocq, J. V. Chocholoušová, J. Vacek, R. Pohl, L. Bednárová, P. Fiedler,

I. Císařová, I. G. Stará and I. Starý, *Angew. Chemie - Int. Ed.*, 2013, **52**, 9970–9975.
81 I. G. Sánchez, M. Šámal, J. Nejedlý, M. Karras, J. Klívar, J. Rybáček, M. Buděšínský, L. Bednárová, B. Seidlerová, I. G. Stará and I. Starý, *Chem. Commun.*, 2017, **53**, 4370–4373.
82 R. Yamano, S. Kinoshita, Y. Shibata and K. Tanaka, *European J. Org. Chem.*, 2018, **2018**, 5916–5920.
83 R. Yamano, Y. Shibata and K. Tanaka, *Chem. - A Eur. J.*, 2018, **24**, 6364–6370.
84 K. Murayama, Y. Oike, S. Furumi, M. Takeuchi, K. Noguchi and K. Tanaka, *European J. Org. Chem.*, 2015, **2015**, 1409–1414.
85 Y. Sawada, S. Furumi, A. Takai, M. Takeuchi, K. Noguchi and K. Tanaka, *J. Am. Chem. Soc.*, 2012, **134**, 4080–4083.
86 M. Satoh, Y. Shibata and K. Tanaka, *Chem. - A Eur. J.*, 2018, **24**, 5434–5438.
87 K. Nakamura, S. Furumi, M. Takeuchi, T. Shibuya and K. Tanaka, *J. Am. Chem. Soc.*, 2014, **136**, 5555–5558.
88 M. Tanaka, Y. Shibata, K. Nakamura, K. Teraoka, H. Uekusa, K. Nakazono, T. Takata and K. Tanaka, *Chem. - A Eur. J.*, 2016, **22**, 9537–9541.
89 K. Usui, K. Yamamoto, Y. Ueno, K. Igawa, R. Hagihara, T. Masuda, A. Ojida, S. Karasawa, K. Tomooka, G. Hirai and H. Suemune, *Chem. - A Eur. J.*, 2018, **24**, 14617–14621.
90 P. Redero, T. Hartung, J. Zhang, L. D. M. Nicholls, G. Zichen, M. Simon, C. Golz and M. Alcarazo, *Angew. Chemie - Int. Ed.*, 2020, DOI:10.1002/anie.202010021.
91 T. Hartung, R. Machleid, M. Simon, C. Golz and M. Alcarazo, *Angew. Chemie - Int. Ed.*, 2020, **59**, 5660–5664.
92 L. D. M. Nicholls, M. Marx, T. Hartung, E. González-Fernández, C. Golz and M. Alcarazo, *ACS Catal.*, 2018, **8**, 6079–6085.
93 E. González-Fernández, L. D. M. Nicholls, L. D. Schaaf, C. Farès, C. W. Lehmann and M. Alcarazo, *J. Am. Chem. Soc.*, 2017, **139**, 1428–1431.
94 M. S. Newman and W. B. Lutz, *J. Am. Chem. Soc.*, 1956, **78**, 2469–2473.
95 J. Míšek, F. Teplý, I. G. Stará, M. Tichý, D. Šaman, I. Císařová, P. Vojtíšek and I. Starý, *Angew. Chemie - Int. Ed.*, 2008, **47**, 3188–3191.
96 S. G. Merica, W. Jędral, S. Lait, P. Keech and N. J. Bunce, *Can. J. Chem.*, 1999, **77**, 1281–1287.
97 S. Graule, M. Rudolph, W. Shen, J. A. Gareth Williams, C. Lescop, J. Autschbach, J. Crassous and R. Réau, *Chem. - A Eur. J.*, 2010, **16**, 5976–6005.
98 D. Dova, S. Cauteruccio, S. Prager, A. Dreuw, C. Graiff and E. Licandro, *J. Org. Chem.*, 2015, **80**, 3921–3928.
99 K. Tanaka, H. Osuga, Y. Shogase and H. Suzuki, *Tetrahedron Lett.*, 1995, **36**, 915–918.
100 B. Laleu, P. Mobian, C. Herse, B. W. Laursen, G. Hopfgartner, G. Bernardinelli and J. Lacour, *Angew. Chemie - Int. Ed.*, 2005, **44**, 1879–1883.
101 K. Tanaka, Y. Shogase, H. Osuga, H. Suzuki and K. Nakamura, *Tetrahedron Lett.*, 1995, **36**, 1675–1678.
102 N. Saleh, C. Shen and J. Crassous, *Chem. Sci.*, 2014, **5**, 3680–3694.
103 J. OuYang and J. Crassous, *Coord. Chem. Rev.*, 2018, **376**, 533–547.
104 K. Soai and H. Hasegawa, *J. Chem. Soc. Perkin Trans. 1*, 1985, **4**, 769–772.
105 B. Ben Hassine, M. Gorsane, J. Pecher and R. H. Martin, *Bull. des Sociétés Chim. Belges*, 1986, **95**, 557–566.
106 M. T. Reetz and S. Sostmann, *Tetrahedron*, 2001, **57**, 2515–2520.
107 A. U. Malik, F. Gan, C. Shen, N. Yu, R. Wang, J. Crassous, M. Shu and H. Qiu, *J. Am. Chem. Soc.*, 2018, **140**, 2769–2772.
108 P. Aillard, A. Voituriez and A. Marinetti, *Dalt. Trans.*, 2014, **43**, 15263–15278.
109 F. Aloui, R. El Abed, A. Marinetti and B. Ben Hassine, *Tetrahedron Lett.*, 2008, **49**, 4092–4095.
110 T. Kawasaki, K. Suzuki, E. Licandro, A. Bossi, S. Maiorana and K. Soai, *Tetrahedron Asymmetry*, 2006, **17**, 2050–2053.
111 M. Gicquel, Y. Zhang, P. Aillard, P. Retailleau, A. Voituriez and A. Marinetti, *Angew. Chemie - Int. Ed.*, 2015, **54**, 5470–5473.
112 P. Aillard, D. Dova, V. Magné, P. Retailleau, S. Cauteruccio, E. Licandro, A. Voituriez and A. Marinetti, *Chem. Commun.*, 2016, **52**, 10984–10987.
113 P. Aillard, A. Voituriez, D. Dova, S. Cauteruccio, E. Licandro and A. Marinetti, *Chem. - A Eur. J.*, 2014, **20**, 12373–12376.

114 K. Yavari, P. Aillard, Y. Zhang, F. Nuter, P. Retailleau, A. Voituriez and A. Marinetti, *Angew. Chemie - Int. Ed.*, 2014, **53**, 861–865.
115 C. S. Demmer, A. Voituriez and A. Marinetti, *Comptes Rendus Chim.*, 2017, **20**, 860–879.
116 T. Beránek, J. Žádný, T. Strašák, J. Karban, I. Císařová, J. Sýkora and J. Storch, *ACS Omega*, 2020, **5**, 882–892.
117 Y. Yang, R. C. Da Costa, D. M. Smilgies, A. J. Campbell and M. J. Fuchter, *Adv. Mater.*, 2013, **25**, 2624–2628.
118 Y. Yang, R. C. Da Costa, M. J. Fuchter and A. J. Campbell, *Nat. Photonics*, 2013, **7**, 634–638.
119 Y. Yang, B. Rice, X. Shi, J. R. Brandt, R. Correa Da Costa, G. J. Hedley, D. M. Smilgies, J. M. Frost, I. D. W. Samuel, A. Otero-De-La-Roza, E. R. Johnson, K. E. Jelfs, J. Nelson, A. J. Campbell and M. J. Fuchter, *ACS Nano*, 2017, **11**, 8329–8338.
120 L. Wan, J. Wade, F. Salerno, O. Arteaga, B. Laidlaw, X. Wang, T. Penfold, M. J. Fuchter and A. J. Campbell, *ACS Nano*, 2019, **13**, 8099–8105.
121 F. Feng, T. Miyashita, H. Okubo and M. Yamaguchi, *J. Am. Chem. Soc.*, 1998, **120**, 10166–10170.
122 M. J. Miah, M. Shahabuddin, M. Karikomi, M. Salim, E. Nasuno, N. Kato and K. I. Iimura, *Bull. Chem. Soc. Jpn.*, 2016, **89**, 203–211.
123 M. Karras, J. Holec, L. Bednárová, R. Pohl, B. Schmidt, I. G. Stará and I. Starý, *J. Org. Chem.*, 2018, **83**, 5523–5538.
124 J. Holec, J. Rybáček, J. Vacek, M. Karras, L. Bednárová, M. Buděšínský, M. Slušná, P. Holý, B. Schmidt, I. G. Stará and I. Starý, *Chem. – A Eur. J.*, 2019, **25**, 11393–11393.
125 Y. Zhao and K. Zhu, *Chem. Soc. Rev.*, 2016, **45**, 655–689.
126 M. I. H. Ansari, A. Qurashi and M. K. Nazeeruddin, *J. Photochem. Photobiol. C Photochem. Rev.*, 2018, **35**, 1–24.
127 C. C. Lee, C. I. Chen, C. Te Fang, P. Y. Huang, Y. T. Wu and C. C. Chueh, *Adv. Funct. Mater.*, 2019, **23**, DOI:10.1002/adfm.201808625.
128 N. Xu, A. Zheng, Y. Wei, Y. Yuan, J. Zhang, M. Lei and P. Wang, *Chem. Sci.*, 2020, **11**, 3418–3426.
129 Z. P. Yan, X. F. Luo, W. Q. Liu, Z. G. Wu, X. Liang, K. Liao, Y. Wang, Y. X. Zheng, L. Zhou, J. L. Zuo, Y. Pan and H. Zhang, *Chem. - A Eur. J.*, 2019, **25**, 5672–5676.
130 K. Yavari, W. Delaunay, N. De Rycke, T. Reynaldo, P. Aillard, M. Srebro-Hooper, V. Y. Chang, G. Muller, D. Tondelier, B. Geffroy, A. Voituriez, A. Marinetti, M. Hissler and J. Crassous, *Chem. - A Eur. J.*, 2019, **25**, 5303–5310.
131 J. Storch, J. Zadny, T. Strasak, M. Kubala, J. Sykora, M. Dusek, V. Cirkva, P. Matejka, M. Krbal and J. Vacek, *Chem. - A Eur. J.*, 2015, **21**, 2343–2347.
132 J. Vacek, J. V. Chocholoušová, I. G. Stará, I. Starý and Y. Dubi, *Nanoscale*, 2015, **7**, 8793–8802.
133 P. Josse, L. Favereau, C. Shen, S. Dabos-Seignon, P. Blanchard, C. Cabanetos and J. Crassous, *Chem. - A Eur. J.*, 2017, **23**, 6277–6281.
134 Y. Ooyama, G. Ito, K. Kushimoto, K. Komaguchi, I. Imae and Y. Harima, *Org. Biomol. Chem.*, 2010, **8**, 2756–2770.
135 V. Kiran, S. P. Mathew, S. R. Cohen, I. Hernández Delgado, J. Lacour and R. Naaman, *Adv. Mater.*, 2016, **28**, 1957–1962.
136 D. Schweinfurth, M. Zalibera, M. Kathan, C. Shen, M. Mazzolini, N. Trapp, J. Crassous, G. Gescheidt and F. Diederich, *J. Am. Chem. Soc.*, 2014, **136**, 13045–13052.
137 M. Srebro, E. Anger, B. Moore, N. Vanthuyne, C. Roussel, R. Réau, J. Autschbach and J. Crassous, *Chem. - A Eur. J.*, 2015, **21**, 17100–17115.
138 S. Sakunkaewkasem, A. Petdum, W. Panchan, J. Sirirak, A. Charoenpanich, T. Sooksimuang and N. Wanichacheva, *ACS Sensors*, 2018, **3**, 1016–1023.
139 J. R. Brandt, F. Salerno and M. J. Fuchter, *Nat. Rev. Chem.*, 2017, 1, 0045.
140 E. Licandro, S. Cauteruccio and D. Dova, *Adv. Heterocycl. Chem.*, 2016, **118**, 1–46.
141 S. Cauteruccio, E. Licandro, M. Panigati, G. D'Alfonso and S. Maiorana, *Coord. Chem. Rev.*, 2019, **386**, 119–137.
142 A. Bossi, E. Licandro, S. Maiorana, C. Rigamonti, S. Righetto, G. Richard Stephenson, M. Spassova, E. Botek and B. Champagne, *J. Phys. Chem. C*, 2008, **112**, 7900–7907.
143 S. Cauteruccio, D. Dova, M. Benaglia, A. Genoni, M. Orlandi and E. Licandro, *European J. Org. Chem.*, 2014, **2014**, 2694–2702.
144 D. Dova, L. Viglianti, P. R. Mussini, S. Prager, A. Dreuw, A. Voituriez, E. Licandro and S. Cauteruccio, *Asian J. Org. Chem.*, 2016, **5**, 537–549.

145 S. Cauteruccio, A. Loos, A. Bossi, M. C. Blanco Jaimes, D. Dova, F. Rominger, S. Prager, A. Dreuw, E. Licandro and A. S. K. Hashmi, *Inorg. Chem.*, 2013, **52**, 7995–8004.
146 S. Arnaboldi, S. Cauteruccio, S. Grecchi, T. Benincori, M. Marcaccio, A. O. Biroli, G. Longhi, E. Licandro and P. R. Mussini, *Chem. Sci.*, 2019, **10**, 1539–1548.
147 S. Cauteruccio, C. Bartoli, C. Carrara, D. Dova, C. Errico, G. Ciampi, D. Dinucci, E. Licandro and F. Chiellini, *Chempluschem*, 2015, **80**, 490–493.
148 Y. Xu, Y. X. Zhang, H. Sugiyama, T. Umano, H. Osuga and K. Tanaka, *J. Am. Chem. Soc.*, 2004, **126**, 6566–6567.
149 K. I. Shinohara, Y. Sannohe, S. Kaieda, K. I. Tanaka, H. Osuga, H. Tahara, Y. Xu, T. Kawase, T. Bando and H. Sugiyama, *J. Am. Chem. Soc.*, 2010, **132**, 3778–3782.
150 K. Yamada, S. Ogashiwa, H. Tanaka, H. Nakagawa and H. Kawazura, *Chem. Lett.*, 1981, **10**, 343–346.
151 S. Maiorana, A. Papagni, E. Licandro, R. Annunziata, P. Paravidino, D. Perdicchia, C. Giannini, M. Bencini, K. Clays and A. Persoons, *Tetrahedron*, 2003, **59**, 6481–6488.
152 C. Baldoli, A. Bossi, C. Giannini, E. Licandro, S. Maiorana, D. Perdicchia and M. Schiavo, *Synlett*, 2005, **7**, 1137–1141.
153 D. Waghray, C. De Vet, K. Karypidou and W. Dehaen, *J. Org. Chem.*, 2013, **78**, 11147–11154.
154 J. Pei, W. Y. Zhang, J. Mao and X. H. Zhou, *Tetrahedron Lett.*, 2006, **47**, 1551–1554.
155 K. Tanaka, H. Suzuki and H. Osuga, *J. Org. Chem.*, 1997, **62**, 4465–4470.
156 K. Tanaka, H. Suzuki and H. Osuga, *Tetrahedron Lett.*, 1997, **38**, 457–460.
157 A. Rajca, M. Miyasaka, S. Xiao, P. J. Boratyński, M. Pink and S. Rajca, *J. Org. Chem.*, 2009, **74**, 9105–9111.
158 I. García-Benito, I. Zimmermann, J. Urieta-Mora, J. Aragó, A. Molina-Ontoria, E. Ortí, N. Martín and M. K. Nazeeruddin, *J. Mater. Chem. A*, 2017, **5**, 8317–8324.
159 R. C. Larock, M. J. Doty, Q. Tian and J. M. Zenner, *J. Org. Chem.*, 1997, **62**, 7536–7537.
160 H. Wynberg, *Acc. Chem. Res.*, 1971, **4**, 65–73.
161 S. Cauteruccio, D. Dova, C. Graiff, C. Carrara, J. Doulcet, G. R. Stephenson and E. Licandro, *New J. Chem.*, 2014, **38**, 2241–2244.
162 N. Hebbar, Y. Ramondenc, G. Plé, G. Dupas and N. Plé, *Tetrahedron*, 2009, **65**, 4190–4200.
163 P. Boontiem and S. Kiatisevi, *Inorganica Chim. Acta*, 2020, **506**, 119538.
164 S. D. Xu, F. Z. Sun, W. H. Deng, H. Hao and X. H. Duan, *New J. Chem.*, 2018, **42**, 16464–16468.
165 A. Hooper, A. Zambon and C. J. Springer, *Org. Biomol. Chem.*, 2016, **14**, 963–969.
166 G. A. Molander, S. L. J. Trice and B. Tschaen, *Tetrahedron*, 2015, **71**, 5758–5764.
167 T. Ishiyama, Y. Itoh, T. Kitano and N. Miyaura, *Tetrahedron Lett.*, 1997, **38**, 3447–3450.
168 L. H. Xie, X. Y. Hou, Y. R. Hua, Y. Q. Huang, B. M. Zhao, F. Liu, B. Peng, W. Wei and W. Huang, *Org. Lett.*, 2007, **9**, 1619–1622.
169 G. Bianchi, G. Schimperna, ENI S.P.A. WO 2013/92648, 2013, A1.
170 R. C. Larock, *Pure Appl. Chem.*, 1999, **71**, 1435–1442.
171 A. Bossi, S. Arnaboldi, C. Castellano, R. Martinazzo and S. Cauteruccio, *Adv. Opt. Mater.*, 2020, **8**, 2001018.
172 Y. P. Ou, J. Zhang, F. Zhang, D. Kuang, F. Hartl, L. Rao and S. H. Liu, *Dalt. Trans.*, 2016, **45**, 6503–6516.
173 M. W. van der Meijden, T. Balandina, O. Ivasenko, S. De Feyter, K. Wurst and R. M. Kellogg, *Chem. - A Eur. J.*, 2016, **22**, 14633–14639.
174 J. Storch, J. Sýkora, J. Čermak, J. Karban, I. Císařová and A. Růžička, *J. Org. Chem.*, 2009, **74**, 3090–3093.
175 A. Bedi and S. S. Zade, *Macromolecules*, 2013, **46**, 8864–8872.
176 R. M. Appa, S. S. Prasad, J. Lakshmidevi, B. R. Naidu, M. Narasimhulu and K. Venkateswarlu, *Appl. Organomet. Chem.*, 2019, **33**, DOI:10.1002/aoc.5126.
177 G. Dilauro, S. M. García, D. Tagarelli, P. Vitale, F. M. Perna and V. Capriati, *ChemSusChem*, 2018, **11**, 3495–3501.
178 H. J. Dauben and L. L. McCoy, *J. Am. Chem. Soc.*, 1959, **81**, 4863–4873.
179 R. Fusco, P. Biagini, S. Maiorana, E. Licandro, WO 2013/098726 2013, A1.
180 S. Gronowitz and T. Dahlgron Chem. Scripta 1977, **12**, 97.
181 R. Rieger, D. Beckmann, A. Mavrinskiy, M. Kastler and K. Müllen, *Chem. Mater.*, 2010, **22**, 5314–5318.

182 E. Licandro, C. Rigamonti, M. T. Ticozzelli, M. Monteforte, C. Baldoli, C. Giannini and S. Maiorana, *Synthesis.*, 2006, **21**, 3670–3678.
183 Y. Liu, Q. Xu, J. Sun, L. Wang, D. He, M. Wang and C. Yang, *Spectrochim. Acta - Part A Mol. Biomol. Spectrosc.*, 2020, **239**, 118475.
184 J. Y. Hu, X. Feng, A. Paudel, H. Tomiyasu, U. Rayhan, P. Thuéry, M. R. J. Elsegood, C. Redshaw and T. Yamato, *European J. Org. Chem.*, 2013, **2013**, 5829–5837.
185 M. Buchta, J. Rybáček, A. Jančařík, A. A. Kudale, M. Buděšínský, J. V. Chocholoušová, J. Vacek, L. Bednárová, I. Císařová, G. J. Bodwell, I. Starý and I. G. Stará, *Chem. - A Eur. J.*, 2015, **21**, 8910–8917.
186 A. C. Bédard, A. Vlassova, A. C. Hernandez-Perez, A. Bessette, G. S. Hanan, M. A. Heuft and S. K. Collins, *Chem. - A Eur. J.*, 2013, **19**, 16295–16302.
187 C. Maeda, K. Nagahata, T. Shirakawa and T. Ema, *Angew. Chemie - Int. Ed.*, 2020, **59**, 7813–7817.
188 T. Chen, B. Zhang, Z. Liu, L. Duan, G. Dong, Y. Feng, X. Luo and D. Cui, *Tetrahedron Lett.*, 2017, **58**, 531–535.
189 W. Hua, Z. Liu, L. Duan, G. Dong, Y. Qiu, B. Zhang, D. Cui, X. Tao, N. Cheng and Y. Liu, *RSC Adv.*, 2015, **5**, 75–84.
190 L. Shi, Z. Liu, G. Dong, L. Duan, Y. Qiu, J. Jia, W. Guo, D. Zhao, D. Cui and X. Tao, *Chem. - A Eur. J.*, 2012, **18**, 8092–8099.
191 M. Tounsi, M. Ben Braiek, A. Baraket, M. Lee, N. Zine, M. Zabala, J. Bausells, F. Aloui, B. Ben Hassine, A. Maaref and A. Errachid, *Electroanalysis*, 2016, **28**, 2892–2899.
192 M. Schubert, S. Trosien, L. Schulz, C. Brscheid, D. Schollmeyer and S. R. Waldvogel, *European J. Org. Chem.*, 2014, **2014**, 7091–7094.
193 K. Górski, J. Mech-Piskorz, B. Leśniewska, O. Pietraszkiewicz and M. Pietraszkiewicz, *J. Org. Chem.*, 2020, **85**, 4672–4681.
194 R. Kuhn, *Stereochemie*, Ed.: K. Freudenberg, Franz Deuticke, Leipzig, 1933, 803-824.
195 U. Bornscheuer, *Angew. Chemie Int. Ed.*, 2008, **47**, 5282–5282.
196 S. R. Laplante, L. D. Fader, K. R. Fandrick, D. R. Fandrick, O. Hucke, R. Kemper, S. P. F. Miller and P. J. Edwards, *J. Med. Chem.*, 2011, **54**, 7005–7022.
197 S. R. Laplante, P. J. Edwards, L. D. Fader, A. Jakalian and O. Hucke, *ChemMedChem*, 2011, **6**, 505–513.
198 I. D'Acquarica, F. Gasparrini, M. Pierini, C. Villani and G. Zappia, *J. Sep. Sci.*, 2006, **29**, 1508–1516.
199 S. Gabrieli, G. Mazzeo, G. Longhi, S. Abbate and T. Benincori, *Chirality*, 2016, **28**, 686–695.
200 G. Longhi, E. Castiglioni, J. Koshoubu, G. Mazzeo and S. Abbate, *Chirality*, 2016, **28**, 696–707.
201 O. Trapp, *Anal. Chem.*, 2006, **78**, 189–198.
202 M. Wierzbicka, I. Bylińska, C. Czaplewski and W. Wiczk, *RSC Adv.*, 2015, **5**, 29294–29303.
203 Y. Nagano, T. Ikoma, K. Akiyama and S. Tero-Kubota, *J. Am. Chem. Soc.*, 2003, **125**, 14103–14112.
204 M. J. Frisch, G. W. Trucks, H. E. Schlegel, G. E. Scuseria, M. A. Robb, J. R. Cheeseman, G. Scalmani, V. Barone, G. A. Petersson, F. O., J. B. Foresman and J. D. Fox, *Gaussian, Inc., Wallingford CT*, 2016.
205 P. J. Stephens, *J. Phys. Chem.*, 1985, **89**, 748–752.
206 G. Longhi, E. Castiglioni, S. Abbate, F. Lebon and D. A. Lightner, *Chirality*, 2013, **25**, 589–599.
207 S. Abbate, G. Longhi, F. Lebon, E. Castiglioni, S. Superchi, L. Pisani, F. Fontana, F. Torricelli, T. Caronna, C. Villani, R. Sabia, M. Tommasini, A. Lucotti, D. Mendola, A. Mele and D. A. Lightner, *J. Phys. Chem. C*, 2014, **118**, 1682–1695.
208 E. Castiglioni, S. Abbate and G. Longhi, in *Applied Spectroscopy*, 2010, **64**, 1416–1419.
209 P. J. Stephens, F. J. Devlin and J. R. Cheeseman, *VCD spectroscopy for organic chemists*, 2012.
210 S. Abbate, G. Longhi, F. Lebon, E. Castiglioni, S. Superchi, L. Pisani, F. Fontana, F. Torricelli, T. Caronna, C. Villani, R. Sabia, M. Tommasini, A. Lucotti, D. Mendola, A. Mele and D. A. Lightner, *J. Phys. Chem. C*, 2014, **118**, 1682–1695.
211 L. A. Nafie, *Vibrational Optical Activity: Principles and Applications*, 2011.
212 P. L. Palavarapu, *CRC Press*, Taylor & Francis Group, 2017.
213 C. Merten, T. P. Golub and N. M. Kreienborg, *J. Org. Chem.*, 2019, **84**, 8797–8814.
214 F. Pfeiffer and G. Mayer, *Front. Chem.*, 2016, **4**, 1–9.
215 A. S. K. Hashmi and G. J. Hutchings, *Angew. Chemie - Int. Ed.*, 2006, **45**, 7896–7936.
216 G. C. Bond, P. A. Sermon, G. Webb, D. A. Buchanan and P. B. Wells, *J. Chem. Soc. Chem. Commun.*, 1973, 444.

217 G. J. Hutchings, *J. Catal.*, 1985, **96**, 292–295.
218 M. Haruta, T. Kobayashi, H. Sano and N. Yamada, *Chem. Lett.*, 1987, **16**, 405–408.
219 Y. Ito, M. Sawamura and T. Hayashi, *J. Am. Chem. Soc.*, 1986, **108**, 6405–6406.
220 M. Paz Muñoz, J. Adrio, J. C. Carretero and A. M. Echavarren, *Organometallics*, 2005, **24**, 1293–1300.
221 C. Bour and V. Gandon, *Synlett*, 2015, **26**, 1427–1436.
222 A. Fürstner, *Chem. Soc. Rev.*, 2009, **38**, 3208–3221.
223 C. Nieto-Oberhuber, S. López, E. Jiménez-Núñez and A. M. Echavarren, *Chem. - A Eur. J.*, 2006, **12**, 5916–5923.
224 E. Jiménez-Núñez and A. M. Echavarren, *Chem. Rev.*, 2008, **108**, 3326–3350.
225 A. Fürstner and P. W. Davies, *Angew. Chemie - Int. Ed.*, 2007, **46**, 3410–3449.
226 W. Zi and F. Dean Toste, *Chem. Soc. Rev.*, 2016, **45**, 4567–4589.
227 B. Ranieri, I. Escofet and A. M. Echavarren, *Org. Biomol. Chem.*, 2015, **13**, 7103–7118.
228 P. Pyykkö, *Angew. Chemie - Int. Ed.*, 2004, **43**, 4412–4456.
229 R. L. Lalonde, B. D. Sherry, E. J. Kang and F. D. Toste, *J. Am. Chem. Soc.*, 2007, **129**, 2452–2453.
230 D. H. Miles, M. Veguillas and F. D. Toste, *Chem. Sci.*, 2013, **4**, 3427–3431.
231 S. G. Sethofer, T. Mayer and F. D. Toste, *J. Am. Chem. Soc.*, 2010, **132**, 8276–8277.
232 H. Teller, S. Flügge, R. Goddard and A. Fürstner, *Angew. Chemie - Int. Ed.*, 2010, **49**, 1949–1953.
233 Y. M. Wang, C. N. Kuzniewski, V. Rauniyar, C. Hoong and F. D. Toste, *J. Am. Chem. Soc.*, 2011, **133**, 12972–12975.
234 J. Francos, F. Grande-Carmona, H. Faustino, J. Iglesias-Sigüenza, E. Díez, I. Alonso, R. Fernández, J. M. Lassaletta, F. López and J. L. Mascareñas, *J. Am. Chem. Soc.*, 2012, **134**, 14322–14325.
235 A. Z. González and F. Dean Toste, *Org. Lett.*, 2010, **12**, 200–203.
236 I. Alonso, H. Faustino, F. López and J. L. Mascareñas, *Angew. Chemie - Int. Ed.*, 2011, **50**, 11496–11500.
237 H. Teller, M. Corbet, L. Mantilli, G. Gopakumar, R. Goddard, W. Thiel and A. Fürstner, *J. Am. Chem. Soc.*, 2012, **134**, 15331–15342.
238 J. Ruiz, A. F. Mesa and D. Sol, *Organometallics*, 2015, **34**, 5129–5135.
239 K. Schwedtmann, R. Schoemaker, F. Hennersdorf, A. Bauzá, A. Frontera, R. Weiss and J. J. Weigand, *Dalt. Trans.*, 2016, **45**, 11384–11396.
240 L. Gu, L. M. Wolf, A. Zieliński, W. Thiel and M. Alcarazo, *J. Am. Chem. Soc.*, 2017, **139**, 4948–4953.
241 E. Haldón, Á. Kozma, H. Tinnermann, L. Gu, R. Goddard and M. Alcarazo, *Dalt. Trans.*, 2016, **45**, 1872–1876.
242 J. W. Dube, Y. Zheng, W. Thiel and M. Alcarazo, *J. Am. Chem. Soc.*, 2016, **138**, 6869–6877.
243 H. Tinnermann, C. Wille and M. Alcarazo, *Angew. Chemie - Int. Ed.*, 2014, **53**, 8732–8736.
244 G. Mehler, P. Linowski, J. Carreras, A. Zanardi, J. W. Dube and M. Alcarazo, *Chem. - A Eur. J.*, 2016, **22**, 15320–15327.
245 J. Carreras, G. Gopakumar, L. Gu, A. Gimeno, P. Linowski, J. Petuškova, W. Thiel and M. Alcarazo, *J. Am. Chem. Soc.*, 2013, **135**, 18815–18823.
246 J. Petuškova, M. Patil, S. Holle, C. W. Lehmann, W. Thiel and M. Alcarazo, *J. Am. Chem. Soc.*, 2011, **133**, 20758–20760.
247 M. Alcarazo, *Acc. Chem. Res.*, 2016, **49**, 1797–1805.
248 L. D. M. Nicholls and M. Alcarazo, *Chem. Lett.*, 2019, **48**, 1–13.
249 L. D. M. Nicholls, Dissertation, Georg-August-Universität Göttingen, 2018.
250 H. Tinnermann, L. D. M. Nicholls, T. Johannsen, C. Wille, C. Golz, R. Goddard and M. Alcarazo, *ACS Catal.*, 2018, **8**, 10457–10463.
251 L. Gu, Y. Zheng, E. Haldón, R. Goddard, E. Bill, W. Thiel and M. Alcarazo, *Angew. Chemie - Int. Ed.*, 2017, **56**, 8790–8794.
252 G. M. Sheldrick, *Acta Crystallogr. Sect. A Found. Crystallogr.*, 2008, **64**, 112–122.
253 O. V. Dolomanov, L. J. Bourhis, R. J. Gildea, J. A. K. Howard and H. Puschmann, *J. Appl. Crystallogr.*, 2009, **42**, 339–341.
254 Hebbar, Y. Ramondenc, G. Ple, G. Dupas, N. Ple, *Tetrahedron*, 2009, **65**, 4190–4200.
255 J. Roncali, *Chem. Rev.*, 1997, **97**, 173–205.
256 T. A. Skotheim and J. R. Reynolds, *Conjugated polymers: Theory, synthesis, properties, and*

characterization, 2007.
257 R. Jean, *Acc. Chem. Res.*, 2009, **42**, 1719–1730.
258 K. Takimiya, S. Shinamura, I. Osaka and E. Miyazaki, *Adv. Mater.*, 2011, **23**, 4347–4370.
259 Y. Xie, T. Fujimoto, S. Dalgleish, Y. Shuku, M. M. Matsushita and K. Awaga, *J. Mater. Chem. C*, 2013, **1**, 3467–3481.
260 G. R. Stephenson, S. Cauteruccio and J. Doulcet, *Synlett*, 2014, **25**, 701–707.
261 C. Rigamonti, M. T. Ticozzelli, A. Bossi, E. Licandro, C. Giannini and S. Maiorana, *Heterocycles*, 2008, **76**, 1439–1470.
262 D. Waghray and W. Dehaen, *Org. Lett.*, 2013, **15**, 2910–2913.
263 P. Gao, H. N. Tsao, M. Grätzel and M. K. Nazeeruddin, *Org. Lett.*, 2012, **14**, 4330–4333.
264 E. Longhi, A. Bossi, G. Di Carlo, S. Maiorana, F. De Angelis, P. Salvatori, A. Petrozza, M. Binda, V. Roiati, P. R. Mussini, C. Baldoli and E. Licandro, *European J. Org. Chem.*, 2013, 84–94.
265 X. Li, K. Wu, L. Zheng, Y. Deng, S. Tan and H. Chen, *Dye. Pigment.*, 2019, **168**, 59–67.
266 K. Tanaka, H. Osuga, N. Tsujiuchi, M. Hisamoto and Y. Sakaki, *Bull. Chem. Soc. Jpn.*, 2002, **75**, 551–557.
267 C. Kim, T. J. Marks, A. Facchetti, M. Schiavo, A. Bossi, S. Maiorana, E. Licandro, F. Todescato, S. Toffanin, M. Muccini, C. Graiff and A. Tiripicchio, *Org. Electron.*, 2009, **10**, 1511–1520.
268 M. Zhang, Y. Sun, X. Guo, C. Cui, Y. He and Y. Li, *Macromolecules*, 2011, **44**, 7625–7631.
269 Y. Nishide, H. Osuga, M. Saito, T. Aiba, Y. Inagaki, Y. Doge and K. Tanaka, *J. Org. Chem.*, 2007, **72**, 9141–9151.
270 A. Bedi and S. S. Zade, *Eur. Polym. J.*, 2014, **59**, 19–24.
271 T. A. Skotheim, J. R. Reynolds, Handbook of Conducting Polymers, 3rd edn.; CRC Press: Boca Raton, FL, 2007.
272 K. Starčević, D. W. Boykin and G. Karminski-Zamola, *Heteroat. Chem.*, 2003, **14**, 218–222.
273 A. Bedi and S. S. Zade, *Org. Biomol. Chem.*, 2014, **12**, 7375–7380.
274 A. Meyer, E. Sigmund, F. Luppertz, G. Schnakenburg, I. Gadaczek, T. Bredow, S. S. Jester and S. Höger, *Beilstein J. Org. Chem.*, 2010, **6**, 1180–1187.
275 D. A. Alonso, A. Baeza, R. Chinchilla, G. Guillena, I. M. Pastor and D. J. Ramón, *European J. Org. Chem.*, 2016, **2016**, 612–632.
276 Q. Zhang, K. De Oliveira Vigier, S. Royer and F. Jérôme, *Chem. Soc. Rev.*, 2012, **41**, 7108–7146.
277 F. M. Perna, P. Vitale and V. Capriati, *Curr. Opin. Green Sustain. Chem.*, 2020, **21**, 27–33.
278 A. P. Abbott, G. Capper, D. L. Davies, R. K. Rasheed and V. Tambyrajah, *Chem. Commun.*, 2003, **1**, 70–71.
279 Y. Dai, J. van Spronsen, G. J. Witkamp, R. Verpoorte and Y. H. Choi, *Anal. Chim. Acta*, 2013, **766**, 61–68.
280 M. Hayyan, M. A. Hashim, A. Hayyan, M. A. Al-Saadi, I. M. AlNashef, M. E. S. Mirghani and O. K. Saheed, *Chemosphere*, 2013, **90**, 2193–2195.
281 K. Radošević, I. Čanak, M. Panić, K. Markov, M. C. Bubalo, J. Frece, V. G. Srček and I. R. Redovniković, *Environ. Sci. Pollut. Res.*, 2018, **25**, 14188–14196.
282 B. Y. Zhao, P. Xu, F. X. Yang, H. Wu, M. H. Zong and W. Y. Lou, *ACS Sustain. Chem. Eng.*, 2015, **3**, 2746–2755.
283 A. Pandey, R. Rai, M. Pal and S. Pandey, *Phys. Chem. Chem. Phys.*, 2014, **16**, 1559–1568.
284 M. Pal, R. Rai, A. Yadav, R. Khanna, G. A. Baker and S. Pandey, *Langmuir*, 2014, **30**, 13191–13198.
285 V. Fischer, J. Marcus, D. Touraud, O. Diat and W. Kunz, *J. Colloid Interface Sci.*, 2015, **453**, 186–193.
286 A. Yadav and S. Pandey, *J. Chem. Eng. Data*, 2014, **59**, 2221–2229.
287 Y. Dai, G. J. Witkamp, R. Verpoorte and Y. H. Choi, *Food Chem.*, 2015, **187**, 14–19.
288 L. Cicco, M. J. Rodríguez-Álvarez, F. M. Perna, J. García-Álvarez and V. Capriati, *Green Chem.*, 2017, **19**, 3069–3077.
289 J. García-Álvarez, E. Hevia and V. Capriati, *Chem. - A Eur. J.*, 2018, **24**, 14854–14863.
290 L. Millia, V. Dall'Asta, C. Ferrara, V. Berbenni, E. Quartarone, F. M. Perna, V. Capriati and P. Mustarelli, *Solid State Ionics*, 2018, **323**, 44–48.
291 C. R. Müller, I. Meiners and P. Domínguez De María, *RSC Adv.*, 2014, **4**, 46097–46101.
292 S. Ghinato, G. Dilauro, F. M. Perna, V. Capriati, M. Blangetti and C. Prandi, *Chem. Commun.*, 2019, **55**, 7741–7744.
293 A. F. Quivelli, P. Vitale, F. M. Perna and V. Capriati, *Front. Chem.*, 2019, **7**, 723.

294 X. Marset, B. Saavedra, N. González-Gallardo, A. Beaton, M. M. León, R. Luna, D. J. Ramón and G. Guillena, *Front. Chem.*, 2019, **7**, 700.
295 R. A. Sheldon, *Chem. - A Eur. J.*, 2016, **22**, 12984–12999.
296 P. Vitale, V. M. Abbinante, F. M. Perna, A. Salomone, C. Cardellicchio and V. Capriati, *Adv. Synth. Catal.*, 2017, **359**, 1049–1057.
297 L. Cicco, N. Ríos-Lombardía, M. J. Rodríguez-Álvarez, F. Morís, F. M. Perna, V. Capriati, J. García-Álvarez and J. González-Sabín, *Green Chem.*, 2018, **20**, 3468–3475.
298 R. Martínez, L. Berbegal, G. Guillena and D. J. Ramón, *Green Chem.*, 2016, **18**, 1724–1730.
299 D. Brenna, E. Massolo, A. Puglisi, S. Rossi, G. Celentano, M. Benaglia and V. Capriati, *Beilstein J. Org. Chem.*, 2016, **12**, 2620–2626.
300 A. Torregrosa-Chinillach, A. Sánchez-Laó, E. Santagostino and R. Chinchilla, *Molecules*, 2019, **24**, 4058.
301 C. L. Boldrini, N. Manfredi, F. M. Perna, V. Trifiletti, V. Capriati and A. Abbotto, *Energy Technol.*, 2017, **5**, 345–353.
302 C. L. Boldrini, N. Manfredi, F. M. Perna, V. Capriati and A. Abbotto, *Chem. - A Eur. J.*, 2018, **24**, 17656–17659.
303 F. Milano, L. Giotta, M. R. Guascito, A. Agostiano, S. Sblendorio, L. Valli, F. M. Perna, L. Cicco, M. Trotta and V. Capriati, *ACS Sustain. Chem. Eng.*, 2017, **5**, 7768–7776.
304 J. Hassan, M. Sévignon, C. Gozzi, E. Schulz and M. Lemaire, *Chem. Rev.*, 2002, **102**, 1359–1469.
305 Y. Hu, E. O. Danilov, B. Wex and D. C. Neckers, *J. Nonlinear Opt. Phys. Mater.*, 2008, **17**, 275–283.